Antigen handling and cross-presentation by dendritic cells
Ho, N.I.S.C.

Cover Page

Universiteit Leiden

Author: Ho, N.I.S.C.
Title: Antigen handling and cross-presentation by dendritic cells
Issue Date: 2020-07-09

ANTIGEN HANDLING & CROSS-PRESENTATION BY DENDRITIC CELLS

Nataschja Ho

Antigen handling and
cross-presentation by dendritic cells

Nataschja Ho

Antigen handling and cross-presentation by dendritic cells
Nataschja Ho

Antigen handling and cross-presentation by dendritic cells

Proefschrift

ter verkrijging van
de graad van Doctor aan de Universiteit Leiden,
op gezag van Rector Magnificus prof.mr. C.J.J.M. Stolker,
volgens besluit van het College voor Promoties
te verdedigen op

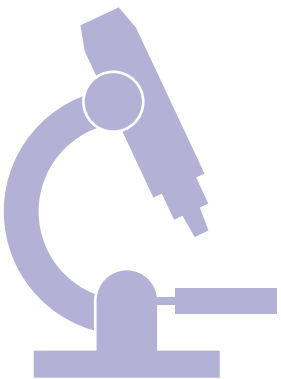donderdag 9 juli 2020, klokke 11:15 uur

door
Nataschja Isabel Suet-Ching Ho
geboren te Amsterdam in 1986

TABLE OF CONTENTS

1

General introduction

THE IMMUNE SYSTEM

Our human body possesses a complex immune system to defend against infections with pathogens, such as bacteria, viruses and parasites but also against malignant cancer cells. The diversity of different immune mechanisms can be divided into an innate immune system and an adaptive immune system. The innate immune system is the first line of defense, and can be activated upon recognition of pathogen-associated molecular patterns (PAMPs), small molecules expressed by pathogens (1, 2). The recognition of PAMPs by the immune system relies on pattern recognition receptors (PRRs), including Toll-like receptors (TLRs), Nod-like receptors (NLRs), and C-type lectin receptors (CLRs) (Fig. 1). Fcγ receptors (FcγRs) recognize antigens bound to antibodies. TLRs can be expressed on the cell surface (TLR1, 2, 4, 5, 6, and 11), recognizing microbial membrane components, but TLRs can also be found on intracellular vesicles (TLR3, 7, 8, and 9), where they recognize microbial nucleic acids. NLRs sense bacterial components which are directly introduced into the cytoplasm. CLRs recognize sugar structures of bacteria and fungi. Macrophages, neutrophils, and dendritic cells are sensor cells of the adaptive immune system that express PRRs and recognize PAMPs that are part of microorganisms but not of the host body's own cells. Activation of PRRs on these sensor cells can induce uptake of pathogen antigen by endocytosis or phagocytosis, resulting in killing of the pathogen, production of cytokines and chemokines to attract immune cells. In addition, inflammation and antigen presentation to other immune cells can be induced.
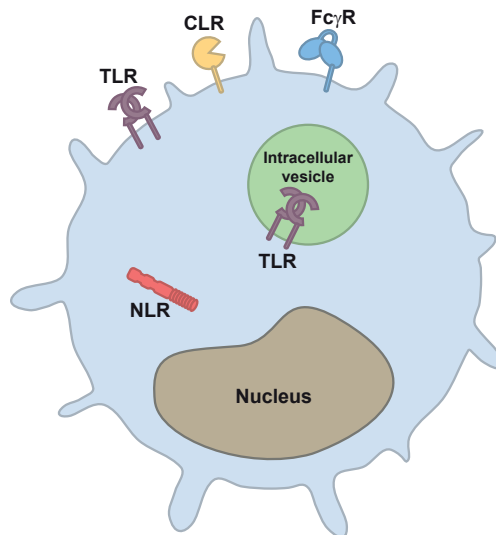
Figure 1. Dendritic cell pattern recognition receptors. Dendritic cells recognize pathogens by pattern recognition receptors, such as Toll-like receptors (TLRs), Nod-like receptors (NLRs), C-type lectin receptors (CLRs). Fcγ receptors (FcγRs) recognize antigens that are bound to antibodies. TLRs can be expressed extracellular or on intracellular vesicles.

Once the pathogen overwhelms the innate defense mechanisms, the adaptive immune response comes into action. The adaptive immune system is composed of B and T lymphocytes (humoral and cellular immunity, respectively). Both B and T lymphocytes (B and T cells) express a unique repertoire of antigen receptors on each individual lymphocyte which are highly specific for a certain antigen. B cells are specialized in binding specific soluble molecules through their B-cell receptor, which facilitates the internalization of antigen via endocytosis and the process of internalized antigen, followed by the display of fragments as peptide:MHCII complexes to helper T cells (Th). When the Th have previously been activated by the same antigen, the B cells will receive signals from the Th that drive the B cells' differentiation into antibody producing cells and class switching, while others become memory B cells residing in the germinal centers. The secretion of antibodies in the blood stream can bind and mark pathogens for clearance and destruction.

T cells recognize specific antigens which are presented on professional antigen presenting cells (APCs). APCs migrate from the infection or tumor site to the lymph nodes upon antigen recognition, antigen uptake, and activation. Antigens are then processed in APCs and presented on MHC class I (MHCI) or MHC class II (MHCII) molecules on the cell surface to CD8$^+$ or CD4$^+$ lymphocytes, respectively. MHCI molecules are expressed by almost all cells, while MHCII molecules are exclusively expressed on APCs. The main function of MHCI in nucleated cells is to display intracellular proteins, derived from endogenous infections and mutations to CD8$^+$ cytotoxic T cells (CTLs). The classical MHCI antigen presentation pathway is mainly used for endogenous antigens, whereas the MHCII antigen pathway is used when exogenous antigens are encountered.

Naïve T cells circulate in the blood stream and secondary lymphoid organs (such as lymph nodes, spleen, and Peyer's patches in the small intestine) until they encounter their specific antigen, presented as a peptide:MHC complex on the surface of APCs, and get activated to proliferate and differentiate into effector T cells including CD4$^+$ Th and CD8$^+$ CTLs. CD4$^+$ T cells can differentiate into specialized effector subsets which can stimulate or regulate specific immunological functions dependent on the type of infection or pathological situation. These include T$_H$1 (T helper 1), T$_H$2, T$_H$17, and T$_{FH}$ (T follicular helper) cells, which can help different immune cell types; and T$_{reg}$ (regulatory T) cells, which inhibit or modulate the extent of immune activation. T$_H$1 cells help eradicating infections by microbes that are phagocytosed by macrophages. Through the release of IFN-γ, macrophages are activated and enhanced in their killing activities. T$_H$2 cells control extracellular parasite infections by mediating class switching of B cells to produce IgE. T$_H$17 cells are important in responses to extracellular bacteria and fungi by inducing neutrophilic responses to clear the pathogens. T$_{FH}$ cells mainly provide B-cell help for high-affinity antibody production. T$_{reg}$ cells suppress T-cell responses and prevents autoimmunity, however high levels of T$_{reg}$ cells are often found in the tumor microenvironment and are associated with poor prognosis in many cancers. A specialized function of the adaptive immune system is the induction of memory T cells

(CD4^{+} or CD8^{+}) after an infection. This is important to enable a more rapid and effective response against pathogens that have been encountered previously. Already for almost a century we make use of the adaptive immune system by vaccinating inactive pathogens to induce long term protective immunity against aggressive infectious diseases. CD8^{+} T cells are the main effector cells that can attack cancer and virus-infected cells. The activation and differentiation of naïve T cells by APCs is also called priming, which is often dependent on both antigen presentation and co-stimulatory signals from the APCs to the T cells. In general, CD8^{+} T cells require more co-stimulatory activity to be activated compared to CD4^{+} T cells. In some viral infections, DCs are sufficient to activate CD8^{+} T cells into CTLs, however the majority of viral infections requires additional help from CD4^{+} effector T cells. The CD4^{+} effector T cells, triggered by MHCII presentation on APCs, upregulate CD40L which binds to CD40 on APCs. This leads to APC maturation and upregulation of various co-stimulatory molecules, including CD80, CD86, 4-1BBL, and MHC molecules. Combined with optimal specific antigen presentation on MHCI by APCs, this will license the APCs to activate CD8^{+} CTLs (license to kill) (3). Thus APCs, especially dendritic cell subsets, play a crucial role in inducing effective CTL responses in order to eradicate tumors and infectious diseases.

ANTIGEN CROSS-PRESENTATION BY DENDRITIC CELLS

Dendritic cells (DCs) are APCs that can capture, process and present antigens to T cells. Two classical antigen presentation pathways have been described in DCs: MHCI and MHCII pathways. MHCI pathway mainly presents endogenous antigens on MHCI molecules to CD8^{+} T cells, whereas MHCII pathway presents exogenous antigens on MHCII molecules to CD4^{+} T cells. However, DCs have a specialized function to present exogenous antigens also on MHCI molecules, called cross-presentation, linking innate and adaptive immunity. Several studies reported the importance of DC cross-presentation for inducing T cell responses which are specific for tumor antigens and infectious diseases (4–6). In order to elicit potent CD8^{+} T cell priming, the levels of DC maturation and DC cross-presentation efficiency are important. DCs express several uptake and sensing receptors (Fig. 1) and undergo maturation after the recognition of pathogen-derived products by PRRs (e.g. TLRs, NLRs) or antibody-antigen complexes by FcγRs. Upon DC maturation, antigen processing is increased followed by upregulation of MHC molecules and co-stimulatory molecules (such as CD40, CD80 and CD86), and induction of cytokine release, which are all important for the interaction with T cells (7). Two main intracellular pathways for antigen cross-presentation in DCs have been proposed: the vacuolar and the cytosolic pathways (Fig. 2). Antigen processing through the vacuolar pathway is proteasome independent and generally also independent of the transporter associated with antigen processing (TAP) (8). It has been suggested that antigen is degraded by proteases (e.g. cathepsin S) and that antigen

processing and loading on MHCI occur in endocytic compartments. In the cytosolic pathway, exogenous antigens are transported from endosomal vesicles into the cell cytosol, where they are degraded by the proteasome. Proteasome-generated peptides are then transported by TAP1 and TAP2 to the endoplasmic reticulum (ER) for loading on MHCI molecules (9–11) (Fig. 2). However, it has been reported that some proteasome-generated peptides may be transported back into endocytic compartments and trimmed by insulin regulated aminopeptidase (IRAP) and directly loaded on MHCI molecules (12).
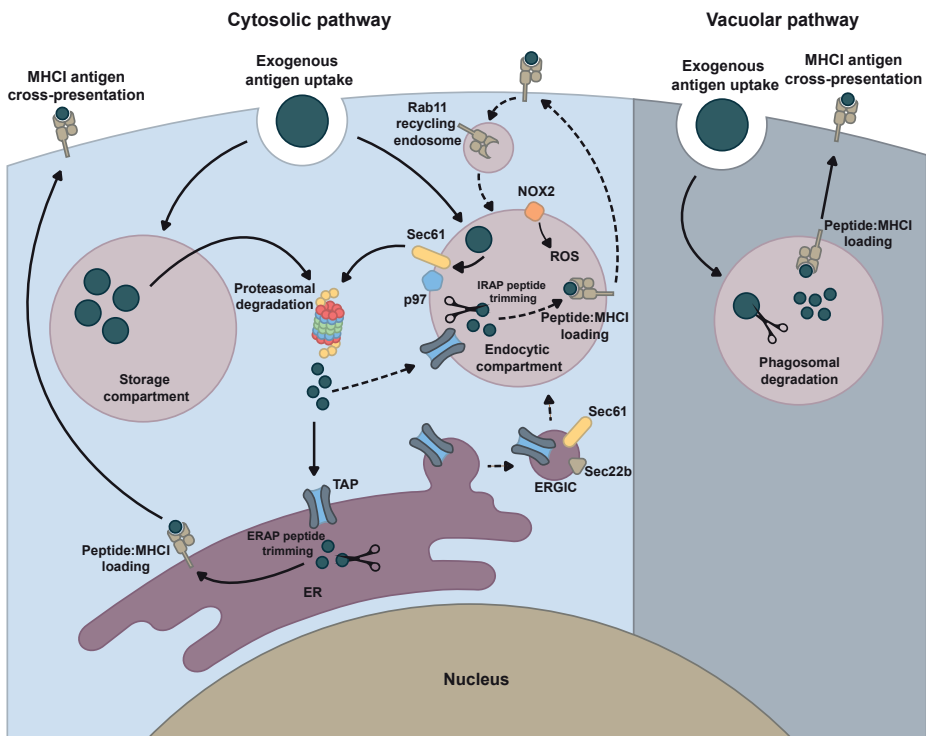
Figure 2. Antigen cross-presentation by dendritic cells. Two main intracellular pathways for antigen cross-presentation in DCs have been proposed: the cytosolic and the vacuolar pathways. In the vacuolar pathway, antigens are degraded by proteases (e.g. cathepsin S). Antigen processing and loading on MHCI occur in endocytic compartments. In the cytosolic pathway, antigens are taken up in endosomal vesicles. It has been proposed that antigens are translocated from endosomal vesicles into the cell cytosol through Sec61 or mediated through p97. Antigens are then degraded by the proteasome and transported by TAP to the endoplasmic reticulum (ER) for loading on MHCI molecules. However, some proteasome-generated peptides may be transported back into endocytic compartments for further peptide trimming and MHCI loading. MHCI molecules could be originated from the cell membrane and translocated via Rab11 recycling endosomes to endocytic compartments. There are indications that the recruitment of ER and ER-Golgi intermediate compartment (ERGIC) components to the phagosomes is mediated by the ER-resident SNARE Sec22b. Recruitment of NOX2 to endosomes and ROS production will induce alkalization and thereby preventing rapid antigen degradation in endosomes. Moreover, exogenous antigen can be taken up and conserved in storage compartments for prolonged antigen presentation. Antigen from the storage compartment is translocated to the cell cytosol where it is degraded by the proteasome and transported by TAP to the ER for MHCI loading and subsequently antigen cross-presentation on the cell surface.

How exogenous antigens are translocated from endocytic compartments into the cytosol is still not clear. It has been demonstrated using exogenous cytochrome *c*, that only cross-presenting DCs transfer cytochrome *c* to their cell cytosol, thereby triggering caspase-dependent apoptosis (13). Extensive studies in murine models identified the recruitment of ER-associated degradation (ERAD) member, Sec61, to endocytic compartments and suggested Sec61 as a possible translocator for antigen from the endosomes into the cytosol (14) (Fig. 2). By blocking Sec61 with a specific intracellular antibody they showed Sec61 was trapped in the ER, preventing its transport towards endosomes, and thereby blocking antigen translocation and cross-presentation. However, a more recent study showed severe inhibition of protein import into the ER but no inhibition of protein export from endocytic compartments when they used mycolactone, which binds Sec61α specifically (15). Although both studies showed inhibition of DC cross-presentation upon Sec61 blocking, it seems that Sec61 plays a more dominant role in inhibiting protein translocation into the ER and altering antigen cross-presentation at a different level than antigen export into the cytosol. Other evidence for the involvement of the ERAD machinery was shown by the Cresswell group, who demonstrated the requirement of p97 (also known as AAA ATPase) in protein export from phagosomes and thereby regulating cross-presentation (10) (Fig. 2). Moreover, they showed that a bead-bound synthetic peptide with an N-glycosylation site was N-glycosylated, which is a characteristic feature of the ER after DC phagocytosis. There has been an ongoing debate about the possible role of ER-resident proteins in endocytic compartments and in the membrane transport pathways. There are indications that the recruitment of ER and ER-Golgi intermediate compartment (ERGIC) components to the phagosomes is mediated by the ER-resident SNARE Sec22b (Fig. 2). The group of Amigorena showed that silencing Sec22b inhibits both the delivery of ER-resident proteins to phagosomes and the export of exogenous proteins from phagosomes to the cytosol (16). In a follow up study they showed impairment of DC cross-presentation in Sec22b-knockout DCs (17). However, conflicting results were found by another group who used similar Sec22b-knockout DCs and demonstrated that Sec22b is not necessary for cross-presentation (18). Therefore, a role for Sec22b in DC cross-presentation still needs to be determined.

Another proposed regulator of antigen cross-presentation in DCs is stromal interaction molecule 1 (STIM1), which is a calcium sensor that conveys the calcium content of the ER to store-operated channels of a cell. STIM1 can promote the contact sites between the ER and phagosomes, altering Ca^{2+} signaling and regulating phago/endosome fusion events (19). The ER membrane protein uncoordinated 93 homolog B1 (UCN93B1), which is activated by TLR triggering, interacts with STIM1 and is critically involved in antigen cross-presentation (20). Ablation of UCN93B1 impairs antigen translocation into the cytosol and antigen cross-presentation. In addition, it has been demonstrated that lipid peroxidation in DCs might play an important role in antigen translocation to the cytosol. The recruitment of NADPH-oxidase

complex (NOX2) and production of reactive oxygen species (ROS) in the endosomes can cause lipid peroxidation, resulting in leakiness of the endosomal membrane and hence, antigen access into the cytosol and enhanced antigen cross-presentation (21). Furthermore, upon NOX2 recruitment and ROS release in endosomes, mediated by Rab27a, endosomal alkalization and pH in endosomes are increased (22, 23) (Fig. 2). This will prevent rapid antigen degradation and thereby enhancing antigen cross-presentation.

We have previously published that antigen can be conserved in DCs in specialized intracellular storage compartments which facilitate prolonged antigen cross-presentation to CD8$^+$ T cells (24) (Fig. 2). These storage compartments are lysosomal-like organelles, distinct from MHCII compartments or MHCI processing/loading compartments. Surface MHCI molecules on DCs have a shorter turnover rate compared to MHCII molecules, most MHCI-peptide complexes disappear from the cell surface within 24 hours. Since the migration of DCs after antigen encountering to the T-cell zones might take up to several days, this high turnover rate of MHCI molecules is not beneficial for efficient CD8$^+$ T-cell cross-presentation (25). Also, the dose of antigen that is expressed on MHCI needs to exceed the required threshold for effective T-cell activation. Therefore, long-term antigen storage in DCs and sustained antigen display on the DC cell-surface are important to ensure T-cell cross-priming. In this thesis we investigate antigen uptake, storage, processing, and sustained cross-presentation mechanisms in DCs *in vitro* and *in vivo*.

MURINE CROSS-PRESENTING DENDRITIC CELL SUBSETS

Over the years it has become clear that DCs are organized in multiple subpopulations, each having specific functions. Only some of the DC subsets have the ability to cross present antigen efficiently. Murine DCs in secondary lymphoid organs can roughly be divided in conventional DCs (cDCs) and plasmacytoid DCs (pDCs) (26). cDCs are further classified into CD8α$^+$ DCs (cDC1) and CD8α$^-$ DCs (cDC2). The development of CD8α$^+$ DCs is mainly regulated by the expression of the transcription factors IRF8 and Batf3, whereas CD8α$^-$ DCs is mainly regulated by IRF4 (27). Deletion of either of these genes can lead to development defects of the DC subsets. In general, CD8α$^+$ DCs are considered to be more efficient at cross-presentation than CD8α$^-$ DCs (28). Some explanations for the superior cross-presentation ability of CD8α$^+$ DCs include higher expression of components that are associated with MHCI processing pathway, reduced antigen degradation in endosomes by ROS production, and higher efficiency in antigen transfer into the cytosol (13, 22, 29). However, studies have shown that CD8α$^-$ DCs can also cross-present antigen efficiently after receptor-mediated endocytosis by CD205 or FcγRs (30, 31). The main DC subset responsible for cross-presentation in the lymph nodes, lung and skin is CD103$^+$ migratory DCs (32, 33).

Murine pDCs are generally considered as poor cross-presenting cells. Although some studies suggested their cross-presenting ability *in vitro*, *ex vivo*, or after TLR activation, their role in cross-presentation *in vivo* seems lacking during viral infections, despite the fact that they are well known for producing large amount of type I interferons (34–39). In human, the BDCA1+ (CD1c+) and BDCA3+ (CD141+) DCs in blood are proposed as the human counterparts of murine CD8α- and CD8α+ DCs, respectively (40). Although in general BDCA3+ are considered to be more efficient in antigen cross-presentation, it has been shown that BDCA1+ DCs reached similar efficiency upon activation with TLR ligands (41). In contrast to murine pDCs, it has been reported that human pDCs can efficiently cross-present soluble and cell-associated antigens. However, a recent study identified a distinct pre-pDC subset which bears similar markers as the classical pDCs. They showed that only the pre-pDC subset was able to present antigen to CD4+ T cells and that the antigen presenting ability for the classical pDCs might be a result of the "contamination" of pre-pDCs. Whether this also applies for antigen cross-presentation to CD8+ T cells still needs to be elucidated. However in both murine and human, it seems that the cross-presentation ability for each subset can depend on factors including the type of antigen, antigen handling and processing, DC location, DC activation, and local inflammatory signals (42).

Recent studies identified a two-step T cell priming model in which CD4+ T cells and CD8+ T cells first encounter their respective antigen on different types of DCs during the first priming step (43–46). During the second priming step, lymph node resident XC-chemokine receptor 1 (XCR1)+ cDC1s are recruited to receive cross-presented antigen from the DCs that carried out the first priming step. The pre-activated CD4+ and CD8+ T cells during the first priming step interact with the cDC1s, where CD4+ T cells induce optimal signals for CD8+ T cell differentiation into CTLs and memory CTLs. These findings highlight the importance of different DC subsets and their distinctive functions for the induction of efficient T cell priming. In **chapter 2** we studied the sustained cross-presentation ability of individual murine DC subsets *in vivo*.

CANCER IMMUNOTHERAPY TARGETING DENDRITIC CELLS

DCs have become the prime target for cancer vaccines since they play a critical role in inducing anti-tumor immunity responses and the formation of anti-tumor memory cells. Extensive studies on DC-based vaccination strategies have been done in order to find an optimal treatment for cancer patients. DC immunotherapy can roughly be divided in *ex vivo* activated DCs and direct *in vivo* targeting of DCs (47, 48). *Ex vivo* DCs are mainly obtained from peripheral blood mononuclear cells (PBMCs) or generated from CD34+ progenitors by culturing them in the presence of cytokines such as IL-4 and GM-CSF. This very labor

1

intensive immunotherapy has shown some clinical successes (49). The autologous DCs cultured in Good Manufacturing Practice (GMP) setting are then loaded with tumor-derived antigens, activated with a maturation cocktail (e.g. TNF-α, IL-1β, IL-6, and PGE2), and injected back into the patients. Despite the fact that *ex vivo* generated DCs can properly initiate tumor-specific CD8+ and CD4+ T cell responses, there is still limited efficacy of DC-based vaccines. This is likely caused by the presence of immune escape, and immunosuppressive mechanisms in the tumor microenvironment (50). Also, determining the ideal antigen-loading is important for optimal therapy. Several methods of antigen loading of DCs have been studied, including short peptides, long peptides, tumor cell lysates, DNA or RNA coding for a specific antigen, immune complexes, and neoantigens (48, 51). Loading DCs with short peptides results in peptides that bind to a limited number of HLA class I molecules. The lack of Th induction might cause suboptimal long-lived CTL responses (3). More ideal is to load all available HLA class I- and class II-presenting molecules on DCs with tumor-derived peptides (52). *Ex vivo* loading of DCs with immune complexes, consisting specific antibodies complexed with tumor-associated protein antigen, have shown efficient MHCI and MHCII antigen presentation, potent DC activation, and efficient tumor control in mice (53).

Another DC vaccination approach is to deliver antigens to DCs directly *in vivo* by coupling the antigens to antibodies specific to DC-expressed receptors, including FcγRs and CLRs. Targeting DC CLRs, such as DEC-205, DC-SIGN, and DNGR-1, have shown efficient MHCI and MHCII immune responses (54–56). However, if these antigen-antibody conjugates are given without additional adjuvant to stimulate DC activation, this type of DC targeting can induce disease-specific tolerance (57). Therefore, additional DC activating compounds such as CD40 and TLR ligands are often required (55, 58). Another highly efficient targeting strategy of *in vivo* DCs is injecting long-peptides conjugated to TLR-ligands, sharing the peptide antigen and adjuvant in one single molecule. This resulted in enhanced antigen presentation, efficient CD8+ T cell priming, and antitumor immunity in mice challenged with aggressive transplantable melanoma or lymphoma (59, 60). This might be a more promising DC targeting vaccination strategy compared to the laborious and expensive *ex vivo* loading of DCs with tumor antigens.

Currently, one of the most innovative developments in DC vaccination developments is the use of RNA sequencing to determine neoantigens derived from somatic mutations in the tumor, which are absent in non-malignant cells. Neoantigens can stimulate expansion of high-affinity CD8+ T cells which are patient and tumor specific. However, the number of somatic mutations is dependent on the tumor type, which can influence the susceptibility of immunotherapy (61). Nevertheless, it becomes more clear that DCs play a vital role in the outcome of vaccines against cancer or infectious diseases.

FCΓ RECEPTORS ON DENDRITIC CELLS

Potent therapeutic vaccination against cancer relies on efficient antigen loading and activation of DCs in priming T cells. Several studies revealed that antibody-mediated targeting of protein antigen via FcγRs are highly effective in inducing T cell-mediated antitumor responses (62–64). DCs express FcγRs on their cell surface to facilitate the uptake of antibody-bound exogenous antigens. In mice, four FcγRs have been described including FcγRI (CD64), FcγRIIB (CD32B), FcγRIII (CD16), and FcγRIV (65). The activating receptors FcγRI, FcγRIII, and FcγRIV have an immunoreceptor tyrosine-based activation motif (ITAM), whereas the inhibitory receptor FcγRII has an immunoreceptor tyrosine-based inhibition motif (ITIM) (Table 1) (65). ITAM activates signaling cascades via SRC family kinases and spleen tyrosine kinase (SYK). ITIM recruits SH2 domain-containing inositol 5'-phophatase 1 (SHIP1) and counteracts activating signals by the activating receptors. Co-expression of activating and inhibitory receptors on the same cell can function as a threshold for activation, thereby defining the outcome of cellular response (66–68). In general, murine cDCs and macrophages express all activating FcγRs and the inhibitory receptor, whereas pDCs only express the inhibitory receptor FcγRII (65). FcγRs have different affinity for binding of different IgG isotypes (Table 1). Although both activating and inhibitory receptors can bind and rapidly endocytose opsonized materials or antigen-antibody immune complexes (ICs), the type of receptor that is triggered influences the degradative pathway in which antigens will be routed (69). Internalization by activating FcγRs favors the degradative route for antigen processing and presentation, whereas the inhibitory FcγR favors a retention pathway preserving the antigen for transfer to B cells. Activating receptors mainly promote antigen presentation due to their ability to activate DCs and to stimulate the MHCI cross-presentation machinery (70). We have demonstrated that FcγR-mediated uptake of model antigen OVA bound to anti-OVA IgG is at least 1000-fold more efficient in antigen cross-presentation than soluble OVA (64). Binding of ICs triggers cross-linking of the FcγRs resulting in DC maturation and internalization of the ICs toward antigen storage and presentation compartments (24, 71). DCs loaded with specific antigen-antibody ICs resulted in priming of CD8+ CTLs, and tumor protection *in vivo* (64, 72). We characterized the antigen storage compartments in more detail in **chapter 4** and described the importance of these storage compartments for prolonged antigen cross-presentation *in vivo* in **chapter 2**. The role of FcγR targeting in sustained DC cross-presentation by DC subsets *in vivo* will be discussed in **chapter 3**.

Table 1. Murine Fcγ receptors

FcγRs	IgG binding affinity	Function	Motif	Expression on APCs
FcγRI	IgG2a > IgG2b > IgG3	Activation	ITAM	CD8α⁺ DCs, CD8α⁻ DCs, macrophages
FcγRIIB	IgG1 > IgG2b > IgG2a	Inhibition	ITIM	CD8α⁺ DCs, CD8α⁻ DCs, pDCs, macrophages, B cells
FcγRIII	IgG2a > IgG2b > IgG1	Activation	ITAM	CD8α⁺ DCs, CD8α⁻ DCs, macrophages
FcγRIV	IgG2a > IG2b	Activation	ITAM	CD8α⁺ DCs, CD8α⁻ DCs, macrophages

1

COMPLEMENT FACTOR C1Q

Complement is one of the main effector mechanisms of antibody-mediated immunity. It plays an important role in defending against bacterial infections, bridging innate and adaptive immunity, and rapid clearance of circulating ICs by binding complement coated ICs to complement receptor-1 on erythrocytes and thereby preventing IC deposition (73, 74). It has been described that patients with systemic lupus erythematosus have defects in IC clearance, resulting in tissue inflammation and damage (75). The complement system can be divided into three different pathways: the classical pathway, the alternative pathway, and the mannose binding lectin pathway (74). Each pathway is activated upon different triggering but all converge at the point of cleavage of complement protein C3 and ultimately cleavage of C5 into C5a and C5b, thereby initiating the membrane attack complex (MAC). MAC is composed of a complex of C5b, C6, C7, and C8, which binds to the cell membrane and can kill or damage the cell by inducing pores in the membrane. The classical pathway is initiated upon binding of the C1 complex (which consists of C1q, two C1r serine proteases, and two C1s serine proteases) to antibodies bound to antigen (Fig. 3). Besides binding to FcγRs, most IgG subclasses can bind to C1q, the first recognition subcomponent of the classical pathway (76). C1q is a hexameric glycoprotein assembled from 18 polypeptide chains that are formed by three types of chains (A, B, and C chain) (77). Each chain consists of a collagen-like domain (the binding site for anti-C1q auto-antibody) to which the serine proteases C1r and C1s are localized. Moreover, each chain comprises a globular head which binds to the Fc part of IgG and IgM when bound to cognate antigen (78). Importantly, it has been reported that IgG hexamerization after antigen binding leads to a more stabilized binding of C1q with high avidity (78, 79) (Fig. 3). The collagen-like regions mediate immune effector mechanisms, including complement activation through interaction with the C1r and C1s proteases (80). Upon binding of C1q to ICs, C1r and C1s are activated, resulting in activation of the classical complement pathway (81). Interestingly, C1q is mainly produced by macrophages and immature DCs (82). We and others have demonstrated that the uptake, processing of ICs, and antigen cross-presentation by DCs in the spleen were hampered in C1q-defiecient mice (83, 84). The crucial role of C1q in antibody-mediated antigen uptake and cross-presentation by APC subsets *in vivo* will be discussed in **chapter 3**.
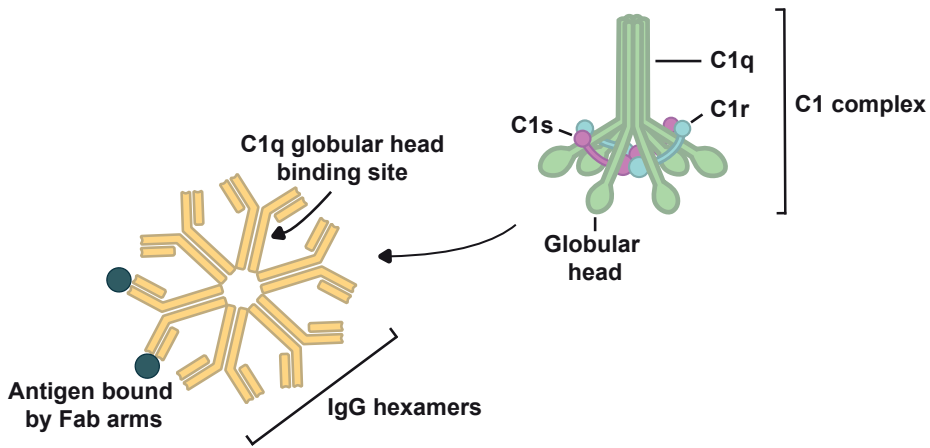
Figure 3. C1q binding to antigen:IgG hexameric complex. C1q is a hexameric glycoprotein with collagen-like domains to which two serine proteases C1r and two C1s are localized. Each chain of the hexamer comprises a globular head that binds to the Fc part of IgG when bound to cognate antigen. It is likely, based on recent data (78, 79), that IgG molecules can form hexameric structures after antigen binding which lead to a more stabilized binding of hexameric C1q multimers with high avidity.

C-TYPE LECTIN RECEPTOR MGL

CLRs have been extensively studied for the development of tumor vaccine that targets specific DC subsets. DCs express a large variety of CLRs, including DEC205, DCIR, CLEC9a/DNGR1, CLEC12, Dectin-1, Langerin, MR, DC-SIGN, and MGL (85). Most CLRs recognize glycosylated antigens through their carbohydrate recognition receptors. Directing antigens to CLRs on DCs (e.g. DEC205, MR, DC-SIGN and CLEC9a), by using antigens conjugated to CLR-specific antibodies, have shown enhanced antigen uptake and presentation (86–89). Targeting strategies using natural or artificial glycan ligands have gained interest since they are easy to develop and relatively cheap to produce. The ligands can be directly conjugated to tumor antigens or incorporated in nanoparticles, and more importantly, they mimic natural functions of the receptors, inducing "natural" signaling cascades in DCs. Glycosylated antigen specific for CLRs have shown efficient antigen uptake and presentation (90–94). However, targeting antigen to different CLRs might result in activating or suppressive downstream signaling events, resulting in different intracellular routing, DC maturation status, and antigen presentation. Therefore, it is important to bear this in mind when targeting specific CLRs for the desirable outcome.

There are two homologs of macrophage galactose-type lectin (MGL) identified in mice, MGL1 and MGL2, whereas in human only one homolog (huMGL) has been found (95, 96). MGL is exclusively expressed on DCs and macrophages and therefore considered to be a

potent target for vaccination strategies. Murine MGL1 binds to the carbohydrate structures Lewis[x] (Le[x]) and Lewis[a] (Le[a]), while murine MGL2 and huMGL have high affinities for *N*-acetylgalactosamine (GalNac) and galactose, including the O-linked Tn-antigen, TF-antigen, and core 2 (97, 98). The difference of glycan specificities between MGL1 and MGL2 provides specific targeting of each receptor. However, their targeting potency in inducing DC cross-presentation is still not fully unraveled yet. It has been shown that GalNac modifications of antigen resulted in antigen presentation to CD4^{+} and CD8^{+} T cells in murine BMDCs (99). Targeting dermal DCs with glycosidic Tn-based vaccines favored CD4^{+} T cell priming *in vivo* and activation of antibody-producing B cells (100). The model protein OVA is mainly binding to the mannose receptor (MR) on DCs and has extensively been used in many DC cross-presentation studies. However, it have been shown that MR mediates cross-presentation only when high doses of OVA were used in combination with TLR-triggering (101). In **chapter 4 and 5**, we redirected OVA targeting to MGL1 on DCs by the modification of OVA with Le[x], and investigated the antigen routing, processing, and cross-presentation outcome.

AUTOPHAGY IN DENDRITIC CELLS

Autophagy is an evolutionary conserved system that degrades and recycle unnecessary or damaged cellular components by lysosomes (102). At least three different pathways for autophagy has been described: macroautophagy, microautophagy and chaperon-mediated autophagy (103) (Fig. 4). Microautophagy involves direct engulfment of small amounts of cytoplasmic material into the lysosome, whereas chaperon-mediated autophagy utilizes heat-shock-cognate protein 70 (Hsc70) and LAMP2A to translocate proteins to the lysosome. Macroautophagy degrades larger structures like damaged organelles or protein aggregates. These are taken up from the cytoplasm by a cup-shaped double membrane which fuses its ends to form double-membrane-surrounded autophagosomes and subsequently fuse with lysosomes.

Cell nutrient starvation and other stresses can initiate autophagy, which is under control of the mammalian target of rapamycin complex 1 (mTORC1) and AMP-activate protein kinase (AMPK). During starvation, mTORC1 is inactivated whereas AMPK is activated, resulting in macroautophagy activation and autophagosome elongation. The autophagosome formation is regulated by autophagy-related gene (Atg) products (104) (Fig. 5). The ULK complex (containing ULK1/2, Atg13, and FIP200) recruits the class III phosphatidylinositol 3-kinase (PI3K) VPS34 complex to the membranes. The VPS34 complex (containing Atg14, VPS34, Atg6/Beclin-1, VPS15, UVRAG, and BIF-1) generates phosphatidylinositol 3-phosphate (PI3P) which leads to the recruitment of two ubiquitin-like molecules, Atg8 (LC3) and Atg12. Atg12 is activated by Atg7 (E1-like conjugation enzyme) and Atg10 (E2-like conjugation enzyme).
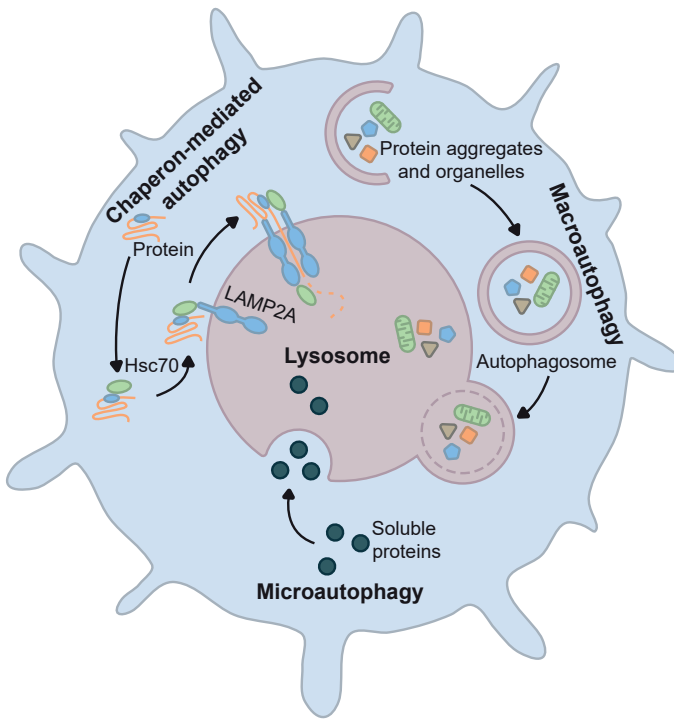
Figure 4. Autophagy pathways. Lysosomal degradation of cellular contents can involve three autophagy pathways, including macroautophagy, microautophagy, and chaperon-mediated autophagy. Protein aggregates or damaged organelles can be delivered to lysosomes via autophagosomes, a process called macroautophagy. Microautophagy involves engulfment of small amounts of cytoplasmic cargo into the lysosome. Chaperon-mediated autophagy utilizes heat-shock-cognate protein (Hsc70) and LAMP2A to translocate cytosolic proteins to the lysosome for degradation.

Activation of these conjugation systems leads to binding of Atg12 with Atg5, followed by binding of Atg16 to form the E3-like ligase of the LC3 conjugation system. LC3 is cleaved by Atg4 to LC3-I, which is then lipidated by Atg3 (E2-like conjugation enzyme) and Atg7 (E1-like conjugation enzyme) to generate phosphatidylethanolamine (PE)-conjugated LC3-II. LC3-II is incorporated into the phagophore membrane which serves as docking site of adaptor proteins. The closure of an elongated phagophore marks the formation of a mature autophagosome. LC3-II is commonly used as autophagosomal marker since it is binding covalently on newly formed autophagosomes until they fuse with lysosomes. Fusion of autophagosomes with lysosomes results in degradation of the cargo and Atg8 homologs coupled to the inner autophagosomal membrane.
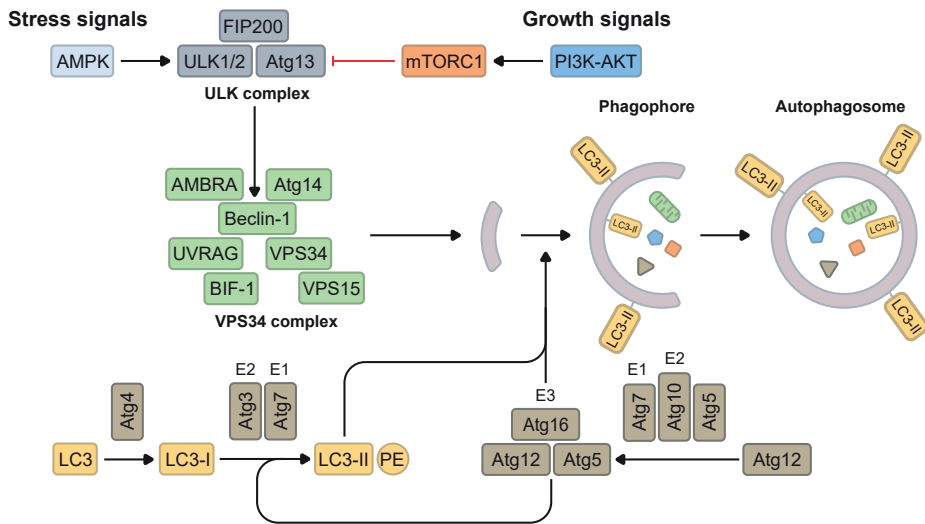
Figure 5. Formation of autophagosome. During starvation or other stress signals, mTORC1 is inactivated whereas AMPK is activated, which results in macroautophagy activation and the formation of autophagosomes. The ULK complex (ULK1/2, Atg13, FIP200) recruits the VPS34 complex (VPS34, VPS15, Beclin-1, AMBRA, Atg14, UVRAG, and BIF-1) which is required for nucleation of the phagophore membrane. The elongation and formation of autophagosomes involve the formation of two ubiquitin-like conjugation systems: Atg16 complex (Atg5, Atg12, and Atg16) and lipidation of Atg8 (LC3). For the formation of Atg16 complex, Atg12 is activated by Atg7 (E1-like conjugating enzyme) and transferred to Atg10 (E2-like conjugation enzyme) which further facilitates the formation of Atg12-Atg5, followed by binding of Atg16. The Atg16 complex is required for the lipidation of LC3. LC3 is first cleaved by Atg4 to LC3-I, which is then activated by Atg7 (E1-like conjugating enzyme) and transferred to Atg3 (E2-conjugating enzyme). The formation of Atg3-LC3-I facilitates the generation of PE-conjugated LC3-II, which is incorporated in the inner and outer membrane of autophagosomes. The closure of an elongated phagophore marks the formation of a mature autophagosome.

A role for macroautophagy has been suggested in intracellular antigen processing for MHCII presentation. Starvation-induced macroautophagy resulted in 50% increase of MHCII presentation of intracellular, cytosolic and nuclear antigens (105). DCs from mice which were Atg5 deficient showed impaired CD4+ T cell priming after herpes simplex virus infection, suggesting the autophagic machinery is required for optimal phagosome-to-lysosome fusion and subsequently processing of antigen for MHCII loading (106). A role for autophagy in extracellular antigen processing for MHCII presentation was observed *in vivo* where OVA was only efficiently processed and presented to CD4+ T cells in the presence of Atg5 (106). It has been suggested that LC3-associated phagocytosis (LAP) plays a role in endocytosis and degradation of extracellular material for efficient MHCII presentation (107, 108). During LAP the single phagosomal membrane recruits LC3 and LAMP phagosomes are either degraded in lysosomes, delayed in their fusion with lysosomes, or fused with compartments that contains PRRs, resulting in increased MHCII presentation of extracellular antigens (107-

110). The induction of LAP is dependent on receptor-mediated antigen uptake, and the attachment of LC3 to the phagosomes requires NOX2. However, LAP is independent of 'classical' macroautophagy proteins such as the Atg1 complex (111).

Several studies have provided evidence for enhancement of the classical MHCI antigen presentation pathway by autophagy. Reduced autophagic degradation of defective ribosomal products (DRiPs) was observed when HeLa cells were treated with the selective PI3K inhibitor 3-Methyladenine (3-MA), resulting in enhanced proteasome degradation and class I antigen presentation (112). During herpes simplex virus-1 (HSV-1) infection, it seems that macroautophagy contributes to antigen processing for efficient MHCI presentation of HSV-1 glycoprotein to CD8+ T cells in a proteasome dependent manner (113). On the contrary, infection with human cytomegalovirus (HCMV) induced autophagy and increased the presentation of HCMV latency-associated protein (pUL138) in a proteasome- and TAP-independent manner that involved MHCI loading in endosomal compartments (114). Several studies have investigated the role of autophagy in DC cross-presentation with contradictory results. Some showed elevated CD8+ T cell responses upon autophagy inhibition in DCs with different antigen targeting systems (115), while others showed autophagy-independent cross-presentation (106) or even lowered immune responses upon blocking autophagy (116, 117). In **chapter 6** we investigated the role of autophagy on long-term DC cross-presentation.

SCOPE OF THESIS

In this thesis we further investigate the underlying mechanisms of DC cross-presentation. Understanding and improving DC cross-presentation is key for the development of cancer vaccines to induce effective CTL responses. In **chapter 2**, we studied the sustained cross-presentation capacity of murine splenic DC subsets *in vivo* after antigen storage. The role of FcyRs and complement factor C1q in prolonged antigen cross-presentation will be described in **chapter 3**. In **chapter 4** we characterized the antigen storage compartments in DCs where antigen is preserved for long-term cross-presentation. By redirecting antigen targeting to MGL1 on DCs, we studied the antigen routing, processing, and cross-presentation outcome in DCs in **chapter 5**. In **chapter 6**, we will investigate how the autophagy machinery regulates long-term cross-presentation by DCs. Specific conjugation of fluorescent dyes to antigenic peptides to study DC uptake and routing was analyzed for cell biological properties, which will be discussed in **chapter 7**. Finally, in **chapter 8** the findings of this thesis are summarized and discussed.

REFERENCES

1. Kawai, T., and S. Akira. The role of pattern-recognition receptors in innate immunity: update on Toll-like receptors. *Nat. Immunol.* 2010. 11: 373–384.
2. Hoffmann, J., and S. Akira. Innate immunity. *Curr. Opin. Immunol.* 2013. 25: 1–3.
3. Melief, C. J. M. "License to kill" Reflects joint action of CD4 and CD8 T cells. *Clin. Cancer Res.* 2013. 19: 4295–4296.
4. Carbone, F. R., and M. J. Bevan. Class I-restricted processing and presentation of exogenous cell-associated antigen in vivo. *J. Exp. Med.* 1990. 171: 377–387.
5. Huang, A. Y., P. Golumbek, M. Ahmadzadeh, E. Jaffee, D. Pardoll, and H. Levitsky. Role of bone marrow-derived cells in presenting MHC class I-restricted tumor antigens. *Science* 1994. 264: 961–965.
6. Sigal, L. J., S. Crotty, R. Andino, and K. L. Rock. Cytotoxic T-cell immunity to virus-infected non-haematopoietic cells requires presentation of exogenous antigen. *Nature* 1999. 398: 77–80.
7. Cohn, L., and L. Delamarre. Dendritic cell-targeted vaccines. *Front. Immunol.* 2014. 5: 255.
8. Shen, L., L. J. Sigal, M. Boes, and K. L. Rock. Important role of cathepsin S in generating peptides for TAP-independent MHC class I crosspresentation in vivo. *Immunity* 2004. 21: 155–165.
9. Kovacsovics-Bankowski, M., and K. L. Rock. A phagosome-to-cytosol pathway for exogenous antigens presented on MHC class I molecules. *Science* 1995. 267: 243–246.
10. Ackerman, A. L., A. Giodini, and P. Cresswell. A Role for the Endoplasmic Reticulum Protein Retrotranslocation Machinery during Crosspresentation by Dendritic Cells. *Immunity* 2006. 25: 607–617.
11. Palmowski, M. J., U. Gileadi, M. Salio, A. Gallimore, M. Millrain, E. James, C. Addey, D. Scott, J. Dyson, E. Simpson, and V. Cerundolo. Role of Immunoproteasomes in Cross-Presentation. *J. Immunol.* 2006. 177: 983–990.
12. Saveanu, L., O. Carroll, M. Weimershaus, P. Guermonprez, E. Firat, V. Lindo, F. Greer, J. Davoust, R. Kratzer, S. R. Keller, G. Niedermann, and P. van Endert. IRAP Identifies an Endosomal Compartment Required for MHC Class I Cross-Presentation. *Science* 2009. 325: 213–217.
13. Lin, M. L., Y. Zhan, A. I. Proietto, S. Prato, L. L. Wu, W. R. Heath, J. A. Villadangos, and A. M. Lew. Selective suicide of cross-presenting CD8+ dendritic cells by cytochrome c injection shows functional heterogeneity within this subset. *Proc. Natl. Acad. Sci. U. S. A.* 2008. 105: 3029–3034.
14. Zehner, M., A. L. L. Marschall, E. Bos, J.-G. G. Schloetel, C. Kreer, D. Fehrenschild, A. Limmer, F. Ossendorp, T. Lang, A. J. J. Koster, S. Dübel, and S. Burgdorf. The Translocon Protein Sec61 Mediates Antigen Transport from Endosomes in the Cytosol for Cross-Presentation to CD8+ T Cells. *Immunity* 2015. 42: 850–863.
15. Grotzke, J. E., P. Kozik, J.-D. Morel, F. Impens, N. Pietrosemoli, P. Cresswell, S. Amigorena, and C. Demangel. Sec61 blockade by mycolactone inhibits antigen cross-presentation independently of endosome-to-cytosol export. *Proc. Natl. Acad. Sci. U. S. A.* 2017. 114: E5910–E5919.
16. Cebrian, I., G. Visentin, N. Blanchard, M. Jouve, A. Bobard, C. Moita, J. Enninga, L. F. Moita, S. Amigorena, and A. Savina. Sec22b regulates phagosomal maturation and antigen crosspresentation by dendritic cells. *Cell* 2011. 147: 1355–1368.
17. Alloatti, A., D. C. Rookhuizen, L. Joannas, J.-M. Carpier, S. Iborra, J. G. Magalhaes, N. Yatim, P. Kozik, D. Sancho, M. L. Albert, and S. Amigorena. Critical role for Sec22b-dependent antigen cross-presentation in antitumor immunity. *J. Exp. Med.* 2017. 214: 2231–2241.
18. Wu, S. J., Y. S. Niknafs, S. H. Kim, K. Oravecz-Wilson, C. Zajac, T. Toubai, Y. Sun, J. Prasad, D. Peltier, H. Fujiwara, I. Hedig, N. D. Mathewson, R. Khoriaty, D. Ginsburg, and P. Reddy. A Critical Analysis of the Role of SNARE Protein SEC22B in Antigen Cross-Presentation. *Cell Rep.* 2017. 19: 2645–2656.
19. Nunes-Hasler, P., S. Maschalidi, C. Lippens, C. Castelbou, S. Bouvet, D. Guido, F. Bermont, E. Y. Bassoy, N. Page, D. Merkler, S. Hugues, D. Martinvalet, B. Manoury, and N. Demaurex. STIM1 promotes migration, phagosomal maturation and antigen cross-presentation in dendritic cells. *Nat. Commun.* 2017. 8: 1852.
20. Maschalidi, S., P. Nunes-Hasler, C. R. Nascimento, I. Sallent, V. Lannoy, M. Garfa-Traore, N. Cagnard, F. E. Sepulveda, P. Vargas, A.-M. Lennon-Duménil, P. van Endert, T. Capiod, N. Demaurex, G. Darrasse-Jèze, and B. Manoury. UNC93B1 interacts with the calcium sensor STIM1 for efficient antigen cross-presentation in dendritic cells. *Nat. Commun.* 2017. 8: 1640.

1

21. Dingjan, I., D. R. Verboogen, L. M. Paardekooper, N. H. Revelo, S. P. Sittig, L. J. Visser, G. F. von Mollard, S. S. Henriet, C. G. Figdor, M. ter Beest, and G. van den Bogaart. Lipid peroxidation causes endosomal antigen release for cross-presentation. *Sci. Rep.* 2016. 24: 22064.

22. Savina, A., C. Jancic, S. Hugues, P. Guermonprez, P. Vargas, I. C. Moura, A.-M. M. Lennon-Duménil, M. C. Seabra, G. Raposo, and S. Amigorena. NOX2 Controls Phagosomal pH to Regulate Antigen Processing during Crosspresentation by Dendritic Cells. *Cell* 2006. 126: 205–218.

23. Jancic, C., A. Savina, C. Wasmeier, T. Tolmachova, J. El-Benna, P. M.-C. Dang, S. Pascolo, M.-A. Gougerot-Pocidalo, G. Raposo, M. C. Seabra, and S. Amigorena. Rab27a regulates phagosomal pH and NADPH oxidase recruitment to dendritic cell phagosomes. *Nat. Cell Biol.* 2007. 9: 367–378.

24. Van Montfoort, N., M. G. Camps, S. Khan, D. V. Filippov, J. J. Weterings, J. M. Griffith, H. J. Geuze, T. van Hall, J. S. Verbeek, C. J. Melief, and F. Ossendorp. Antigen storage compartments in mature dendritic cells facilitate prolonged cytotoxic T lymphocyte cross-priming capacity. *Proc. Natl. Acad. Sci. U. S. A.* 2009. 106: 6730–6735.

25. Henrickson, S. E., T. R. Mempel, I. B. Mazo, B. Liu, M. N. Artyomov, H. Zheng, A. Peixoto, M. P. Flynn, B. Senman, T. Junt, H. C. Wong, A. K. Chakraborty, and U. H. von Andrian. T cell sensing of antigen dose governs interactive behavior with dendritic cells and sets a threshold for T cell activation. *Nat. Immunol.* 2008. 9: 282–291.

26. Shortman, K., and Y.-J. Liu. Mouse and human dendritic cell subtypes. *Nat. Rev. Immunol.* 2002. 2: 151–161.

27. Mildner, A., and S. Jung. Development and Function of Dendritic Cell Subsets. *Immunity* 2014. 40: 642–656.

28. Shortman, K., and W. R. Heath. The CD8+ dendritic cell subset. *Immunol. Rev.* 2010. 234: 18–31.

29. Dudziak, D., A. O. Kamphorst, G. F. Heidkamp, V. R. Buchholz, C. Trumpfheller, S. Yamazaki, C. Cheong, K. Liu, H.-W. H.-W. H. W. Lee, G. P. Chae, R. M. Steinman, M. C. Nussenzweig, C. G. Park, R. M. Steinman, and M. C. Nussenzweig. Differential antigen processing by dendritic cell subsets in vivo. *Science* 2007. 315: 107–111.

30. den Haan, J. M. M., and M. J. Bevan. Constitutive versus activation-dependent cross-presentation of immune complexes by CD8(+) and CD8(-) dendritic cells in vivo. *J. Exp. Med.* 2002. 196: 817–827.

31. Kamphorst, A. O., P. Guermonprez, D. Dudziak, and M. C. Nussenzweig. Route of Antigen Uptake Differentially Impacts Presentation by Dendritic Cells and Activated Monocytes. *J. Immunol.* 2010. 185: 3426–3435.

32. Bedoui, S., P. G. Whitney, J. Waithman, L. Eidsmo, L. Wakim, I. Caminschi, R. S. Allan, M. Wojtasiak, K. Shortman, F. R. Carbone, A. G. Brooks, and W. R. Heath. Cross-presentation of viral and self antigens by skin-derived CD103+ dendritic cells. *Nat. Immunol.* 2009. 10: 488–495.

33. Desch, A. N., G. J. Randolph, K. Murphy, E. L. Gautier, R. M. Kedl, M. H. Lahoud, I. Caminschi, K. Shortman, P. M. Henson, and C. V Jakubzick. CD103+ pulmonary dendritic cells preferentially acquire and present apoptotic cell-associated antigen. *J. Exp. Med.* 2011. 208: 1789–1797.

34. Di Pucchio, T., B. Chatterjee, A. Smed-Sörensen, S. Clayton, A. Palazzo, M. Montes, Y. Xue, I. Mellman, J. Banchereau, and J. E. Connolly. Direct proteasome-independent cross-presentation of viral antigen by plasmacytoid dendritic cells on major histocompatibility complex class I. *Nat. Immunol.* 2008. 9: 551–557.

35. Mouries, J., G. Moron, G. Schlecht, N. Escriou, G. Dadaglio, and C. Leclerc. Plasmacytoid dendritic cells efficiently cross-prime naive T cells in vivo after TLR activation. *Blood* 2008. 112: 3713–3722.

36. GeurtsvanKessel, C. H., M. A. M. Willart, L. S. van Rijt, F. Muskens, M. Kool, C. Baas, K. Thielemans, C. Bennett, B. E. Clausen, H. C. Hoogsteden, A. D. M. E. Osterhaus, G. F. Rimmelzwaan, and B. N. Lambrecht. Clearance of influenza virus from the lung depends on migratory langerin+CD11b- but not plasmacytoid dendritic cells. *J. Exp. Med.* 2008. 205: 1621–1634.

37. Lee, H. K., M. Zamora, M. M. Linehan, N. Iijima, D. Gonzalez, A. Haberman, and A. Iwasaki. Differential roles of migratory and resident DCs in T cell priming after mucosal or skin HSV-1 infection. *J. Exp. Med.* 2009. 206: 359–370.

38. Moffat, J. M., E. Segura, G. Khoury, I. Caminschi, P. U. Cameron, S. R. Lewin, J. A. Villadangos, and J. D. Mintern. Targeting antigen to bone marrow stromal cell-2 expressed by conventional and plasmacytoid dendritic cells elicits efficient antigen presentation. *Eur. J. Immunol.* 2013. 43: 595–605.

39. Oberkampf, M., C. Guillery, J. Mouriès, P. Rosenbaum, C. Fayolle, A. Bobard, A. Savina, E. Ogier-Denis, J. Enninga, S. Amigorena, C. Leclerc, and G. Dadaglio. Mitochondrial reactive oxygen species regulate the induction of CD8+ T cells by plasmacytoid dendritic cells. *Nat. Commun.* 2018. 9: 2241.

40. Ziegler-Heitbrock, L., P. Ancuta, S. Crowe, M. Dalod, V. Grau, D. N. Hart, P. J. M. Leenen, Y.-J. Liu, G. MacPherson, G. J. Randolph, J. Scherberich, J. Schmitz, K. Shortman, S. Sozzani, H. Strobl, M. Zembala, J. M. Austyn, and M. B. Lutz. Nomenclature of monocytes and dendritic cells in blood. *Blood* 2010. 116: e74–e80.

41. Nizzoli, G., J. Krietsch, A. Weick, S. Steinfelder, F. Facciotti, P. Gruarin, A. Bianco, B. Steckel, M. Moro, M. Crosti, C. Romagnani, K. Stölzel, S. Torretta, L. Pignataro, C. Scheibenbogen, P. Neddermann, R. De Francesco, S. Abrignani, and J. Geginat. Human CD1c+ dendritic cells secrete high levels of IL-12 and potently prime cytotoxic T-cell responses. *Blood* 2013. 122: 932–942.

42. Nierkens, S., J. Tel, E. Janssen, and G. J. Adema. Antigen cross-presentation by dendritic cell subsets: One general or all sergeants? *Trends Immunol.* 2013. 34: 361–370.

43. Eickhoff, S., A. Brewitz, M. Y. Gerner, F. Klauschen, K. Komander, H. Hemmi, N. Garbi, T. Kaisho, R. N. Germain, and W. Kastenmüller. Robust Anti-viral Immunity Requires Multiple Distinct T Cell-Dendritic Cell Interactions. *Cell* 2015. 162: 1322–1337.

44. Hor, J. L., P. G. Whitney, A. Zaid, A. G. Brooks, W. R. Heath, and S. N. Mueller. Spatiotemporally Distinct Interactions with Dendritic Cell Subsets Facilitates CD4+ and CD8+ T Cell Activation to Localized Viral Infection. *Immunity* 2015. 43: 554–565.

45. Kitano, M., C. Yamazaki, A. Takumi, T. Ikeno, H. Hemmi, N. Takahashi, K. Shimizu, S. E. Fraser, K. Hoshino, T. Kaisho, and T. Okada. Imaging of the cross-presenting dendritic cell subsets in the skin-draining lymph node. *Proc. Natl. Acad. Sci. U. S. A.* 2016. 113: 1044–1049.

46. Borst, J., T. Ahrends, N. Bąbała, C. J. M. Melief, and W. Kastenmüller. CD4+ T cell help in cancer immunology and immunotherapy. *Nat. Rev. Immunol.* 2018. 18: 635–647.

47. Palucka, K., and J. Banchereau. Dendritic-Cell-Based Therapeutic Cancer Vaccines. *Immunity* 2013. 39: 38–48.

48. Bol, K. F., G. Schreibelt, W. R. Gerritsen, I. J. M. de Vries, and C. G. Figdor. Dendritic Cell-Based Immunotherapy: State of the Art and Beyond. *Clin. Cancer Res.* 2016. 22: 1897–1906.

49. Sprooten, J., J. Ceusters, A. Coosemans, P. Agostinis, S. De Vleeschouwer, L. Zitvogel, G. Kroemer, L. Galluzzi, and A. D. Garg. Trial watch: dendritic cell vaccination for cancer immunotherapy. *Oncoimmunology* 2019. 8: e1638212.

50. Mittal, D., M. M. Gubin, R. D. Schreiber, and M. J. Smyth. New insights into cancer immunoediting and its three component phases—elimination, equilibrium and escape. *Curr. Opin. Immunol.* 2014. 27: 16–25.

51. Melief, C. J. M. Cancer Immunotherapy by Dendritic Cells. *Immunity* 2008. 29: 372–383.

52. Melief, C. J. M., and S. H. van der Burg. Immunotherapy of established (pre)malignant disease by synthetic long peptide vaccines. *Nat. Rev. Cancer* 2008. 8: 351–360.

53. Schuurhuis, D. H., N. van Montfoort, A. Ioan-Facsinay, R. Jiawan, M. Camps, J. Nouta, C. J. M. Melief, J. S. Verbeek, and F. Ossendorp. Immune Complex-Loaded Dendritic Cells Are Superior to Soluble Immune Complexes as Antitumor Vaccine. *J. Immunol.* 2006. 176: 4573–4580.

54. Tacken, P. J., I. J. M. de Vries, K. Gijzen, B. Joosten, D. Wu, R. P. Rother, S. J. Faas, C. J. A. Punt, R. Torensma, G. J. Adema, and C. G. Figdor. Effective induction of naive and recall T-cell responses by targeting antigen to human dendritic cells via a humanized anti-DC-SIGN antibody. *Blood* 2005. 106: 1278–1285.

55. Trumpfheller, C., J. S. Finke, C. B. López, T. M. Moran, B. Moltedo, H. Soares, Y. Huang, S. J. Schlesinger, C. G. Park, M. C. Nussenzweig, A. Granelli-Piperno, and R. M. Steinman. Intensified and protective CD4 [+] T cell immunity in mice with anti–dendritic cell HIV gag fusion antibody vaccine. *J. Exp. Med.* 2006. 203: 607–617.

56. Sancho, D., D. Mourão-Sá, O. P. Joffre, O. Schulz, N. C. Rogers, D. J. Pennington, J. R. Carlyle, and C. R. Sousa. Tumor therapy in mice via antigen targeting to a novel, DC-restricted C-type lectin. *J. Clin. Invest.* 2008. 118: 2098–2110.

57. Mukhopadhaya, A., T. Hanafusa, I. Jarchum, Y.-G. Chen, Y. Iwai, D. V Serreze, R. M. Steinman, K. V Tarbell, and T. P. DiLorenzo. Selective delivery of beta cell antigen to dendritic cells in vivo leads to deletion and tolerance of autoreactive CD8+ T cells in NOD mice. *Proc. Natl. Acad. Sci. U. S. A.* 2008. 105: 6374–6379.

58. Dhodapkar, M. V., M. Sznol, B. Zhao, D. Wang, R. D. Carvajal, M. L. Keohan, E. Chuang, R. E. Sanborn, J. Lutzky, J. Powderly, H. Kluger, S. Tejwani, J. Green, V. Ramakrishna, A. Crocker, L. Vitale, M. Yellin, T. Davis, and T. Keler. Induction of antigen-specific immunity with a vaccine targeting NY-ESO-1 to the dendritic cell receptor DEC-205. *Sci. Transl. Med.* 2014. 6: 232ra51.

1

59. Khan, S., M. S. Bijker, J. J. Weterings, H. J. Tanke, G. J. Adema, T. van Hall, J. W. Drijfhout, C. J. M. Melief, H. S. Overkleeft, G. A. van der Marel, D. V. Filippov, S. H. van der Burg, and F. Ossendorp. Distinct Uptake Mechanisms but Similar Intracellular Processing of Two Different Toll-like Receptor Ligand-Peptide Conjugates in Dendritic Cells. *J. Biol. Chem.* 2007. 282: 21145–21159.

60. Zom, G. G., S. Khan, C. M. Britten, V. Sommandas, M. G. M. Camps, N. M. Loof, C. F. Budden, N. J. Meeuwenoord, D. V. Filippov, G. A. van der Marel, H. S. Overkleeft, C. J. M. Melief, and F. Ossendorp. Efficient induction of antitumor immunity by synthetic toll-like receptor ligand-peptide conjugates. *Cancer Immunol. Res.* 2014. 2: 756–764.

61. Schumacher, T. N., and R. D. Schreiber. Neoantigens in cancer immunotherapy. *Science* 2015. 348: 69–74.

62. Kalergis, A. M., and J. V. Ravetch. Inducing tumor immunity through the selective engagement of activating Fcγ receptors on dendritic cells. *J. Exp. Med.* 2002. 195: 1653–1659.

63. Rafiq, K., A. Bergtold, and R. Clynes. Immune complex-mediated antigen presentation induces tumor immunity. *J. Clin. Invest.* 2002. 110: 71–79.

64. Schuurhuis, D. H., A. Ioan-Facsinay, B. Nagelkerken, J. J. van Schip, C. Sedlik, C. J. M. Melief, J. S. Verbeek, and F. Ossendorp. Antigen-Antibody Immune Complexes Empower Dendritic Cells to Efficiently Prime Specific CD8 + CTL Responses In Vivo. *J. Immunol.* 2002. 168: 2240–2246.

65. Guilliams, M., P. Bruhns, Y. Saeys, H. Hammad, and B. N. Lambrecht. The function of Fcγ receptors in dendritic cells and macrophages. *Nat. Rev. Immunol.* 2014. 14: 94–108.

66. Ravetch, J. V., and R. A. Clynes. Divergent roles for Fc receptors and complement in vivo. *Annu. Rev. Immunol.* 1998. 16: 421–432.

67. Clynes, R., J. S. Maizes, R. Guinamard, M. Ono, T. Takai, and J. V Ravetch. Modulation of immune complex-induced inflammation in vivo by the coordinate expression of activation and inhibitory Fc receptors. *J. Exp. Med.* 1999. 189: 179–185.

68. van Montfoort, N., P. A. C. 't Hoen, S. M. Mangsbo, M. G. M. Camps, P. Boross, C. J. M. Melief, F. Ossendorp, and J. S. Verbeek. Fcγ Receptor IIb Strongly Regulates Fcγ Receptor-Facilitated T Cell Activation by Dendritic Cells. *J. Immunol.* 2012. 189: 92–101.

69. Bergtold, A., D. D. Desai, A. Gavhane, and R. Clynes. Cell Surface Recycling of Internalized Antigen Permits Dendritic Cell Priming of B Cells. *Immunity* 2005. 23: 503–514.

70. Yada, A., S. Ebihara, K. Matsumura, S. Endo, T. Maeda, A. Nakamura, K. Akiyama, S. Aiba, and T. Takai. Accelerated antigen presentation and elicitation of humoral response in vivo by FcγRIIB- and FcγRI/III-mediated immune complex uptake. *Cell. Immunol.* 2003. 225: 21–32.

71. Baker, K., T. Rath, W. I. Lencer, E. Fiebiger, and R. S. Blumberg. Cross-presentation of IgG-containing immune complexes. *Cell. Mol. Life Sci.* 2013. 70: 1319–1334.

72. Regnault, A., D. Lankar, V. Lacabanne, A. Rodriguez, C. Thery, M. Rescigno, T. Saito, S. Verbeek, C. Bonnerot, P. Ricciardi-Castagnoli, S. Amigorena, C. Théry, M. Rescigno, T. Saito, S. Verbeek, C. Bonnerot, P. Ricciardi-Castagnoli, and S. Amigorena. Fcgamma receptor-mediated induction of dendritic cell maturation and major histocompatibility complex class I-restricted antigen presentation after immune complex internalization. *J. Exp. Med.* 1999. 189: 371–380.

73. Naama, J. K., A. O. Hamilton, A. C. Yeung-Laiwah, and K. Whaley. Prevention of immune precipitation by purified classical pathway complement components. *Clin. Exp. Immunol.* 1984. 58: 486–492.

74. Walport, M. J. Complement. *N. Engl. J. Med.* 2001. 344: 1058–1066.

75. Walport, M. J., K. A. Davies, and M. Botto. C1q and Systemic Lupus Erythematosus. *Immunobiology* 1998. 199: 265–285.

76. Thielens, N. M., F. Tedesco, S. S. Bohlson, C. Gaboriaud, and A. J. Tenner. C1q: A fresh look upon an old molecule. *Mol. Immunol.* 2017. 89: 73–83.

77. Sellar, G. C., D. J. Blake, and K. B. Reid. Characterization and organization of the genes encoding the A-, B- and C-chains of human complement subcomponent C1q. The complete derived amino acid sequence of human C1q. *Biochem. J.* 1991. 274 (Pt 2): 481–490.

78. Diebolder, C. A., F. J. Beurskens, R. N. de Jong, R. I. Koning, K. Strumane, M. A. Lindorfer, M. Voorhorst, D. Ugurlar, S. Rosati, A. J. R. R. Heck, J. G. J. J. Van De Winkel, I. A. Wilson, A. J. Koster, R. P. Taylor, E. O. Saphire, D. R. Burton, J. Schuurman, P. Gros, and P. W. H. I. H. I. Parren. Complement is activated by IgG hexamers assembled at the cell surface. *Science* 2014. 343: 1260–1263.

79. Wang, G., R. N. de Jong, E. T. J. van den Bremer, F. J. J. Beurskens, A. F. F. Labrijn, D. Ugurlar, P. Gros, J. Schuurman, P. W. H. I. W. H. I. Parren, A. J. R. J. R. Heck, R. N. de Jong, E. T. J. van den Bremer, F. J. J. Beurskens, A. F. F. Labrijn, D. Ugurlar, P. Gros, J. Schuurman, P. W. H. I. W. H. I. Parren, and A. J. R. J. R. Heck. Molecular Basis of Assembly and Activation of Complement Component C1 in Complex with Immunoglobulin G1 and Antigen. *Mol. Cell* 2016. 63: 135–145.

1

80. Siegel, R. C., and V. N. Schumaker. Measurement of the association constants of the complexes formed between intact C1q or pepsin-treated C1q stalks and the unactivated or activated C1r2C1s2 tetramers. *Mol. Immunol.* 1983. 20: 53–66.

81. Daha, N. A., N. K. Banda, A. Roos, F. J. Beurskens, J. M. Bakker, M. R. Daha, and L. A. Trouw. Complement activation by (auto-) antibodies. *Mol. Immunol.* 2011. 48: 1656–1665.

82. Castellano, G., A. M. Woltman, A. J. Nauta, A. Roos, L. A. Trouw, M. A. Seelen, F. P. Schena, M. R. Daha, and C. Van Kooten. Maturation of dendritic cells abrogates C1q production in vivo and in vitro. *Blood* 2004. 103: 3813–3820.

83. Nash, J. T., P. R. Taylor, M. Botto, P. J. Norsworthy, K. A. Davies, and M. J. Walport. Immune complex processing in C1q-deficient mice. *Clin. Exp. Immunol.* 2001. 123: 196–202.

84. van Montfoort, N., J. M. H. de Jong, D. H. Schuurhuis, E. I. H. van der Voort, M. G. M. Camps, T. W. J. Huizinga, C. van Kooten, M. R. Daha, J. S. Verbeek, F. Ossendorp, and R. E. M. Toes. A Novel Role of Complement Factor C1q in Augmenting the Presentation of Antigen Captured in Immune Complexes to CD8 + T Lymphocytes. *J. Immunol.* 2007. 178: 7581–7586.

85. van Dinther, D., D. A. Stolk, R. van de Ven, Y. van Kooyk, T. D. de Gruijl, and J. M. M. den Haan. Targeting C-type lectin receptors: a high-carbohydrate diet for dendritic cells to improve cancer vaccines. *J. Leukoc. Biol.* 2017. 102: 1017–1034.

86. Bonifaz, L. C., D. P. Bonnyay, A. Charalambous, D. I. Darguste, S.-I. Fujii, H. Soares, M. K. Brimnes, B. Moltedo, T. M. Moran, and R. M. Steinman. In vivo targeting of antigens to maturing dendritic cells via the DEC-205 receptor improves T cell vaccination. *J. Exp. Med.* 2004. 199: 815–824.

87. Hawiger, D., K. Inaba, Y. Dorsett, M. Guo, K. Mahnke, M. Rivera, J. V Ravetch, R. M. Steinman, and M. C. Nussenzweig. Dendritic cells induce peripheral T cell unresponsiveness under steady state conditions in vivo. *J. Exp. Med.* 2001. 194: 769–779.

88. Caminschi, I., A. I. Proietto, F. Ahmet, S. Kitsoulis, J. Shin Teh, J. C. Y. Lo, A. Rizzitelli, L. Wu, D. Vremec, S. L. H. van Dommelen, I. K. Campbell, E. Maraskovsky, H. Braley, G. M. Davey, P. Mottram, N. van de Velde, K. Jensen, A. M. Lew, M. D. Wright, W. R. Heath, K. Shortman, and M. H. Lahoud. The dendritic cell subtype-restricted C-type lectin Clec9A is a target for vaccine enhancement. *Blood* 2008. 112: 3264–3273.

89. Chatterjee, B., A. Smed-Sorensen, L. Cohn, C. Chalouni, R. Vandlen, B.-C. Lee, J. Widger, T. Keler, L. Delamarre, and I. Mellman. Internalization and endosomal degradation of receptor-bound antigens regulate the efficiency of cross presentation by human dendritic cells. *Blood* 2012. 120: 2011–2020.

90. Aarnoudse, C. A., M. Bax, M. Sánchez-Hernández, J. J. García-Vallejo, and Y. van Kooyk. Glycan modification of the tumor antigen gp100 targets DC-SIGN to enhance dendritic cell induced antigen presentation to T cells. *Int. J. cancer* 2008. 122: 839–846.

91. Singh, S. K., J. Stephani, M. Schaefer, H. Kalay, J. J. García-Vallejo, J. den Haan, E. Saeland, T. Sparwasser, and Y. van Kooyk. Targeting glycan modified OVA to murine DC-SIGN transgenic dendritic cells enhances MHC class I and II presentation. *Mol. Immunol.* 2009. 47: 164–174.

92. Singh, S. K., I. Streng-Ouwehand, M. Litjens, H. Kalay, S. Burgdorf, E. Saeland, C. Kurts, W. W. Unger, and Y. van Kooyk. Design of neo-glycoconjugates that target the mannose receptor and enhance TLR-independent cross-presentation and Th1 polarization. *Eur. J. Immunol.* 2011. 41: 916–925.

93. Unger, W. W., C. T. Mayer, S. Engels, C. Hesse, M. Perdicchio, F. Puttur, I. Streng-Ouwehand, M. Litjens, H. Kalay, L. Berod, T. Sparwasser, and Y. van Kooyk. Antigen targeting to dendritic cells combined with transient regulatory T cell inhibition results in long-term tumor regression. *Oncoimmunology* 2015. 4: e970462.

94. Fehres, C. M., A. J. van Beelen, S. C. M. Bruijns, M. Ambrosini, H. Kalay, L. van Bloois, W. W. J. Unger, J. J. Garcia-Vallejo, G. Storm, T. D. de Gruijl, and Y. van Kooyk. In situ Delivery of Antigen to DC-SIGN(+) CD14(+) Dermal Dendritic Cells Results in Enhanced CD8(+) T-Cell Responses. *J. Invest. Dermatol.* 2015. 135: 2228–2236.

95. Higashi, N., K. Fujioka, K. Denda-Nagai, S. Hashimoto, S. Nagai, T. Sato, Y. Fujita, A. Morikawa, M. Tsuiji, M. Miyata-Takeuchi, Y. Sano, N. Suzuki, K. Yamamoto, K. Matsushima, and T. Irimura. The Macrophage C-type Lectin Specific for Galactose/ *N* -Acetylgalactosamine Is an Endocytic Receptor Expressed on Monocyte-derived Immature Dendritic Cells. *J. Biol. Chem.* 2002. 277: 20686–20693.

96. Suzuki, N., K. Yamamoto, S. Toyoshima, T. Osawa, and T. Irimura. Molecular cloning and expression of cDNA encoding human macrophage C-type lectin. Its unique carbohydrate binding specificity for Tn antigen. *J. Immunol.* 1996. 156: 128–135.

97. van Vliet, S. J., E. van Liempt, E. Saeland, C. A. Aarnoudse, B. Appelmelk, T. Irimura, T. B. H. Geijtenbeek, O. Blixt, R. Alvarez, I. van Die, and Y. van Kooyk. Carbohydrate profiling reveals a distinctive role for the C-type lectin MGL in the recognition of helminth parasites and tumor antigens by dendritic cells. *Int. Immunol.* 2005. 17: 661–669.

98. Singh, S. K., I. Streng-Ouwehand, M. Litjens, D. R. Weelij, J. J. García-Vallejo, S. J. van Vliet, E. Saeland, and Y. van Kooyk. Characterization of murine MGL1 and MGL2 C-type lectins: Distinct glycan specificities and tumor binding properties. *Mol. Immunol.* 2009. 46: 1249–1249.

99. Singh, S. K., I. Streng-Ouwehand, M. Litjens, H. Kalay, E. Saeland, and Y. van Kooyk. Tumour-associated glycan modifications of antigen enhance MGL2 dependent uptake and MHC class I restricted CD8 T cell responses. *Int. J. Cancer* 2011. 128: 1371–1383.

100. Freire, T., X. Zhang, E. Deriaud, C. Ganneau, S. Vichier-Guerre, E. Azria, O. Launay, R. Lo-Man, S. Bay, and C. Leclerc. Glycosidic Tn-based vaccines targeting dermal dendritic cells favor germinal center B-cell development and potent antibody response in the absence of adjuvant. *Blood* 2010. 116: 3526–3536.

101. Burgdorf, S., C. Schölz, A. Kautz, R. Tampé, and C. Kurts. Spatial and mechanistic separation of cross-presentation and endogenous antigen presentation. *Nat. Immunol.* 2008. 9: 558–566.

102. Murrow, L., and J. Debnath. Autophagy as a Stress-Response and Quality-Control Mechanism: Implications for Cell Injury and Human Disease. *Annu. Rev. Pathol. Mech. Dis.* 2013. 8: 105–137.

103. Münz, C. Autophagy proteins in antigen processing for presentation on MHC molecules. *Immunol. Rev.* 2016. 272: 17–27.

104. Mizushima, N., T. Yoshimori, and Y. Ohsumi. The Role of Atg Proteins in Autophagosome Formation. *Annu. Rev. Cell Dev. Biol.* 2011. 27: 107–132.

105. Dengjel, J., O. Schoor, R. Fischer, M. Reich, M. Kraus, M. Muller, K. Kreymborg, F. Altenberend, J. Brandenburg, H. Kalbacher, R. Brock, C. Driessen, H.-G. Rammensee, and S. Stevanovic. Autophagy promotes MHC class II presentation of peptides from intracellular source proteins. *Proc. Natl. Acad. Sci. U. S. A.* 2005. 102: 7922–7927.

106. Lee, H. K., L. M. Mattei, B. E. Steinberg, P. Alberts, Y. H. Lee, A. Chervonsky, N. Mizushima, S. Grinstein, and A. Iwasaki. In Vivo Requirement for Atg5 in Antigen Presentation by Dendritic Cells. *Immunity* 2010. 32: 227–239.

107. Sanjuan, M. A., C. P. Dillon, S. W. G. Tait, S. Moshiach, F. Dorsey, S. Connell, M. Komatsu, K. Tanaka, J. L. Cleveland, S. Withoff, and D. R. Green. Toll-like receptor signalling in macrophages links the autophagy pathway to phagocytosis. *Nature* 2007. 450: 1253–1257.

108. Romao, S., N. Gasser, A. C. Becker, B. Guhl, M. Bajagic, D. Vanoaica, U. Ziegler, J. Roesler, J. Dengjel, J. Reichenbach, and C. Münz. Autophagy proteins stabilize pathogen-containing phagosomes for prolonged MHC II antigen processing. *J. Cell Biol.* 2013. 203: 757–766.

109. Henault, J., J. Martinez, J. M. Riggs, J. Tian, P. Mehta, L. Clarke, M. Sasai, E. Latz, M. M. Brinkmann, A. Iwasaki, A. J. Coyle, R. Kolbeck, D. R. Green, and M. A. Sanjuan. Noncanonical autophagy is required for type I interferon secretion in response to DNA-immune complexes. *Immunity* 2012. 37: 986–997.

110. Ma, J., C. Becker, C. A. Lowell, and D. M. Underhill. Dectin-1-triggered Recruitment of Light Chain 3 Protein to Phagosomes Facilitates Major Histocompatibility Complex Class II Presentation of Fungal-derived Antigens. *J. Biol. Chem.* 2012. 287: 34149–34156.

111. Münz, C. Autophagy Beyond Intracellular MHC Class II Antigen Presentation. *Trends Immunol.* 2016. 37: 755–763.

112. Wenger, T., S. Terawaki, V. Camosseto, R. Abdelrassoul, A. Mies, N. Catalan, N. Claudio, G. Clavarino, A. de Gassart, F. de A. Rigotti, E. Gatti, and P. Pierre. Autophagy inhibition promotes defective neosynthesized proteins storage in ALIS, and induces redirection toward proteasome processing and MHCI-restricted presentation. *Autophagy* 2012. 8: 350–363.

113. English, L., M. Chemali, J. Duron, C. Rondeau, A. Laplante, D. Gingras, D. Alexander, D. Leib, C. Norbury, R. Lippé, and M. Desjardins. Autophagy enhances the presentation of endogenous viral antigens on MHC class I molecules during HSV-1 infection. *Nat. Immunol.* 2009. 10: 480–487.

114. Tey, S. K. S.-K., and R. Khanna. Autophagy mediates transporter associated with antigen processing- independent presentation of viral epitopes through MHC class I pathway. *Blood* 2012. 120: 994–1004.

115. Loi, M., A. Müller, K. Steinbach, J. Niven, R. Barreira da Silva, P. Paul, L. A. Ligeon, A. Caruso, R. A. Albrecht, A. C. Becker, N. Annaheim, H. Nowag, J. Dengjel, A. García-Sastre, D. Merkler, C. Münz, and M. Gannagé. Macroautophagy Proteins Control MHC Class I Levels on Dendritic Cells and Shape Anti-viral CD8+ T Cell Responses. *Cell Rep.* 2016. 15: 1076–1087.
116. Ravindran, R., N. Khan, H. I. Nakaya, S. Li, J. Loebbermann, M. S. Maddur, Y. Park, D. P. Jones, P. Chappert, J. Davoust, D. S. Weiss, H. W. Virgin, D. Ron, and B. Pulendran. Vaccine activation of the nutrient sensor GCN2 in dendritic cells enhances antigen presentation. *Science* 2014. 343: 313–317.
117. Mintern, J. D., C. Macri, W. J. Chin, S. E. Panozza, E. Segura, N. L. Patterson, P. Zeller, D. Bourges, S. Bedoui, P. J. Mcmillan, A. Idris, C. J. Nowell, A. Brown, K. J. Radford, A. P. R. Johnston, and J. A. Villadangos. Differential use of autophagy by primary dendritic cells specialized in cross-presentation. *Autophagy* 2015. 11: 906–917.

1

2
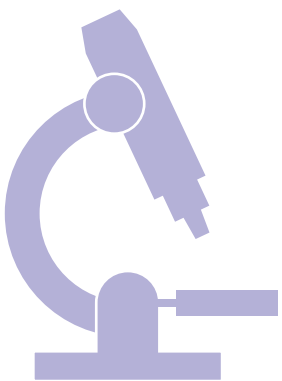
Sustained cross-presentation capacity of murine splenic dendritic cell subsets in vivo

Nataschja I. Ho, Marcel G. M. Camps, Edwin F. E. de Haas, Ferry Ossendorp

ABSTRACT

An exclusive feature of dendritic cells (DCs) is their ability to cross-present exogenous antigens in MHC class I molecules. We analyzed the fate of protein antigen in antigen presenting cell (APC) subsets after uptake of naturally formed antigen-antibody complexes *in vivo*. We observed that murine splenic DC subsets were able to present antigen *in vivo* for at least a week. After *ex vivo* isolation of four APC subsets, the presence of antigen in the storage compartments was visualized by confocal microscopy. Although all APC subsets stored antigen for many days, their ability and kinetics in antigen presentation was remarkably different. CD8α+ DCs showed sustained MHC class I-peptide specific CD8+ T cell activation for more than 4 days. CD8α- DCs also presented antigenic peptides in MHC class I but presentation decreased after 48 h. In contrast, only the CD8α- DCs were able to present antigen in MHC class II to specific CD4+ T cells. Plasmacytoid DCs and macrophages were unable to activate any of the two T cell types despite detectable antigen uptake. These results indicate that naturally occurring DC subsets have functional antigen storage capacity for prolonged T cell activation and have distinct roles in antigen presentation to specific T cells *in vivo*.

INTRODUCTION

Dendritic cells (DCs) are professional antigen presenting cells (APCs) that can capture, process and present exogenous antigen on MHC class I (MHCI) molecules. This cross-presentation pathway is considered to be a specialized function of DCs. We have previously demonstrated that the uptake of the protein antigen ovalbumin (OVA) bound to OVA-specific IgG antibodies, also called OVA immune complexes (OVA IC), by DCs is at least 100-fold more efficient than uptake of free OVA (1). This antibody-dependent uptake route of OVA IC results in DC maturation, specific CD8$^+$ T cell priming and tumor protection *in vivo* (2, 3). Moreover, we have reported that DCs can store OVA IC for many days in a lysosome-like organelle, distinct from MHC class II compartments or MHCI processing/ loading compartments. Despite the rapid turnover rate of MHCI-peptide complexes on the cell surface, this storage compartment serves as an antigen source for continuous supply of MHCI ligands and thereby enhancing sustained cross-presentation to CD8$^+$ T cells (1).

Lymphoid organs harbor different DC subsets *in vivo* and their role in antigen presentation have been studied extensively. The secondary lymphoid organs in mouse contain two main DC subtypes: plasmacytoid DCs (pDCs) and conventional DCs (cDCs). In murine spleen, resident cDCs can be further subdivided into CD8α$^+$ DCs and CD8α$^-$ DCs based on the expression of a wide variety of surface markers (4, 5). Although both cDC subsets have the ability to take up and present exogenous antigens on MHCI, CD8α$^+$ DCs are known for their specialized and much more efficient cross-presentation of cell-associated, antibody-bound, or soluble antigen to CD8$^+$ T cells *in vivo* and *ex vivo* (6–11). On the other hand, CD8α$^-$ DCs preferentially present antigen on MHCII to CD4$^+$ T cells to a greater extent than CD8α$^+$ DCs.

In the current study we injected mice sequentially with anti-OVA IgG and OVA to form OVA IC *in vivo*. We have previously demonstrated that this natural formation of antigen-IgG complexes *in vivo* leads to efficient antigen cross-presentation to CD8$^+$ T cells in which C1q plays an important role (12, 13). Four APC subsets from murine spleen were studied here: CD8α$^+$ DCs, CD8α$^-$ DCs, pDCs and macrophages. We show that all APC subsets were able to take up and store antigen for several days *in vivo*. However, their ability and kinetics in antigen presentation was remarkably different. CD8α$^+$ DCs showed more efficient MHCI cross-presentation to CD8$^+$ T cells for several days compared to CD8α$^-$ DCs. Only CD8α$^-$ DCs showed effective and prolonged MHCII presentation to CD4$^+$ T cells. Despite detectable uptake of antigen, pDCs and macrophages were incapable to activate T cells. Our results show for the first time that naturally occurring DC subsets have functional compartments to store antigen for prolonged T cell activation *in vivo* and each DC subset appears to play a distinct role in their antigen presentation function to specific T cells.

RESULTS

Long lasting MHCI and MHCII antigen presentation *in vivo*
We previously reported that DCs have the ability to conserve exogenous protein antigen for several days in intracellular antigen containing compartments which facilitate prolonged antigen cross-presentation to CD8^{+} T cells (1). This specialized function of DCs has primarily been shown using cultured dendritic cells *in vitro*. To analyze the capacity and duration of naturally occurring APC subsets to present antigen to CD8^{+} and CD4^{+} T cells *in vivo*, naïve C57BL/6 mice were first intravenously injected with OVA-specific IgG antibody and after a recovery period of 30 min followed by an i.v. injection of OVA protein antigen (Fig. 1A). Separate injection of antibody followed by antigen will allow natural formation of antigen-antibody immune complexes (IC). Antigen presentation *in vivo* was analyzed by injecting OVA-specific transgenic CD8^{+} and CD4^{+} T cells, OTI or OTII cells respectively, several time points after OVA antigen administration. Twenty-four hours after IgG and OVA injection strong CD8^{+} and CD4^{+} T cell proliferation was observed (Fig. 1B). Mice injected with only OVA did not activate either of the T cell subsets, underlining the efficiency of antibody-mediated targeting of soluble protein. Mice that received OTI cells 24 h after IgG and OVA injection showed ~90% T cell proliferation. This effect hardly diminished in time to ~80% after 4 days and even one week after IgG and OVA injection 30-40% of the CD8^{+} T cells still proliferated (Fig. 1C). The same we observed for OTII CD4^{+} T cell proliferation. Although the proliferation of CD4^{+} T cells decreased faster in time compared to CD8^{+} T cells, there was still some activity detected after 1 week. These results show that *in vivo* formed antigen-antibody complexes are efficiently presented to CD8^{+} and CD4^{+} T cells for at least a week suggesting that antigen is stored in APCs for many days.

Effective and sustained cytotoxic T cell killing capacity
Beside the prolonged antigen presentation *in vivo*, we determined whether these antigen-containing resident APCs were able to induce functional CD8^{+} T cells with killing capacity. C57BL/6 mice that have been injected with OVA specific antibody followed by OVA antigen received OTI T cell adoptive transfer after 48 h or 1 week (Fig. 2A). The induction of effector CD8^{+} T cells was determined by the decrease of CD127^{+} (IL-7Rα) and the increase of CD44^{+} expression on OTI T cells (data not shown). To determine whether these T cells were able to kill specific target cells *in vivo*, splenic target cells were loaded with OVA peptide or control peptide and injected in mice 4 days after OTI adoptive transfer. The next day, *in vivo* killing of target cells was analyzed in the spleen. Mice that received anti-OVA antibody and OVA, 48 h prior to the OTI adoptive transfer, showed near 80% specific killing and a higher percentage of OTI cells of total CD8^{+} T cells compared to mice that only received OVA (Fig. 2B). Mice that were injected with OTI cells 1 week after they first received anti-OVA antibody and OVA also

showed higher numbers of OTI cells with almost 60% specific killing of the target cells and no detectable killing in mice that only received soluble OVA (Fig. 2C). Similar results were found when *in vivo* killing of target cells was analyzed in the lymph nodes derived from the same mice (Supplemental Fig. 1).


2
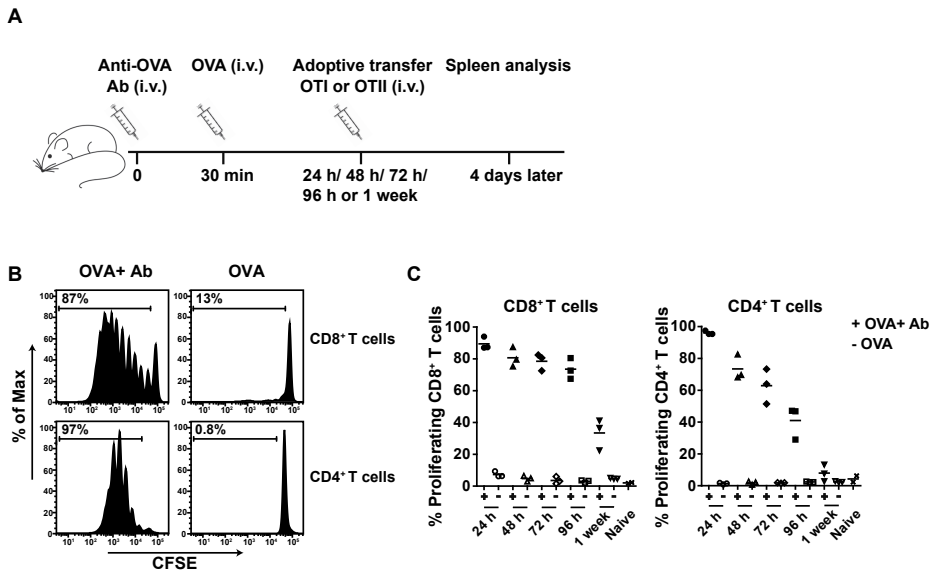
Figure 1. Sustained T cell proliferation *in vivo*. C57BL/6 (BL/6) mice were i.v. injected with anti-OVA IgG (Ab) followed by OVA i.v. injection 30 min later. At different time points mice were i.v. injected with CFSE-labeled spleen cells from OTI or OTII mice. Spleens were then collected after 4 days and analyzed by flow cytometry **(A)**. OTI (CD8+/ CD90.1+ cells) and OTII (CD4+/ CD45.1+ cells) proliferation analysis (percentages indicated) from the spleens of mice that received OVA and Ab or OVA only injections for 24 h **(B)**, and percentage proliferated T cells of three mice per group indicated for all time points (24 h/ 48 h/ 72 h/ 96 h/ 1 week) combined **(C)**. Flow cytometry data are from a single experiment with 3 mice per group, representative of two experiments.

APC subsets take up and store antigen for several days *in vivo*

We have previously shown that CD11c+ cells are crucially involved in antigen presentation of *in vivo* complexed antigen (12). Since we observed prolonged T cell activation, proliferation and killing capacity above, we set out to determine which APC subsets play a role in sustained antigen storage *in vivo*. Four subsets in the spleen of mice were distinguished by the following markers: CD8α+ DCs (CD11c^high CD8α+ CD11b-), CD8α- DCs (CD11c^high CD8α- CD11b+), pDCs (CD11c^int Ly6C- B220+) and macrophages (CD11c^int CD11b+ F4/80+) using flow cytometry (Fig. 3A). The major population is the macrophages (~3% of total spleen cells), followed by CD8α- DCs (~2%), CD8α+ DCs (~1%) and pDCs (<0.5%). Mice were injected sequentially with anti-OVA IgG antibody and Alexa Fluor 647 labeled OVA to track the uptake in the APC subsets.
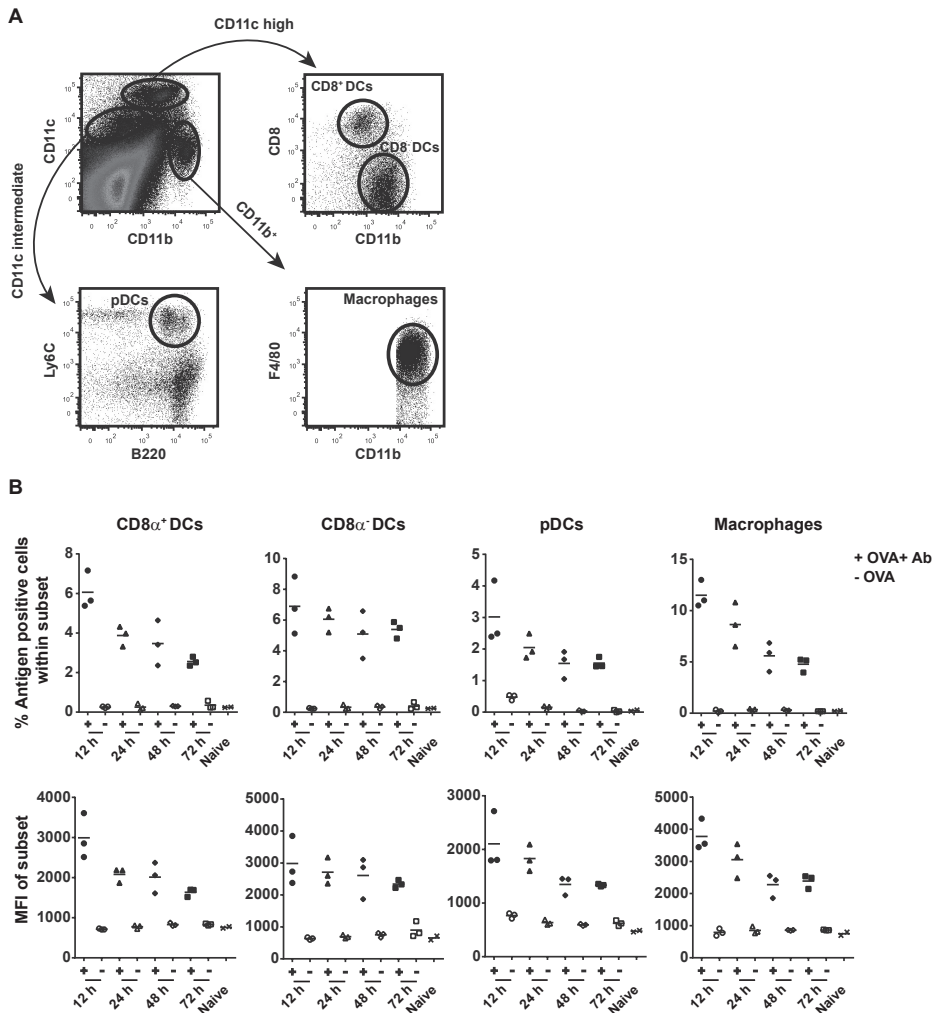
Approximately 6% of the CD8α⁺ DCs were antigen positive after 12 h of antibody and OVA injection (Fig. 3B upper panel, Supplemental Fig. 2A). This remains sustained in time up to 72 h where 2% antigen positive CD8α⁺ DCs were found in the spleen (Fig. 3B upper panel). A similar pattern of sustained antigen presence in time was found in the other APC subsets. Measuring the mean Alexa 647 fluorescence intensity (MFI) of the subsets showed less than 50% decrease from 12 h up to 72 h after antibody and OVA injection (Fig. 3B lower panel). Mice that only received OVA without antibody did not show any detectable uptake indicating the efficiency of antibody-mediated uptake of OVA (Fig. 3B, Supplemental Fig. 2A). Similar uptake with soluble OVA was only reached when 40 times more OVA was given compared to antibody-mediated uptake (data now shown).
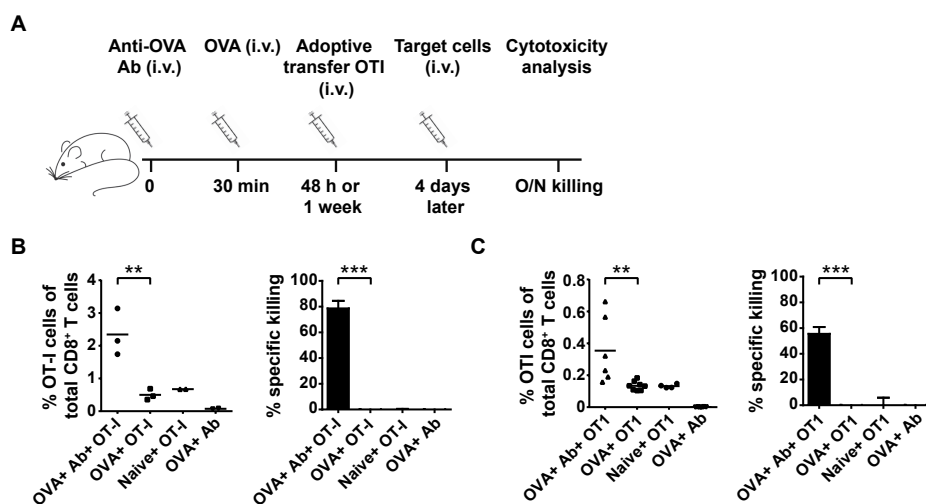
Figure 2. Sustained induction of cytotoxic T cell activity *in vivo*. BL/6 mice were injected i.v. with Ab followed 30 min later by OVA i.v. injection **(A)**. After 48 h **(B)** or 1 week **(C)**, mice received i.v. adoptive transfer of OTI cells, followed by target cells 4 days later. OTI cell (CD8⁺/ CD90.1⁺) proliferation and specific cytotoxic killing of target cells were measured overnight by spleen analysis. Data are from a single experiment representative of three experiments with each dot representing one mouse. **p < 0.01, ***p <0.001.

Using an irrelevant antibody against HPV E6 protein we observed no detectable antigen uptake by all APC subsets, indicating that antigen uptake is only achieved with the use of antigen specific antibodies (Supplemental Fig. 2B). To show that this highly efficient antibody-mediated antigen uptake was not due to the use of rabbit specific IgG, mice were prime-boost vaccinated with OVA protein to generate endogenous murine anti-OVA IgG antibodies (Supplemental Fig. 2C). Two weeks after the booster vaccination, seropositive mice were injected with OVA (Alexa Fluor 647 labeled) and efficient antigen uptake in all APC subsets

was detected (Supplemental Fig. 2D). Moreover, when serum from OVA-vaccinated mice, containing anti-OVA antibodies, was transferred to naïve mice followed by Alexa Fluor 647 labeled OVA injection, antigen uptake was detected in all APC subsets in contrast to control mice (Supplemental Fig. 2E).

Figure 3. Sustained antigen presence in APC subsets *in vivo*. Four splenic APC subsets in BL/6 mice were distinguished by the following markers in flow cytometry: CD8α+ DCs (CD11c^high CD8α+ CD11b-), CD8α- DCs (CD11c^high CD8α- CD11b+), pDCs (CD11c^int Ly6C- B220+) and macrophages (CD11c^int CD11b+ F4/80+) **(A)**. BL/6 mice were injected with Ab i.v. followed by OVA (Alexa Fluor 647 labeled) i.v. injection 30 min later. Antigen presence in spleens (each dot represents one mouse) was analyzed after 12 h/ 24 h/ 48 h/ 72 h, indicated by percentage positive cells and mean fluorescence intensity (MFI) of Alexa Fluor 647 **(B)**. Flow cytometry data are from a single experiment with 3 mice per group, representative of four independent experiments.

Next, we analyzed the presence of OVA protein in serum during our experiments. A possible explanation for the sustained antigen presence in APCs is that OVA protein is remaining in the circulation of the mice which may allow continuous uptake of fresh OVA by APCs over time. This is however an unlikely option since most of the single injection of OVA was cleared from the circulation already after 2 h and was non-detectable after 24 h (Supplemental Fig. 3). Taken together, these data demonstrate that APC subsets *in vivo* have the ability to efficiently engulf and store antigen in an antibody-dependent fashion for several days.

Antigen is stored in punctuated compartments in APC subsets *in vivo*

In order to visualize and localize where antigen was stored in APC subsets, all four subsets were sorted from the spleen at different time points after the injection of anti-OVA antibody and Alexa Fluor 647 labeled OVA and analyzed by confocal microscopy. An overlay of the fluorescence signal and differential interference contrast (DIC) observed in optical slices from the *ex vivo* isolated APC subsets show the location of antigen within the cells. After 12 h of antibody and OVA injection several intensely fluorescent punctuated "hotspots" were found in all APC subsets (Fig. 4). Co-staining with Lysotracker, a marker for endo-lysosomal compartments, showed partial co-localization with OVA indicating intracellular localization and storage of antigen in DCs in endo-lysosomal compartments (Supplemental Fig. 4), similar as we described previously for DCs *in vitro* (1). In general, the number of hotspots decreased in time in all four subsets but remained detectable even after 72 h. These results are in line with the MFI detection in figure 3B, indicating localized storage and gradual decrease of antigen in time in these APC subsets *in vivo*.

Sustained and selective MHC I and II antigen presentation by CD8α⁺ and CD8⁻ DCs

To address the question which APC subsets contributes to sustained antigen presentation to CD8⁺ and CD4⁺ T cells, mice were injected sequentially with anti-OVA antibody and OVA. At different time points four APC subsets were separately sorted from the spleen, as described before, and incubated *ex vivo* with either CD8⁺ OTI or CD4⁺ OTII cells. Both CD8α⁺ DCs and CD8α⁻ DCs cross-presented antigen to OTI cells, with CD8α⁺ DCs being the most potent cross-presenting subset (Fig. 5A). On the other hand, CD8α⁻ DCs were the only subset that could present antigen to OTII cells. All four subsets that were isolated from spleens of mice that were injected with the same dose of soluble OVA protein did not show any detectable antigen presentation to either OTI or OTII cells. Following the CD8α⁺ DC subset in time showed their sustained capacity to cross-present antigen to OTI cells: 40% OTI cells proliferated upon encountering CD8α⁺ DCs that had stored antigen for 96 h (Fig. 5B). Although the CD8α⁻ DCs were able to cross-present antigen, it was in a lesser extent compared to the CD8α⁺ DCs, e.g. only 10% OTI cells proliferated after being exposed to CD8α⁻ DCs that had stored antigen for 72 h. However, the CD8α⁻ DCs showed potent and
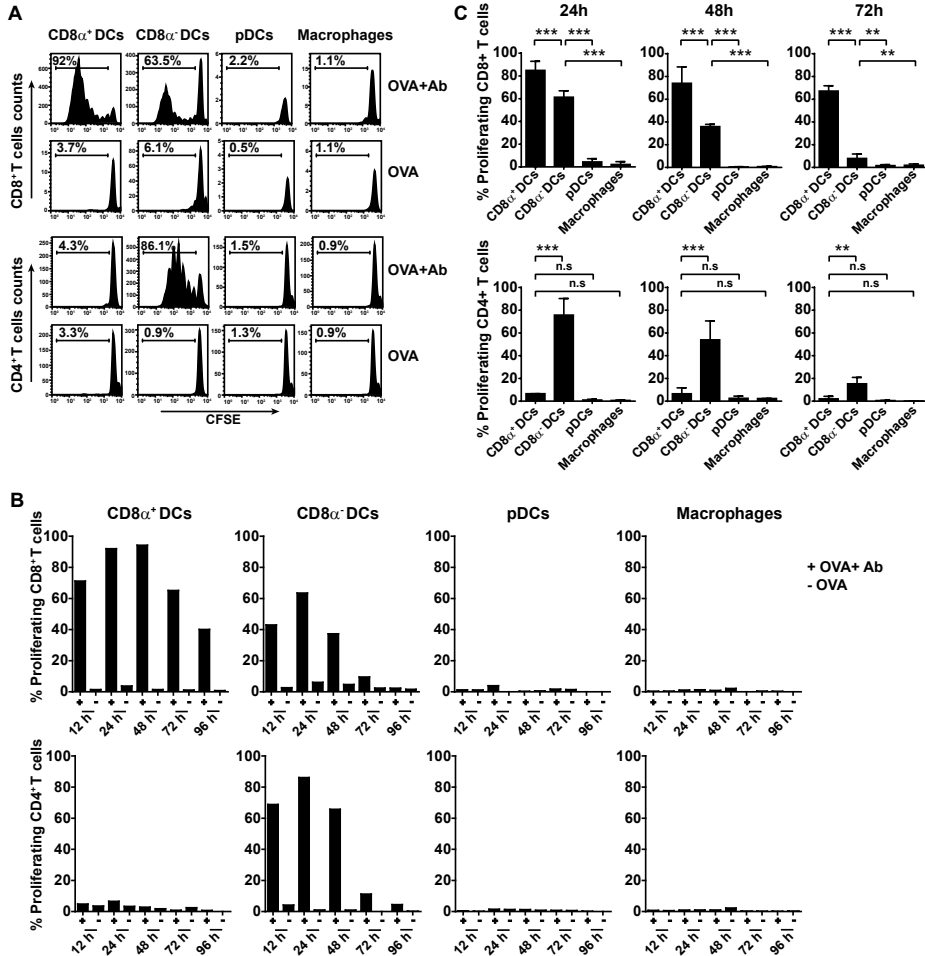
sustained antigen presentation to OTII T cells up to 72 h, whereas the CD8α+ DCs failed to do so at any time point. In contrast, the pDCs and macrophages could not present antigen to either OTI or OTII cells in any extent.
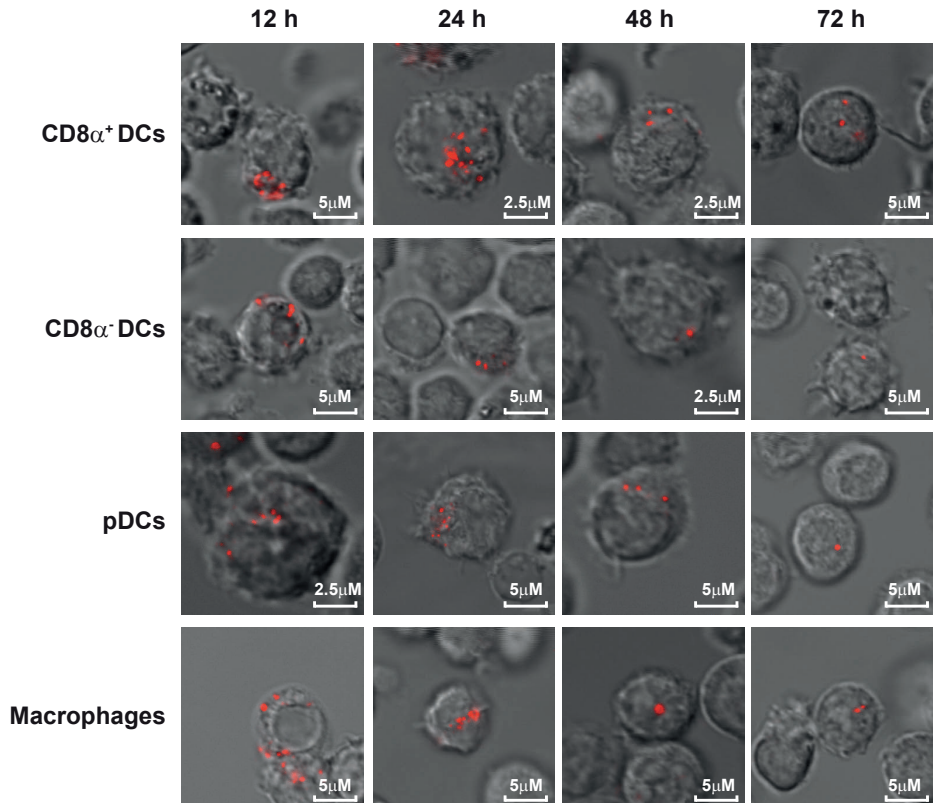
Figure 4. Localization of antigen storage in APC subsets *in vivo*. BL/6 mice were injected with Ab i.v. followed by OVA (Alexa Fluor 647 labeled) injection after 30 min. Four APC subsets were sorted at different time points according to the markers described in Fig. 3A and antigen presence in live cells was visualized by confocal microscopy. Data are from a single experiment representative of three experiments with 2 mice per experiment.

Figure 5C shows significant higher antigen cross-presentation ability of CD8α+ DCs compared to other APC subsets which was most pronounced after 72 h. The CD8α- DCs was the only subset showing significant and sustained antigen presentation to CD4+ T cells (Fig. 5C). In order to investigate whether the differences found in antigen presentation ability of the four subsets were due to the lack of MHCI or MHCII expression on their cell surface, spleens from naïve mice were sorted and loaded with antigenic peptides (Supplemental Fig. 5). All four subsets that were loaded with the MHCI binding peptide OVA8 were fully competent to activate OTI cells. The APC subsets that were loaded with the MHCII binding T helper peptide OVA17

were also able to present in MHCII to OTII cells, although the pDCs and macrophages in a lower degree. Taken together, these data show that all four APC subsets take up and store antigen for several days, but there is a clear functional distinction in their antigen presentation ability.

Figure 5. Sustained and selective antigen presentation by splenic CD8α⁺ and CD8α⁻ DCs. BL/6 mice (two mice per group) were injected with Ab followed by OVA i.v. injection 30 min later. At different time points (12 h/ 24 h/ 48 h/ 72 h and 96 h), splenic APC subsets were isolated of individual mice by FACS sorting according to the markers described in Fig. 3A and incubated with CFSE-labeled OTI (CD8⁺/ CD90.1⁺) or OTII (CD4⁺/ CD45.1⁺) cells *ex vivo* for 3 days. CD8⁺ T cell and CD4⁺ T cell proliferation by APC subsets was measured in mice that received OVA and Ab or only OVA for 24 h, indicated by the percentage of divided T cells **(A)**. Percentage of CD8⁺ T cell and CD4⁺ T cell proliferation activated by APC subsets at all time points is shown from one representative experiment out of 3 performed **(B)**. Average proliferation data of 3 independent experiments showing MHCI cross-presentation (upper panel) and MHCII antigen presentation (lower panel) by each APC subset after 24 h, 48 h and 72 h **(C)**. **p < 0.01, ***p <0.001, n.s: non-significant.

DISCUSSION

DCs are a heterogeneous cell population *in vivo* where each subset has different capacities in antigen-presentation. We have previously reported that DCs can conserve exogenous protein antigen in a storage organelle, distinct from MHC class II compartments or MHCI processing/ loading compartments, for several days that corresponds with sustained CTL cross-priming *in vivo* (1). In the current study we further investigate the antigen storage and presentation abilities of APC subsets (CD8α+ DCs, CD8α- DCs, pDCs and macrophages) *in vivo*. In contrast to most studies that used *in vitro* preformed Ag-Ab immune complexes (IC), we sequentially injected mice with antibody followed by cognate protein antigen (i.v.) to allow natural formation of IC in circulation. We show here for the first time that all APC subsets take up antigen and have the ability to store antigen for several days *in vivo*. This corresponds with long-lasting *in vivo* antigen presentation to CD8+ and CD4+ T cells and effective cytotoxic T cell killing of target cells up to a week after antigen injection. From all APC subsets, CD8α+ DCs were superior in antigen cross-presentation and showed sustained CD8+ T-cell activation after isolation. On the other hand, only CD8α- DCs were able to present antigen to CD4+ T cells several days after antigen injection. These results are in line with other studies that show distinct antigen presentation capacities by CD8α+ DCs and CD8α- DCs to T cells (6, 7, 9–11). It has been suggested that cross-presentation by CD8α- DCs depends on activating Fcγ receptors (FcγRs), since MHCI antigen presentation by CD8α- DCs was hampered in γ-chain-deficient mice (8). Cross-presentation by CD8α+ DCs from γ-chain-deficient mice remained intact, indicating that activation of CD8α+ DCs is not necessary for efficient cross-presentation. However, we have recently shown that complement factor C1q, and not FcγRs, plays a major role in antibody-mediated antigen uptake from blood circulation and presentation by APCs *in vivo* (13). Mice lacking C1q showed no detectable antigen uptake in APCs and strongly reduced antigen presentation to CD8+ or CD4+ T cells.

Despite that pDCs and macrophages take up antigen, we showed no detectable antigen presentation to T cells. Both pDCs and macrophages have been described as poor antigen cross-presenting APCs compared to cDCs (14–20). Several studies have addressed the contribution of pDCs in cross-priming of CD8+ T cells with different infection models since pDCs are unique in their ability to produce large amounts of type I interferons (IFN I) upon viral infections, however no specific role for pDCs was found in MHCI cross-presentation (21, 22). pDCs probably play a more important role in endogenous viral infections or there still might be unidentified specific antigen targeting routes that can induce the cross-presentation ability of pDCs. Macrophages mostly function as the first line of defense against pathogens by its rapid particle and immune complex removal and degradation abilities. One study showed that macrophages were able to prime naïve T cells *in vivo* by using 10-fold more antigen compared with DCs (23). Based on our data we however feel that macrophages

2

are far less effective in T cell priming than DCs. Although it has been suggested that macrophages have more acidic endosomal environments with many lysosomal proteases that results in faster antigen degradation compared to DCs (24, 25), we could still detect similar amounts of stored protein antigen in splenic macrophages compared to other DC subsets 3 days after antigen and antibody injection. Moreover, others have shown that the antigen uptake capacity does not determine cross-presentation efficiency in APC subsets (11). Therefore, it is more likely that, at least in this targeting system, other mechanisms located downstream from antigen uptake and storage determine the cross-presentation outcome of APC subsets.

We have previously demonstrated that the processing of antigen from the storage organelle in DCs involves a cytosolic and TAP-dependent pathway since inhibiting proteasomal activity or using TAP deficient DCs almost completely inhibits MHCI cross-presentation (1). Therefore, it is presumable that antigens from the storage compartment are degraded by the proteasome in the cell cytosol and loaded on MHCI in the ER, although it is not excluded that peptides, after proteasome degradation, are transported back into endocytic compartments where they are trimmed by IRAP and loaded on MHCI as reported by Van Endert and colleagues (26). It is still unclear how antigens are transferred from endosomes into the cytosol for proteasomal degradation. One study used exogenous cytochrome c, which induces apoptosis upon release in the cell cytosol, to show that CD8+ DCs was the major DC subset reduced by the treatment *in vivo* (27). These data suggest that CD8+ DCs possess a highly efficient mechanism for endosome-to-cytosol transport compared to other APC subsets. Some reports suggested Sec61 as the translocator for endosome-to-cytosol transport of antigens for DC cross-presentation to CD8+ T cells (28, 29), however a more recent study showed the opposite (30). Others showed that by silencing Sec22b, an ER-resident SNARE, cross-presentation by DCs is impaired due to antigen transfer inhibition from phagosomes to the cytosol (31). Nevertheless, it is still not clear which specific translocator on DC endosomal membranes regulate antigen transportation from endosomes to the cytosol. Characterizing translocator function might give better insight into the different cross-presentation outcome of APC subsets.

We have shown previously that cell surface MHCI on DCs have a shorter turnover rate compared to MHCII (1). Most MHCI-peptide complexes disappear from the cell surface within 24 h. Since the migration of DCs after antigen encountering to the T cell zones might take up to several days, this high turnover rate of MHCI is not beneficial for efficient CD8+ T cell cross-presentation (32). Also, the dose of antigen that is expressed on MHCI needs to exceed the required threshold for effective T cell activation. Therefore, long term antigen storage in DCs and sustained antigen display on the DC cell-surface is important to ensure T cell cross-priming. Several reports have shown that DCs *in vivo* have relative rapid turnover rates (33–35). It has been suggested that cDCs in mouse spleen undergo faster turnover and

have a shorter lifespan than pDCs, approximately a half-life of 2 days and 8 days respectively. Some studies suggest that rapid turnover of cDCs favors the engulfment by other DCs which facilitate antigen processing and presentation (36, 37). In regard to our observations of sustained in vivo antigen presentation of splenic APCs, the significance of different lifespans of APC subsets may also contribute to modulation of immune control.

In conclusion, we show here for the first time that *in vivo* DC subsets can store antigen for several days in storage compartments and that this contributes to sustained and selective antigen cross-presentation to CD8+ and CD4+ T cells. Further characterization of the downstream antigen processing pathways within each APC subset may reveal why specific subsets are superior in MHCI cross-presentation or MHCII antigen presentation.

2

MATERIALS AND METHODS

Mice
All animal experiments in this paper have been approved by the review board of Leiden University Medical Center. C57BL/6 mice were purchased from Charles River Laboratories. CD45.1 congenic mice on C57BL/6 background, OTI mice (CD8+ T cell transgenic mice expressing a TCR recognizing the OVA derived K^b associated epitope SIINFEKL) and OTII mice (CD4+ T cell transgenic mice expressing a TCR recognizing the OVA derived Th epitope ISQAVHAAHAEINEAGR in association with I A^b) were bred and kept at the LUMC animal facility under SPF conditions. All mice were used at 8-12 weeks of age.

In vivo formed OVA-IgG complexes
C57BL/6 mice were intravenously injected with 100 µg polyclonal rabbit anti-OVA IgG (ICN Biomedicals). After 30 min of antibody circulation, mice were injected intravenously with 5 µg Ovalbumin (OVA, Worthington Biochemical Corporation) or OVA conjugated with Alexa Fluor 647 (Life Technologies). As control antibody, polyclonal rabbit anti-human papilloma virus (HPV) E6 IgG were generated in our lab by vaccinating New Zealand rabbits with recombinant E6 protein.

T cell proliferation *in vivo*
Recipient mice received intravenously CFSE-labeled spleen cells from OTI or OTII mice (purified with CD8 and CD4 T lymphocyte enrichment kit respectively, BD Biosciences). After 4 days, spleens from the recipient mice were collected and proliferation of CFSE- labeled T lymphocytes was analyzed by flow cytometry. OTI cells were gated as CD8+/ CD90.1+ cells. OTII cells were gated as CD4+/ CD45.1+ cells.

In vivo cytotoxicity assay

C57BL/6 mice were injected with anti-OVA antibody and OVA to form OVA-IgG complexes *in vivo* as described before or only with OVA. After different time points mice received spleen cells from OTI mice (CD8$^+$ T cell enriched) intravenously. 4 days later Ly5.1$^+$ splenocytes were used as target cells. The target cells were labeled with 5 μmol/L CFSE and pulsed with OVA peptide SIINFEKL (0.5μg/ml, 1 h at 37°C), or labeled with 0.5 μmol/L CFSE and pulsed with the control D^b- binding flu-peptide ASNENMDAM (1μg/ml, 1 h at 37°C). The target cells were mixed 1:1 ratio and injected intravenously. Spleen cells and lymph nodes were isolated the next day and the number of specific CFSE^{high} and control CFSE^{lo} Ly5.1$^+$ were measured by flow cytometry. CD8$^+$/ CD90.1$^+$ OTI cells were stained for effector T cell markers CD127 and CD44. The percentage of specific killing is calculated as follows: (1-(ratio injected mice/ ratio background mice)) x 100%. Ratio is defined by the number of SIINFEKL CFSE^{high} target cells/ number of control CFSE^{lo} target cells. Background mice are C57BL/6 mice injected with only OTI cells.

Ex vivo antigen presentation

Spleens from C57BL/6 mice with *in vivo* formed OVA-IgG complexes or only OVA were isolated at different time points. APC subsets sorting was performed on BD FACSAria II SORP (BD Biosciences). The purity of each subset after the sort was determined by flow cytometry: CD8α$^+$ DCs (86%), CD8α$^-$ DCs (81%), pDCs (50%) and macrophages (67%). Contaminations by other subsets were less than 1%. Each APC subset (50.000 cells) was incubated with CFSE labeled and purified OTI (50.000) or OTII cells (50.000) in a 96 well round bottom plate. CD8$^+$ and CD4$^+$ T cell proliferation was measured after 4 days by flow cytometry. Minimal peptide loading controls were performed with APC subsets from naïve C57BL/6 mice. After isolation, each subset was incubated with 100 pg/ml OVA8 (SIINFEKL) or 1 μg/ml OVA17 (ISQAVHAAHAEINEAGR) for 1 h and washed extensively afterwards. Each subset was then incubated with either CFSE labeled OTI or OTII cells and T cell proliferation was measured by flow cytometry 3 days later.

Antigen presence in splenic APC subsets

C57BL/6 mice with *in vivo* formed OVA-IgG complexes or only OVA (Alexa Fluor 647 labeled, Life Technologies) were sacrificed at different time points. Spleens were isolated and dissociated with Liberase (Thermolysin Low, research grade, Roche) for 20 min at 37°C. The antigen presence was measured by the percentage of Alexa Fluor 647 positive cells and the mean fluorescence intensity (MFI) within each APC subset. Background levels were determined by naïve mice without any injections.

In addition, antigen presence in splenic APC subsets was visualized by confocal scanning laser microscopy. APC subsets sorting was performed as described before and sorted cells

were incubated for 30 min with Lysotracker (Green DND-26, ThermoFisher) at 37°C, washed and transferred to glass bottom dishes (MatTek corporation, Ashland, USA). Live cells were imaged using Leica SP5 STED confocal microscope with a 63x objective lens. Differential interference contrast (DIC) was additionally used to image cell contrast. Images were acquired by taking optical slices in 10x magnification and were processed with Leica LAS AF software. Co-localization was measured by a line scan drawn on a single optical slice and plotted in histograms. Each arrow indicates co-localization between OVA and Lysotracker.

Ovalbumin specific mouse IgG generation and transfer

C57BL/6 mice were injected s.c. with 100 µg OVA emulsified in Incomplete Freund's Adjuvant (IFA) and boosted 2 weeks later with 100 µg OVA in IFA. After two weeks, blood was withdrawn from the lateral tail vein and the presence of mouse anti-OVA IgG was determined by ELISA. Seropositive C57BL/6 mice were injected i.v. with 5 µg OVA (Alexa Fluor 647 labeled) and spleen APCs were analyzed 24 h later for the presence of fluorescent OVA by flow cytometry. Furthermore, sera from OVA seropositive C57BL/6 mice were collected and transferred i.v. into naïve C57BL/6 mice followed by i.v. injection of 5 µg OVA (Alexa Fluor 647 labeled). The presence of fluorescent OVA was measured 24 h later in spleen APCs by flow cytometry.

Quantification of ovalbumin in mouse serum

Naïve C57BL/6 mice were injected i.v. with 100 µg polyclonal rabbit anti-OVA IgG. After 30 min, mice were injected i.v. with 5 µg OVA (Alexa Fluor 647 labeled). At indicated time points 50 µl blood was withdrawn from the lateral tail vein and serum was collected. Five µl serum was mixed with sample buffer, heated at 95°C for 5 min and loaded on SDS/PAGE. Fluorescent OVA was quantified directly from the SDS/PAGE gels by using a Typhoon 9410 Variable mode imager (GE Healthcare Bio-Sciences) and ImageQuant TL v8.1 software (GE Healthcare Life Sciences), indicated by relative pixel intensity.

Statistical analysis

Statistical analysis was performed using one-way analysis of variance (ANOVA) test. Tukey's *post hoc* test was performed to correct for multiple comparisons. The following indications are used in all figures: $*p < 0.05$, $**p < 0.01$, $***p < 0.001$, n.s: non-significant.

ACKNOWLEDGEMENTS

REFERENCES

1. Van Montfoort, N., M. G. Camps, S. Khan, D. V. Filippov, J. J. Weterings, J. M. Griffith, H. J. Geuze, T. van Hall, J. S. Verbeek, C. J. Melief, and F. Ossendorp. Antigen storage compartments in mature dendritic cells facilitate prolonged cytotoxic T lymphocyte cross-priming capacity. *Proc. Natl. Acad. Sci. U. S. A.* 2009. 106: 6730–6735.
2. Regnault, A., D. Lankar, V. Lacabanne, A. Rodriguez, C. Thery, M. Rescigno, T. Saito, S. Verbeek, C. Bonnerot, P. Ricciardi-Castagnoli, S. Amigorena, C. Théry, M. Rescigno, T. Saito, S. Verbeek, C. Bonnerot, P. Ricciardi-Castagnoli, and S. Amigorena. Fcgamma receptor-mediated induction of dendritic cell maturation and major histocompatibility complex class I-restricted antigen presentation after immune complex internalization. *J. Exp. Med.* 1999. 189: 371–380.
3. Schuurhuis, D. H., A. Ioan-Facsinay, B. Nagelkerken, J. J. van Schip, C. Sedlik, C. J. M. Melief, J. S. Verbeek, and F. Ossendorp. Antigen-Antibody Immune Complexes Empower Dendritic Cells to Efficiently Prime Specific CD8 + CTL Responses In Vivo. *J. Immunol.* 2002. 168: 2240–2246.
4. Villadangos, J. a, and P. Schnorrer. Intrinsic and cooperative antigen-presenting functions of dendritic-cell subsets in vivo. *Nat. Rev. Immunol.* 2007. 7: 543–555.
5. Hey, Y. Y., and H. C. O'Neill. Murine spleen contains a diversity of myeloid and dendritic cells distinct in antigen presenting function. *J. Cell. Mol. Med.* 2012. 16: 2611–2619.
6. den Haan, J. M., S. M. Lehar, and M. J. Bevan. CD8(+) but not CD8(-) dendritic cells cross-prime cytotoxic T cells in vivo. *J. Exp. Med.* 2000. 192: 1685–1696.
7. Pooley, J. L., W. R. Heath, and K. Shortman. Cutting edge: intravenous soluble antigen is presented to CD4 T cells by CD8- dendritic cells, but cross-presented to CD8 T cells by CD8+ dendritic cells. *J. Immunol.* 2001. 166: 5327–5330.
8. den Haan, J. M. M., and M. J. Bevan. Constitutive versus activation-dependent cross-presentation of immune complexes by CD8(+) and CD8(-) dendritic cells in vivo. *J. Exp. Med.* 2002. 196: 817–827.
9. Dudziak, D., A. O. Kamphorst, G. F. Heidkamp, V. R. Buchholz, C. Trumpfheller, S. Yamazaki, C. Cheong, K. Liu, H.-W. H.-W. H. W. Lee, G. P. Chae, R. M. Steinman, M. C. Nussenzweig, C. G. Park, R. M. Steinman, and M. C. Nussenzweig. Differential antigen processing by dendritic cell subsets in vivo. *Science* 2007. 315: 107–111.
10. Hildner, K., B. T. Edelson, W. E. Purtha, M. S. Diamond, H. Matsushita, M. Kohyama, B. Calderon, B. U. Schraml, E. R. Unanue, M. S. Diamond, R. D. Schreiber, T. L. Murphy, and K. M. Murphy. Batf3 deficiency reveals a critical role for CD8α+ dendritic cells in cytotoxic T cell immunity. *Science* 2008. 322: 1097–1100.
11. Schnorrer, P., G. M. N. Behrens, N. S. Wilson, J. L. Pooley, C. M. Smith, D. El-Sukkari, G. Davey, F. Kupresanin, M. Li, E. Maraskovsky, G. T. Belz, F. R. Carbone, K. Shortman, W. R. Heath, and J. A. Villadangos. The dominant role of CD8+ dendritic cells in cross-presentation is not dictated by antigen capture. *Proc. Natl. Acad. Sci. U. S. A.* 2006. 103: 10729–10734.
12. van Montfoort, N., S. M. Mangsbo, M. G. M. M. Camps, W. W. C. C. van Maren, I. E. C. C. Verhaart, A. Waisman, J. W. Drijfhout, C. J. M. M. Melief, J. S. Verbeek, and F. Ossendorp. Circulating specific antibodies enhance systemic cross-priming by delivery of complexed antigen to dendritic cells in vivo. *Eur. J. Immunol.* 2012. 42: 598–606.
13. Ho, N. I., M. G. M. Camps, E. F. E. de Haas, L. A. Trouw, J. S. Verbeek, and F. Ossendorp. C1q-Dependent Dendritic Cell Cross-Presentation of In Vivo–Formed Antigen–Antibody Complexes. *J. Immunol.* 2017. 198: 4235–4243.
14. Jaehn, P. S., K. S. Zaenker, J. Schmitz, and A. Dzionek. Functional dichotomy of plasmacytoid dendritic cells: Antigen-specific activation of T cells versus production of type I interferon. *Eur. J. Immunol.* 2008. 38: 1822–1832.
15. Salio, M., M. J. Palmowski, A. Atzberger, I. F. Hermans, and V. Cerundolo. CpG-matured murine plasmacytoid dendritic cells are capable of in vivo priming of functional CD8 T cell responses to endogenous but not exogenous antigens. *J. Exp. Med.* 2004. 199: 567–579.
16. Sapoznikov, A., J. A. A. Fischer, T. Zaft, R. Krauthgamer, A. Dzionek, and S. Jung. Organ-dependent in vivo priming of naive CD4+, but not CD8+, T cells by plasmacytoid dendritic cells. *J. Exp. Med.* 2007. 204: 1923–1933.
17. Banchereau, J., and R. M. Steinman. Dendritic cells and the control of immunity. *Nature* 1998. 392: 245–252.
18. Norbury, C. C., D. Malide, J. S. Gibbs, J. R. Bennink, and J. W. Yewdell. Visualizing priming of virus-specific CD8+ T cells by infected dendritic cells in vivo. *Nat. Immunol.* 2002. 3: 265–271.

19. Jung, S., D. Unutmaz, P. Wong, G. I. Sano, K. De Los Santos, T. Sparwasser, S. Wu, S. Vuthoori, K. Ko, F. Zavala, E. G. Pamer, D. R. Littman, and R. A. Lang. In vivo depletion of CD11c+ dendritic cells abrogates priming of CD8+ T cells by exogenous cell-associated antigens. *Immunity* 2002. 17: 211–220.

20. Rodriguez, A., A. Regnault, M. Kleijmeer, P. Ricciardi-Castagnoli, and S. Amigorena. Selective transport of internalized antigens to the cytosol for MHC class I presentation in dendritic cells. *Nat. Cell Biol.* 1999. 1: 362–368.

21. GeurtsvanKessel, C. H., M. A. M. Willart, L. S. van Rijt, F. Muskens, M. Kool, C. Baas, K. Thielemans, C. Bennett, B. E. Clausen, H. C. Hoogsteden, A. D. M. E. Osterhaus, G. F. Rimmelzwaan, and B. N. Lambrecht. Clearance of influenza virus from the lung depends on migratory langerin+CD11b- but not plasmacytoid dendritic cells. *J. Exp. Med.* 2008. 205: 1621–1634.

22. Belz, G. T., K. Shortman, M. J. Bevan, and W. R. Heath. CD8alpha+ dendritic cells selectively present MHC class I-restricted noncytolytic viral and intracellular bacterial antigens in vivo. *J. Immunol.* 2005. 175: 196–200.

23. Pozzi, L.-A. M., J. W. Maciaszek, and K. L. Rock. Both Dendritic Cells and Macrophages Can Stimulate Naive CD8 T Cells In Vivo to Proliferate, Develop Effector Function, and Differentiate into Memory Cells. *J. Immunol.* 2005. 175: 2071–2081.

24. Savina, A., C. Jancic, S. Hugues, P. Guermonprez, P. Vargas, I. C. Moura, A.-M. M. Lennon-Duménil, M. C. Seabra, G. Raposo, and S. Amigorena. NOX2 Controls Phagosomal pH to Regulate Antigen Processing during Crosspresentation by Dendritic Cells. *Cell* 2006. 126: 205–218.

25. Delamarre, L., M. Pack, H. Chang, I. Mellman, and E. S. Trombetta. Differential Lysosomal Proteolysis in Antigen-Presenting Cells Determines Antigen Fate. *Science* 2005. 307: 1630–1634.

26. Saveanu, L., O. Carroll, M. Weimershaus, P. Guermonprez, E. Firat, V. Lindo, F. Greer, J. Davoust, R. Kratzer, S. R. Keller, G. Niedermann, and P. van Endert. IRAP Identifies an Endosomal Compartment Required for MHC Class I Cross-Presentation. *Science* 2009. 325: 213–217.

27. Lin, M. L., Y. Zhan, A. I. Proietto, S. Prato, L. L. Wu, W. R. Heath, J. A. Villadangos, and A. M. Lew. Selective suicide of cross-presenting CD8+ dendritic cells by cytochrome c injection shows functional heterogeneity within this subset. *Proc. Natl. Acad. Sci. U. S. A.* 2008. 105: 3029–3034.

28. Zehner, M., A. L. L. Marschall, E. Bos, J.-G. G. Schloetel, C. Kreer, D. Fehrenschild, A. Limmer, F. Ossendorp, T. Lang, A. J. J. Koster, S. Dübel, and S. Burgdorf. The Translocon Protein Sec61 Mediates Antigen Transport from Endosomes in the Cytosol for Cross-Presentation to CD8+ T Cells. *Immunity* 2015. 42: 850–863.

29. Ackerman, A. L., A. Giodini, and P. Cresswell. A Role for the Endoplasmic Reticulum Protein Retrotranslocation Machinery during Crosspresentation by Dendritic Cells. *Immunity* 2006. 25: 607–617.

30. Grotzke, J. E., P. Kozik, J.-D. Morel, F. Impens, N. Pietrosemoli, P. Cresswell, S. Amigorena, and C. Demangel. Sec61 blockade by mycolactone inhibits antigen cross-presentation independently of endosome-to-cytosol export. *Proc. Natl. Acad. Sci. U. S. A.* 2017. 114: E5910–E5919.

31. Alloatti, A., D. C. Rookhuizen, L. Joannas, J.-M. Carpier, S. Iborra, J. G. Magalhaes, N. Yatim, P. Kozik, D. Sancho, M. L. Albert, and S. Amigorena. Critical role for Sec22b-dependent antigen cross-presentation in antitumor immunity. *J. Exp. Med.* 2017. 214: 2231–2241.

32. Henrickson, S. E., T. R. Mempel, I. B. Mazo, B. Liu, M. N. Artyomov, H. Zheng, A. Peixoto, M. P. Flynn, B. Senman, T. Junt, H. C. Wong, A. K. Chakraborty, and U. H. von Andrian. T cell sensing of antigen dose governs interactive behavior with dendritic cells and sets a threshold for T cell activation. *Nat. Immunol.* 2008. 9: 282–291.

33. O'Keeffe, M., H. Hochrein, D. Vremec, I. Caminschi, J. L. Miller, E. M. Anders, L. Wu, M. H. Lahoud, S. Henri, B. Scott, P. Hertzog, L. Tatarczuch, and K. Shortman. Mouse plasmacytoid cells: long-lived cells, heterogeneous in surface phenotype and function, that differentiate into CD8(+) dendritic cells only after microbial stimulus. *J. Exp. Med.* 2002. 196: 1307–1319.

34. Kamath, A. T., S. Henri, F. Battye, D. F. Tough, and K. Shortman. Developmental kinetics and lifespan of dendritic cells in mouse lymphoid organs. *Blood* 2002. 100: 1734–1741.

35. Chen, M., L. Huang, Z. Shabier, and J. Wang. Regulation of the lifespan in dendritic cell subsets. *Mol. Immunol.* 2007. 44: 2558–2565.

36. Zimmermann, V. S., A. Bondanza, A. Monno, P. Rovere-Querini, A. Corti, and A. a Manfredi. TNF-alpha coupled to membrane of apoptotic cells favors the cross-priming to melanoma antigens. *J. Immunol.* 2004. 172: 2643–2650.

37. Schnurr, M., Q. Chen, A. Shin, W. Chen, T. Toy, C. Jenderek, S. Green, L. Miloradovic, D. Drane, I. D. Davis, J. Villadangos, K. Shortman, E. Maraskovsky, and J. Cebon. Tumor antigen processing and presentation depend critically on dendritic cell type and the mode of antigen delivery. *Blood* 2005. 105: 2465–2472.

2
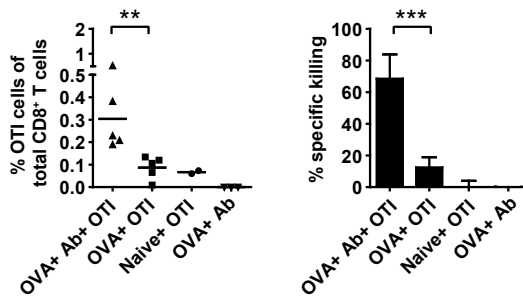
Supplemental Figure 1. Sustained induction of cytotoxic T cell activity in lymph nodes *in vivo*. BL/6 mice were injected i.v. with Ab followed 30 min later by OVA i.v. injection. After 1 week, mice received i.v. adoptive transfer of OTI cells, followed by target cells 4 days later. OTI cell proliferation and specific cytotoxic killing of target cells were measured overnight in the inguinal lymph nodes. Data are from a single experiment representative of three experiments with each dot representing one mouse. **p < 0.01, ***p <0.001.
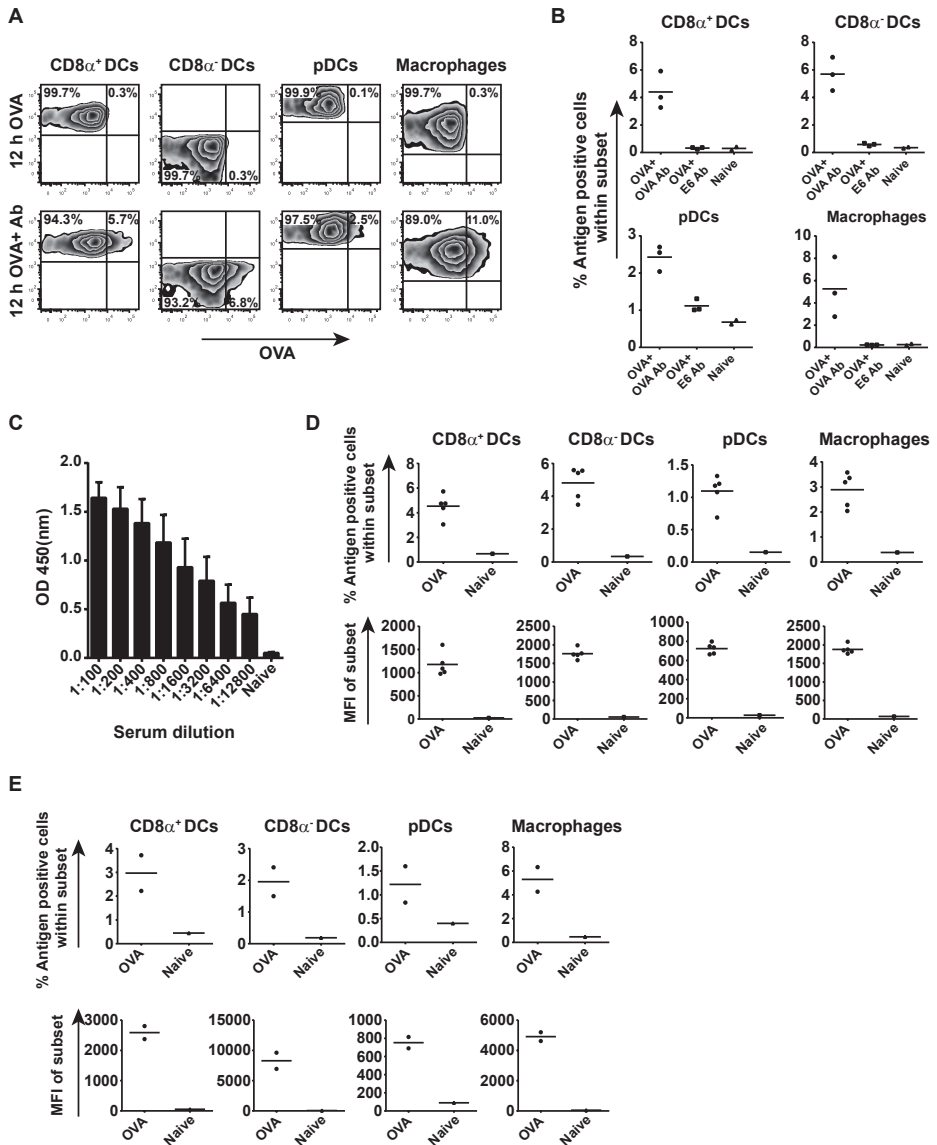
Supplemental Figure 2. Endogenous mouse anti-OVA IgG mediates efficient OVA uptake in splenic APC subsets. BL/6 mice were injected and analyzed as described in Fig.3 **(A)**. BL/6 mice (each dot represents one mouse) were injected with 100 μg polyclonal rabbit anti-OVA IgG or with 100 μg anti-HPV E6 antibody followed 30 minutes later by 5 μg OVA (Alexa Fluor 647 labeled). After 24 h the presence of OVA was measured in splenic APC subsets by flow cytometry **(B)**. BL/6 mice (N=5) were vaccinated with OVA s.c. and boosted 2 weeks later with OVA. After two weeks, blood was taken from mice and the presence of anti-OVA in mouse serum was determined by ELISA **(C)**. Seropositive BL/6 mice (each dot represents one mouse) were i.v. injected with OVA (Alexa Fluor 647 labeled) and the presence of OVA was measured in splenic APC subsets after 24 h by flow cytometry **(D)**. Serum containing anti-OVA IgG from OVA-vaccinated BL/6 mice was transferred i.v. into naïve BL/6 mice followed by i.v. injection of OVA (Alexa Fluor 647 labeled). The presence of OVA was measured 24 h later by flow cytometry **(E)**.
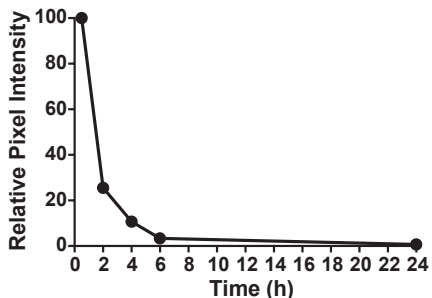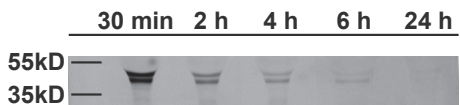
Supplemental Figure 3. Rapid clearance of OVA in Ab positive mice. BL/6 mice received polyclonal rabbit anti-OVA IgG i.v. followed 30 minutes later by OVA (Alexa Fluor 647 labeled). At different time points serum was collected and the presence of fluorescent OVA was quantified from SDS/PAGE gels and indicated by relative pixel intensity. Data are from a single experiment representative of two experiments.
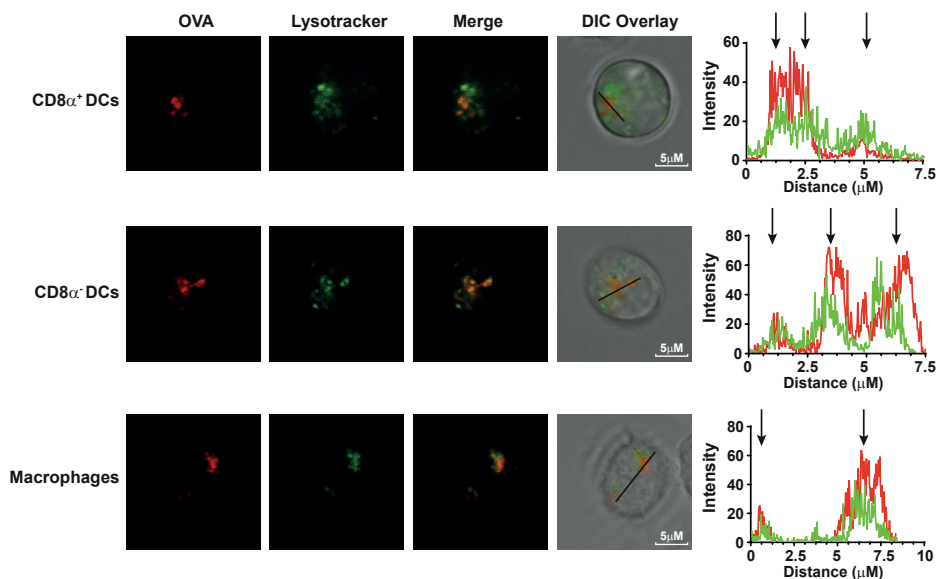

Supplemental Figure 4. Intracellular localization of antigen storage. Experiment was performed as described in Fig. 4. After sorting the splenic APC subsets 24 h after injection of Ab and OVA (Alexa Fluor 647 labeled), Lysotracker Green was added for 30 min *ex vivo* and co-localization with OVA antigen in live cells was visualized by confocal microscopy. Co-localization was analyzed by a line scan drawn on a single optical slice and plotted in histograms. Arrows indicate co-localization between OVA and Lysotracker.
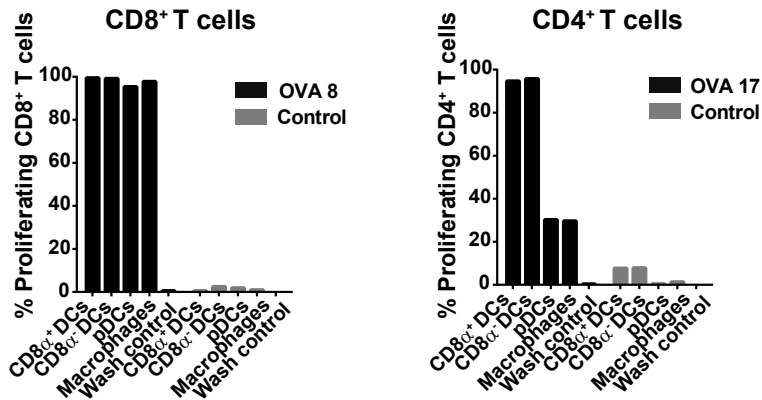
Supplemental Figure 5. All four APC subsets are competent in MHCI and MHCII antigen presentation. Four splenic APC subsets from naïve BL/6 mice were sorted according to the markers described in Fig. 3A and incubated with OVA8 (SIINFEKL) or OVA17 (ISQAVHAAHAEINEAGR) synthetic peptides. After extensively washing, each APC subset was incubated with CFSE-labeled OTI (CD8+/ CD90.1+) or OTII (CD4+/ CD45.1+) cells. T cell proliferation was measured after 3 days by flow cytometry. Wash controls were done without the presence of cells. Data are from a single experiment representative of two experiments.
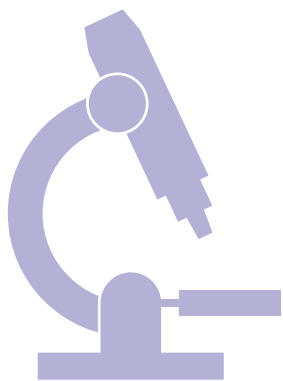
2

3

C1q-dependent dendritic cell cross-presentation of in vivo-formed antigen-antibody complexes

Nataschja I. Ho, Marcel G. M. Camps, Edwin F. E. de Haas, Leendert A. Trouw, J. Sjef Verbeek, Ferry Ossendorp

ABSTRACT

Dendritic cells (DCs) are specialized in antigen engulfment via a wide variety of uptake receptors on their cell surface. In the current study we investigated antigen uptake and presentation of *in vivo* formed antigen-antibody complexes by injecting intravenously mice with antigen-specific antibodies followed by the cognate antigen. We show by this natural antibody-mediated antigen targeting system that uptake by splenic APC subsets is severely hampered in mice lacking complement factor C1q (C1qa$^{-/-}$). Moreover, no detectable antigen cross-presentation by CD8α$^+$ DCs from C1qa$^{-/-}$ mice was found. On the contrary, antigen uptake was not hampered by APCs in FcγRI/II/III/IV-deficient (FcγR quadruple$^{-/-}$) mice and the cross-presentation ability of CD8α$^+$ DCs was not affected.

In conclusion, we show that C1q rather than FcγR controls the antibody- mediated antigen uptake and its presentation by spleen APC subsets to T cells.

INTRODUCTION

Dendritic cells (DCs) are professional antigen presenting cells (APCs) bridging innate and adaptive immunity. DCs are specialized in antigen uptake and internalization via pinocytosis, phagocytosis or receptor mediated endocytosis and subsequently process and present the antigen peptides in MHC molecules to specific T cells (1). DCs express a wide variety of pathogen recognition receptors on their cell surface including C-type lectin receptors, toll-like receptors and Fcγ receptors (FcγR) (2). Several studies revealed that FcγR are important in T cell mediated anti-tumor responses (3, 4). DCs loaded with specific antigen-IgG-immune complexes resulted in induction of DC maturation, priming of specific CD8^{+} CTL responses and tumor protection *in vivo* (5, 6). We have demonstrated that FcγR mediated uptake of model antigen ovalbumin (OVA) bound to anti-OVA IgG, also called OVA immune complexes (OVA IC), is at least 1000 fold more efficient in antigen cross-presentation than soluble OVA (6). Binding of antigen-IgG complexes triggers crosslinking of the Fcγ receptors resulting in internalization of the IC towards antigen storage and presentation compartments (7, 8). In mice, four FcγR have been described, FcγRI (CD64), FcγRIIB (CD32B), FcγRIII (CD16) and FcγRIV (9). The activating receptors FcγRI, FcγRIII and FcγRIV have an immunoreceptor tyrosine-based activation motif (ITAM), whereas the inhibitory receptor FcγRII has an immunoreceptor tyrosine-based inhibitory motif (ITIM). Both activating and inhibitory FcγR can be co-expressed on the same cell, which can regulate and determine the cellular response (10, 11).

Besides binding to FcγR, most IgG subclasses can also activate complement by binding to C1q, the first recognition subcomponent of the classical pathway (12, 13). C1q is a hexameric glycoprotein, composed of 18 polypeptide chains that are formed by 3 types of chains (A-chain, B-chain and C-chain) (14, 15). Each chain consists of a collagen-like domain (binding site for anti-C1q autoantibody) to which the serine proteases C1r and C1s are localized, and a globular head, which binds to the Fc part of IgG and IgM when bound to the cognate antigen (16). Upon binding of C1q to IC, the serine proteases C1r and C1s are activated, resulting in the activation of the classical complement pathway (17). C1q is mainly produced by macrophages and immature DCs (18).

The complement system plays an important role in the physiological clearance of IC by binding complement coated IC to complement receptor-1 (CR1) on erythrocytes and thereby preventing IC deposition (19). Defects in IC clearance mechanisms, resulting in tissue inflammation and damage, have been described in patients with systemic lupus erythematosus (SLE) (20). Several studies have also shown the importance of C1q in adaptive immunity as the uptake and processing of IC in the spleen and antigen cross-presentation *in vivo* were hampered in C1q deficient mice (21, 22).

3

In the present study we used *in vivo* formed OVA IC obtained by injecting mice sequentially with anti-OVA IgG and OVA to investigate the contribution of FcγR and C1q in IC uptake in splenic APC subsets. We have previously reported that this natural formation of antigen-IgG complexes *in vivo* leads to efficient antigen cross-presentation to CD8^{+} T cells (23). We now show that FcγR play minor roles in antibody-mediated antigen uptake *in vivo*, as the antigen uptake and cross-presentation were not hampered in APCs from FcγRI/II/III/IV-deficient (FcγR quadruple^{-/-}) mice. On the contrary, our results indicate a dominant role for C1q in controlling antigen targeting and handling by dendritic cells *in vivo*, as mice lacking C1q (C1qa^{-/-}) showed no detectable antigen uptake in APCs and strongly reduced antigen presentation to CD8^{+} or CD4^{+} T cells.

RESULTS

Efficient antibody-dependent antigen uptake by dendritic cell subsets *in vivo*

We have previously demonstrated by using a classical haptenated protein that circulating hapten-specific antibodies enhanced antigen uptake by DCs *in vivo* which can activate naïve CD4^{+} and CD8^{+} T lymphocytes (23). Here, we analyzed the uptake of the model antigen ovalbumin (OVA) by murine splenic APC subsets *in vivo* mediated by circulating OVA specific antibodies. Mice were first i.v. injected with anti-OVA Ab followed by OVA after 30min to allow natural formation of immune complexes (IC) by circulating antibodies *in vivo* (Fig. 1A). Antigen uptake was analyzed in four splenic APC subsets: CD8α^{+} DCs, CD8α^{-} DCs, pDCs and CD11b^{+} Macrophages. Mice with circulating anti-OVA Ab showed OVA uptake in all four APC subsets (Fig. 1B). Although the percentage of antigen positive cells differed between the subsets (~2%- 10%), the overall level of uptake (MFI) was comparable. Mice that were injected with OVA without anti-OVA Ab showed no detectable antigen uptake in any APC subsets, indicating antibody dependence of antigen engulfment.

### Antibody-mediated antigen uptake by APC subsets *in vivo* is Fcγ receptor independent

Several studies have shown that FcγR are involved in Ab-mediated uptake of antigen (6, 10, 24). Here, we investigated the role of FcγR in antigen-antibody complex uptake by APC subsets *in vivo* by using FcγRI/II/III/IV-deficient (FcγR quadruple^{-/-}) mice. Expression of all four FcγR was analyzed on BL/6 WT and FcγR quadruple^{-/-} murine spleen APC subsets (Supplemental Fig. 1). CD8α[+] DCs, CD8α[-] DCs and Macrophages from BL/6 mice expressed all four FcγR, whereas pDCs only expressed FcγRII. OVA was injected in mice with circulating anti-OVA Ab as described above (Fig. 1A). Unexpectedly, all four APC subsets in FcγR quadruple^{-/-} mice showed significant uptake of OVA (Fig. 2 and Supplemental Fig. 2A).
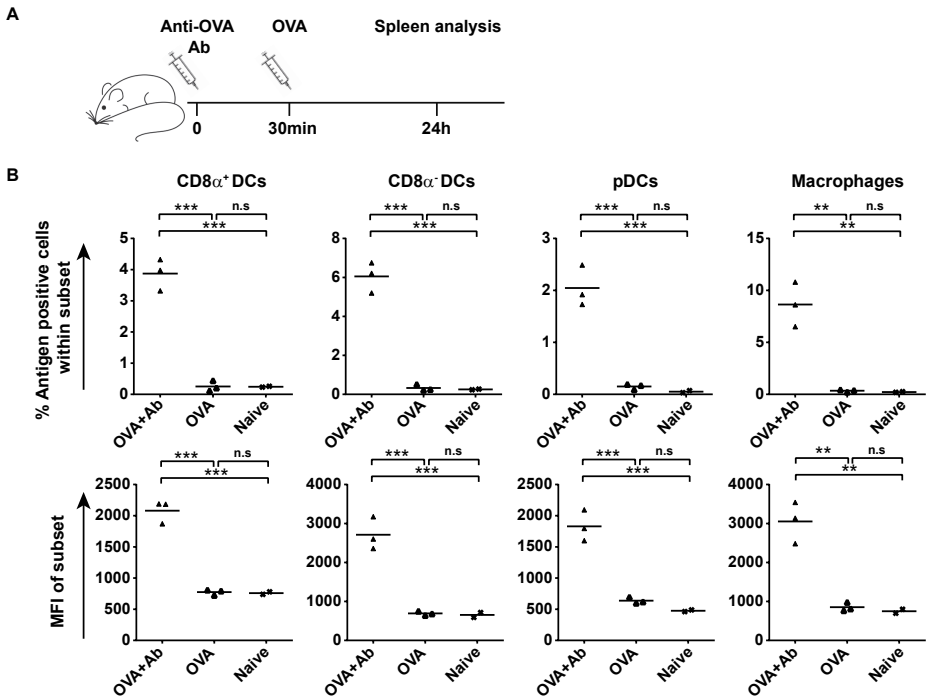
Figure 1. Antibody-mediated antigen uptake by APCs *in vivo*. C57BL/6 (BL/6) mice (each dot represents one mouse) were i.v. injected with 100μg anti-OVA IgG (Ab) and 30min later i.v. injected with 5μg OVA (Alexa Fluor 647 labeled). Antigen presence was measured in spleen APC subsets after 24h **(A)**. Antigen presence in spleen APC subsets measured after 24h, indicated by percentage antigen positive cells and MFI within each subset. Representative experiment is shown for 4 independent experiments **(B)**.

The antigen uptake was slightly higher in CD8α⁺ DCs and pDCs from FcγR quadruple⁻/⁻ mice compared to BL/6 mice, indicated by percentage positive cells and MFI. The OVA uptake by CD11b^high^F4/80⁺ Macrophages was lower when all four FcγR were lacking. FcγR are also known for their function in antigen-antibody complex clearance from the blood (25). By measuring the OVA amount in serum of mice after anti-OVA Ab and OVA injection in time, we could show that FcγR indeed play a role in rapid antigen clearance (Supplemental Fig. 3). Most of the circulating OVA was already cleared after 30min of injection in BL/6 mice, while the clearance was delayed in FcγR quadruple⁻/⁻ mice and OVA was still detectable in circulation after 4h. This lower antigen clearance in FcγR quadruple⁻/⁻ mice, and therefore more availability of OVA antigen, is likely the explanation for the higher uptake found in some of the APC subsets compared to BL/6 WT mice. Importantly, the uptake of OVA in FcγR quadruple⁻/⁻ mice is antibody dependent, as mice injected with only OVA showed no significant OVA uptake in any APC subset (Supplemental Fig. 2B). These results indicate that antibody-mediated antigen uptake by *in vivo* APC subsets is FcγR independent and is likely facilitated by a different uptake route.
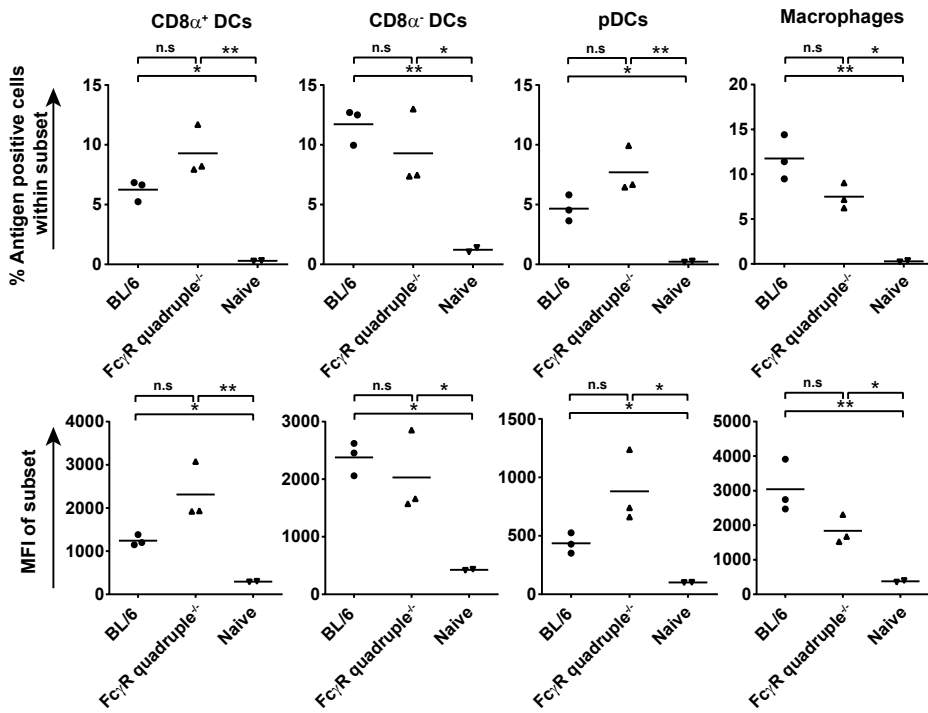
Figure 2. FcγR independent uptake of antigen-antibody complexes by APCs *in vivo*. BL/6 and FcγR quadruple^{-/-} mice (each dot represents one mouse) were injected i.v. with 100μg anti-OVA Ab, followed by 5μg OVA (Alexa Fluor 647 labeled) i.v. injection 30min later. After 24h hours, antigen presence was measured in spleen APC subsets with flow cytometry. The percentage antigen positive cells within each subset is indicated in the upper panel. The mean fluorescence intensity (MFI) of antigen within each APC subset is shown in the bottom panel. Representative FACS data from one representative experiment are shown for 3 independent experiments.

MHCI cross-presentation by CD8α⁺ DCs of antibody bound antigen is Fc receptor independent

Since APC subsets lacking all four FcγR were still able to take up antigen-antibody complexes, we further investigate the possible role of FcγR in antigen presentation to CD4⁺ and CD8⁺ T cells. APC subsets were freshly sorted from spleens of mice that were 24h before injected with anti-OVA Ab and OVA. Each *ex vivo* isolated subset was incubated with either CD8⁺ (OTI) or CD4⁺ (OTII) T cells. CD8α⁺ DCs from BL/6 WT mice showed efficient antigen cross-presentation (~87% dividing cells) to OTI cells (Fig. 3A). CD8α⁻ DCs were also able to cross-present antigen, although in a lower extent (~57% division) compared to CD8α⁺ DCs. The antigen cross-presentation ability of CD8α⁺ DCs from FcγR quadruple^{-/-} was comparable to BL/6 WT mice (~85%), but antigen cross-presentation by CD8α⁻ DCs lacking FcγR was drastically hampered. pDCs and Macrophages from both BL/6 WT and FcγR quadruple^{-/-} showed no detectable antigen cross-presentation to OTI cells. CD8α⁻ DCs from BL/6 WT was the only subset capable of presenting antigen to OTII cells, but again hampered when

lacking FcγR (Fig. 3B). In conclusion, in this circulating antigen-antibody uptake model, *ex vivo* isolated CD8α⁺ DCs can cross-present antigen regardless of the presence of FcγR. On the other hand, FcγR play a role in CD8α⁻ DC mediated cross-presentation.

A

B
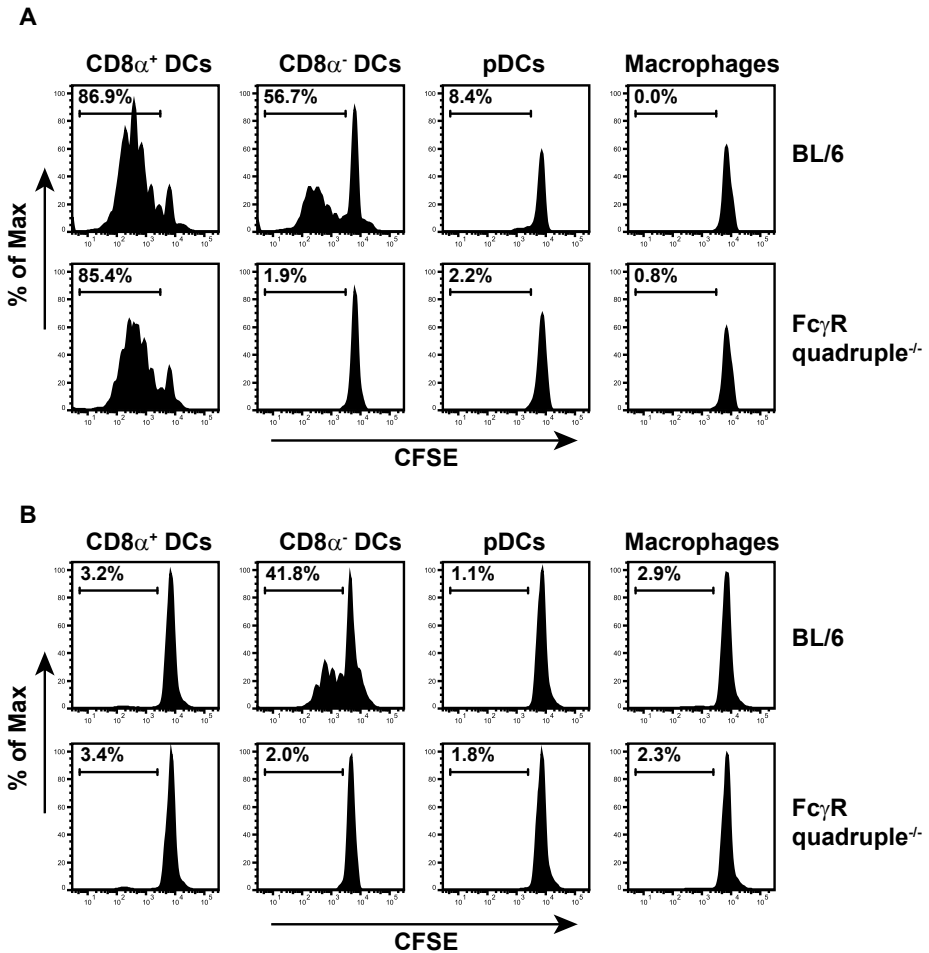
Figure 3. Antibody-mediated antigen cross-presentation by CD8α⁺ DCs is FcγR independent.
BL/6 and FcγR quadruple⁻/⁻ mice (2 mice per group) were injected i.v. with 100μg anti-OVA Ab, 30min later 5μg OVA was i.v. injected. 24h later, spleen APC subsets were sorted and incubated with CFSE labeled OTI (CD8⁺) T cells **(A)** or OTII (CD4⁺) T cells **(B)**. T cell proliferation was measured after 4 days by flow cytometry. Representative FACS data are shown for 3 experiments.

Antigen uptake mediated by circulating antibodies *in vivo* is C1q dependent

Several studies suggest that the complement system is involved in IC clearance which is mainly mediated by C1q, the activating molecule of the classical complement pathway (21, 22, 26). To investigate the possible role of C1q in *in vivo* formed IC, we analyzed antigen uptake

in splenic APC subsets of BL/6 WT in comparison with FcγR quadruple^{-/-} and C1qa^{-/-} mice. As shown previously, antigen uptake by all APC subsets in FcγR quadruple^{-/-} mice is comparable to BL/6 WT mice (Fig. 4). However, mice lacking C1q showed no uptake of antigen in CD8α[+] DCs, pDCs and macrophages, and a strongly reduced uptake in CD8α[-] DCs. The antigen clearance rate is not affected in mice lacking C1q (Supplemental Fig. 3). These results indicate that C1q plays a crucial role in the uptake of antigen bound to circulating antibodies *in vivo*.
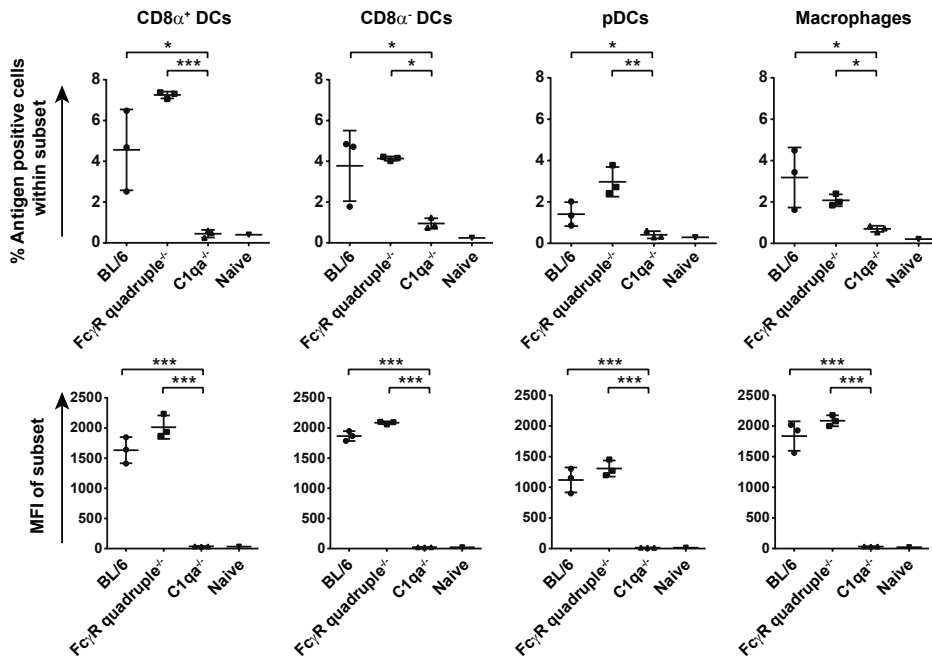
Figure 4. C1q dependent uptake of antibody-mediated antigen by APCs *in vivo*. BL/6, FcγR quadruple^{-/-} and C1qa^{-/-} mice (each dot represents one mouse) were i.v. injected with 100µg anti-OVA Ab and 30min later i.v. with 5µg OVA (Alexa Fluor 647 labeled). Antigen presence in spleen APC subsets were measured after 24h by flow cytometry, indicated by percentage antigen positive cells (upper panel) and MFI (bottom panel) within each subset. Representative FACS data are shown for 3 experiments.

MHCI cross-presentation of antibody bound antigen is C1q dependent

To determine whether C1q is important in antigen presentation to T cells, C1qa^{-/-} mice were injected with anti-OVA Ab and subsequently with OVA. Splenic APC subsets were sorted after 24h and incubated with either CD8^{+} (OTI) or CD4^{+} (OTII) T cells. CD8α^{+} DCs, pDCs and macrophages from mice lacking C1q showed no detectable antigen presentation to CD8^{+} T cells (Fig. 5A). However, CD8α^{-} DCs from C1qa^{-/-} mice were still able to present antigen to CD8^{+} T cells (~54% proliferating T cells) although in a lower extent than BL/6 WT mice (~69% proliferating T cells). All four APC subsets from C1qa^{-/-} mice showed no efficient antigen

presentation to CD4$^+$ T cells (Fig. 5B). Taken together, C1q drastically affects *in vivo* circulating antibody-mediated antigen uptake and thereby controlling antigen presentation efficiency by spleen APC subsets to T cells.

A

B
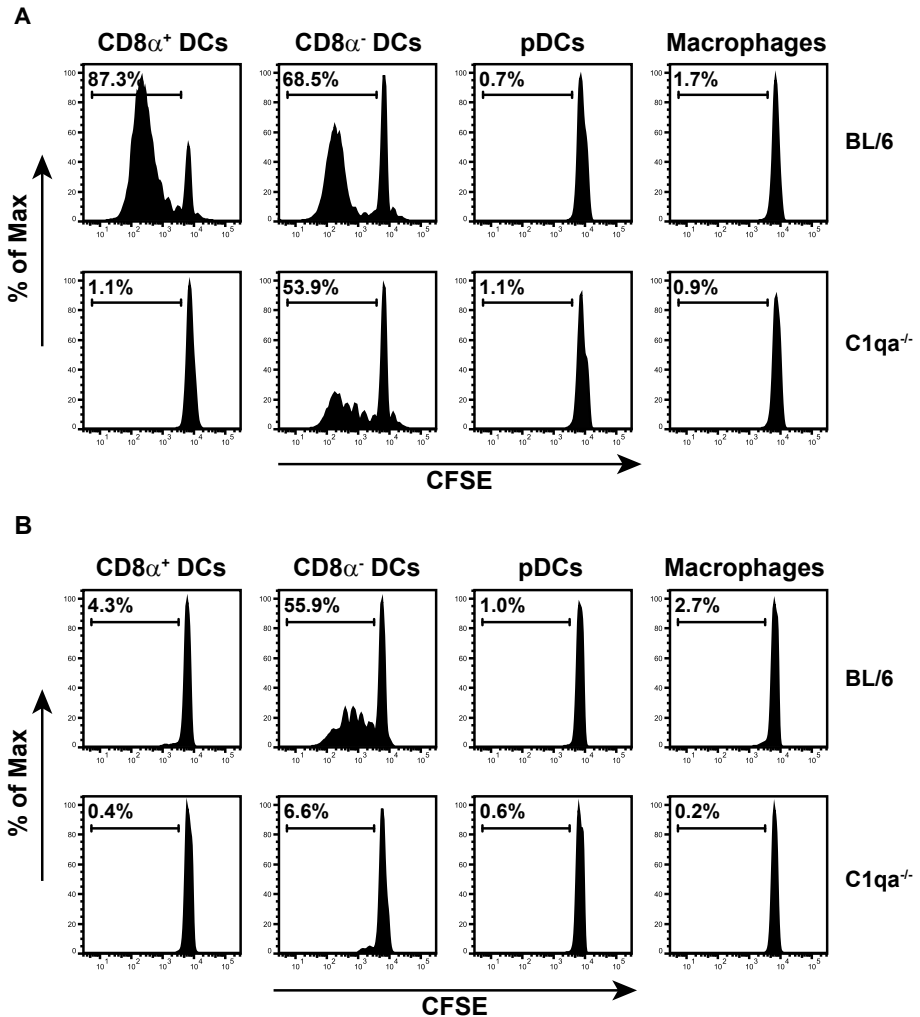

Figure 5. C1q dependent antigen presentation by APCs *in vivo*. BL/6 and C1qa$^{-/-}$ mice (2 mice per group) were i.v. injected with 100μg anti-OVA Ab, followed by 5μg OVA i.v. injection 30min later. Spleen APC subsets were sorted after 24h and incubated with CFSE labeled OTI **(A)** or OTII **(B)** cells. T cell proliferation was measured after 4 days by flow cytometry. Representative data are shown for 3 experiments.

In vivo antigen uptake is reduced by C1q depleting antibodies

To further analyze the crucial role of serum C1q in circulating antibody-mediated antigen uptake *in vivo*, BL/6 WT mice were injected with C1q depleting antibody (27) prior to anti-OVA Ab and OVA injection. All four splenic APC subsets showed reduced uptake of antigen when C1q was depleted from the serum (Fig. 6A). The C1q levels in mice that received C1q depletion treatment were monitored, showing reduced C1q in circulation even up to 24h (Fig. 6B). The antigen clearance rate from the system was not affected in the presence of C1q depleting antibodies (Fig. 6C). These results show that C1q in circulation plays an important role in antibody-mediated antigen uptake by splenic APC subsets *in vivo*.
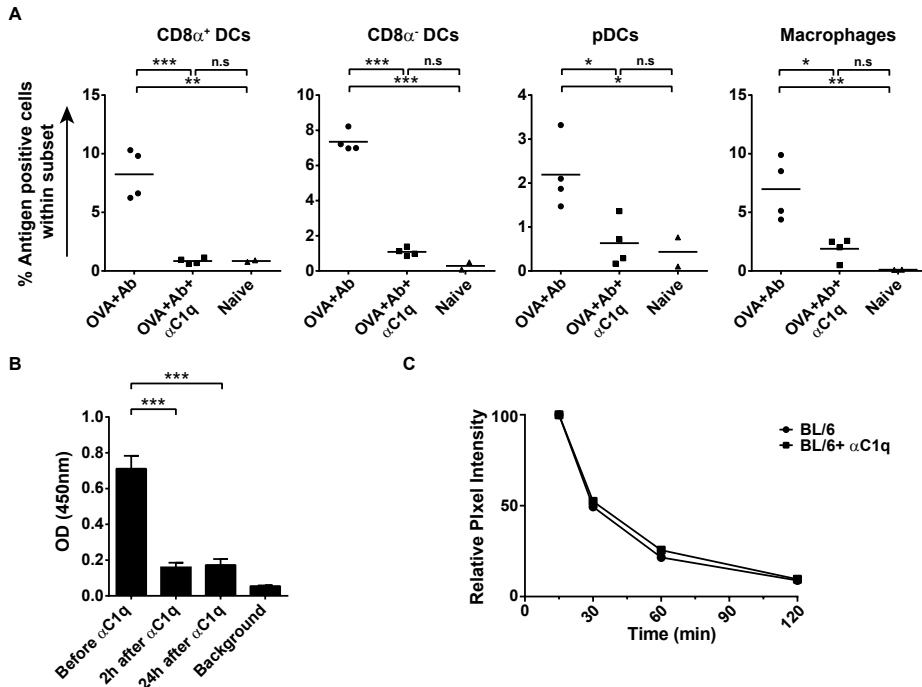
Figure 6. Antibody-mediated antigen uptake after C1q depletion. BL/6 mice (each dot represents one mouse) were i.p. injected with 1mg anti-C1q mAb (αC1q). Two hours later, mice were injected i.v. with 100µg anti-OVA Ab and after 30min i.v. with 5µg OVA (Alexa Fluor 647 labeled). Antigen presence in APC subsets were measured after 24h with flow cytometry **(A)**. C1q levels in serum were measured by C1q ELISA at indicated time points before or after C1q depletion **(B)**. OVA antigen clearance from mice serum was analyzed by withdrawing blood at the indicated time points. Serum was loaded on SDS/PAGE and the amount of fluorescent OVA was quantified, indicated by relative pixel intensity **(C)**. Representative data are shown for at least 2 independent experiments.

**Antigen-antibody complex uptake *in vitro* is improved by C1q**

In apparent contrast to the *in vivo* results from the current study, we have previously shown by using FcR gamma chain deficient mice (lacking FcγR I/III/IV) that the uptake of antibody-bound antigen by bone marrow derived DCs (BMDCs) is FcγR dependent *in vitro* (7). We confirmed these results with the use of BMDCs from FcγR quadruple^{-/-} mice, showing no antigen uptake and antigen cross-presentation to CD8^{+} T cells *in vitro* (Supplemental Fig. 4A). Together, these studies show that FcγR are crucial in the uptake of antigen-antibody complexes by DCs *in vitro*. To determine whether this uptake can be improved by adding additional C1q, spleen cells from untreated BL/6 or FcγR quadruple^{-/-} mice were incubated with different combinations of anti-OVA Ab, OVA and C1q *ex vivo*. Splenic APC subsets from BL/6 WT mice showed an increased antigen uptake when C1q was added to anti-OVA Ab and OVA (Fig. 7). As expected, the uptake of antigen-antibody complexes in splenic APC subsets in absence of all four FcγR is much lower compared to BL/6 WT, however, by adding C1q the uptake increased significantly. The uptake in FcγR quadruple^{-/-} subsets could be increased in the presence of C1q, however the levels are only comparable with those in BL/6 WT without adding additional C1q. Adding additional C1q to OVA without anti-OVA Ab did not enhance antigen uptake by FcγR quadruple^{-/-} APC subsets, indicating the antibody dependence for antigen uptake *in vitro* (Supplemental Fig. 4B). These results indicate that although C1q can facilitate the uptake of antigen-antibody complexes, FcγR are the more dominant uptake receptors under *in vitro* conditions.

3
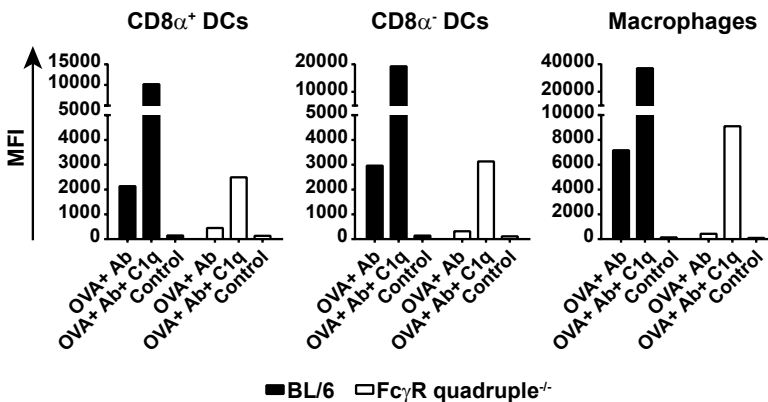
Figure 7. C1q induced antigen-antibody complex uptake by APCs *in vitro*. Naïve spleens from BL/6 or FcγR quadruple^{-/-} mice (2 mice per group) were depleted for B cells and incubated with anti-OVA Ab and OVA (Alexa Fluor 488 labeled) with or without C1q for 1h. Antigen uptake in APC subsets was measured by flow cytometry, indicated by MFI. Representative FACS data are shown for 3 independent experiments showing similar results.

DISCUSSION

It is well established that targeting antigens to dendritic cells (DCs) via FcγR results in high efficient antigen uptake, DC maturation and antigen processing and presentation to T cells (5, 8, 9). Antibody-bound soluble antigen is much more efficient than free antigen since binding of immune complexes triggers crosslinking of FcγR, resulting in DC activation, prolonged antigen presentation, priming of specific CD8^{+} CTL responses and tumor protection *in vivo* (6, 7, 28). In contrast to most studies that used *in vitro* preformed antigen-antibody complexes before injecting in mice, we injected mice sequentially with antibody followed by antigen (i.v.) to allow natural *in vivo* binding of IgG with cognate protein in circulation. As we have previously shown this leads to functional cross-presentation *in vivo* (23). In the present study we show a crucial role for complement factor C1q in antibody-mediated antigen uptake in DCs *in vivo* (illustrated in Fig. 8). Antibody-mediated antigen uptake in APC subsets of C1qa^{-/-} mice was severely hampered in CD8α[+] DCs, pDCs and macrophages, and strongly reduced in CD8α[-] DCs. Moreover, CD8α[+] DCs, pDCs and macrophages isolated from C1qa^{-/-} mice that were injected with circulating antibody and antigen, showed no detectable MHCI and MHCII antigen presentation.
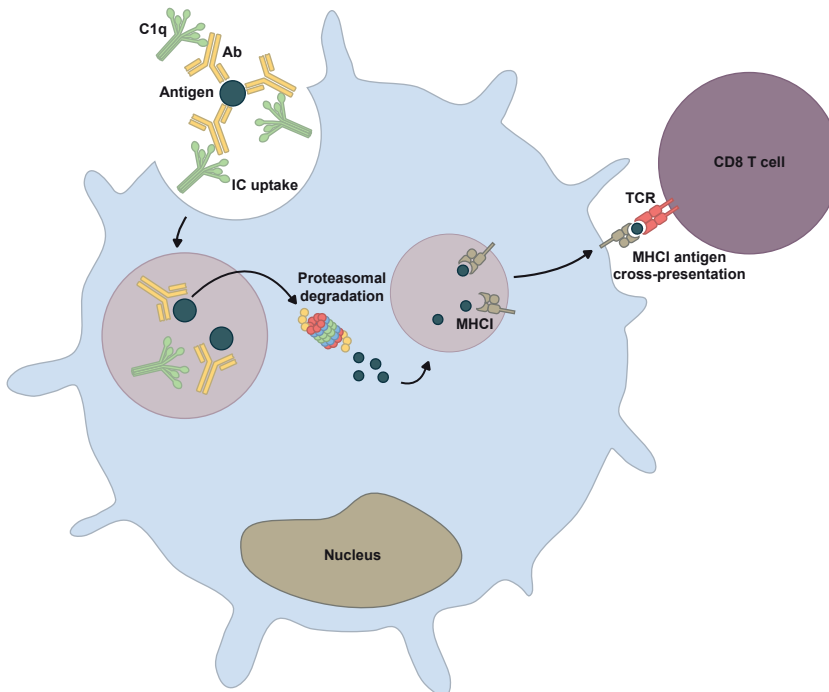
Figure 8. C1q-dependent dendritic cell cross-presentation of antigen-antibody complexes.
Soluble protein antigen binds to antibodies in circulation to form antigen-antibody complexes. C1q facilitates the uptake of these complexes by dendritic cells via an as yet undefined uptake route *in vivo*. After antigen uptake, cross-presentation takes place and MHCI molecules are loaded with processed peptides and presented on the cell surface to CD8^{+} T cells.

By using FcγRI/II/III/IV-deficient (FcγR quadruple$^{-/-}$) mice, we show that antibody-mediated antigen uptake was not hampered but slightly increased in all APC subsets compared to wildtype mice *in vivo*. Detailed characterization study of the FcγR quadruple$^{-/-}$ mice has been done by Fransen *et al.* (29) and no significant differences in circulating levels of C1q or other complement factors were observed. A likely explanation for the enhanced uptake in FcγR quadruple$^{-/-}$ mice is the prolonged presence of antigen in circulation since the clearance of antigen was lower in mice lacking all FcγR. Elimination of circulating antigen-antibody IC is generally assumed to be mediated by Kupffer cells and endothelial cells expressing FcγR in the liver. Although antigen uptake by APC subsets is FcγR independent, we showed that CD8α$^-$ DC antigen cross-presentation was hampered in the absence of FcγR. On the other hand, CD8α$^+$ DCs could still cross-present antigen regardless of the presence of FcγR. These results are in line with earlier work using FcRγchain$^{-/-}$ mice where it was shown that FcR γ-chain activation is necessary for CD8α$^-$ DCs to enable MHCI cross-presentation (30). Taken together, we show that C1q drastically affects *in vivo* circulating antibody-mediated antigen uptake and thereby controlling antigen presentation efficiency by splenic APC subsets to T cells, a process which is mostly independent of FcγR targeting.

In contrast to the *in vivo* results in the present study, we have previously shown in FcRγchain$^{-/-}$ BMDCs that IC uptake *in vitro* is FcγR dependent (7). Here, we show that *in vitro* uptake of IC in FcγR quadruple$^{-/-}$ BMDCs is also hampered compared to wildtype BMDCs, suggesting a distinct contribution of FcγR in antibody-mediated antigen uptake *in vitro* compared to *in vivo*. By adding additional C1q, antigen uptake was highly improved in wildtype APC subsets *in vitro*. The uptake in FcγR quadruple$^{-/-}$ APC subsets could be increased by the presence of C1q, however the levels are only comparable with those in wildtype cells without adding additional C1q. These results indicate that although C1q can facilitate the uptake of antigen-antibody complexes, FcγR are the more dominant uptake receptors *in vitro* compared to C1q mediated uptake, in contrast to their role *in vivo*. One possible explanation is that FcγR *in vivo* are more important in IC clearance from the circulation by FcγR expressing cells in the liver than in IC uptake by DCs in the spleen. Another possible explanation could be the fact that DCs *in vivo* are strategically positioned for efficient take up of antigen to initiate adaptive immunity. Studies on the anatomy of mouse spleen show high organization of immune cells in different zones within the spleen. DCs in the spleen are a heterogeneous population that can be distinguished into numerous smaller subsets according to specific markers. It has been shown that CD8α$^+$ DCs that express higher levels of DEC205/CD205 are more restricted to periarterial lymphoid sheaths (PALS) in the spleen, whereas CD8α$^-$ DCs that express DCIR2 are restricted to the bridging region of the marginal zone (MZ) (31). Moreover, it has been shown that Langerin/CD207$^+$CD103$^+$CD8α$^+$ DCs were mainly localized to the MZ, but migrated into the T cell zone for cross-presentation after phagocytosis of apoptotic cells (32). Since distinct DC subsets are distributed differently

3

in the spleen, there is a possibility that DCs expressing a receptor for C1q-mediated IC uptake is better positioned in the spleen and therefore having better access to circulating IC compared to DCs that lack C1q receptor. Considering the fact that we only found a small percentage of antigen positive cells within each APC subset after i.v. injection, it is possible that this is a subpopulation that is either expressing high levels of C1q receptor and/or better positioned in the spleen. Further anatomic studies on the spleen are needed to determine the distribution of subpopulations expressing FcγR and C1q receptors.

Many C1q receptors have been described over the years, however it is still unclear which C1q receptor is expressed on DCs to mediate IC uptake (14, 33, 34). Both the collagen-like region and the globular head are suggested as binding sites for C1q receptors. Several studies demonstrated that a monomeric IgG binding to one C1q head domains is of low affinity and gives poor complement activation (35, 36). More recent studies showed that IgG molecules form ordered hexamerix structures after binding to antigen that bind C1q with high avidity and promote efficient complement activation (16, 37). By using different Ab mutants that either promote or inhibit hexamerization in solution, they showed that IgG hexamerization is prerequisite to C1q binding and C1 activation. These findings present possibilities to further fine-tune C1q-mediated IC uptake by DCs and thereby enhancing immune responses.

In conclusion, we have shown that antibody-mediated antigen uptake from blood circulation and presentation by APCs *in vivo* is mainly controlled by C1q, independent of FcγR. Further studies on C1q-mediated IC uptake mechanisms by DCs may be relevant for the design of vaccination strategies for optimal induction of T cell immunity against cancer and infectious diseases.

MATERIALS AND METHODS

Mice
All animal experiments in this paper have been approved by the review board of Leiden University Medical Center. C57BL/6 (BL/6) mice were purchased from Charles River laboratories. FcγRI/II/III/IV-deficient (FcγR quadruple^{-/-}) (29) and C1q-deficient (C1qa^{-/-}) mice were on C57BL/6 genetic background (38). OTI mice (CD8^{+} T cell transgenic mice expressing a TCR recognizing the OVA derived K[b] associated epitope SIINFEKL) and OTII mice (CD4^{+} T cell transgenic mice expressing a TCR recognizing the OVA derived Th epitope ISQAVHAAHAEINEAGR in association with IA[b]) were bred and kept at the LUMC animal facility under SPF conditions. All mice were used at 8-12 weeks of age.

In vivo formed OVA-IgG complexes

Mice were intravenously (i.v.) injected with 100µg polyclonal rabbit anti-OVA IgG (Ab, ICN Biomedicals). After 30 min of antibody circulation, mice were injected i.v. with 5µg Ovalbumin (OVA, Worthington Biochemical Corporation) or OVA conjugated with Alexa Fluor 647 (Life Technologies).

Antigen presence in splenic APC subsets

Mice with *in vivo* formed OVA-Ab complexes or only OVA (Alexa Fluor 647 labeled) were sacrificed at different time points. Spleens were isolated and dissociated with Liberase (Thermolysin Low, research grade, Roche) for 20 min at 37°C. The antigen presence was measured by the percentage of Alexa Fluor 647 positive cells and the mean fluorescence intensity (MFI) within each APC subset. Background fluorescence levels were determined by naïve mice without any injections. APC subsets were gated according to the following markers: CD8α^+ DCs (CD11c^{high}CD11b^{low}CD8$^+$), CD8α^- DCs (CD11c^{high}CD11b^{high}CD8$^-$), pDCs (CD11c^{int}CD11b^{low}CD45R$^+$Ly6C$^-$) and macrophages (CD11c^{low}CD11b^{high}F4/80$^+$).

Ex vivo antigen presentation

Spleens from mice with *in vivo* formed OVA-Ab complexes or only OVA were isolated at different time points. Sorting of APC subsets was performed by BD FACSAria II SORP (BD Biosciences). Each APC subset (50.000 cells) was incubated with CFSE labeled and purified OTI (50.000) or OTII cells (50.000) in a 96 well round bottom plate. CD8$^+$ and CD4$^+$ T cell proliferation was measured after 4 days by flow cytometry.

Quantification of ovalbumin in mouse serum

Age- and weight-matched naïve mice received 100µg polyclonal rabbit anti-OVA IgG i.v. followed 30 minutes later by 5µg Alexa Fluor 647 conjugated Ovalbumin (Life Technologies) i.v.. At indicated time points 50µl blood was withdrawn from the lateral tail vein and serum was collected. 5µl serum was mixed with sample buffer, heated at 95°C for 5 minutes and loaded on SDS/PAGE. Fluorescent Ovalbumin was quantified directly from the SDS/PAGE gels by using a Typhoon 9410 Variable mode imager (GE Healthcare Bio-Sciences) and ImageQuant TL v8.1 software (GE Healthcare Life Sciences), indicated by relative pixel intensity.

C1q depletion *in vivo*

C57BL/6 mice were intraperitoneal injected with 1mg anti-C1q mAb JL-1, which recognizes the collagen-like region of mouse C1q (27). Two hours later, mice were injected i.v. with 100µg polyclonal rabbit anti-OVA IgG followed by i.v. injection of OVA conjugated with Alexa Fluor 647 30min later. Antigen presence in spleens was analyzed after 24h. C1q in mouse serum was measured 2h and 24h after anti-C1q mAb injection with the use of C1q ELISA (39).

Antigen uptake and presentation by DCs *in vitro*

Bone marrow cells from C57BL/6 or FcγR quadruple$^{-/-}$ mice were cultured in the presence of 30% R1 supernatant from NIH3T3 fibroblasts transfected with GM-CSF for 10 days. The generated bone marrow dendritic cells (BMDCs) were incubated with titrated amounts of Alexa 488 labeled or unlabeled OVA IC for 1h. Antigen uptake (OVA IC Alexa 488) was measured by flow cytometry indicated by MFI. BMDCs that were incubated with unlabeled OVA IC for 1h were washed and incubated with CFSE labeled OTI cells. CD8$^+$ T cell proliferation was measured after 3 days by flow cytometry.

Spleen cell suspensions from naïve C57BL/6 or FcγR quadruple$^{-/-}$ mice were depleted from B cells (Anti-mouse CD45R/B220 magnetic particles, BD Biosciences) and incubated with 1μg/ml Alexa 488 labeled OVA and 300μg/ml rabbit anti-OVA IgG (LSBio) with or without 10μg/ml hC1q (kindly provided by Cees van Kooten, LUMC). Antigen uptake in APC subsets was measured after 1h with flow cytometry indicated by MFI.

Statistical analysis

Statistical analysis was performed using one-way analysis of variance (ANOVA) test. Tukey's *post hoc* test was performed to correct for multiple comparisons. The following indications are used in all figures: n.s non-significant, * $p<0.05$, ** $p<0.01$ and *** $p<0.001$.

ACKNOWLEDGMENTS

REFERENCES

1. Joffre, O. P., E. Segura, A. Savina, and S. Amigorena. Cross-presentation by dendritic cells. *Nat. Rev. Immunol.* 2012. 12: 557–569.
2. Tacken, P. J., I. J. M. De Vries, R. Torensma, and C. G. Figdor. Dendritic-cell immunotherapy: From ex vivo loading to in vivo targeting. *Nat. Rev. Immunol.* 2007. 7: 790–802.
3. Kalergis, A. M., and J. V. Ravetch. Inducing tumor immunity through the selective engagement of activating Fcγ receptors on dendritic cells. *J. Exp. Med.* 2002. 195: 1653–1659.
4. Rafiq, K., A. Bergtold, and R. Clynes. Immune complex-mediated antigen presentation induces tumor immunity. *J. Clin. Invest.* 2002. 110: 71–79.
5. Regnault, A., D. Lankar, V. Lacabanne, A. Rodriguez, C. Thery, M. Rescigno, T. Saito, S. Verbeek, C. Bonnerot, P. Ricciardi-Castagnoli, S. Amigorena, C. Théry, M. Rescigno, T. Saito, S. Verbeek, C. Bonnerot, P. Ricciardi-Castagnoli, and S. Amigorena. Fcgamma receptor-mediated induction of dendritic cell maturation and major histocompatibility complex class I-restricted antigen presentation after immune complex internalization. *J. Exp. Med.* 1999. 189: 371–380.
6. Schuurhuis, D. H., A. Ioan-Facsinay, B. Nagelkerken, J. J. van Schip, C. Sedlik, C. J. M. Melief, J. S. Verbeek, and F. Ossendorp. Antigen-Antibody Immune Complexes Empower Dendritic Cells to Efficiently Prime Specific CD8 + CTL Responses In Vivo. *J. Immunol.* 2002. 168: 2240–2246.
7. Van Montfoort, N., M. G. Camps, S. Khan, D. V. Filippov, J. J. Weterings, J. M. Griffith, H. J. Geuze, T. van Hall, J. S. Verbeek, C. J. Melief, and F. Ossendorp. Antigen storage compartments in mature dendritic cells facilitate prolonged cytotoxic T lymphocyte cross-priming capacity. *Proc. Natl. Acad. Sci. U. S. A.* 2009. 106: 6730–6735.
8. Baker, K., T. Rath, W. I. Lencer, E. Fiebiger, and R. S. Blumberg. Cross-presentation of IgG-containing immune complexes. *Cell. Mol. Life Sci.* 2013. 70: 1319–1334.
9. Guilliams, M., P. Bruhns, Y. Saeys, H. Hammad, and B. N. Lambrecht. The function of Fcγ receptors in dendritic cells and macrophages. *Nat. Rev. Immunol.* 2014. 14: 94–108.
10. Ravetch, J. V., and R. A. Clynes. Divergent roles for Fc receptors and complement in vivo. *Annu. Rev. Immunol.* 1998. 16: 421–432.
11. van Montfoort, N., P. A. C. 't Hoen, S. M. Mangsbo, M. G. M. Camps, P. Boross, C. J. M. Melief, F. Ossendorp, and J. S. Verbeek. Fcγ Receptor IIb Strongly Regulates Fcγ Receptor-Facilitated T Cell Activation by Dendritic Cells. *J. Immunol.* 2012. 189: 92–101.
12. Duncan, A. R., and G. Winter. The binding site for C1q on IgG. *Nature* 1988. 332: 738–740.
13. Dunkelberger, J. R., and W. C. Song. Complement and its role in innate and adaptive immune responses. *Cell Res.* 2010. 20: 34–50.
14. Kishore, U., and K. B. M. Reid. C1q: Structure, function, and receptors. *Immunopharmacology* 2000. 49: 159–170.
15. Sellar, G. C., D. J. Blake, and K. B. Reid. Characterization and organization of the genes encoding the A-, B- and C-chains of human complement subcomponent C1q. The complete derived amino acid sequence of human C1q. *Biochem. J.* 1991. 274 (Pt 2): 481–490.
16. Diebolder, C. A., F. J. Beurskens, R. N. de Jong, R. I. Koning, K. Strumane, M. A. Lindorfer, M. Voorhorst, D. Ugurlar, S. Rosati, A. J. R. R. Heck, J. G. J. J. Van De Winkel, I. A. Wilson, A. J. Koster, R. P. Taylor, E. O. Saphire, D. R. Burton, J. Schuurman, P. Gros, and P. W. H. I. H. I. Parren. Complement is activated by IgG hexamers assembled at the cell surface. *Science* 2014. 343: 1260–1263.
17. Daha, N. A., N. K. Banda, A. Roos, F. J. Beurskens, J. M. Bakker, M. R. Daha, and L. A. Trouw. Complement activation by (auto-) antibodies. *Mol. Immunol.* 2011. 48: 1656–1665.
18. Castellano, G., A. M. Woltman, A. J. Nauta, A. Roos, L. A. Trouw, M. A. Seelen, F. P. Schena, M. R. Daha, and C. Van Kooten. Maturation of dendritic cells abrogates C1q production in vivo and in vitro. *Blood* 2004. 103: 3813–3820.
19. Naama, J. K., A. O. Hamilton, A. C. Yeung-Laiwah, and K. Whaley. Prevention of immune precipitation by purified classical pathway complement components. *Clin. Exp. Immunol.* 1984. 58: 486–492.
20. Walport, M. J., K. A. Davies, and M. Botto. C1q and Systemic Lupus Erythematosus. *Immunobiology* 1998. 199: 265–285.
21. Nash, J. T., P. R. Taylor, M. Botto, P. J. Norsworthy, K. A. Davies, and M. J. Walport. Immune complex processing in C1q-deficient mice. *Clin. Exp. Immunol.* 2001. 123: 196–202.

3

22. van Montfoort, N., J. M. H. de Jong, D. H. Schuurhuis, E. I. H. van der Voort, M. G. M. Camps, T. W. J. Huizinga, C. van Kooten, M. R. Daha, J. S. Verbeek, F. Ossendorp, and R. E. M. Toes. A Novel Role of Complement Factor C1q in Augmenting the Presentation of Antigen Captured in Immune Complexes to CD8 + T Lymphocytes. *J. Immunol.* 2007. 178: 7581–7586.

23. van Montfoort, N., S. M. Mangsbo, M. G. M. M. Camps, W. W. C. C. van Maren, I. E. C. C. Verhaart, A. Waisman, J. W. Drijfhout, C. J. M. M. Melief, J. S. Verbeek, and F. Ossendorp. Circulating specific antibodies enhance systemic cross-priming by delivery of complexed antigen to dendritic cells in vivo. *Eur. J. Immunol.* 2012. 42: 598–606.

24. Hamano, Y., H. Arase, H. Saisho, and T. Saito. Immune Complex and Fc Receptor-Mediated Augmentation of Antigen Presentation for in Vivo Th Cell Responses. *J. Immunol.* 2000. 164: 6113–6119.

25. Kurlander, R. J., D. M. Ellison, and J. Hall. The blockade of Fc receptor-mediated clearance of immune complexes in vivo by a monoclonal antibody (2.4G2) directed against Fc receptors on murine leukocytes. *J. Immunol.* 1984. 133: 855–862.

26. Naama, J. K., I. P. Niven, A. Zoma, W. S. Mitchell, and K. Whaley. Complement, antigen-antibody complexes and immune complex disease. *J. Clin. Lab. Immunol.* 1985. 17: 59–67.

27. Trouw, L. A., T. W. L. Groeneveld, M. A. Seelen, J. M. G. J. Duijs, I. M. Bajema, F. A. Prins, U. Kishore, D. J. Salant, J. S. Verbeek, C. Van Kooten, and M. R. Daha. Anti C1q autoantibodies deposit in glomeruli but are only pathogenic in combination with glomerular C1q-containing immune complexes. *J. Clin. Invest.* 2004. 114: 679–688.

28. Schuurhuis, D. H., N. van Montfoort, A. Ioan-Facsinay, R. Jiawan, M. Camps, J. Nouta, C. J. M. Melief, J. S. Verbeek, and F. Ossendorp. Immune Complex-Loaded Dendritic Cells Are Superior to Soluble Immune Complexes as Antitumor Vaccine. *J. Immunol.* 2006. 176: 4573–4580.

29. Fransen, M. F., H. Benonisson, W. W. van Maren, H. S. Sow, C. Breukel, M. M. Linssen, J. W. C. Claassens, C. Brouwers, J. van der Kaa, M. Camps, J. W. Kleinovink, K. K. Vonk, S. van Heiningen, N. Klar, L. van Beek, V. van Harmelen, L. Daxinger, K. S. Nandakumar, R. Holmdahl, C. Coward, Q. Lin, S. Hirose, D. Salvatori, T. van Hall, C. van Kooten, P. Mastroeni, F. Ossendorp, and J. S. Verbeek. A Restricted Role for FcγR in the Regulation of Adaptive Immunity. *J. Immunol.* 2018. 200: 2615–2626.

30. den Haan, J. M. M., and M. J. Bevan. Constitutive versus activation-dependent cross-presentation of immune complexes by CD8(+) and CD8(-) dendritic cells in vivo. *J. Exp. Med.* 2002. 196: 817–827.

31. Qiu, C.-H. C.-H., Y. Miyake, H. Kaise, H. Kitamura, O. Ohara, and M. Tanaka. Novel Subset of CD8α + Dendritic Cells Localized in the Marginal Zone Is Responsible for Tolerance to Cell-Associated Antigens. *J. Immunol.* 2009. 182: 4127–4136.

32. Idoyaga, J., N. Suda, K. Suda, C. G. Park, and R. M. Steinman. Antibody to Langerin/CD207 localizes large numbers of CD8 + dendritic cells to the marginal zone of mouse spleen. *Proc. Natl. Acad. Sci. U. S. A.* 2009. 106: 1524–1529.

33. Ghiran, I., S. R. Tyagi, L. B. Klickstein, and A. Nicholson-Weller. Expression and function of C1q receptors and C1q binding proteins at the cell surface. *Immunobiology* 2002. 205: 407–420.

34. Peerschke, E. I. B., and B. Ghebrehiwet. CC1qR/CR and gC1qR/p33: Observations in cancer. *Mol. Immunol.* 2014. 61: 100–109.

35. Hughes-Jones, N. C., and B. Gardner. Reaction between the isolated globular sub-units of the complement component C1q and IgG-complexes. *Mol. Immunol.* 1979. 16: 697–701.

36. Sledge, C. R., and D. H. Bing. Binding properties of the human complement protein C1q. *J. Biol. Chem.* 1973. 248: 2818–2823.

37. Wang, G., R. N. de Jong, E. T. J. van den Bremer, F. J. J. Beurskens, A. F. F. Labrijn, D. Ugurlar, P. Gros, J. Schuurman, P. W. H. I. W. H. I. Parren, A. J. R. J. R. Heck, R. N. de Jong, E. T. J. van den Bremer, F. J. J. Beurskens, A. F. F. Labrijn, D. Ugurlar, P. Gros, J. Schuurman, P. W. H. I. W. H. I. Parren, and A. J. R. J. R. Heck. Molecular Basis of Assembly and Activation of Complement Component C1 in Complex with Immunoglobulin G1 and Antigen. *Mol. Cell* 2016. 63: 135–145.

38. Botto, M., C. Dell'Agnola, A. E. Bygrave, E. M. Thompson, H. T. Cook, F. Petry, M. Loos, P. P. Pandolfi, and M. J. Walport. Homozygous C1q deficiency causes glomerulonephritis associated with multiple apoptotic bodies. *Nat. Genet.* 1998. 19: 56–59.

39. Trouw, L. A., M. A. Seelen, J. M. G. J. Duijs, H. Benediktsson, C. Van Kooten, and M. R. Daha. Glomerular deposition of C1q and anti-C1q antibodies in mice following injection of antimouse C1q antibodies. *Clin. Exp. Immunol.* 2003. 132: 32–39.
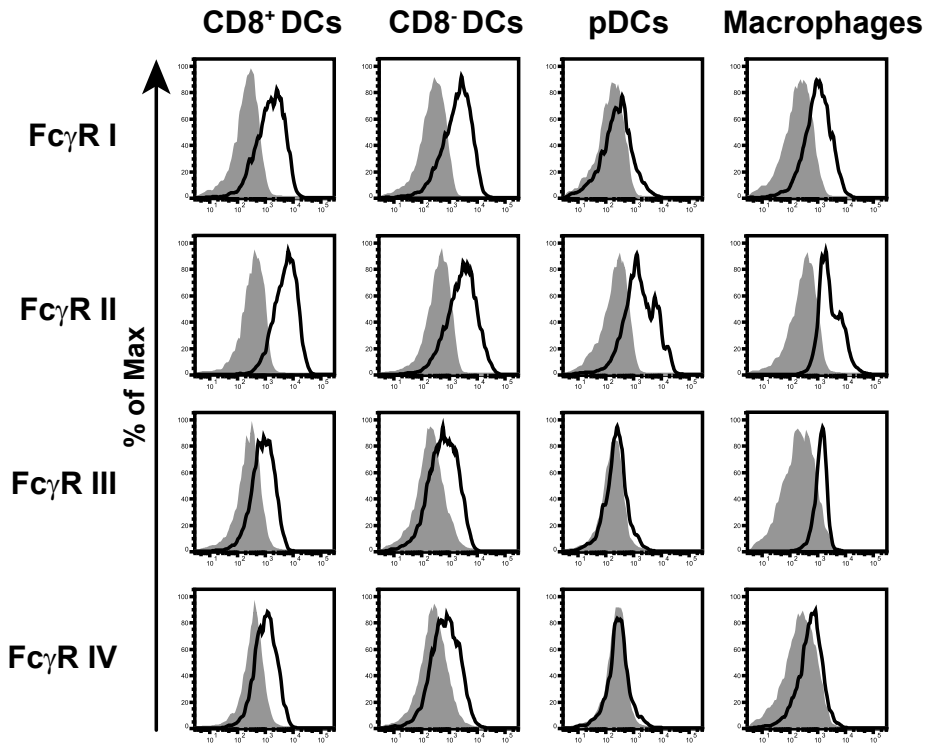
Supplemental Figure 1. FcγR expression on spleen APC subsets. Spleen cells from naïve BL/6 and FcγR quadruple^{-/-} mice were stained with FcγRI-IV antibodies. FcγR expression was measured on each APC subset from BL/6 mice with flow cytometry (black histograms) compared to FcγR quadruple^{-/-} mice (grey histograms). Representative FACS data are shown here for 3 experiments.

A

B
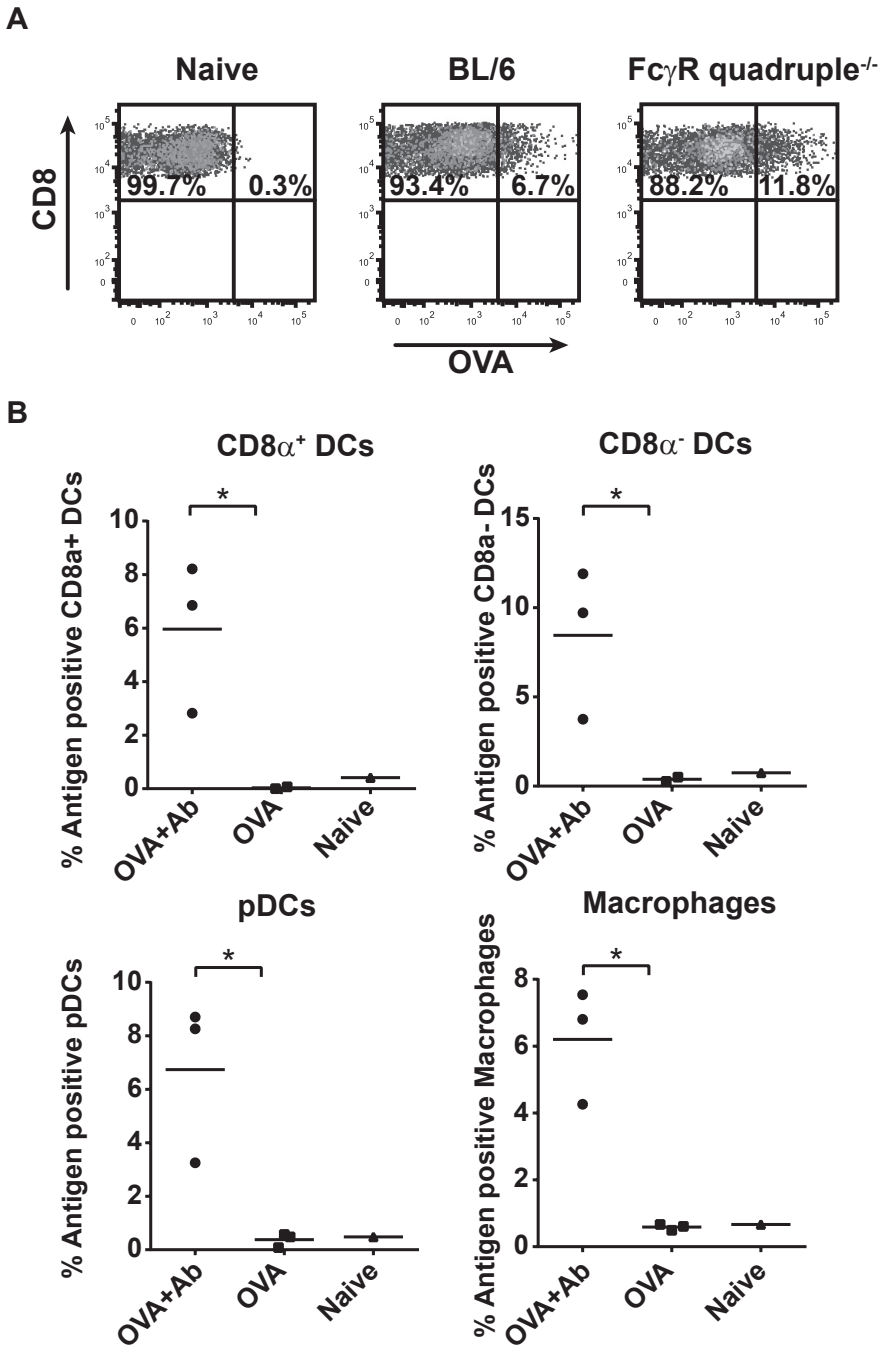
Supplemental Figure 2. Antigen-antibody IC uptake in APC subsets. Mice we injected as described in figure 2. Representative FACS plots of antigen uptake in CD8α⁺ DCs from BL/6 and FcγR quadruple⁻/⁻ mice **(A)**. FcγR quadruple⁻/⁻ mice were injected i.v. with 100µg anti-OVA Ab and 30min later i.v. with 5µg OVA (Alexa Fluor 647 labeled) or with OVA (Alexa Fluor 647 labeled) only without Ab. Antigen presence in spleen APCs was measured after 24h by flow cytometry **(B)**. Representative data for 4 experiments.
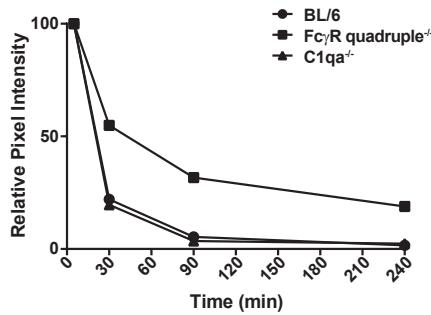
Supplemental Figure 3. Antigen clearance in mouse serum. BL/6, FcγR quadruple^{-/-} and C1qa^{-/-} mice (each dot represents one mouse) were injected with 100µg anti-OVA Ab i.v. followed by 5µg OVA (Alexa Fluor 647 labeled) i.v. after 30min. OVA antigen clearance from mice serum was analyzed by withdrawing blood at the indicated time points. Serum was loaded on SDS/PAGE and the amount of fluorescent OVA was quantified, indicated by relative pixel intensity. Representative data are shown for 4 independent experiments.

3
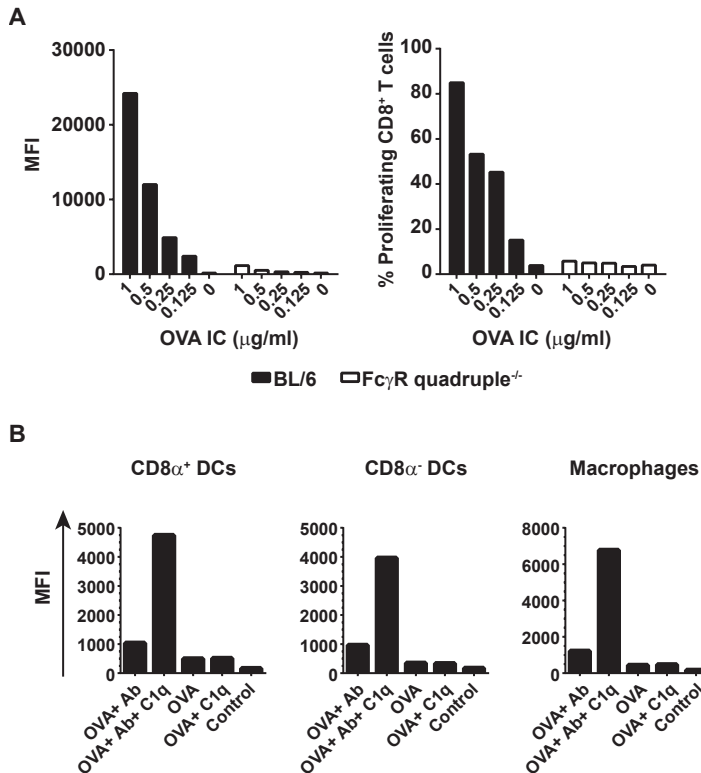
Supplemental Figure 4. Antigen-antibody IC uptake by DCs *in vitro*. BMDCs from BL/6 and FcγR quadruple^{-/-} mice were incubated with titrated amounts of Alexa 488 labeled or unlabeled OVA IC for 1h. Antigen uptake (OVA IC Alexa 488) was measured by flow cytometry indicated by MFI. BMDCs that were incubated with unlabeled OVA IC for 1h were washed and incubated with CFSE labeled OTI cells. CD8+ T cell proliferation was measured after 3 days by flow cytometry. Representative data are shown for 4 experiments **(A)**. Spleen cells from FcγR quadruple^{-/-} mice were depleted for B cells and incubated with different combinations of anti-OVA Ab, OVA (Alexa Fluor 488 labeled) and C1q for 1h. Antigen uptake in APC subsets was measured by flow cytometry, indicated by MFI. Representative FACS data are shown for 3 experiments **(B)**.

4

Characterization of antigen-containing compartments after Fcy receptor or C-type lectin receptor-mediated uptake in dendritic cells

Nataschja I. Ho, Marcel G. M. Camps, Juan J. Garcia-Vallejo, Erik Bos, Abraham J. Koster, Martijn Verdoes, Yvette van Kooyk, Ferry Ossendorp

ABSTRACT

An exclusive feature of dendritic cells (DCs) is their capacity to present exogenous antigens by MHC class I molecules, called cross-presentation. Here we showed that protein antigen can be conserved in mature DCs for several days in a lysosome-like storage compartment, distinct from MHC class II and early endosomal compartments, as an internal source for the supply of MHC class I ligands. Using two different uptake routes via Fcy receptors and C-type lectin receptors, we characterized the antigen-containing organelle 48 hours after antigen uptake as a LAMP1+ compartment lacking the early endosomal markers EEA1 and Rab5. The antigen-containing compartments lacked co-expression of molecules involved in MHC class I processing and presentation including TAP, proteasome subunits and cathepsin proteases. The lack of cathepsin S but the elevated presence of active cathepsin X in the storage compartments in time indicate a role of cathepsin X in antigen processing and cross-presentation by DCs. We could further conclude that the two independent receptor-mediated uptake routes resulted in co-localization of antigen in the same lysosome-like compartments after 48 hours. Our data suggest that these antigen-containing compartments in DC can conserve protein antigens from different uptake routes and contribute to long-lasting antigen cross-presentation.

INTRODUCTION

Dendritic cells (DCs) are an important target for the design and improvement of cancer immunotherapeutic vaccines due to their exclusive ability to cross-present tumor antigens to initiate $CD8^+$ T cell response (1–3). DCs scan the peripheral tissue and take up antigens they encounter through receptors, such as Fcγ receptors (FcγRs) and C-type lectin receptors (CLRs). Upon antigen internalization and DC activation, DCs migrate toward the draining lymph node where they can present antigens to T cells. However, the underlying mechanism of DC cross-presentation is not fully unraveled yet. Two main intracellular pathways for antigen cross-presentation in DCs have been proposed: the vacuolar and the cytosolic pathways. Antigen processing through the vacuolar pathway is mainly dependent on antigen degradation in endosomes, probably by proteases such as cathepsin S, but independent of transporter associated with antigen processing (TAP) and the proteasome (4). Thus, antigen processing and loading on MHCI probably occurs in endocytic compartments. In the cytosolic pathway, exogenous antigens in endosomal vesicles are transported in the cell cytosol and degraded by the proteasome. The peptides that are generated by the proteasome are then transported by TAP to the endoplasmic reticulum (ER) where they are loaded on MHCI molecules (5–7). However, it has been reported that some proteasome-generated peptides can be transported back into endocytic compartments where they are trimmed by insulin regulated aminopeptidase (IRAP) and directly loaded on MHCI molecules (8).

4

   We have reported before that antigen can be stored in DCs for several days which facilitates prolonged cytotoxic T-lymphocyte (CTL) cross-priming capacity (9). Sustained antigen cross-presentation may be important since it can take up to a few days for DCs to migrate from the infection site to the lymph nodes to encounter T cells. Moreover, the turnover rate of surface MHCI molecules is shorter compared to MHCII, most MHCI-peptide complexes disappear from the cell surface within 24 hours (9). Therefore, prolonged antigen storage in DCs and sustained supply of newly synthesized MHCI-peptide complexes is beneficial to ensure efficient T-cell cross-priming (10). Here we further characterize the compartments where antigen is stored in DCs by using immunofluorescent staining of several proteins related to the endosomal trafficking and antigen processing pathways. The lack of cathepsin S indicate that cathepsin S is not involved in antigen degradation in these storage compartments. Interestingly, the increased presence of cathepsin X in the storage compartments in time, suggest there might be a distinct but yet unidentified function of cathepsin X in antigen storage or processing in DCs. Moreover, we compared the routing of antigens targeted to FcγRs and C-type lectin receptor MGL1. Our results revealed that antigens targeted to FcγRs or MGL1 end up in the same storage compartment. The storage compartment is characterized as LAMP1 positive, distinct from early endosomal or MCHI/ MHCII loading compartments. Our data suggest that these storage compartments can conserve antigens from different uptake routes which can contribute to long-lasting DC antigen cross-presentation.

A

B
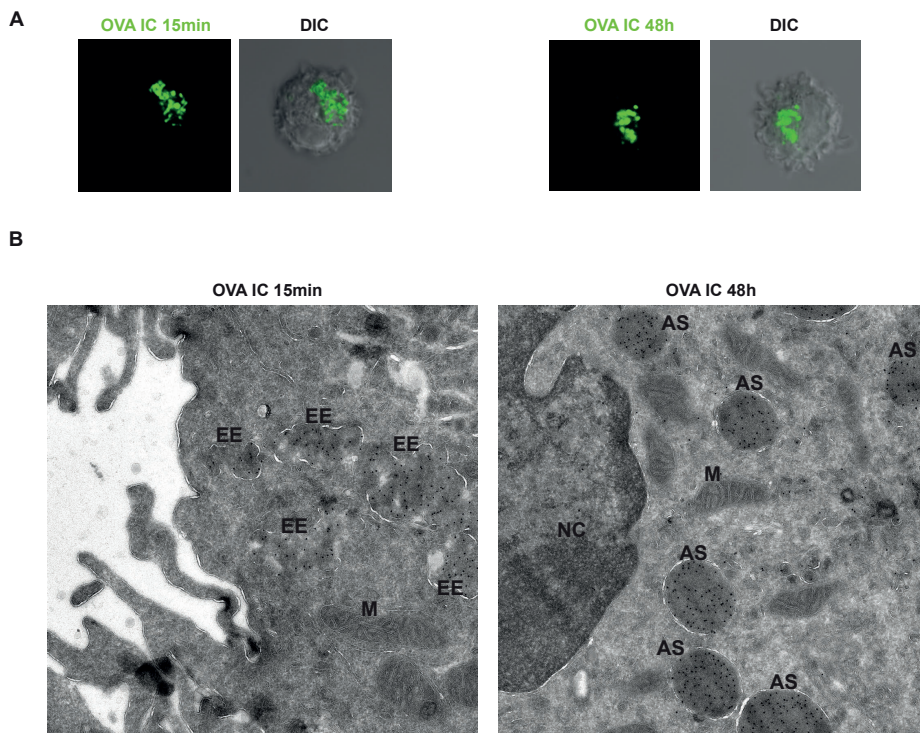
Figure 1. Antigen storage in dendritic cells. DCs were pulsed with OVA IC (Alexa Fluor 488) for 15 min **(A, left panel)** or pulsed with OVA IC for 2 hours and chased for 48 hours **(A, right panel)**. OVA IC uptake and presence in DCs were imaged by confocal microscopy and differential interference contrast (DIC) was additionally used to image cell contrast. Immuno-electron microscopy images of DCs after 15min OVA IC (Alexa Fluor 488) pulse **(B, left)** and DCs pulsed with OVA IC for 2 hours and chased for 48 hours **(B, right)**. Sections were labelled with immunogold for Alexa488 with 10nm gold particle size. EE= early endosome, M= mitochondria, AS= antigen storage compartment, NC= nucleus.

RESULTS

Antigen-antibody complexes are stored in LAMP1 positive compartments in dendritic cells

We have studied the uptake kinetics before of OVA bound to OVA-specific IgG antibodies (OVA immune complexes, OVA IC) and showed that the uptake of OVA IC is a 1000-fold more efficient than soluble OVA (9). Indeed, large amounts of fluorescently labeled OVA IC were already taken up by DCs after only 15 min pulse with OVA IC, visualized by confocal microscopy (Fig. 1A, left panel). Interestingly, DCs that were pulsed with OVA IC for 2 hours, washed, and chased for 48 hours still contain extensive amounts of OVA IC (Fig 1A, right panel). These OVA IC are located perinuclear in a condensed fashion. More detailed visualization of the uptake of OVA IC was done by 10 nm gold particle labeling for electron

microscopy. After 15 min OVA IC pulse in DCs, many gold beads were detected in cloud shaped compartments (Fig. 1B, left). Strikingly, 48 hours after pulse-loading DCs with OVA IC, large spherical structures filled with gold beads were visualized near the nucleus (Fig. 1B, right). These results confirmed once more that antigen can be stored in DCs for several days in compartments proportionate to endosomal structures. Therefore, we performed co-staining with antibodies against several members of the endosomal trafficking pathways to further characterize the storage compartments with confocal microscopy. After the initial 15 min uptake of OVA IC by DCs, OVA IC are taken up in EEA1 and Rab5 positive compartments (Fig. 2, Supplemental Fig. 1). However, after the 48h chase, OVA IC were not found in EEA1 or Rab5 compartments. Rab7, which is a marker for more matured endosomes, did not show any co-localization with OVA IC after 15 min or 48 hours. The lysosomal marker LAMP1 was spread out through the cell cytosol after 15 min and no co-localization was found with OVA IC. However, a clear perinuclear reorganization of LAMP1 was detected after 48 hours and co-localization with OVA IC was observed. MHCI and MHCII positive compartments in the cell cytosol were detected at 15 min time point, and co-localization with OVA IC was observed (Fig. 2, Supplemental Fig. 1). As described before, targeting FcγRs on DCs with OVA IC induced strong DC maturation, including an increased expression of MHCI and MHCII (9). Indeed, 48 hours after antigen pulse, most MHCI and MHCII were detected on the cell surface, and not co-localizing anymore with OVA IC (Fig. 2, Supplemental Fig. 1). Since we have shown before that antigens from the storage compartments are cross-presented in a TAP and proteasome dependent pathway (9), antibody staining for TAP1 and PA28β was performed. The proteasome activator PA28b subunit is known to be strongly upregulated in maturing dendritic cells (11). However, neither TAP1 nor PA28β co-localized with OVA IC at any measured time point (Fig. 2, Supplemental Fig. 1).

In order to follow the co-localization kinetics of OVA IC after uptake by DCs, we used imaging flow cytometry, a method that allows high-throughput image analysis of cells in flow with near-confocal resolution to analyze intracellular routing of fluorescently labeled OVA IC. OVA IC enters EEA1 positive compartments after DC uptake but the co-localization score decreased swiftly within 15 min (Fig. 3). One hour after the initial antigen pulse, most OVA IC were not present in EEA1 positive compartments. Similar kinetics were observed for Rab5, OVA IC enters Rab5 positive compartments, but after 1 hour, the co-localization score between Rab5 and OVA IC had diminished. In line with the confocal analysis, Rab7 did not show any remarkable co-localization with OVA IC, although a slight increase could be observed after 48 hours. OVA IC was strongly co-localizing with LAMP1 after 24 and 48 hours, confirming our previous confocal data. MHCI and MHCII co-localized with OVA IC at early time points (10 min, 1 hour) but the co-localization score was decreased after 24 and 48 hours. The co-localization kinetics for both TAP1 and PA28β with OVA IC did not change in time.
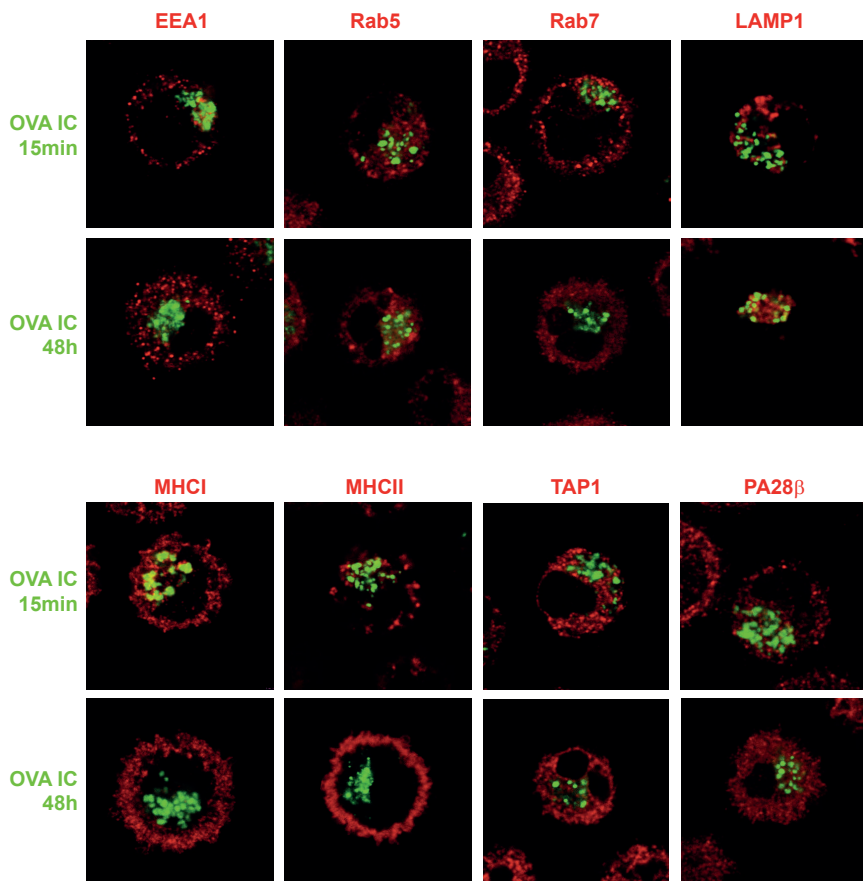
Co-localization	EEA1	Rab5	Rab7	LAMP1	MHCI	MHCII	TAP1	PA28β
OVA IC 15min	+	+	-	-	+	+	-	-
OVA IC 48h	-	-	-	+	-	-	-	-

Figure 2. Characterization of the antigen storage compartments in DCs upon FcγR targeting.
DCs were pulsed with OVA IC (Alexa Fluor 488, green) for 15 min or pulsed with OVA IC for 2 hours and chased for 48 hours. OVA IC presence in DCs was imaged by confocal microscopy and DIC was used to image cell contrast. Specific antibodies against EEA1, Rab5, Rab7, LAMP1, MHCI, MHCII, TAP1, and PA28β (red) were used and analyzed for co-localization with OVA IC. Co-localization between OVA IC and the antibodies is summarized in a table, "+" indicates co-localization, "-" indicates no co-localization.
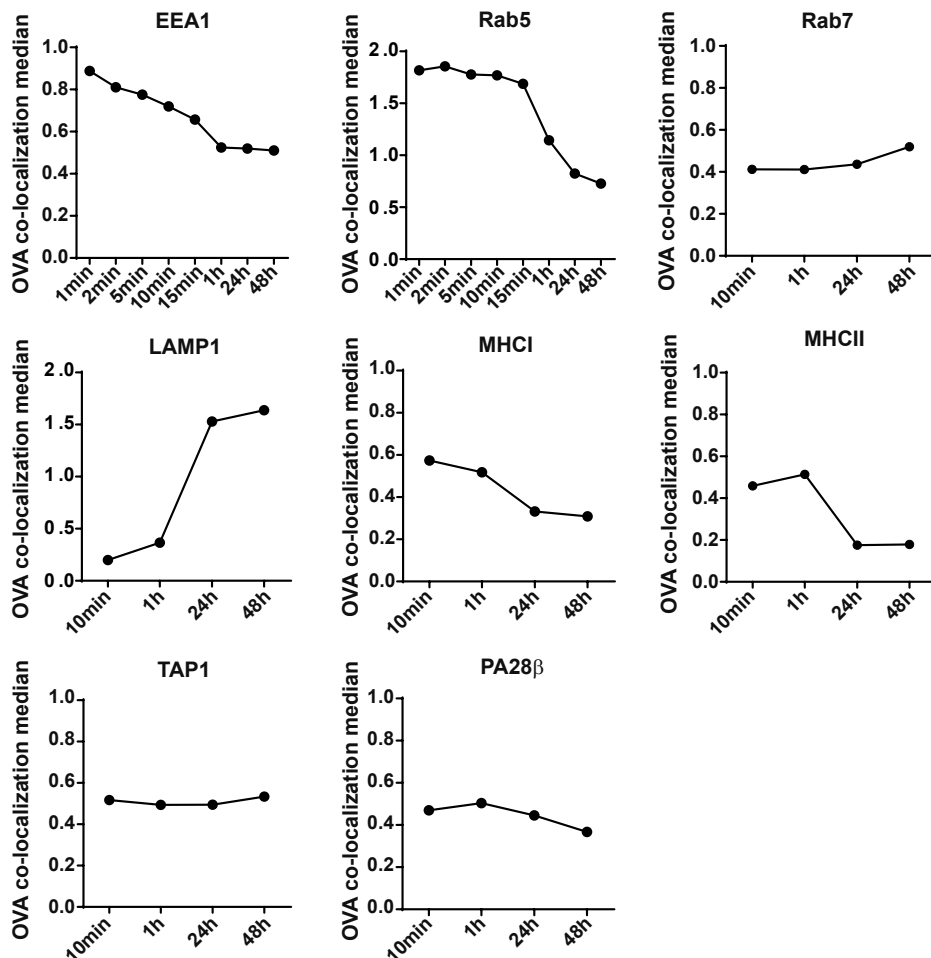
Figure 3. Characterization of the antigen storage compartments in DCs with imaging flow cytometry. DCs were pulsed with OVA IC (Alexa Fluor 647 labeled OVA) for 1, 2, 5, 10, 15 min, or 1 hour (different for each antibody), and pulsed for 2 hours and chased for 24 and 48 hours. Co-localization between OVA IC and EEA1, Rab5, Rab7, LAMP1, MHCI, MHCII, TAP1, and PA28β was analyzed by imaging flow cytometry.

Taken together, we observed that OVA IC enter the early endosomal pathway after uptake by DCs. Besides, OVA IC are present in endosomal compartments that contain MHCI and MHCII at early time points. However, at later time points (24 and 48 hours), OVA IC are stored in LAMP1 positive compartments, distinct from early endosomal and MHCII loading compartments. Since TAP1 and PA28β were not detected in the antigen storage compartments, but shown before to be crucial in antigen processing and cross-presentation (11, 9), this suggests that antigen is translocated from the storage compartments into the cell cytosol for further processing.

Antigen storage compartments contain cathepsin X but no cathepsin S

Since antigen storage compartments can be characterized as lysosomal-like compartments, we investigated the role of lysosomal proteases, such as cysteine cathepsins. The role of cathepsin S in antigen degradation have been described for the vacuolar pathway in DC cross-presentation (4). Whether cysteine cathepsins play a role in endosome-to-cytosol pathway is not excluded. Therefore we investigated the presence of proteolytically active cysteine cathepsins in antigen storage compartments in DCs with the use of the cysteine cathepsin quenched activity-based probe (qABP) BMV109 (12). This intrinsically dark qABP reacts with active cathepsin X, B, S, and L to yield a fluorescent Cy5 conjugate. Lysates of naïve DCs exposed to 1 μM BMV109 for 1 hour were run on 15% PAGE gel and scanned for Cy5 fluorescence to show the presence of active cathepsin X, B, S, and L, with cathepsin S being the most dominantly labeled (Fig. 4A, left lane). Interestingly, after 2 hours OVA IC pulse and 24 hours chase, the amount of cathepsin X was increased compared to immature DCs (Fig. 4A, right lane). We continued to investigate cathepsin S and X with the use of confocal microscopy to analyze their presence in the antigen storage compartments. BMV109 labeling showed partial co-localization with antibody-stained cathepsin S in naïve DCs (Fig. 4B, Supplemental Fig. 2A). DCs that were pulsed with fluorescently labeled OVA IC for 30 min revealed co-localization of OVA IC with BMV109 labeling, but not with cathepsin S (Fig. 4B, Fig. 4D, Supplemental Fig. 2B). After 2 hours OVA IC pulse and 24 hours chase, co-localization between OVA IC and BMV109 labeling was more distinct, but no co-localization was observed with cathepsin S (Fig. 4B, Fig. 4D, Supplemental Fig. 2B). A more detailed kinetic experiment following co-localization of OVA IC with cysteine cathepsin activity and cathepsin X in time revealed that BMV109 labeling and cathepsin X were distributed in the cell cytosol in naïve DCs, but became more clustered to a central location 3 hours after OVA IC uptake (Fig. 4C, Supplemental Fig. 2C). Moreover, after 30 min, one hour, or 2 hours OVA IC pulse, OVA IC were co-localizing with BMV109 fluorescence but not with cathepsin X (Fig. 4C, Fig. 4D, Supplemental Fig. 2D). After 3 hours OVA IC pulse, co-localization between OVA IC and BMV109 labeling, and partial co-localization between OVA IC with cathepsin X was observed. When DCs were pulse-loaded with OVA IC for 2 hours and chased for 24 hours, both the BMV109 fluorescence and cathepsin X were co-localizing with OVA IC (Fig. 4C, Fig. 4D, Supplemental Fig. 2D). These results indicate that the antigen storage compartments in DCs contain cathepsin X and possibly other yet unidentified cathepsins, such as cathepsins B or L.
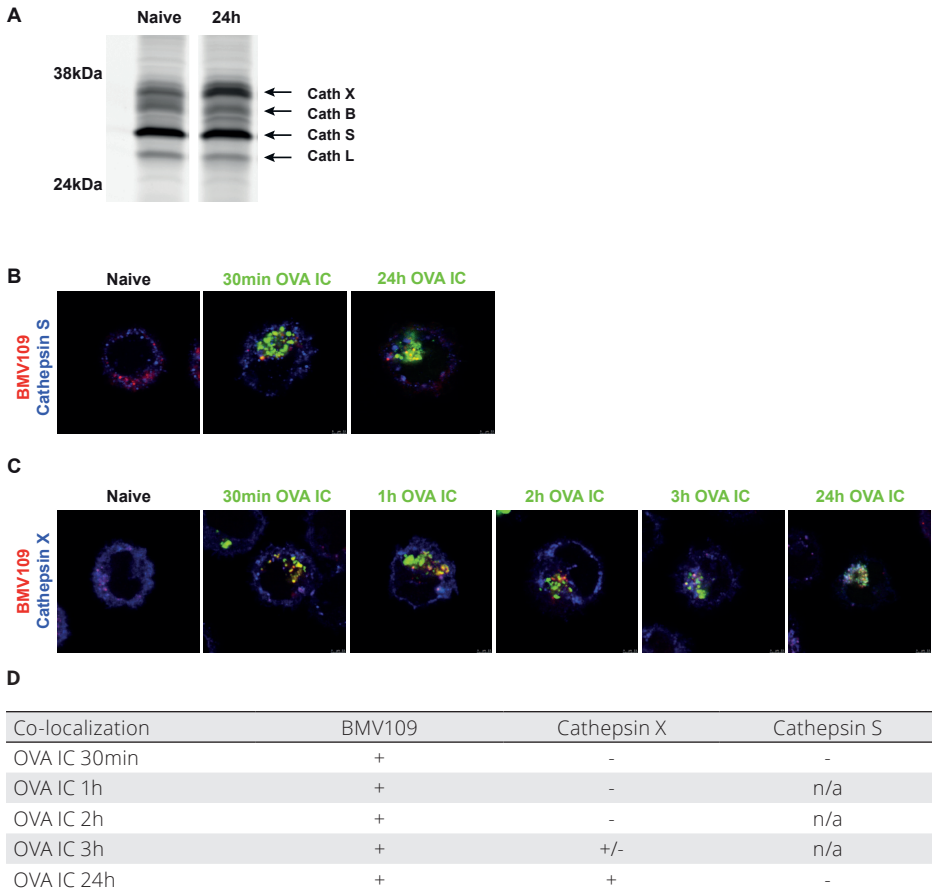
Figure 4. The presence of cathepsins in the antigen storage compartments in DCs. Naïve DCs or DCs pulsed with OVA IC for 2 hours and chased for 24 hours were run on a 15% PAGE gel. Quenched activity-based probe BMV109 was used to stain active cathepsin X, B, S, and L, indicated by arrows **(A)**. Co-localization between BMV109 (red) and specific antibody against cathepsin S (blue) was analyzed in naïve DCs with confocal microscopy. DCs were pulsed with OVA IC (Alexa Fluor 488) for 30 min or pulsed for 2 hours and chased for 24 hours. Co-localization between OVA IC (green), cathepsin S (blue), and BMV109 (red) was analyzed by confocal microscopy **(B)**. Naïve DCs, DCs pulsed with OVA IC (Alexa Fluor 488) for 30 min, 1, 2, 3 hours or DCs pulsed for 2 hours and chased for 24 hours were stained with cathepsin X antibody and BMV109. Co-localization between OVA IC (green), cathepsin X (blue), and BMV109 (red) was analyzed by confocal microscopy **(C)**. Co-localization between OVA IC, BMV109, cathepsin X, and cathepsin S is summarized in a table, "+" indicates co-localization, "+/-" indicates partial co-localization, "-" indicates no co-localization, "n/a" indicates not applicable **(D)**.

Antigen uptake by FcγRs and MGL1 routes the antigen to the same storage compartments

To investigate whether the fate of antigen taken up by a different DC uptake receptor is similar to antigen taken up by FcγRs, we investigated antigen targeting via the C-type lectin receptor MGL1. We have described before that modification of OVA with the glycan-structure

Lewis^x (Le^x) re-directs OVA to MGL1 and induce enhanced T cell cross-priming (13). Here we pulsed DCs with fluorescently labeled OVA IC and OVA-Le^x and followed the antigen in time. Fifteen minutes after antigen pulse, great amounts of both OVA IC and OVA-Le^x were already taken up by DCs (Fig. 5A, Supplemental Fig. 3). Punctuated hotspots of OVA IC and OVA-Le^x were spread through the cell cytosol and showed partial co-localization. After one hour, OVA IC and OVA-Le^x were more compactly distributed in the cell cytosol compared to 15 minutes, still showing partial co-localization (Fig. 5A, Supplemental Fig. 3). More strikingly, after 2 hours pulse loading DCs and 24 hours or 48 hours chase, both OVA IC and OVA-Le^x appeared as concentrated hotspots near the nucleus of DCs (Fig. 5A, Supplemental Fig. 3). Co-localization analysis showed complete overlap of both OVA IC and OVA-Le^x indicating the antigens were present in the same compartments (Supplemental Fig. 3). These results demonstrate that targeting antigen to DCs through FcγRs and MGL1 routes the antigen to the same storage compartments at later time points.

Antigen targeted to MGL1 is stored in LAMP1 positive compartments in DCs

Our previous results suggest that antigen taken up via MGL1 by DCs end up in the same compartments as antigen targeted to FcγRs. To further characterize the routing, DCs were pulsed with fluorescently labeled OVA-Le^x for 15 min or pulsed for 2 hours and chased for 48 hours. Co-staining between OVA-Le^x and several members of the endosomal trafficking and processing pathways was performed and analyzed by confocal microscopy. After 15 min pulse, OVA-Le^x was distributed through the cell cytosol and co-localization with EEA1 and partially with Rab5 was observed (Fig. 5B, Supplemental Fig. 4). After 48 hours, OVA-Le^x was redistributed in a more compact manner located near the nucleus and not co-localizing with either EEA1 or Rab5. No co-localization between OVA-Le^x and Rab7 was observed at the measured time points (Fig. 5B, Supplemental Fig. 4). Since we showed that OVA IC and OVA-Le^x co-localized after 24 hours chase, and we observed co-localization of OVA IC with LAMP1 after 48 hours, one could speculate that OVA-Le^x also ends up in similar LAMP1 positive compartments. Indeed, we observed an overlap of OVA-Le^x with LAMP1 after 48 hours, whereas no co-localization was observed after 15 min antigen pulse (Fig. 5B, Supplemental Fig. 4). Interestingly, OVA-Le^x is present in intracellular MHCI and MHCII positive compartments during the early stage of antigen uptake, but after 48 hours chase both MHCI and MHCII were mainly expressed on the cell surface and not co-localizing with OVA-Le^x (Fig. 5B, Supplemental Fig. 4). Both TAP1 and PA28β did not co-localize with OVA-Le^x regardless of the measured time points (Fig. 5B, Supplemental Fig. 4). These results indicate that OVA-Le^x is following a similar uptake routing as FcγR-targeted OVA IC and both end up in the same LAMP1 positive storage compartments.

Co-localization	EEA1	Rab5	Rab7	LAMP1	MHCI	MHCII	TAP1	PA28β
OVA-Le^x 15min	+	+	-	-	+	+	-	-
OVA-Le^x 48h	-	-	-	+	-	-	-	-
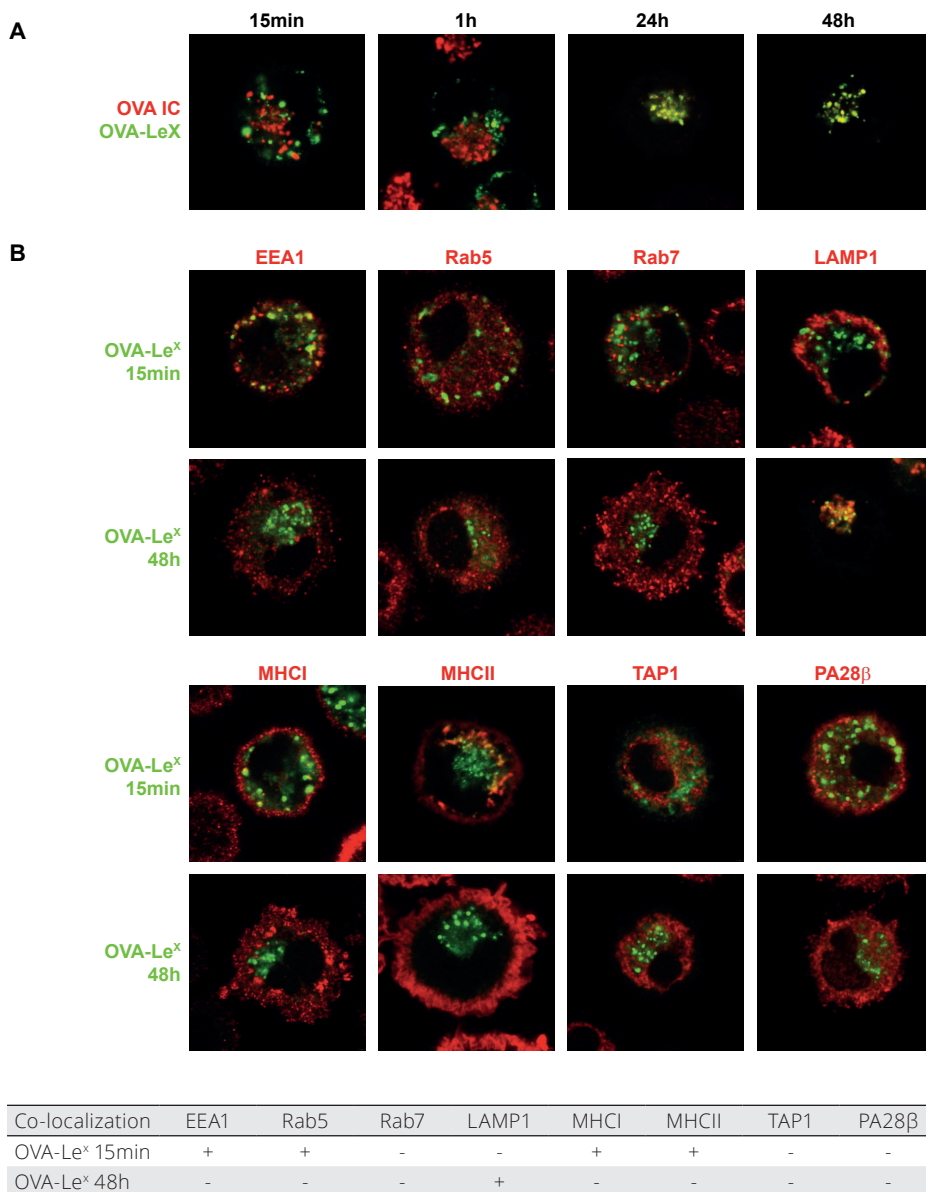
Figure 5. Antigens targeted to FcγRs and MGL1 on DCs end up in the same compartment. DCs were pulsed with OVA IC (Alexa Fluor 647) or OVA-Le^x (Dylight 488) for 15 min and 1 hour, or pulsed for 2 hours and chased for 24 or 48 hours. Co-localization between OVA IC (red) and OVA-Le^x (green) was visualized by confocal microscopy **(A)**. DCs were pulsed with OVA-Le^x (Dylight 488) for 15 min or pulsed with OVA-Le^x for 2 hours and chased for 48 hours. OVA-Le^x presence in DCs was imaged by confocal microscopy and specific antibodies against EEA1, Rab5, Rab7, LAMP1, MHCI, MHCII, TAP1, and PA28β (red) were used and analyzed for co-localization with OVA-Le^x (green). Co-localization between OVA-Le^x and the antibodies is summarized in a table, "+" indicates co-localization, "-" indicates no co-localization **(B)**.

DISCUSSION

We have previously described that antigen can be stored in dendritic cells (DCs) for several days which is beneficial for prolonged antigen presentation to CD8^{+} and CD4^{+} T cells (9). In the current study, we have characterized the storage compartments in DCs by tracking protein antigens targeted to FcγRs and C-type lectin receptor MGL1. Several markers of the endosomal trafficking and antigen processing pathways were investigated for co-localization with fluorescently labeled antibody-bound OVA immune complexes (OVA IC) targeted to FcγRs at different time points and detected by confocal microscopy and imaging flow cytometry. We observed that OVA IC were efficiently taken up by DCs already after 15 min. The antigen first entered early endosomal compartments characterized by the presence of EEA1 and Rab5. Co-localization with MHCI and MHCII was also detected after 15 min OVA IC uptake, suggesting a route for early antigen presentation. However, when DCs were pulse loaded with OVA IC and chased for 48 hours, OVA IC were stored in LAMP1 positive compartments, distinct from EEA1, Rab5 or MHCI/ MHCII loading compartments. Moreover, TAP1 or the proteasomal activator PA28β were not present in the storage compartments. We have shown before that antigen cross-presentation from the storage compartments is TAP1 and proteasome dependent, suggesting that antigen is translocated from the storage compartments into the cytosol for further processing before loading on MHCI (9). It has been reported that in the endosome-to-cytosol pathway antigens need to be transported from endosomal compartments into the cytosol where they are degraded by the proteasome (6, 7). After proteasomal degradation, these derived peptides are further transported by TAP into the ER. However, it has also been reported that some proteasome-generated peptides may be transported back into endocytic compartments and trimmed by IRAP and then directly loaded on MHCI molecules (8).

Lysosomal proteases, such as cathepsin S, are essential for the generation of antigenic peptides for MHCII antigen presentation, Ii degradation and dissociation from MHCII (14, 15). Besides, cathepsin S, B, H, and L redistribute from lysosomes to MHCII-containing endosomal antigen-processing compartments upon DC activation (16). The role of cathepsin S in antigen degradation has been described for the vacuolar pathway in DC cross-presentation (4). Whether cathepsins play a role in endosome-to-cytosol antigen cross-presentation pathway is not reported yet. Here we show that the antigen storage compartments containing OVA IC lack cathepsin S activity, but do possess cathepsin X activity, as determined by qABP (BMV109) labeling of cysteine cathepsin activity in combination with immunofluorescence staining. We observed co-localization of cysteine cathepsin activity with OVA IC already after 30 min uptake. However, staining with antibodies against cathepsin S or cathepsin X did not show any co-localization with OVA IC after 30 min uptake. The storage compartments where

antigen is conserved during later stage were cathepsin S negative but contained cathepsin X, however the presence of other cathepsins could not be ruled out.

Rapid antigen degradation of internalized antigen is assumed to be negatively affecting cross-presentation outcome. It has been demonstrated that DCs expressed lower levels of lysosomal proteases compared to macrophages (17). Expression of cathepsin L, S, D, and B in DC phagosomes was reduced compared to macrophages, which could impair phagolysosomal degradation and sustained antigen stability in DCs. Cathepsin X is predominantly found in monocytes, macrophages, and dendritic cells (18). It has been described that cathepsin X played a role in β2 integrin activation in DCs, which was crucial for affective antigen presentation and initiation of T cell immune response (19). Obermajer *et al.* showed that during DC maturation, cathepsin X translocated to the plasma membrane and enabled Mac-1 activation and cell adhesion (20). Moreover, cathepsin X redistributed from the membrane to the perinuclear region in mature DCs, which coincided with de-adhesion of DCs, cell cluster formation, and acquisition of the mature phenotype. Importantly, they showed that inhibition of cathepsin X in DCs reduced cell surface expression of co-stimulatory molecules, abolished cytokine production, diminished DC migration, and decreased stimulation of CD4+ T cells. However, the role of cathepsin X on DC cross-presentation still needs to be elucidated.

We found similar endosomal trafficking results of fluorescently labeled antigen targeted to the C-type lectin receptor MGL1 compared to FcγRs targeting. The antigen was first present in EEA1/ Rab5 positive early endosomes, containing MHCI and MHCII, but was subsequently stored in LAMP1 positive compartments lacking TAP and PA28β after 48 hours chase. These results indicate that antigen targeted to FcγRs or MGL1 on DCs follows a similar antigen routing pathway, ending up in the same storage compartments. We have published before that MGL1 targeting involved antigen routing to a Rab11/LAMP1 positive compartment and that the cross-presentation is TAP and cathepsin S independent (13). This seems contradictory to our previous results where we showed that antigen cross-presentation after targeting FcγRs is TAP and proteasome dependent (9). However, an important note is that relative early cross-presentation was measured in the MGL1 setting, only 4 hours after antigen pulse, whereas antigen cross-presentation from the storage compartments occurred at later time points, as described for OVA IC targeted to FcγRs after 48 hours chase. Nevertheless, antigen uptake by MGL also induced sustained antigen cross-presentation when measured after 48 hours chase (13). It could be possible that there is a distinction between early and late antigen processing and cross-presentation in DCs. One can speculate that during the early stage after antigen uptake, antigen is processed and loaded on MHCI directly in early endosomes, which is TAP and proteasome independent. In this case, MHCI molecules could be derived from Rab11 positive endosomal recycling compartments (21). However, when antigen stays longer in DCs and resides in LAMP1

4

positive compartments, which lack direct processing and loading machineries, the antigen needs to be translocated from the storage compartments to the cytosol for proteasomal degradation and subsequently transported via TAP to MHCI loading sites.

Since the turnover rate of surface MHCI molecules is shorter compared to MHCII, most MHCI-peptide complexes disappear from the cell surface within 24 hours (9). The migration of DCs after antigen encountering to the T-cell zones might take up to several days, therefore prolonged antigen storage in DCs and sustained supply of newly synthesized MHCI-peptide complexes is beneficial to ensure efficient T-cell cross-priming (10). The current study was performed with *in vitro* cultured BMDCs, however the existence and relevance of antigen storage compartments *in vivo* was confirmed by our previous work where we showed sustained antigen presence in different DC subsets and prolonged cross-presentation *in vivo* (22). The presence of storage compartments was visible after isolation of both CD8α$^+$ and CD8α$^-$ DC subsets after *in vivo* antigen uptake, showing similar punctuated endosomal structures. These DC subsets could efficiently present antigen to CD8$^+$ and CD4$^+$ T cells, respectively. Taken together, our studies indicate the importance of antigen storage compartments in DCs *in vitro* as well as *in vivo*.

Next to direct antigen uptake, processing, and presentation, also carry-over of antigen from one DC type to another is currently accepted as a feasible model of cross presentation *in vivo* (23–25) as the role of multiple DC subsets in T cell priming become more evident (26–29). In this two-step priming model, naïve CD4$^+$ and CD8$^+$ T cells are activated by different DC populations. The activated CD8$^+$ T cells recruit lymph node-resident XCR1$^+$ DCs which receive cross-presented antigen from the DCs that carried out the first priming step (30, 31). The XCR1$^+$ DCs interact with both activated CD4$^+$ and CD8$^+$ T cells and thereby inducing optimal signals for CD8$^+$ T cell differentiation into cytotoxic T lymphocytes (CTLs) and memory CTLs. We speculate that antigen storage compartments may play a central role in these processes between cell types as well since prolonged antigen storage and presentation by DCs would be beneficial for this multi-step T cell priming model.

Here we show that antigen targeted to different uptake receptors on DCs can result in the same antigen routing and ultimately conserved in LAMP1 positive storage compartments. The absence of core components of the antigen processing and loading machineries in these compartments suggest that the main function of the compartments is to store antigen for sustained antigen presentation, which is crucial to elicit prolonged efficient T cell priming. Furthermore, antigen degradation in the storage compartments could be slower due to the lack of cathepsin S. Additional research is needed to determine the role of cathepsin X in antigen storage and DC cross-presentation. The current understanding of the intracellular pathways underlying DC cross-presentation reveals a complex molecular and subcellular interplay.

MATERIALS AND METHODS

Cells and antigen stimulation

Bone marrow-derived dendritic cells (BMDCs) from C57BL/6 mice were generated in the presence of 30% R1 supernatant from NIH3T3 fibroblasts transfected with GM-CSF for 10 days. OVA-IgG immune complexes (OVA IC) were formed by incubating 1 µg/ml OVA (Alex Fluor 488 or 647 conjugated; Life Technologies) and 300 µg/ml anti-OVA IgG (rabbit polyclonal, LSBio) for 30 min at 37^0C. BMDCs were loaded with OVA IC for different time points, as indicated in each experiment. For the pulse-chase experiments, BMDCs were pulsed for 2 hours with OVA IC, washed, and chased for 24 or 48 hours. BMDCs were incubated with 30µg/ml OVA-Le^x (Dylight 488) (kindly gifted by Yvette van Kooyk) for 15 min or pulsed for 2 hours, washed, and chased for 48 hours.

Confocal microscopy

BMDCs were incubated with OVA IC (Alexa Fluor 488, or 647 conjugated) or OVA-Le^x (Dylight 488) for the indicated time points. Cells were washed and transferred to glass bottom dishes (MatTek corporation, Ashland, USA), fixed with 4% formaldehyde (Merck) and permeabilized with 0.5% saponin. Cells were then incubated with one of the following primary antibodies: goat anti-EEA-1 (C-15, Santa Cruz Biotechnology), LAMP-1 (CD107a, Alexa Fluor 647, BioLegend), mouse anti-Rab5 (D11, Santa Cruz Biotechnology), mouse anti-Rab7 (Rab7-117, Sigma-Aldrich), rat anti-MHCI ((H-2D^b, ER-HR 52, Abcam), rat anti-MHCII (I-A/I-E, M5/114.15.2, BioLegend), goat anti-TAP1 (B-8, Santa Cruz Biotechnology), and goat anti-PA28β (L-19, Santa Cruz Biotechnology). The following secondary antibodies were used: goat anti-mouse IgG (H+L) Alexa Fluor 647, rabbit anti-goat IgG (H+L) Alexa Fluor 647, and donkey anti-rat IgG (H+L) Alexa Fluor 647, all from ThermoFisher Scientific. For the cathepsin experiments, BMDCS were incubated with OVA IC (Alexa Fluor 488) for the indicated time points. Cells were fixed and permeabilized as described before and then incubated for 30 min with 1µM cysteine cathepsin activity-based probe BMV109 which was provided by Martijn Verdoes (12). The cathepsin probe covalently reacts with the active site of Cathepsin X, B, S, and L. Once the probe binds to the target enzyme, the quencher is removed and the probe emits the fluorophore Cy5. Co-staining was performed with the following primary antibodies: mouse anti-cathepsin S (E-3, Santa Cruz Biotechnology), and polyclonal goat anti-cathepsin X/Z/P (R&D systems). The following secondary antibodies were used: goat anti-mouse IgG A568 (H+L, ThermoFisher Scientific), and rabbit anti-goat A568 (H+L, ThermoFisher Scientific). The cells were imaged using Leica SP5 STED confocal microscope with a 63x objective lens. Differential interference contrast (DIC) was additionally used to image cell contrast. Images were acquired in 10x magnification and processed with ImageJ software.

4

Imaging flow cytometry

BMDCs were incubated with OVA IC (Alexa Fluor 647) for the indicated time points, fixed with 4% formaldehyde (Merck) and permeabilized with 0.5% Saponin. Cells were stained with primary antibodies as described under the confocal microscopy section and subsequently stained with the following secondary antibodies: goat anti-mouse IgG F(ab')$_2$ Alexa Fluor 488, donkey anti-rat IgG (H+L) Alexa Fluor 488 (both from ThermoFisher Scientific), and rabbit anti-goat IgG Cy3 (Jackson ImmunoResearch). Cells were acquired on an ImageStream X100 (Amnis) imaging flow cytometer. A minimum of 15000 cells was measured per sample at a flow rate ranging between 50 and 100 cells/sec at 60x magnification, the analysis was performed using the IDEAS v6.1 software (Amnis). Cells were first gated based on the Gradient RMS (brightfield) feature and then further gated based on area vs aspect ratio intensity (both on brightfield). The first gating identified the cells which appeared in focus, while the second gating excluded doublets and other cells than BMDCs. Co-localization between OVA IC and the markers was calculated using the bright detail co-localization feature.

Electron microscopy

BMDCs were incubated with OVA IC (Alexa Fluor 488) for 15 min or 2 hours, washed, and chased for 48 hours. Cells were fixed for 2 hours in PHEM buffer containing 2% paraformaldehyde and 0.2% glutaraldehyde. The cells were rinsed in PBS and pelleted in pre-warmed PBS containing 12% gelatin. The cell pellet was prepared for cryo sectioning and immunogold labelling as described elsewhere (32). Briefly, small blocks were cut form the cold cell pellet, which were infiltrated in 2.3M sucrose in phosphate buffer for 3 hours. The cryo-protected samples were plunged in liquid nitrogen and sectioned with a cryo ultramicrotome (Leica, Vienna) using a diamond knife (Diatome, Biel). Ultra-thin sections (70 nm) were labelled with protein A gold (10 nm, CMC, Utrecht) and embedded in 2% methylcellulose in water containing 0.6% uranyl acetate and subsequently air-dried. The sections were imaged in a Tecnai 12 transmission electron microscope (Thermo Fisher) operating at 120kV equipped with a 4K Eagle camera (Thermo Fisher).

Fluorescent SDS-PAGE

BMDCs were left untreated or were incubated with OVA IC for 24 hours and 48 hours. Residual immune complexes were removed by washing with culture medium. Subsequently, cells were incubated with 1 μM quenched activity-based probe BMV109 for 1 hour at 37°C. After washing with PBS total cell lysates were prepared and proteins were separated by SDS-PAGE (200.000 cells/lane) on a 15% polyacrylamide gel. Cy5 labeled cathepsins were measured directly in the gel with the Typhoon Imager.

ACKNOWLEDGEMENTS

4

REFERENCES

1. Fehres, C. M., W. W. J. Unger, J. J. Garcia-Vallejo, and Y. van Kooyk. Understanding the Biology of Antigen Cross-Presentation for the Design of Vaccines Against Cancer. *Front. Immunol.* 2014. 5: 149.
2. Embgenbroich, M., and S. Burgdorf. Current Concepts of Antigen Cross-Presentation. *Front. Immunol.* 2018. 9: 1643.
3. Ho, N. I., L. G. M. Huis in 't Veld, T. K. Raaijmakers, and G. J. Adema. Adjuvants Enhancing Cross-Presentation by Dendritic Cells: The Key to More Effective Vaccines? *Front. Immunol.* 2018. 9: 2874.
4. Shen, L., L. J. Sigal, M. Boes, and K. L. Rock. Important role of cathepsin S in generating peptides for TAP-independent MHC class I crosspresentation in vivo. *Immunity* 2004. 21: 155–165.
5. Kovacsovics-Bankowski, M., and K. L. Rock. A phagosome-to-cytosol pathway for exogenous antigens presented on MHC class I molecules. *Science* 1995. 267: 243–246.
6. Ackerman, A. L., C. Kyritsis, R. Tampe, and P. Cresswell. Early phagosomes in dendritic cells form a cellular compartment sufficient for cross presentation of exogenous antigens. *Proc. Natl. Acad. Sci.* 2003. 100: 12889–12894.
7. Palmowski, M. J., U. Gileadi, M. Salio, A. Gallimore, M. Millrain, E. James, C. Addey, D. Scott, J. Dyson, E. Simpson, and V. Cerundolo. Role of Immunoproteasomes in Cross-Presentation. *J. Immunol.* 2006. 177: 983–990.
8. Saveanu, L., O. Carroll, M. Weimershaus, P. Guermonprez, E. Firat, V. Lindo, F. Greer, J. Davoust, R. Kratzer, S. R. Keller, G. Niedermann, and P. van Endert. IRAP Identifies an Endosomal Compartment Required for MHC Class I Cross-Presentation. *Science* 2009. 325: 213–217.
9. Van Montfoort, N., M. G. Camps, S. Khan, D. V. Filippov, J. J. Weterings, J. M. Griffith, H. J. Geuze, T. van Hall, J. S. Verbeek, C. J. Melief, and F. Ossendorp. Antigen storage compartments in mature dendritic cells facilitate prolonged cytotoxic T lymphocyte cross-priming capacity. *Proc. Natl. Acad. Sci. U. S. A.* 2009. 106: 6730–6735.
10. Henrickson, S. E., T. R. Mempel, I. B. Mazo, B. Liu, M. N. Artyomov, H. Zheng, A. Peixoto, M. P. Flynn, B. Senman, T. Junt, H. C. Wong, A. K. Chakraborty, and U. H. von Andrian. T cell sensing of antigen dose governs interactive behavior with dendritic cells and sets a threshold for T cell activation. *Nat. Immunol.* 2008. 9: 282–291.
11. Ossendorp, F., N. Fu, M. Camps, F. Granucci, S. J. P. Gobin, P. J. van den Elsen, D. Schuurhuis, G. J. Adema, G. B. Lipford, T. Chiba, A. Sijts, P.-M. Kloetzel, P. Ricciardi-Castagnoli, and C. J. M. Melief. Differential Expression Regulation of the α and β Subunits of the PA28 Proteasome Activator in Mature Dendritic Cells. *J. Immunol.* 2005. 174: 7815–7822.
12. Verdoes, M., K. Oresic Bender, E. Segal, W. A. van der Linden, S. Syed, N. P. Withana, L. E. Sanman, and M. Bogyo. Improved quenched fluorescent probe for imaging of cysteine cathepsin activity. *J. Am. Chem. Soc.* 2013. 135: 14726–14730.
13. Streng-Ouwehand, I., N. I. Ho, M. Litjens, H. Kalay, M. A. Boks, L. A. M. Cornelissen, S. K. Singh, E. Saeland, J. J. Garcia-Vallejo, F. A. Ossendorp, W. W. J. Unger, and Y. van Kooyk. Glycan modification of antigen alters its intracellular routing in dendritic cells, promoting priming of T cells. *Elife* 2016. 5: pii: e11765.
14. Nakagawa, T. Y., W. H. Brissette, P. D. Lira, R. J. Griffiths, N. Petrushova, J. Stock, J. D. McNeish, S. E. Eastman, E. D. Howard, S. R. Clarke, E. F. Rosloniec, E. A. Elliott, and A. Y. Rudensky. Impaired invariant chain degradation and antigen presentation and diminished collagen-induced arthritis in cathepsin S null mice. *Immunity* 1999. 10: 207–217.
15. Shi, G. P., J. A. Villadangos, G. Dranoff, C. Small, L. Gu, K. J. Haley, R. Riese, H. L. Ploegh, and H. A. Chapman. Cathepsin S required for normal MHC class II peptide loading and germinal center development. *Immunity* 1999. 10: 197–206.
16. Lautwein, A., T. Burster, A.-M. Lennon-Duménil AM, H. S. Overkleeft, E. Weber, H. Kalbacher, C. Driessen, A.-M. Lennon-Duménil, H. S. Overkleeft, E. Weber, H. Kalbacher, and C. Driessen. Inflammatory stimuli recruit cathepsin activity to late endosomal compartments in human dendritic cells. *Eur. J. Immunol.* 2002. 32: 3348–3357.
17. Delamarre, L., M. Pack, H. Chang, I. Mellman, and E. S. Trombetta. Differential Lysosomal Proteolysis in Antigen-Presenting Cells Determines Antigen Fate. *Science* 2005. 307: 1630–1634.
18. Perišić Nanut, M., J. Sabotič, A. Jewett, and J. Kos. Cysteine cathepsins as regulators of the cytotoxicity of NK and T cells. *Front. Immunol.* 2014. 5: 616.

19. Kos, J., Z. Jevnikar, and N. Obermajer. The role of cathepsin X in cell signaling. *Cell Adh. Migr.* 2009. 3: 164–166.

20. Obermajer, N., U. Svajger, M. Bogyo, M. Jeras, and J. Kos. Maturation of dendritic cells depends on proteolytic cleavage by cathepsin X. *J. Leukoc. Biol.* 2008. 84: 1306–1315.

21. Nair-Gupta, P., A. Baccarini, N. Tung, F. Seyffer, O. Florey, Y. Huang, M. Banerjee, M. Overholtzer, P. A. Roche, R. Tampé, B. D. Brown, D. Amsen, S. W. Whiteheart, and J. M. Blander. TLR signals induce phagosomal MHC-I delivery from the endosomal recycling compartment to allow cross-presentation. *Cell* 2014. 158: 506–521.

22. Ho, N. I., M. G. M. Camps, E. F. E. de Haas, and F. Ossendorp. Sustained cross-presentation capacity of murine splenic dendritic cell subsets in vivo. *Eur. J. Immunol.* 2018. 48: 1164–1173.

23. Allan, R. S., J. Waithman, S. Bedoui, C. M. Jones, J. A. Villadangos, Y. Zhan, A. M. Lew, K. Shortman, W. R. Heath, and F. R. Carbone. Migratory Dendritic Cells Transfer Antigen to a Lymph Node-Resident Dendritic Cell Population for Efficient CTL Priming. *Immunity* 2006. 25: 153–162.

24. Srivastava, S., and J. D. Ernst. Cell-to-cell transfer of M. tuberculosis antigens optimizes CD4 T cell priming. *Cell Host Microbe* 2014. 15: 741–752.

25. Gurevich, I., T. Feferman, I. Milo, O. Tal, O. Golani, I. Drexler, and G. Shakhar. Active dissemination of cellular antigens by DCs facilitates CD8+ T-cell priming in lymph nodes. *Eur. J. Immunol.* 2017. 47: 1802–1818.

26. Eickhoff, S., A. Brewitz, M. Y. Gerner, F. Klauschen, K. Komander, H. Hemmi, N. Garbi, T. Kaisho, R. N. Germain, and W. Kastenmüller. Robust Anti-viral Immunity Requires Multiple Distinct T Cell-Dendritic Cell Interactions. *Cell* 2015. 162: 1322–1337.

27. Hor, J. L., P. G. Whitney, A. Zaid, A. G. Brooks, W. R. Heath, and S. N. Mueller. Spatiotemporally Distinct Interactions with Dendritic Cell Subsets Facilitates CD4+ and CD8+ T Cell Activation to Localized Viral Infection. *Immunity* 2015. 43: 554–565.

28. Kitano, M., C. Yamazaki, A. Takumi, T. Ikeno, H. Hemmi, N. Takahashi, K. Shimizu, S. E. Fraser, K. Hoshino, T. Kaisho, and T. Okada. Imaging of the cross-presenting dendritic cell subsets in the skin-draining lymph node. *Proc. Natl. Acad. Sci. U. S. A.* 2016. 113: 1044–1049.

29. Borst, J., T. Ahrends, N. Bąbała, C. J. M. Melief, and W. Kastenmüller. CD4+ T cell help in cancer immunology and immunotherapy. *Nat. Rev. Immunol.* 2018. 18: 635–647.

30. Bachem, A., S. Güttler, E. Hartung, F. Ebstein, M. Schaefer, A. Tannert, A. Salama, K. Movassaghi, C. Opitz, H. W. Mages, V. Henn, P.-M. Kloetzel, S. Gurka, and R. A. Kroczek. Superior antigen cross-presentation and XCR1 expression define human CD11c+CD141+ cells as homologues of mouse CD8+ dendritic cells. *J. Exp. Med.* 2010. 207: 1273–1281.

31. Brewitz, A., S. Eickhoff, S. Dähling, T. Quast, S. Bedoui, R. A. Kroczek, C. Kurts, N. Garbi, W. Barchet, M. Iannacone, F. Klauschen, W. Kolanus, T. Kaisho, M. Colonna, R. N. Germain, and W. Kastenmüller. CD8 + T Cells Orchestrate pDC-XCR1 + Dendritic Cell Spatial and Functional Cooperativity to Optimize Priming. *Immunity* 2017. 46: 205–219.

32. Peters, P. J., E. Bos, and A. Griekspoor. Cryo-immunogold electron microscopy. *Curr. Protoc. cell Biol.* 2006. Chapter 4: Unit 4.7.

4
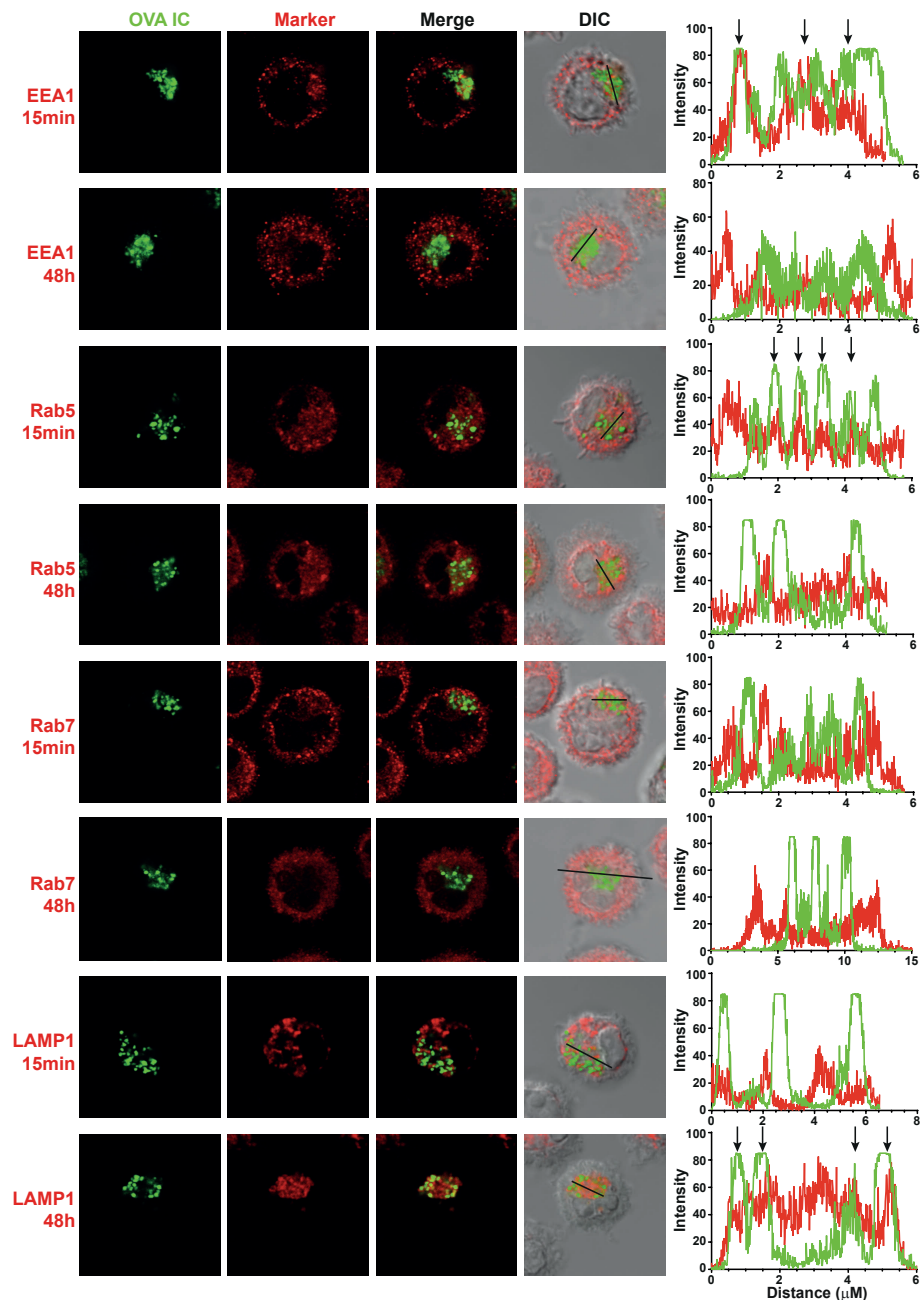
Supplemental Figure 1. Characterization of the antigen storage compartments in DCs upon FcγR targeting. DCs were pulsed with OVA IC (Alexa Fluor 488, green) for 15 min or pulsed with OVA IC for 2 hours and chased for 48 hours. OVA IC presence in DCs was imaged by confocal microscopy and DIC was used to image cell contrast. Specific antibodies against EEA1, Rab5, Rab7, LAMP1, MHCI, MHCII, TAP1, and PA28β (red) were used and analyzed for co-localization with OVA IC (green). Histograms for each fluorophore were created for a selected area (indicated by a line on the image) and overlays were made with the ImageJ software. Arrows indicate co-localization between OVA IC (green) and the specific antibody (red).
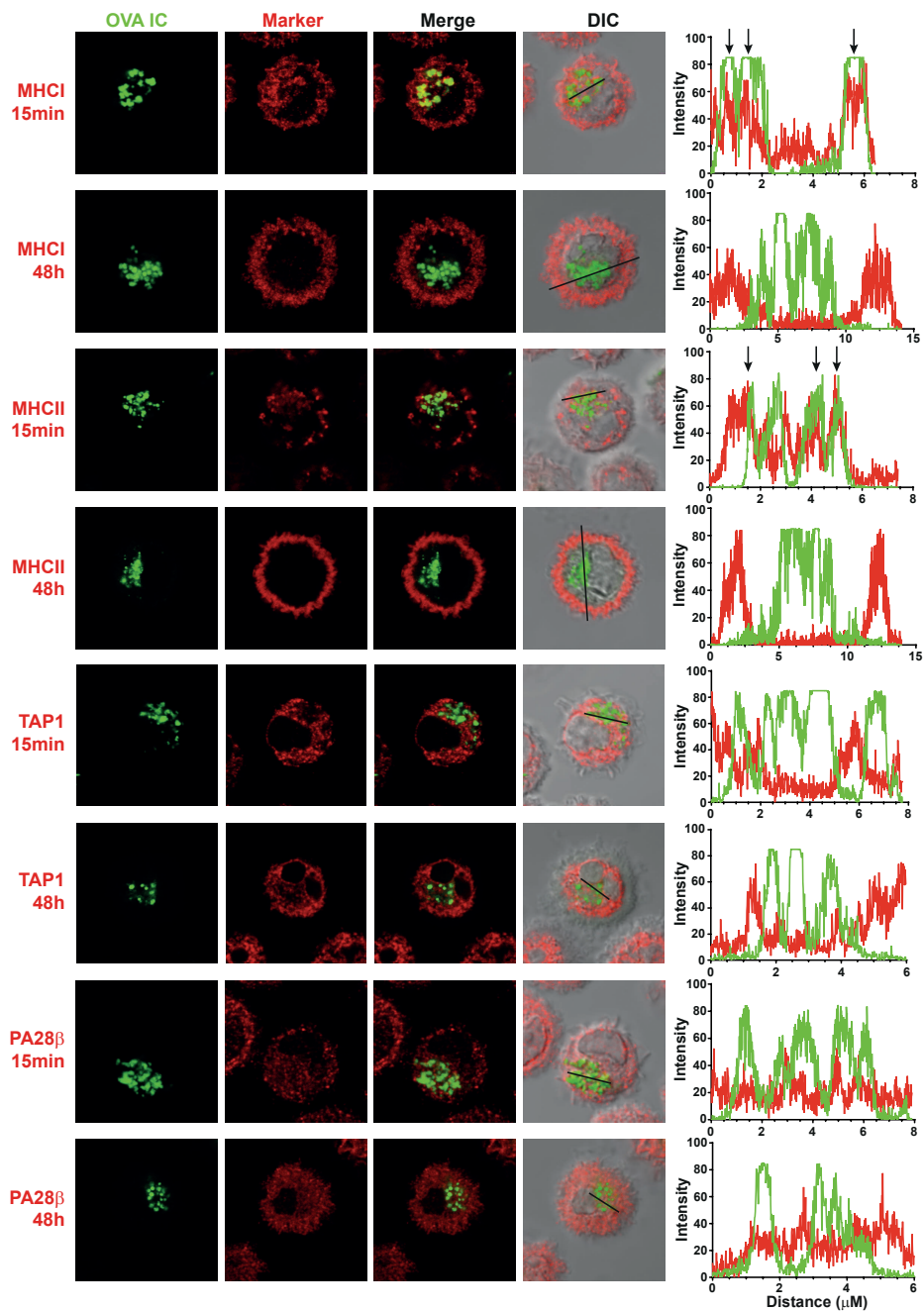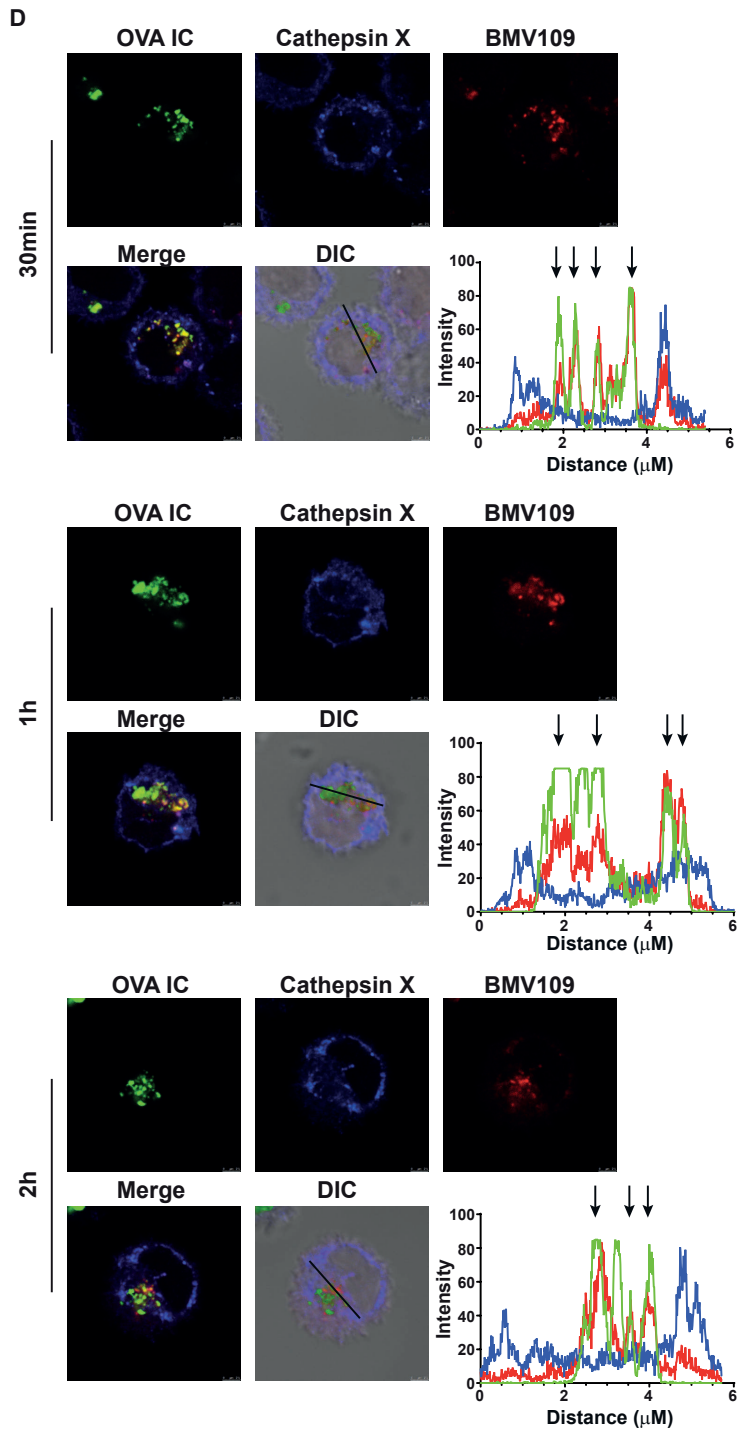
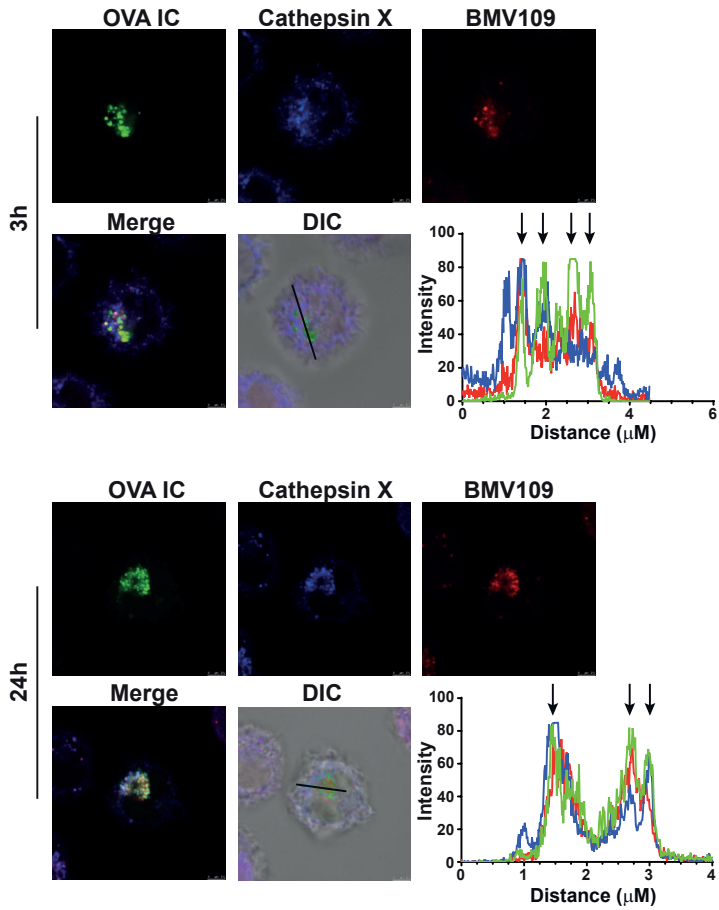**Supplemental Figure 1. Continued.**
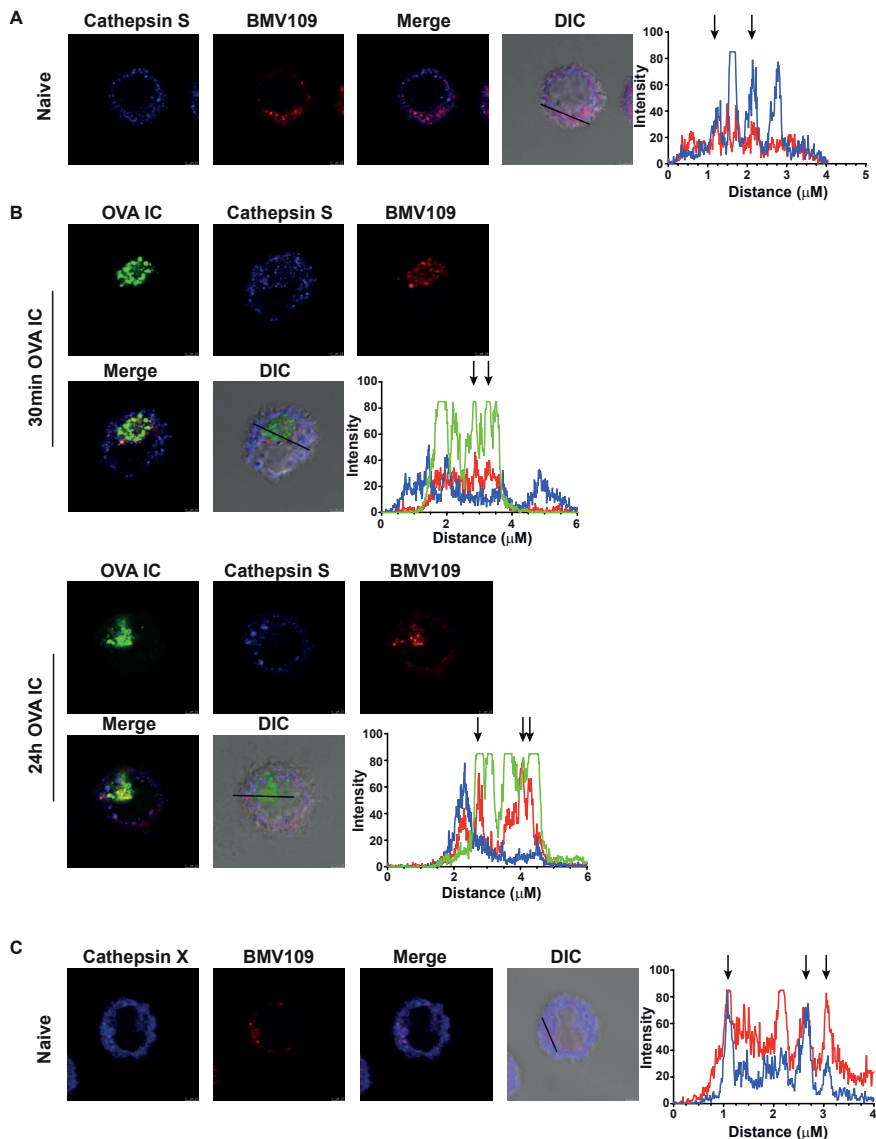
Supplemental Figure 2. The presence of cathepsins in the antigen storage compartments in DCs. Co-localization between quenched activity-based probe BMV109 and specific antibody against cathepsin S was analyzed in naïve DCs with confocal microscopy and DIC was used to image cell contrast. Histograms for each fluorophore were created for a selected area (indicated by a line on the image) and overlays were made with the ImageJ software. Arrows indicate co-localization between cathepsin S (blue) and BMV109 (red) **(A)**. DCs were pulsed with OVA IC (Alexa Fluor 488) for 30 min or pulsed for 2 hours and chased for 24 hours. Co-localization between OVA IC (green), cathepsin S (blue), BMV109 (red) was analyzed by confocal microscopy and indicated by arrows **(B)**. Co-localization between BMV109 and specific antibody against cathepsin X was analyzed in naïve DCs with confocal microscopy. Arrows indicate co-localization between cathepsin X (blue) and BMV109 (red) **(C)**. DCs pulsed with OVA IC (Alexa Fluor 488) for 30 min, 1, 2, 3 hours or DCs pulsed for 2 hours and chased for 24 hours were stained for cathepsin X or BMV109. Co-localization between OVA IC (green), cathepsin X (blue) or BMV109 (red) was analyzed by confocal microscopy and indicated by arrows **(D)**.

Supplemental Figure 2. Continued.

Supplemental Figure 2. Continued.
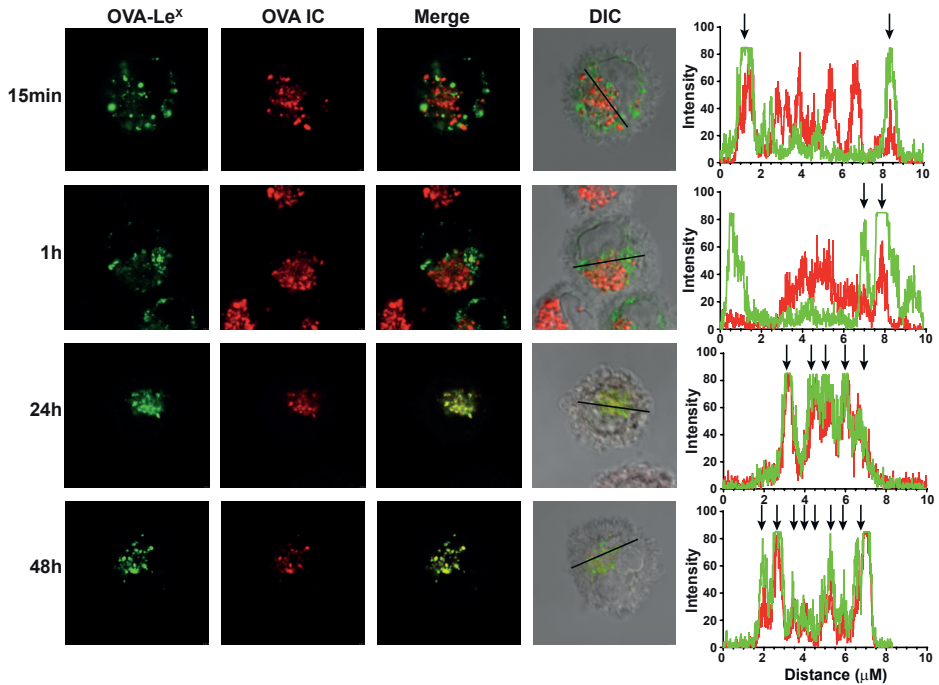
Supplemental Figure 3. Antigens targeted to FcγRs and MGL1 on DCs end up in the same compartment. DCs were pulsed with OVA IC (Alexa Fluor 647) or OVA-Le^x (Dylight 488) for 15 min and 1 hour, or pulsed for 2 hours and chased for 24 or 48 hours. Co-localization between OVA IC and OVA-Le^x was visualized by confocal microscopy and DIC was used to image cell contrast. Histograms for each fluorophore were created for a selected area (indicated by a line on the image) and overlays were made with the ImageJ software. Arrows indicate co-localization between OVA IC (red) and OVA-Le^x (green).
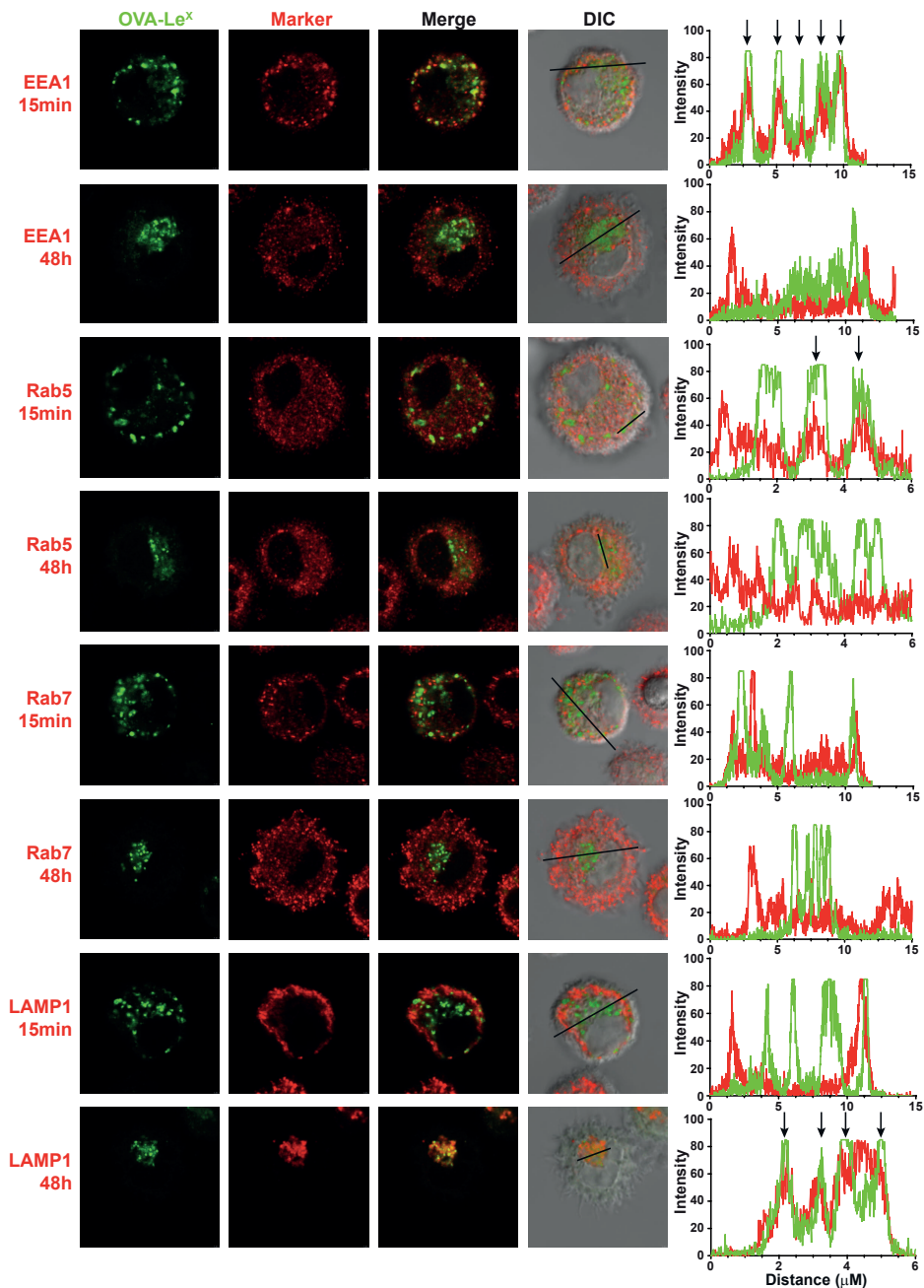
Supplemental Figure 4. Characterization of the antigen storage compartments in DCs upon MGL1 targeting. DCs were pulsed with OVA-Le^x (Dylight 488) for 15 min or pulsed with OVA-Le^x for 2 hours and chased for 48 hours. OVA-Le^x presence in DCs was imaged by confocal microscopy and DIC was used to image cell contrast. Specific antibodies against EEA1, Rab5, Rab7, LAMP1, MHCI, MHCII, TAP1, and PA28β (red) were used and analyzed for co-localization with OVA-Le^x (green). Histograms for each fluorophore were created for a selected area (indicated by a line on the image) and overlays were made with the ImageJ software. Arrows indicate co-localization between OVA-Le^x (green) and the specific antibody (red).
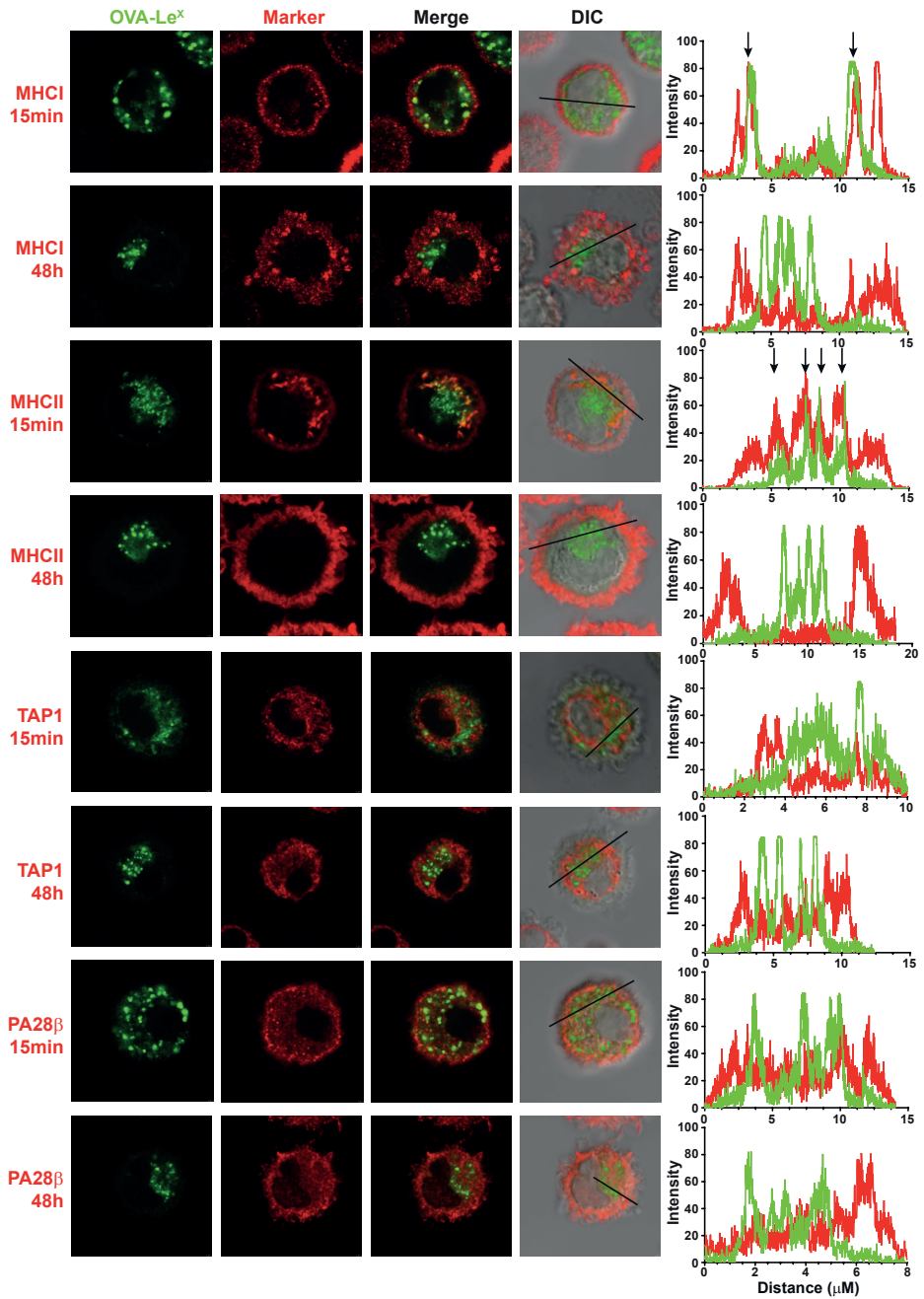
Supplemental Figure 4. Continued.

Glycan modification of antigen alters its intracellular routing in dendritic cells, promoting priming of T cells

Ingeborg Streng-Ouwehand, Nataschja I. Ho, Manja Litjens, Hakan Kalay, Martine A. Boks, Lenneke A.M Cornelissen, Satwinder Kaur Singh, Eirikur Saeland, Juan J. García-Vallejo, Ferry Ossendorp, Wendy W.J. Unger, Yvette van Kooyk

ABSTRACT

Antigen uptake by dendritic cells and intracellular routing of antigens to specific compartments is regulated by C-type lectin receptors that recognize glycan structures. We show that modification of Ovalbumin (OVA) with the glycan-structure Lewis^X (Le^X) re-directs OVA to the C-type lectin receptor MGL1. Le^X-modification of OVA favored Th1 skewing of CD4$^+$ T cells and enhanced cross-priming of CD8$^+$ T cells. While cross-presentation of native OVA requires high antigen dose and TLR stimuli, Le^X modification reduces the required amount 100-fold and obviates its dependence on TLR signaling. The OVA-Le^X induced enhancement of T cell cross-priming is MGL1-dependent as shown by reduced CD8$^+$ effector T cell frequencies in MGL1-deficient mice. Moreover, MGL1-mediated cross-presentation of OVA-Le^X neither required TAP-transporters nor cathepsin S and was still observed after prolonged intracellular storage of antigen in Rab11$^+$LAMP1$^+$ compartments. We conclude that controlled neo-glycosylation of antigens can crucially influence intracellular routing of antigens, the nature and strength of immune responses and should be considered for optimizing current vaccination strategies.

INTRODUCTION

The induction of T cell immunity to viruses or tumors involves the presentation of viral or tumor antigens by antigen-presenting cells (APC) in the context of major histocompatibility complex (MHC) molecules. Loading of exogenously-derived antigens onto MHC class I molecules, a process known as cross-presentation (1) is required to activate antigen-specific CD8$^+$ T cells. Furthermore, cognate CD4$^+$ T cell help is important for licensing the APC, which is essential for effective CD8$^+$ T cell priming and induction of long-lasting memory (2, 3). The molecular mechanisms underlying cross-presentation have been studied intensively, however, little is still known on the nature of the antigens and stimuli that are required for APC to route exogenous antigens efficiently into the MHC class I presentation pathway. Most exogenous antigens that originate from tumor cells or viruses are glycosylated in their native form (4). The relative composition of the glycosylation machinery, which includes all the necessary glycosylation-related enzymes and co-factors, determines the final configuration of the glycan structures that decorate *N*- or *O*-linked glycosylation sites present in glycoproteins. The glycosylation machinery can be affected by multiple physio-pathological cues, including proliferation, activation, and the transformation status of the cell (5), and depends on environmental factors. APC, such as dendritic cells (DCs) and macrophages are able to sense glycans exposed on either self- or pathogen-derived antigens via glycan-binding proteins. Amongst these glycan-binding proteins are C-type lectin receptors (CLRs) that recognize defined carbohydrate-structures through their carbohydrate recognition domain (CRD). Depending on the amino acid sequence, the CRD bears specificity for mannose, fucose, galactose, sialylated-, or sulfated structures. CLRs function both as antigen uptake and/or signaling receptors that modify DC-induced cytokine responses thereby influencing T cell differentiation (6). The specialized internalization motifs in the cytoplasmic domains of CLRs allow the rapid internalization of antigens upon interaction (7, 8). This suggests that DCs use CLRs to "sense" the natural glycan composition of tissues and invading pathogens and, in response to this recognition, are able to modulate immune responses (9).

    The conjugation of antigens to CLRs-specific antibodies, such as DEC205, mannose receptor (MR), Dendritic Cell-Specific Intercellular adhesion molecule-3-Grabbing Non-integrin (DC-SIGN) or CLEC9A, has proven to be an effective way to direct antigens to DCs, resulting in enhanced antigen uptake and presentation on MHC molecules (10–13). Also glycans specific for CLRs have shown their targeting specificity and potential to improve antigen uptake and presentation in MHC class I and II molecules when coupled to antigen formulations (14–20). To achieve immunity rather than tolerance inclusion of a strong adjuvant is necessary. Little is known on how naturally glycosylated antigens or alterations

in the glycosylation of antigens may change and re-direct antigen internalization via CLRs, in addition to subsequent processing and presentation.

MR was shown to mediate cross-presentation of the model-antigen ovalbumin (OVA) in a Toll-like receptor (TLR)-dependent manner and to recruit TAP-1 to endocytic organelles (21, 22). Importantly, cross-presentation of OVA was only effective using high amounts of antigen (21, 22). The interaction of OVA with MR, which has specificity for mannose (23), was speculated to be dependent on the presence of mannose glycans on OVA (22). In the current study, we investigated the effect of modifying the glycan composition of OVA on the efficacy of cross-presentation, priming and differentiation of T cells. We hypothesized that modification of the antigen with specific glycans would re-direct antigens to other CLRs resulting in altered intracellular routing and presentation of antigen and Th differentiation. We have chosen to conjugate the carbohydrate structure Lewis[x] (Le[x]) to 2 free cysteine residues within the native OVA glycoprotein. Le[x] is a ligand of the murine C-type lectin macrophage galactose-type lectin (MGL)-1 (24), which is expressed on murine plasmacytoid DCs, CD8^{+} and CD8^{-} splenic DCs, DCs in the small intestines, the sub-capsular and intra-follicular sinuses of T cell areas in lymph nodes, and on DCs and macrophages in the dermis of skin (25–28). Murine MGL1 is one of two homologues (MGL1 and MGL2) of human MGL (huMGL), which has been shown to interact with tumor cells through glycans exposed on MUC1 as well as with various pathogens (29). However, MGL1 and MGL2 bind different glycan structures: while MGL1 binds Le[x] and Le[a] glycans, MGL2 binds N-acetylgalactosamine (GalNAc) and galactose glycan structures (24). The YENF motif in the cytoplasmic tail of huMGL is essential for uptake of soluble antigens, which are subsequently presented to CD4^{+} T cells (30). Murine MGL1 contains a similar motif (YENL) in its cytoplasmic tail, which likely plays a similar and important role in antigen uptake (31). Glycan binding to the CLRs DC-SIGN, Dectin-1 and Dectin-2 has been demonstrated to trigger the signaling capacity of these receptors, modulating DC-mediated T helper cell (Th) differentiation and cytokine production by DCs (9). This illustrates that glycan epitopes may not only improve antigen presentation, but may also affect Th differentiation and shape specific adaptive immune responses. This is underlined by the observation that DC-SIGN signaling induced upon sensing of specific mannose or fucose structures on pathogens differentially directed Th differentiation (32).

Here, we demonstrate that conjugation of the Le[x] carbohydrate to the model antigen OVA alters its routing from a MR- and TAP-1-dependent cross-presentation pathway into a TAP-1- and cathepsin S-independent pathway, devoid of any TLR-signaling dependence, which simultaneously enhanced CD8^{+} T cell priming and Th1 skewing of CD4^{+} T cells. Cross-presentation was associated with prolonged intracellular storage of antigen in Rab11^{+}LAMP1^{+} vesicles. Our results illustrate that small changes in the glycosylation profile of protein antigens can have a great impact on antigen routing within DCs, affecting cross-presentation and Th cell differentiation.

RESULTS

Identification of glycans on native and glycan-modified OVA, and the consequences for CLR-specific binding and cross-presentation

The well-known model antigen OVA carries one *N*-glycosylation site at N293 and, although the variety of OVA glycans have been previously described, their relative abundance has never been characterized in detail. We determined the glycan profile of OVA by normal-phase HPLC coupled to electrospray ionization mass spectrometry with an intercalated fluorescence detector. We found that the majority of glycan species on OVA corresponded to the complex-type (54.9%), while mannose-rich glycans (mainly Man5 and Man6, potential ligands of the MR (33) represented only 23% of all glycoforms (Figure 1A). The remaining glycoforms were of the hybrid (16.2%) and oligomannose (Man3, 3%) type. The presence of mannose rich glycans on OVA correlate with the earlier reports that in particular MR interacted with OVA (34) and mediated the TLR dependent and TAP-1 dependent cross-presentation of OVA (21). We reasoned that the conjugation of additional glycans to OVA would alter its CLR-dependent effects. To do this, we conjugated the tri-saccharide glycan structure Le[x] (Galβ1-4(Fucα1-3)GlcNAc) to the free cysteins of OVA using standard thiol-maleimide chemistry via the bifunctional crosslinker MPBH. Le[x] is a well characterized carbohydrate ligand of the C-type lectin MGL1 (11, 24). Using mass spectrometry (MALDI-TOF/TOF), we confirmed that OVA-Le[x] increases to 1.2 KDa in mass, indicating that at least 40 % of the total OVA-Le[x] preparation contained the Le[x] (Figure 1-figure supplement 1). This increase corresponded to the addition of two Le[x] molecules per OVA molecule. Furthermore, using anti-Le[x] antibodies the presence of Le[x] was detected on OVA-Le[x], whereas absent on native glycosylated OVA, indicating that the glycan was successfully conjugated to OVA (Figure 1B). While native OVA interacted with the MR (MR-Fc, Figure 1B) and as earlier described (22), the conjugation of Le[x] to OVA conferred high-avidity binding to MGL1 as revealed using the soluble recombinant form of MGL1 (MGL1-Fc, Figure 1B). Moreover, the addition of Le[x] to OVA did not result in increased binding to the MR binding, indicating that Le[x] selectively binds MGL1. Similar binding with an anti-OVA antibody was determined, which indicates that similar protein concentrations in the preparations of OVA and OVA-Le[x] used in our study are present (Figure 1B, right panel). In conclusion, through glycan profiling we identified 23% mannose-rich glycans on native OVA that may facilitate MR binding. Addition of the glycan Le[x], next to these mannose glycans, on cysteine residues (two Le[x] moieties per molecule), conveyed MGL1 specificity to OVA.

5
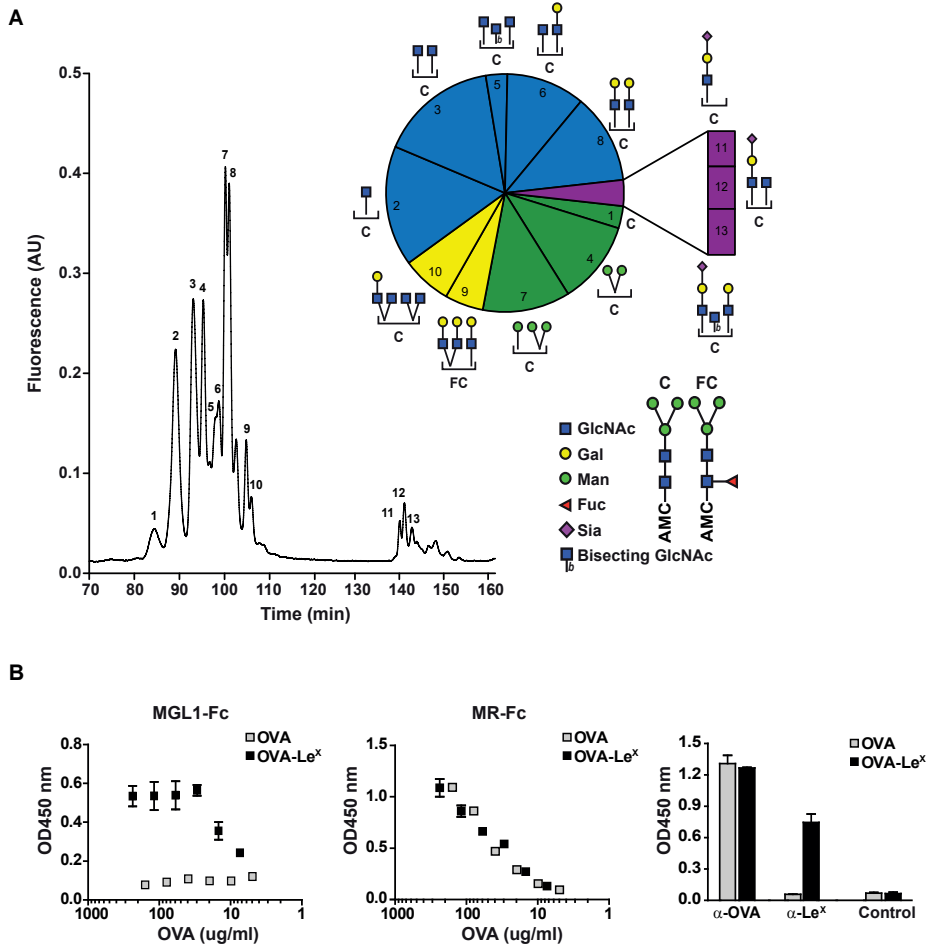
Figure 1. Generation of OVA-neo-glycoconjugates with Le^x that confers binding of OVA to MGL1.
(**A**) A glycan profile of OVA was generated using a multidimensional normal phase nano-HPLC coupled to an electrospray ionization interface mass spectrometer with an intercalated nanofluorescence detector. The different glycan species, indicated by numbers, are shown on the right; their relative proportion is represented in a pie chart. (**B**) ELISA showing functional modification of OVA with Le^x glycans, as detected with anti-Le^x antibodies and resulting in binding of MGL1-Fc. Unconjugated OVA does not carry any ligands for MGL1. Modification of OVA with Le^x did not alter the ability to bind to MR as illustrated by equal binding kinetics of MR-Fc to native OVA and OVA-Le^x. OVA and OVA-Le^x preparations contain similar amounts of OVA as detected with anti-OVA antibodies.

OVA-Le^x binds MGL1 and augments priming of OVA-specific CD8^+ T cells in-vivo

We explored the potency of OVA-Le^x to enhance T cell priming *in vivo*. Since DCs are crucial for priming of naive T cells, we first established the presence of MGL on both splenic and bone marrow-derived DCs (spDCs and BM-DCs) of C57BL/6 mice by staining with the anti-

MGL antibody ER-MP23 (Figure 2A). Since the ER-MP23 antibody does not discriminate between the two murine MGL homologues MGL1 and MGL2, MGL1 expression in wild type (WT) CD11c$^+$ DCs was confirmed using qRT-PCR (Figure 2B). Immunization of mice with OVA-Le^x mixed with agonistic anti-CD40 antibodies resulted in the enhanced priming of OVA-specific CD8$^+$ T cells as revealed from both higher numbers of OVA/H-2K^b tetramer binding CD8$^+$ T cells and OVA-specific IFN-γ and TNF-producing CD8$^+$ T cells than obtained with native OVA (Figure 2C, Figure 2-figure supplement 1). Using MGL1 KO mice, that lack MGL1 expression on DCs (Figure 2B), we ascertained that MGL1 is the prime lectin involved in boosting the generation of antigen-specific effector T cells as upon immunization of these mice with Le^x-conjugated OVA no enhanced frequencies of OVA-specific IFN-γ and TNFα-double-producing T cells were detected (Figure 2D, Figure 2-figure supplement 2). In fact, the OVA-Le^x immunized MGL1 KO mice displayed comparable numbers of effector T cells as WT mice immunized with native OVA. Together, these data show that the conjugation of two Le^x glycans on OVA re-directs OVA to the CLR MGL1 and thereby enhances CD8$^+$ T cell priming *in vivo.*

OVA-Le^x induces Th1 skewing of naive CD4$^+$ T cells

Since we observed that Le^x-modified OVA increased priming of antigen-specific CD8$^+$ T cells we examined whether this also enhanced antigen-presentation to CD4$^+$ T cells. Both OVA-Le^x-loaded and native OVA-loaded spDCs induced CD4$^+$ OT-II T cell proliferation to a similar extent (Figure 3A), illustrating that the altered antigen uptake mediated by Le^x did not affect loading on MHC class II molecules. Similar results were obtained using BM-DCs (Figure 3A). Although we did not observe any differential effect of Le^x on CD4$^+$ T cell expansion, neoglycosylation of antigens could induce signaling via CLRs and herewith potentially influence Th cell differentiation (32). We therefore investigated whether OVA-Le^x affected the differentiation of naive CD4$^+$ T cells. Hereto BM-DCs and spDCs of C57BL/6 mice were pulsed with OVA-Le^x and subsequently co-cultured with naive CD4$^+$CD62L^{hi} OT-II cells. Co-cultures containing OVA-Le^x loaded BM-DCs or spDCs contained significantly more IFN-γ-producing T cells than those containing OVA-loaded DCs (Figure 3B). Neither induction of IL-4- nor IL-17A-producing CD4$^+$ T cells was observed (Figure 3B, upper and middle panel and data not shown). In addition, induction of Foxp3$^+$ T cells was not detected (data not shown). To exclude that the Th1 skewing by OVA-Le^x loaded DCs was attributed to the more Th1 prone status of C57BL/6 (35), we also performed the Th-differentiation assay with cells derived from Th2 prone BALB/c mice (36). We observed that naive OVA-specific CD4$^+$ T cells from DO11.10 Tg mice that were stimulated with OVA-loaded BM-DCs differentiated into IL-4 secreting T cells (Figure 3B, lower panels). However, the generation of IL-4-producing T cells was not influenced by loading DCs with OVA-Le^x as these cultures contained comparable percentages of IL-4-producing DO11.10 T cells. Using these Th2-prone T cells, OVA-Le^x-pulsed
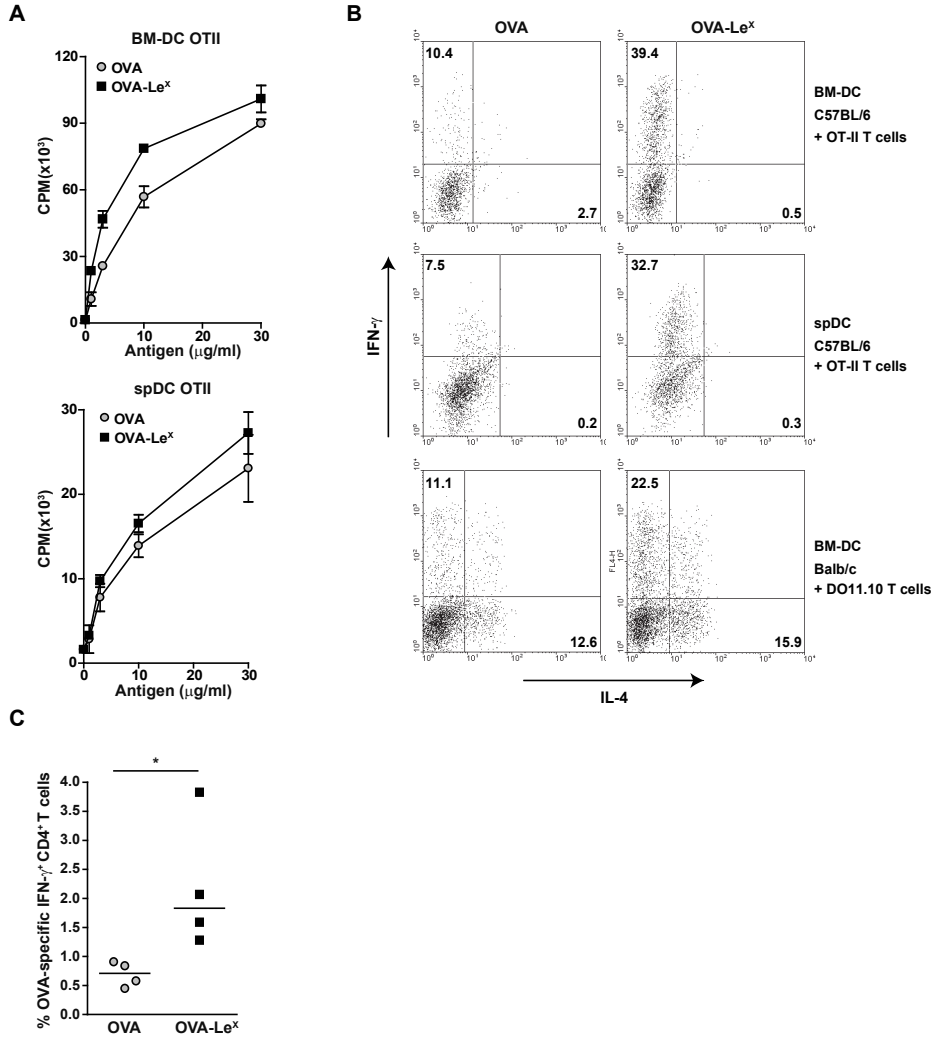
5

DCs still induced considerably more IFN-γ-producing CD4$^+$ T cells than native OVA-pulsed DCs (Figure 3B, lower panel). Since this assay takes three days longer than the antigen-presentation assay, it is possible that the higher frequency of IFN-γ-producing CD4$^+$ T cells is due to increased division of OVA-specific CD4$^+$ T cells. However, we found that the amount of proliferation of OVA-specific CD4$^+$ T cells induced by stimulation with OVA-Le^x-loaded DCs after 6 days is similar to that induced by OVA-loaded DCs (Figure 3-figure supplement 1). The augmented induction of CD4$^+$ Th1 cells was also observed *in vivo* as revealed from the higher frequencies of IFN-γ-producing OVA-specific CD4$^+$ T cells in the spleens of OVA-Le^x immunized mice than in mice immunized with native OVA (Figure 3C, Figure 3-figure supplement 2). These data indicate that the increased numbers of Th1 cells induced by OVA-Le^x-loaded DCs are not due to increased proliferation of OT-II cells, but probably due to MGL1-mediated signaling.

MGL1 mediates cross-presentation of OVA-Le^x independently of TLR signaling

Since we observed a great enhancement of antigen-specific CD8$^+$ T cell priming *in vivo* when immunizing with OVA-Le^x to target MGL1, we wanted to reveal the mechanism that regulates this augmented cross-priming. The internalization of OVA by BM-DCs was significantly increased when OVA was modified with Le^x (Figure 4A, Figure 4-figure supplement 1). To investigate whether the addition of Le^x glycans affected the efficiency of cross-presentation of OVA by DCs, we loaded murine BM-DCs or spDCs with OVA-Le^x and measured their potency to present OVA-derived peptides in MHC class I by measuring the proliferation of OVA-specific OT-I T cells. Strikingly, both BM-DCs as well as spDCs induced substantially more proliferation of OT-I T cells when they were pulsed with OVA-Le^x compared to native OVA (Figure 4B, Figure 4-figure supplement 2). Even at low concentrations of antigen (*i.e.* 7.5 µg/ml), the proliferating OT-I T cells were doubled (30% to 60%) using OVA-Le^x compared to using OVA (Figure 4B), indicating that the modification of OVA with Le^x greatly affected the cross-presentation of OVA. Moreover, detection of SIINFEKL/H-2K^b complexes on the cell membrane of OVA-Le^x-loaded DCs by staining with the 25.1D1 antibody confirmed enhanced antigen loading on MHC-I molecules and transportation to the cell-surface of internalized OVA-Le^x compared to native OVA (Figure 4C, Figure 4-figure supplement 3). Cross-presentation of OVA-Le^x was clearly mediated by MGL1 as demonstrated using MGL1 KO BM-DCs or steady-state spDCs (Figure 4D).
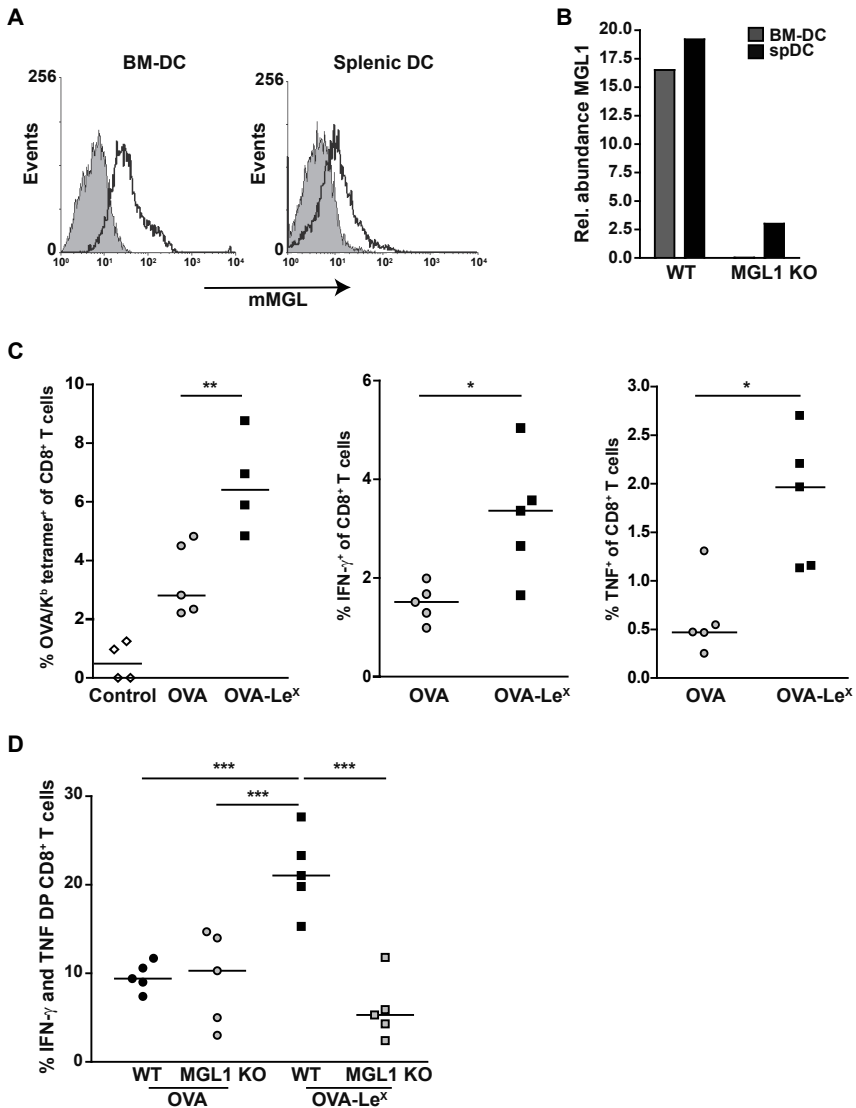
Figure 2. Immunization with OVA-Le^x induces increased CD8+ T cell responses *in vivo*. (**A**) Expression of murine MGL on BM-DCs and CD11c+ spDCs was analyzed by flow cytometry. (**B**) MGL1 mRNA expression by BM-DCs and splenic DCs from WT and MGL1 KO mice was determined using qRT-PCR. GAPDH was used as a reference gene and results are representative of three independent experiments. (**C**) C57BL/6 mice were immunized *s.c.* with either OVA-Le^x or native OVA mixed with anti-CD40 using a prime-boost protocol. Spleens were analyzed by flow cytometry to determine the frequency of H2-K^b/SIINFEKL-tetramer-binding CD8+ T cells and IFN-γ or TNF production by activated CD8+ T cells was determined by intracellular staining after OVA-specific re-stimulation *ex vivo*. Dots represent individual mice (n=4-5 mice/group; **, *P*<0.01). Bars indicate median of each group. Graphs shown are representative of two independent experiments. (**D**) C57BL/6 and MGL1 KO mice were prime-boosted with either OVA-Le^x or native OVA mixed with anti-CD40. Frequencies of IFN-γ and TNF-double-producing CD8+ T cells were determined by intracellular staining after OVA-specific re-stimulation of splenocytes *ex vivo*. Dots represent individual mice (n=4-5 mice/group; * *P* <0.05 ***, *P* <0.001). Bars indicate median of each group. Data are representative of 2 independent experiments.

A

BM-DC OTII

○ OVA
■ OVA-Le^x

spDC OTII

○ OVA
■ OVA-Le^x

B

BM-DC
C57BL/6
+ OT-II T cells

spDC
C57BL/6
+ OT-II T cells

BM-DC
Balb/c
+ DO11.10 T cells

C

Figure 3. Modification of OVA with Le^x structures skews naive CD4$^+$ T cells towards the Th1-effector lineage. (**A**) Pulsing of CD11c$^+$ spDCs or BM-DCs with OVA-Le^x results in equal OT-II proliferation as native OVA. Expansion of OVA-specific T cells was determined using ^{3}H-thymidine incorporation. Data are shown as mean±SD of triplicate cultures, representative of three independent experiments. (**B**) Flow cytometric analysis of OT-II or DO11.10 T cells differentiated by OVA-Le^x or OVA-loaded spDCs or BM-DCs. Cells were gated on CD4$^+$ T cells. Numbers in dot plots indicate the percentage of IFN-γ$^+$ or IL-4$^+$ of CD4$^+$ T cells. Dot plots are representative of five independent experiments. (**C**) C57BL/6 mice were immunized s.c. with either OVA-Le^x or native OVA mixed with anti-CD40 using a prime-boost protocol and the frequency of IFN-γ-producing activated CD4$^+$ T cells in spleen was determined by intracellular staining after OVA-specific re-stimulation *ex vivo*. Dots represent individual mice, bars indicate median of each group (n=5 mice/group, **P<0.01). Graphs shown are representative of two independent experiments

Cross-presentation of OVA via the MR was shown previously to be dependent on TLR signaling and the presence of high amounts of antigen ((34, 21, 37) and Figure 4-figure supplement 4, left panel). The observed differences in cross-presentation between OVA and OVA-Le[x] were not due to any potential contamination with the TLR4 ligand LPS, as both protein preparations did not trigger IL-8 production by TLR4-transfected HEK293 cells (Figure 4-figure supplement 5). In addition, both OVA preparations neither induced maturation of BM-DCs nor altered their cytokine production (data not shown). To exclude any potential role of TLR signaling on the MGL1-mediated cross-presentation of OVA-Le[x] we made use of BM-DCs from mice that lack both MyD88 and TRIF (*i.e.* MyD88/TRIF DKO). However, MyD88/TRIF DKO BM-DCs still induced more OT-I proliferation when targeted with OVA-Le[x] than with OVA (Figure 4E) and only a slight reduction of cross-presentation was observed compared to that induced by WT BM-DCs, suggesting a minor role for MyD88- or TRIF-signaling in MGL1-induced cross-presentation. In line with previous findings, neither exogenous loading of MHC-I molecules with OVA257-264 peptides (Figure 4E) nor MHC class II presentation of OVA-Le[x] and OVA was dependent on MyD88- or TRIF- signaling and resulted in comparable expansion of OVA-specific T cells (data not shown).

Cross-presentation induced by MGL1-targeting is independent of TAP-transport and cathepsin S -induced endosomal degradation

Several cross-presentation pathways have been described, one of which is dependent on the transport of peptides from the cytosol into MHC-class I loading compartments via TAP-molecules (38, 39), whereas another cross-presentation pathway depends on endosomal degradation by the cysteine protease cathepsin S (40). To study a role for TAP transporters in our model, BM-DCs of TAP-1 KO and WT control mice were pulsed with OVA-Le[x] followed by incubation with OT-I T cells. Surprisingly, cross-presentation induced by OVA-Le[x] was not reduced by the absence of TAP as OT-I proliferation induced by OVA-Le[x]-loaded TAP-1 KO BM-DCs was not decreased compared to OVA-Le[x]-loaded WT BM-DCs (Figure 5A). In accordance with previous publications (21) we showed that administration of OVA with LPS is cross-presented in a TAP-dependent manner (Figure 4-figure supplement 4, right panel).

Furthermore, the possibility that the results are confounded by reduced levels of MHC-class I on TAP-1 KO BM-DCs was excluded as the presentation of exogenously loaded OVA257-264 peptide is equal by both WT and TAP-1 KO BM-DCs (Figure 5A). In addition, we excluded the involvement of the cathepsin S pathway for cross-presentation of OVA-Le[x] as cross-presentation of OVA-Le[x] by BM-DCs from cathepsin S KO mice (Cat-S KO) was not reduced compared to WT BM-DCs (Figure 5B). As expected, the MHC-class II-restricted CD4^{+} T cell proliferation was compromised in the Cat-S KO BM-DCs (data not shown), illustrating the involvement of cathepsin S in cleaving the invariant chain of the MHC-class II molecule (41).

5
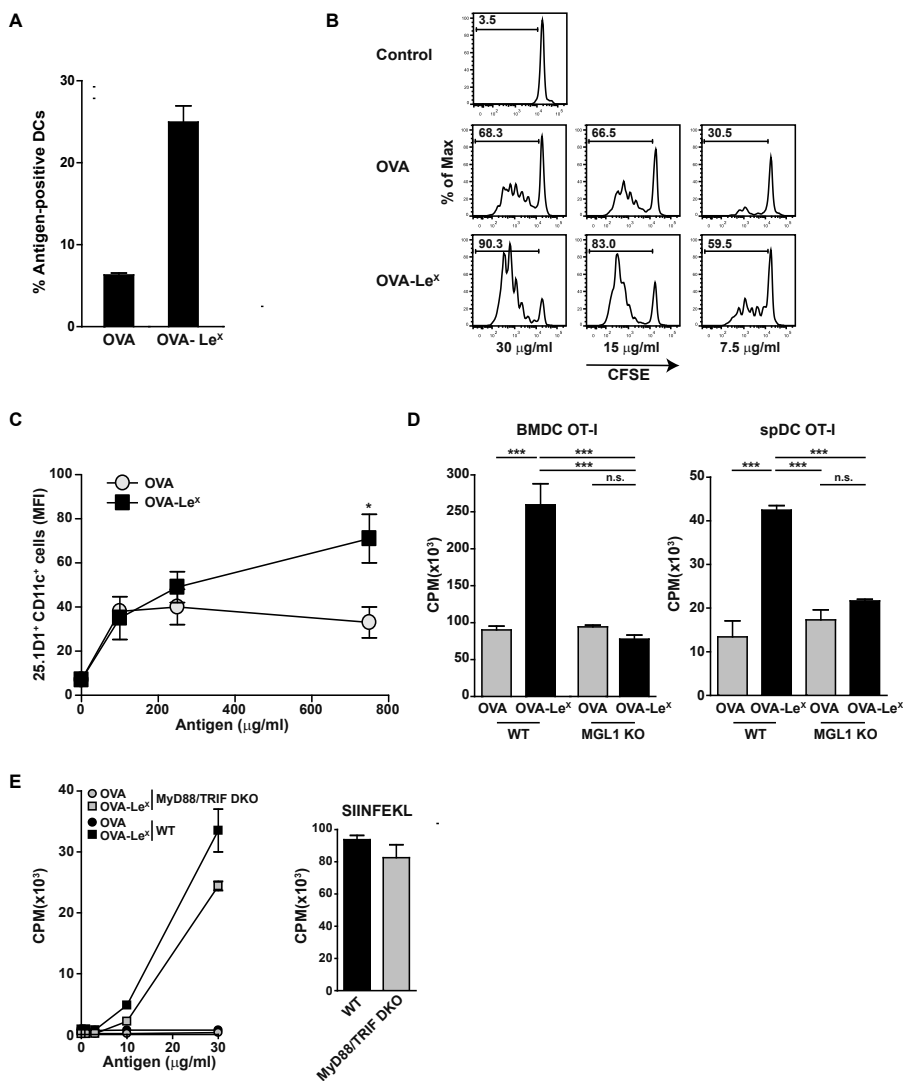
Figure 4. MGL1 mediates cross-presentation of OVA-Le^x independently of TLR signaling. (**A**) Uptake of fluorescent-labeled OVA-Le^x or native OVA (30 μg/ml) by WT BM-DCs was analyzed by flow cytometry after 90 min. Graphs indicate the mean±SD of triplicates and are representative of three independent experiments. (**B**) CFSE-labeled OT-I T cells were incubated with BM-DCs pulse-loaded with indicated concentrations of OVA-Le^x or OVA for 4h. Un-loaded DCs served as controls. Proliferation of OT-I T cells was analyzed after 3 days by flow cytometry. Percentages of divided OT-I cells are indicated. (**C**) OVA-Le^x induces more OVA257-264/H2-K^b I complexes at the cell-surface of DCs than native OVA, as shown by 25.1D1 staining 18h after pulse loading of BM-DCs with OVA-Le^x or native OVA. *P<0.05. (**D**) WT or MGL1 KO BM-DCs or CD11c^+ spDCs are pulsed with OVA-Le^x (black bars) or native OVA and OT-I proliferation was determined on day 3 by [3H]-thymidine uptake. Data are presented as mean±SD of triplicates, representative of three independent experiments. ***P<0.001, ns not significant. (**E**) Cross-presentation of OVA-Le^x is independent of MyD88 and/or TRIF signaling. BM-DCs from WT or MyD88/TRIF DKO mice were pulsed with indicated concentrations of antigen and co-cultured with OT-I T cells. DCs pulsed with the nominal epitope SIINFEKL served as controls (right panel). Proliferation was determined by [3H]-thymidine uptake. Data are representative of two experiments and indicated as mean±SD of triplicates.
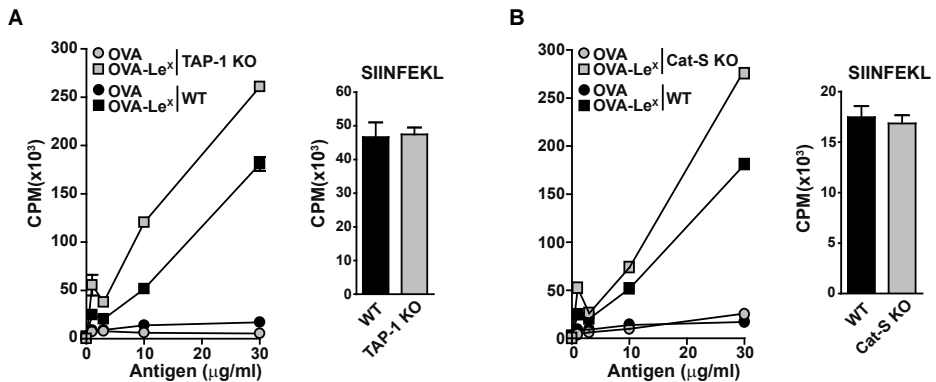
Figure 5. Le^x-modified antigen is cross-presented in a TAP- and cathepsin S-independent fashion. To examine whether cross-presentation of OVA-Le^x involves TAP or cathepsin S (**A**) TAP-1 KO and (**B**) Cat-S KO BM-DCs and WT BM-DCs were pulsed with OVA-Le^x or native OVA and co-cultured with OT-I T cells for 3 days. DCs exogenously loaded with SIINFEKL for 3h served as control. Proliferation was determined by [^{3}H]-Thymidine uptake and data are presented as mean±SD of triplicates (representative of three experiments).

Modification of OVA with Le^x alters the intracellular routing of OVA

As the dominant cross-presentation of Le^x-modified OVA was neither dependent on TAP nor required TLR signaling, we hypothesized that this may be due to the altered uptake and intracellular routing of OVA in DCs. We therefore used imaging flow cytometry, a method that allows high-throughput image analysis of cells in flow with near-confocal resolution to analyze the intracellular routing of fluorescent labeled OVA-Le^x. Co-staining with markers for early endosomal (EEA-1), late endosomal/lysosomal (LAMP1) and recycling endosomal (Rab11) compartments illustrated a swift co-localization of OVA-Le^x with EEA1 and Rab11 as shown by high co-localization scores at 15 min (Figure 6A, Figure 6-figure supplement 1). However, this co-localization score was strongly decreased after 60 min. At this time-point, higher co-localization scores were detected for OVA-Le^x with LAMP1 and Rab11 (Figure 6B, Figure 6-figure supplement 2). We then further dissected the intracellular pathway of OVA-Le^x using confocal laser scan microscopy (CLSM) and compared it to the intracellular routing of native OVA. We confirmed that native OVA, which internalized via MR, was routed to EEA1$^+$Rab11$^+$ compartments within two hours (Figure 6C, upper-left panel and (21)). However, the neoglycosylation with Le^x altered the intracellular routing of OVA, showing its presence predominantly within LAMP1$^+$Rab11$^+$ compartments (Figure 6C, upper-right panel). Moreover, OVA-Le^x internalized by BM-DCs from MGL1 KO mice was routed to EEA1$^+$Rab11$^+$ compartments and did not end up in LAMP1$^+$Rab11$^+$ compartments, similar to OVA in WT BM-DCs (Figure 6C, lower panels, Figure 6-figure supplement 3). Together, these data suggest that upon internalization, OVA-Le^x is rapidly shuttled to Rab11$^+$EEA1$^+$ compartments from where it moves to Rab11$^+$LAMP1$^+$ compartments, where it persists for

longer periods (*i.e.* >24h). Thus, these results indicate that internalization via MGL1 allows the antigen to enter the endosomal/lysosomal pathway. The development of early endosome into late endosome/lysosome coincides with a decreasing pH gradient. The pH at which MGL1 dissociates from its ligand is indicative of the compartment in which the antigen becomes available for degradation and loading on MHC-molecules. We therefore analyzed MGL1-binding to its ligand Le^x at different pH that resembled the pH of the intracellular compartments. MGL1 starts dissociating from Le^x already at pH 6.5 (Figure 6D). This indicates that OVA-Le^x becomes available for degradation in the early and late endosomal compartments, compartments both associated with cross-presentation.

The sustained presence of OVA-Le^x in Rab11$^+$LAMP1$^+$ compartments (Figure 6B and C) prompted us to investigate whether these compartments facilitate prolonged cross-presentation, as shown by van Montfoort *et al.* for OVA-immune complexes (42). Indeed, even two days after antigen pulse, OVA-Le^x-loaded DCs induced strong expansion of OT-I T cells, suggesting that OVA-Le^x-loaded DCs have prolonged cross-presentation capacity (Figure 7A). At the highest antigen concentration used (*i.e.* 30 µg/ml), the percentage of proliferated OT-I T cells was only slightly reduced 48h after pulse compared to that induced by DCs that were pulsed with OVA-Le^x for 4h (Figure 7A). Expansion of OT-I T cells driven by 48h pulse loaded DCs was even detectable at low antigen concentrations (3.75 µg/ml). OT-II proliferation induced by DCs pulsed with OVA-Le^x for 48h was also still detectable although less pronounced than the OT-I induced proliferation (Figure 7B), suggesting that the prolonged storage of antigen in these intracellular compartments predominantly favored cross-presentation. Taken together, these data suggest that antigen internalized by MGL1 is routed from RAb11$^+$EEA1$^+$ compartments towards Rab11$^+$LAMP1$^+$ compartments, which seem to associate with the extended antigen-processing and cross-presentation.

DISCUSSION

We here demonstrate that the glycosylation-profile of antigens has a major influence on antigen uptake and intracellular compartmentalization, thereby affecting both antigen presentation and the type and strength of the induced immune response. Modification of the model-antigen OVA with Le^x glycans directs OVA towards MGL1, skewing naive CD4$^+$ T cell differentiation towards IFNγ-producing Th1 cells. Moreover, targeting OVA to MGL1 through the conjugation of Le^x, substantially enhanced cross-presentation as revealed by the increased frequency of OVA-specific CD8$^+$ effector T cells *in vitro* and *in vivo*. Importantly, MGL1-dependent cross-presentation occurred at low antigen dose and independently of TLR-signaling. Moreover, this cross-presentation pathway did not involve TAP-transporters and cathepsin S. MGL1 targeting involved antigen routing to a Rab11$^+$LAMP1$^+$ compartment in which antigen was present for prolonged periods.
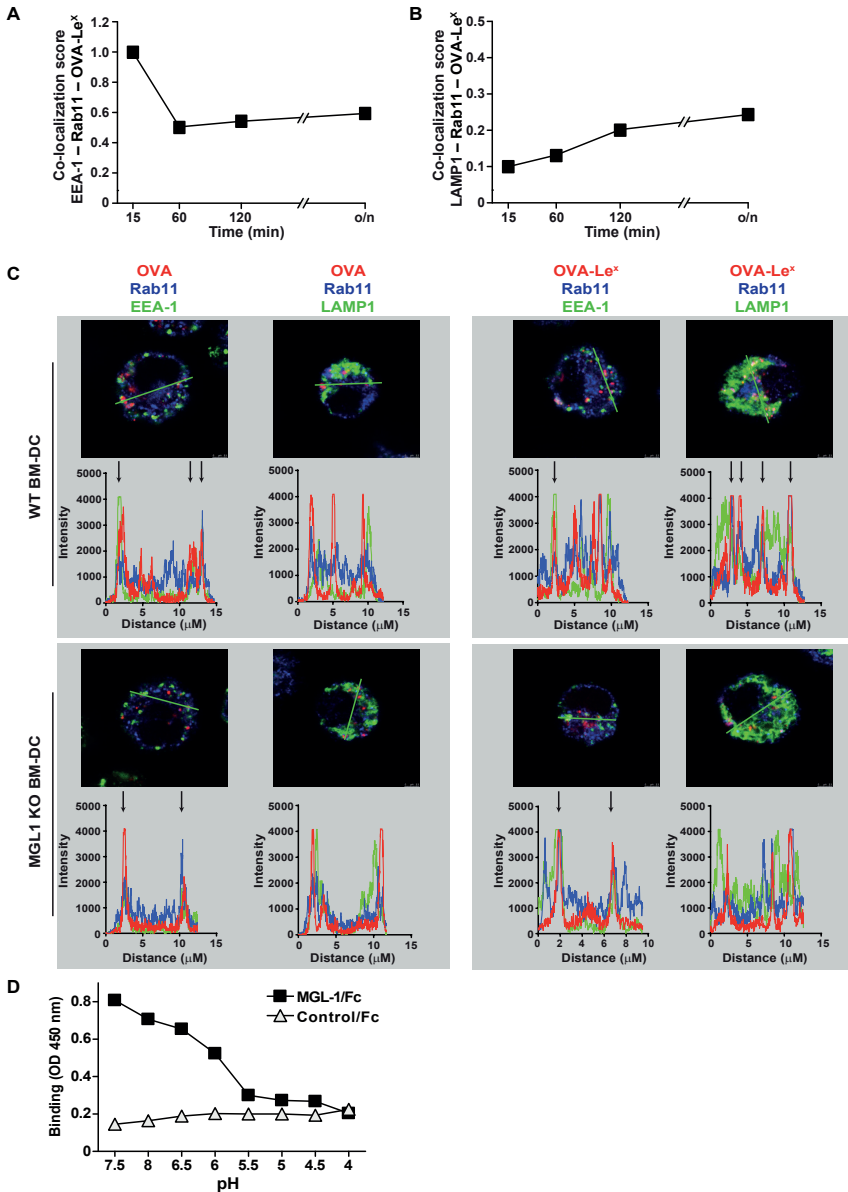
Figure 6. OVA-Le^x is routed to Rab11$^+$LAMP1$^+$ compartments where it is stored for presentation in MHC class I. (**A, B**) WT BM-DCs were pulsed with Alexa Fluor 674-OVA-Le^x (30 µg/ml) and chased at the indicated time-points to assess triple co-localization scores of OVA-Le^x with (**A**) EEA-1 and Rab11 or (**B**) LAMP1 and Rab11 using imaging flow cytometry. (**C**) WT (upper panels) and MGL1 KO (lower panels) BM-DCs were incubated with Dylight-633-OVA-Le^x or native OVA (30 µg/ml) and 2h later co-localization of OVA antigen (Red) with early endosomal (EEA-1, Green) or endosomal/lysosomal (LAMP1, Green) and recycling endosomal (Rab11, Blue) compartments was analyzed using CSLM. From a z-stack, histograms were created for a selected area (indicated by a line, upper part of each panel) using the Leica confocal software. Histograms were created from each fluorochrome and overlays were made by the program. Arrows indicate co-localization of antigen (Red) with EEA1&Rab11 or LAMP1&Rab11. (**D**) MGL1-Fc binding to Le^x-PAA was determined at indicated pH by ELISA.
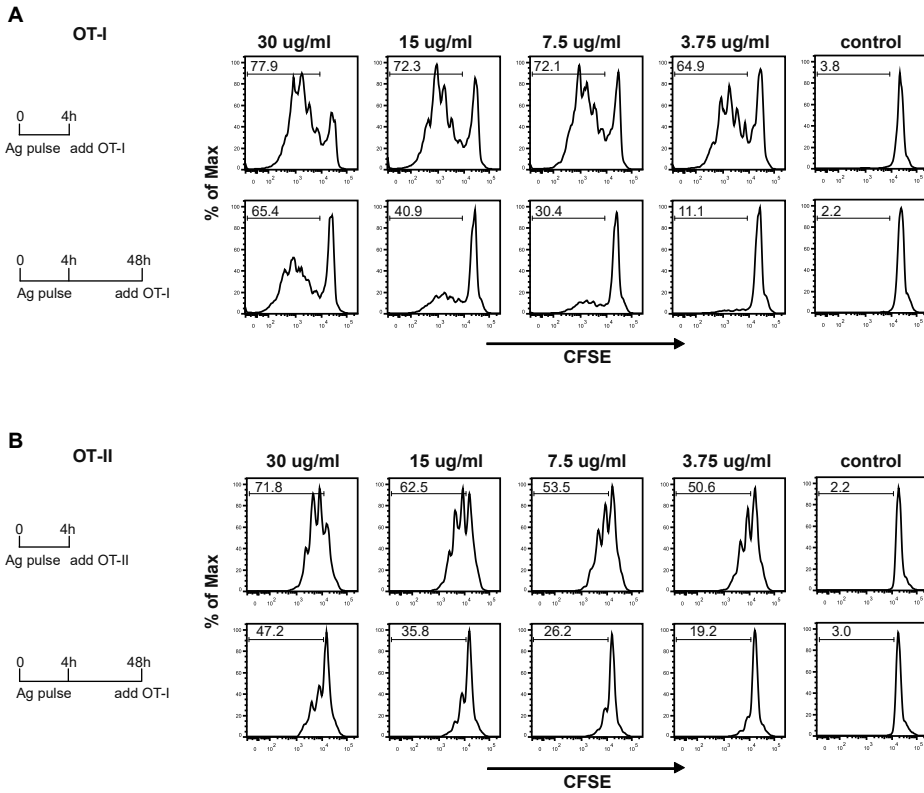
Figure 7. MGL1 targeting with OVA-Le^x shows sustained antigen presentation in MHC-I. WT BM-DCs were pulsed for 4h with titrated amounts of OVA-Le^x and washed with culture medium. DCs were then chased for 48h in antigen-free medium. (**A**) BM-DCs pulsed for 4h with OVA-Le^x induced MHC-I antigen presentation as measured by CFSE-labeled OVA-specific OT-I cells (upper panel). Sustained presentation is shown after 48h (lower panel). (**B**) MHC-II antigen presentation 4h and 48h after pulse-loading with OVA-Le^x, analyzed by OT-II proliferation. Data are presented as percentage of proliferated T cells and representative of three independent experiments.

Previous studies on CLR-mediated antigen uptake and cross-presentation, in particular by the MR, demonstrated a clear requirement for a TLR ligand (43, 21, 44, 45). A common denominator in some of these studies is that the use of antibody-antigen conjugates could potentially induce a different signal than the natural ligand, due to binding to different part of the receptor or through co-engagement of Fc-receptors. The fact that the addition of Le^x glycans to OVA obviates the need for TLR signals for the induction of cross-presentation and Th1 priming in vitro, may indicate that MGL1 signaling is involved in these processes. Some CLR, like DC-SIGN, Clec9A and Dectin-1 are known to induce signaling after triggering by their natural ligands (9, 46). Till now, no signaling pathway has been described for MGL1. Triggering of huMGL resulted in ERK1/2 and NF-κB activation, and results in elevated levels of IL-10 and TNF (47, 48). In our studies the uptake of Le^x-modified OVA through MGL1 was

not associated with any DC maturation or altered cytokine production by DCs. The fact that OVA-Le[x] induced an enhanced frequency of Th1 cells in vitro and of antigen-specific effector T cells *in vivo* when combined with agonistic anti-CD40 Abs illustrates that a yet to be determined costimulatory signal is essential for the induction of effector CD8^{+} and CD4^{+} T cells. This powerful function of MGL1 to establish antigen-specific immunity, stands opposite to its recently demonstrated anti-inflammatory function, which include induction of IL-10 production and altered adhesive function by APC (49, 50).

Various models for cross-presentation of antigens have been contemplated. The "cytosolic pathway" of cross-presentation allows receptor-mediated endocytosis or phagocytosis and antigen translocation into the cytosol, where they are degraded into antigenic peptides by the proteasome and transported into the lumen of the endoplasmic reticulum (ER) (43, 40) or ER/phagosomal fusion compartments (51, 52) by TAP-transporters. A variation to the cytosolic pathway was described in which soluble OVA is taken up via the MR and is supplied to stable early endosomal compartments (22). In these compartments, the MHC class I machinery as well as TAP-transporters are selectively recruited, facilitating direct loading of antigen-derived peptides onto MHC class I molecules without trafficking to the ER. The "vacuolar pathway" allows antigens to be degraded into peptides in early endosomal compartments by endosomal proteases like cathepsin S, to be loaded on MHC class I molecules in the same compartment, thus is TAP-independent (40). The current described models for cross-presentation depend on peptide-transport by TAP from the cytosol to either ER or ER/phagosomal fusion compartments or on endosomal degradation of antigens via cathepsin S (reviewed in (38, 53, 54, 39)). Although we observed localization of OVA-Le[x] in early endosomes, absence of either TAP molecules or cathepsin S did not influence the enhanced cross-presentation of OVA-Le[x]. Our data indicate that the MGL1 cross-presentation pathway is different than that of the MR and may occur via antigen storage compartments similar to those described for FcγR-targeted antigens (42). We observed prolonged presence in Rab11^{+}LAMP1^{+} compartments in the absence of a maturation stimulus or apparent DC maturation. It is tempting to speculate that in these compartments cross-presentation of OVA is facilitated by Rab11 as it was recently shown that Rab11 activity mediates delivery of MHC-I molecules to phagosomes used for cross-presentation during infection (55). However, recruitment of additional components involved in antigen cross-presentation by the SNARE Sec22b40 complex cannot be excluded (56)**.** The prolonged antigen cross-presentation via MGL1 allows sustained cross-priming of CD8^{+} T cells *in vivo* and thus the efficacy of tumor vaccines that target MGL1 may be higher than of conventional vaccines containing non-targeted antigens.

In the current study, we show that already at very low concentrations, soluble protein antigens are efficiently cross-presented upon uptake by MGL1. DCs pulsed with a low dose of OVA-Le[x] (7.5 μg/ml) induced significant CD8^{+} T cell proliferation, whereas

5

the same concentration of native OVA was hardly cross-presented (Figure 4). Others have demonstrated that native OVA can only be cross-presented when a high dose was used (0.5-1.0 mg/ml) and when accompanied with TLR-triggering (21, 45). Although the glycan-modification was associated with increased antigen uptake and enhanced cross-presentation, it did not result in enhanced presentation of antigen on MHC-class II indicating that increased uptake of antigen is not per se a requirement to facilitate MHC class I and II presentation. Therefore, it is most likely that the CLR (and thus the glycosylation of the antigen) dictates how efficiently an antigen is cross-presented. Based on our study MGL1 cross-presents antigen much more efficiently than the MR. The activity of the glycosylation machinery is subjected to subtle regulation and depends on the cell-type or activation status of the cell. Upon malignant transformation glycan profiles may change dramatically. Le^x carbohydrate structures are described to be expressed in the brain (57), and can be *de novo* expressed on cancer stem cells (58) or pathogens, and the glycosylation pattern of *in vivo* accumulating antigens, being brain tissue, tumor tissue or pathogen structure, is crucial for directing specific CLR antigen uptake and cross-presentation (59, 60). Although in our studies only two Le^x glycans were conjugated to each OVA molecule, it cannot be ruled out that multivalent presentation of Le^x, such as often observed on tumors or pathogens (61, 62), may alter avidity-induced MGL-1 signaling and antigen presentation, and induce an anti-inflammatory immune repertoire. At this stage we do not know whether high glycan valency further enhances or inhibits the MGL1-mediated (cross-) priming.

The fact that pulsing of DCs with OVA-Le^x resulted in improved cross-priming and Th1-skewing indicates that conjugation of these carbohydrates to tumor-antigens could be beneficial for induction of potent anti-tumor responses. Therefore, the use of glycans for targeting CLR for anti-cancer immunotherapy could have several advantages. First, they mimic natural function of the receptors, inducing 'natural' signaling cascades in DCs. Furthermore, they are very small molecules, easy to use and relatively cheap to produce. Importantly, many glycans may be considered self-antigens, in contrast to recombinant antibodies that are often not completely of human origin. These properties make it possible to decorate any antigen of choice with glycans to target specific receptors.

In conclusion, our studies indicate that the glycan composition of protein antigens is of fundamental importance in dictating the intracellular routing and Th-skewing, and should be considered as a major determinant in the design of therapeutic vaccines against cancer and infectious diseases.

MATERIALS AND METHODS

Mice

C57BL/6 mice (Charles River Laboratories) were used at 8-12 weeks of age. MGL1 KO mice, which have a null mutation within the *Clec10a* gene, are on the C56BL/6 background and were kindly provided through the Consortium for Functional Glycomics. TAP-1 KO mice have a null mutation within the *Tap1* gene. MGL1 KO, TAP-1 KO, OT-I and OT-II TCR transgenic mice were bred in our animal facilities under specific pathogen-free conditions. All experiments were performed according to institutional, state and federal guidelines.

Antibodies and Fc-chimeric constructs

Fluorochrome-conjugated antibodies used: anti-CD11c-APC, anti-IFNγ-APC, anti-TNFα-PE-cy7, anti-IL-4-PE, anti-IL17-PE, anti-Foxp3-PE (e-Bioscience), and anti-LAMP-1-v450 (BD-Pharmingen). Unconjugated mouse anti-OVA (Sigma Aldrich), mouse anti-Le^x (Calbiochem), rat anti-mMGL (ER-MP23; kind gift from Dr. P. Leenen, Erasmus MC, Rotterdam, The Netherlands), rat anti-LAMP1 (BD-Pharmingen), rabbit anti-Rab11 (Life Technologies), goat anti-EEA1 (Santa Cruz Biotechnology) and rabbit anti-EEA-1 (Dianova). Secondary antibodies used: peroxidase-labeled F(ab')$_2$ fragment goat anti-human IgG, F(ab')$_2$ fragment goat anti-mouse IgG, (Jackson), peroxidase-labeled goat anti-mouse IgM (Nordic Immunology), goat anti-rat Alexa 448, goat anti-rat Alexa 647, donkey anti-goat Alexa488, donkey anti-goat Alexa 647, donkey anti-rabbit Alexa 555 and donkey anti-rabbit Alexa 488 (Molecular Probes). MGL-1-Fc was generated as described earlier (24). MR-Fc was kindly provided by L. Martinez-Pomares (University of Nottingham, Nottingham, UK).

Generation of neo-glycoconjugates

Le^x (lacto-N-fucopentose III; Dextra Labs, UK) carbohydrate structures were conjugated to OVA (Calbiochem) as previously described (14). In short, the bifunctional cross-linker (4-*N*-maleimidophenyl) butyric acid hydrazide (MPBH; Pierce) was covalently linked to the reducing end of the Le^x and the maleimide moiety of the linker was later used for coupling the Le^x to OVA. Neo-glycoconjugates were separated from reaction by-products using PD-10 desalting columns (Pierce). Additionally, a Dylight 549-*N*-hydroxysuccimide (NHS) label (Thermo Scientific) was covalently coupled to OVA or OVA-Le^x (Dylight-549-OVA). Free label was removed using a PD-10 column (Pierce). The presence of Le^x and CLR binding to OVA was measured by ELISA. In brief, OVA-conjugates were coated directly on ELISA plates (NUNC) and binding of MR-Fc, MGL1-Fc, anti-Le^x and anti-OVA antibodies to OVA was determined as described (14, 11). The presence of endotoxin was measured using a LAL assay (Lonza) following manufacturer's protocol.

5

Glycan analysis

OVA was deglycosylated by incubation in 5 IU of PNGase F (Roche Applied Sciences) o/n at 37°C. Proteins were extracted by reverse phase chromatography using Sep-Pak Vac C18 disposable cartridges (Waters). Glycans were further purified by reverse phase chromatography using Superclean ENVI-Carb cartridges disposable columns (Supelco). Glycans were lyophilized and re-dissolved in 30 ml of 7-Amino-4-methylcoumarin (160 mM, Sigma Aldrich) and 2-Picoline borane (270 mM, Sigma Aldrich) in DMSO:acetic acid (4:1, Riedel deHaën). 4-AMC-labelled glycans were purified by size exclusion chromatography using a Bio-Gel P2 (Bio-Rad) column with 50 mM ammonium formate (Sigma Aldrich) as running buffer. 4-AMC-labelled glycans were lyophilized and analyzed by multidimensional normal phase HPLC (UltiMate 3000 nanoLC, Dionex) using a Prevail Carbohydrate ES 0.075 x 200 mm column (Grace) coupled to an LCQ Deca XP with electrospray interface mass spectrometer (Thermo Finnigan) tuned with maltoheptoase (Sigma Aldrich) labeled with 4-AMC and with an intercalated fluorescence detector (Jasco FP-2020 Plus, Jasco) (maximum excitation 350 nm, band width 40 nm; maximum emission 448 nm, band width 40 nm) as previously described (63).

Molecular weight determination

Matrix-assisted laser desorption/ionization-time of flight (MALDI-TOF) mass spectrometry measurements were done using a 4800 MALDI-TOF/TOF Analyzer (Applied Biosystems). Mass spectra were recorded in the range from to 19000 to 155000 m/z in the linear positive ion mode. The data were recorded using 4000 Series Explorer Software and processed with Data Explorer Software version 4.9 (all from Applied Biosystems).

Immunization of mice

C57BL/6 or Mgl1^{-/-} mice were injected *s.c.* either with 100 μg OVA-Le[X] or OVA mixed with 25 μg anti-CD40 Ab (1C10) on day 0 and day 14. Mice were sacrificed one week after boost and the amount of antigen-specific CD8^{+} T cells was analyzed in the spleen by staining with H2-Kb-SIINFEKL tetramers (Sanquin). Additionally, frequencies of OVA-specific cytokine-secreting T cells were analyzed by flow cytometry. Hereto, spleen cells were re-stimulated overnight with either 2 μg/ml SIINFEKL or 200 μg/ml EKLTEWTSSNMEER OVA peptides in the presence of 5μg/ml Brefeldin A, then IFN-γ and TNFα expression were assessed by intracellular staining using specific antibodies.

Cells

BM-DCs were cultured as previously described (14). BM of *Myd88/Ticam1* DKO (referred to as MyD88/TRIF DKO) and *Ctss^{-/-}* (referred to as Cat-S KO) mice was kindly provided by Dr. T. Sparwasser (Twincore, Hannover, Germany) and Dr. K. Rock (Massachusetts Medical School,

Worcester, MA, USA), respectively. CD11c^{+} spDCs were isolated as previously described (Singh et al., 2009a). OVA-specific CD4^{+} and CD8^{+} T cells were isolated from spleen and lymph nodes cell suspensions from OT-II and OT-I mice, respectively using the mouse CD4 and CD8 negative isolation kit (Invitrogen, CA, USA) according to manufacturer's protocol. T cell proliferation assays were performed as described (14). In short, DCs were pulsed with OVA-Le[x] or OVA for 4h before incubation with OVA-specific OT-I or OT-II T cells (2:1 DC:T). [^{3}H]-Thymidine (1 µCi/well; Amersham Biosciences) was present during the last 16h of a 72h culture. [^{3}H]-Thymidine incorporation was measured using a Wallac microbeta counter (Perkin-Elmer). Alternatively, OT-I or OT-II T cells were labeled with CFSE and after 3 days dilution of CFSE was analyzed by flow cytometry. Differentiation of naive OT-II T cells, induced by OVA-Le[x] or OVA -pulsed BM-DCs or spDCs, was measured by an in vitro Th differentiation assay described earlier (20).

cDNA synthesis and Real-Time PCR
mRNA was isolated by capturing poly(A[+])RNA in streptavidin-coated tubes using a mRNA Capture kit (Roche, Basel, Switzerland). cDNA was synthesized using the Reverse Transcription System kit (Promega, WI, USA) following manufacturer's guidelines. Real-Time PCR reactions were performed using the SYBR Green method in an ABI 7900HT sequence detection system (Applied Biosystems).

5

Confocal microscopy and imaging flow cytometry
BM-DCs were incubated with 30 µg/ml Dylight-633-OVA or OVA-Le[x] for 30min or 2h at 37°C, fixed and permeabilized for 20 min on ice, and stained with primary and secondary antibodies. Co-localization was analyzed using a confocal laser scanning microscope (Leica SP5 STED) system containing a 63x objective lens; images were acquired in 10x magnification and processed with Leica LAS AF software. For imaging flow cytometry, approximately 1x10^{6} BM-DCs were incubated with OVA-Le[x] for 30 min at 4°C, washed twice in ice-cold PBS and then transferred to 37°C. At the indicated time-points cells were washed twice and fixated in ice-cold 4% paraformaldehyde (PFA, Electron Microscopy Sciences) in PBS for 20 min. Cells were then permeabilized in 0.1% saponin (Sigma) in PBS for 30 min at RT and subsequently blocked using PBS containing 0.1% saponin and 2% BSA for 30 min at RT. Stainings were performed at room temperature (RT) in PBS supplemented with 0.1% saponin and 2% BSA. After staining, cells were washed twice in PBS, resuspended in PBS containing 1% BSA and 0.02% NaN3 and kept at 4°C until analysis. Cells were acquired on an ImageStream X100 (Amnis) imaging flow cytometer. A minimum of 15000 cells was acquired per sample at a flow rate ranging between 50 and 100 cells/second at 60x magnification. At least 2000 cells were acquired from single stained samples to allow for compensation. Analysis was performed using the IDEAS v6.1 software (Amnis). Cells were first gated based on the Gradient RMS

(brightfield) feature and then based on area *vs* aspect ratio intensity (both on brightfield). The first gating identified the cells that appeared in focus, while the second excluded doublets and cells other than BM-DCs. 3-colour co-localization was calculated using the bright detail co-localization 3 feature.

pH dependency of MGL1 binding

The pH dependency of MGL1 binding to Le[x] on antigens was determined by ELISA. Hereto, Le[x]-PAA (Lectinity Holdings) was coated onto NUNC Maxisorp plates o/n at RT. Plates were blocked with 1% BSA in TSM buffer (20 mM Tris-HCl; 150 mM NaCl; 2 mM $CaCl_2$; 2 mM $MgCl_2$). After washing, MGL1-Fc was added in TSA with different pH and were kept in this buffer throughout the assay. Binding was detected using peroxidase-labeled F(ab')$_2$ fragment goat anti-human IgG.

Statistical analysis

Graphpad prism 5.0 was used for statistical analysis. The Student's t-test and one-way ANOVA with Bonferroni correction were used to determine statistical significance. Statistical significance was defined as *P*< 0.05.

ACKNOWLEDGEMENTS

AUTHOR CONTRIBUTIONS

I.S-O designed and performed experiments, analyzed and interpreted data, and wrote paper; N.I.H., M.B. and L.A.M.C. performed experiments, analyzed and interpreted data; M.L., R.R., and S.K.S. performed experiments; H.K. produced glycan-antigen conjugates; J.J.G.V. performed glycan-analysis and imaging flow cytometric analysis and analyzed and interpreted data; E.S. and F.O. designed experiments and interpreted data; W.W.J.U. and Y.v.K. designed experiments, interpreted data, wrote paper and supervised the study.

REFERENCES

1.	Carbone, F. R., and M. J. Bevan. Class I-restricted processing and presentation of exogenous cell-associated antigen in vivo. *J. Exp. Med.* 1990. 171: 377–387.
2.	Bennett, S. R. M., F. R. Carbone, F. Karamalis, J. F. A. P. Miller, and W. R. Heath. Induction of a CD8+ cytotoxic T lymphocyte response by cross-priming requires cognate CD4+ T cell help. *J. Exp. Med.* 1997. 186: 65–70.
3.	Schoenberger, S. P., R. E. M. Toes, E. I. H. Van Dervoort, R. Offringa, and C. J. M. Melief. T-cell help for cytotoxic T lymphocytes is mediated by CD40-CD40L interactions. *Nature* 1998. 393: 480–483.
4.	Apweiler, R., H. Hermjakob, and N. Sharon. On the frequency of protein glycosylation, as deduced from analysis of the SWISS-PROT database. *Biochim. Biophys. Acta - Gen. Subj.* 1999. 1473: 4–8.
5.	Ohtsubo, K., and J. D. Marth. Glycosylation in Cellular Mechanisms of Health and Disease. *Cell* 2006. 126: 855–867.
6.	van Kooyk, Y., and G. A. Rabinovich. Protein-glycan interactions in the control of innate and adaptive immune responses. *Nat. Immunol.* 2008. 9: 593–601.
7.	Engering, A., T. B. H. Geijtenbeek, S. J. van Vliet, M. Wijers, E. van Liempt, N. Demaurex, A. Lanzavecchia, J. Fransen, C. G. Figdor, V. Piguet, and Y. van Kooyk. The Dendritic Cell-Specific Adhesion Receptor DC-SIGN Internalizes Antigen for Presentation to T Cells. *J. Immunol.* 2002. 168: 2118–2126.
8.	Herre, J., A. S. J. Marshall, E. Caron, A. D. Edwards, D. L. Williams, E. Schweighoffer, V. Tybulewicz, C. Reis E Sousa, S. Gordon, and G. D. Brown. Dectin-1 uses novel mechanisms for yeast phagocytosis in macrophages. *Blood* 2004. 104: 4038–4045.
9.	Geijtenbeek, T. B. H., and S. I. Gringhuis. Signalling through C-type lectin receptors: Shaping immune responses. *Nat. Rev. Immunol.* 2009. 9: 465–479.
10.	Bonifaz, L. C., D. P. Bonnyay, A. Charalambous, D. I. Darguste, S.-I. Fujii, H. Soares, M. K. Brimnes, B. Moltedo, T. M. Moran, and R. M. Steinman. In vivo targeting of antigens to maturing dendritic cells via the DEC-205 receptor improves T cell vaccination. *J. Exp. Med.* 2004. 199: 815–824.
11.	Hawiger, D., K. Inaba, Y. Dorsett, M. Guo, K. Mahnke, M. Rivera, J. V Ravetch, R. M. Steinman, and M. C. Nussenzweig. Dendritic cells induce peripheral T cell unresponsiveness under steady state conditions in vivo. *J. Exp. Med.* 2001. 194: 769–779.
12.	Caminschi, I., A. I. Proietto, F. Ahmet, S. Kitsoulis, J. Shin Teh, J. C. Y. Lo, A. Rizzitelli, L. Wu, D. Vremec, S. L. H. van Dommelen, I. K. Campbell, E. Maraskovsky, H. Braley, G. M. Davey, P. Mottram, N. van de Velde, K. Jensen, A. M. Lew, M. D. Wright, W. R. Heath, K. Shortman, and M. H. Lahoud. The dendritic cell subtype-restricted C-type lectin Clec9A is a target for vaccine enhancement. *Blood* 2008. 112: 3264–3273.
13.	Chatterjee, B., A. Smed-Sorensen, L. Cohn, C. Chalouni, R. Vandlen, B.-C. Lee, J. Widger, T. Keler, L. Delamarre, and I. Mellman. Internalization and endosomal degradation of receptor-bound antigens regulate the efficiency of cross presentation by human dendritic cells. *Blood* 2012. 120: 2011–2020.
14.	Singh, S. K., J. Stephani, M. Schaefer, H. Kalay, J. J. García-Vallejo, J. den Haan, E. Saeland, T. Sparwasser, and Y. van Kooyk. Targeting glycan modified OVA to murine DC-SIGN transgenic dendritic cells enhances MHC class I and II presentation. *Mol. Immunol.* 2009. 47: 164–174.
15.	García-Vallejo, J. J., M. Ambrosini, A. Overbeek, W. E. van Riel, K. Bloem, W. W. J. Unger, F. Chiodo, J. G. Bolscher, K. Nazmi, H. Kalay, and Y. van Kooyk. Multivalent glycopeptide dendrimers for the targeted delivery of antigens to dendritic cells. *Mol. Immunol.* 2013. 53: 387–397.
16.	Unger, W. W. J., A. J. Van Beelen, S. C. Bruijns, M. Joshi, C. M. Fehres, L. Van Bloois, M. I. Verstege, M. Ambrosini, H. Kalay, K. Nazmi, J. G. Bolscher, E. Hooijberg, T. D. De Gruijl, G. Storm, and Y. Van Kooyk. Glycan-modified liposomes boost CD4 + and CD8 + T-cell responses by targeting DC-SIGN on dendritic cells. *J. Control. Release* 2012. 160: 88–95.
17.	Unger, W. W., C. T. Mayer, S. Engels, C. Hesse, M. Perdicchio, F. Puttur, I. Streng-Ouwehand, M. Litjens, H. Kalay, L. Berod, T. Sparwasser, and Y. van Kooyk. Antigen targeting to dendritic cells combined with transient regulatory T cell inhibition results in long-term tumor regression. *Oncoimmunology* 2015. 4: e970462.
18.	Aarnoudse, C. A., M. Bax, M. Sánchez-Hernández, J. J. García-Vallejo, and Y. van Kooyk. Glycan modification of the tumor antigen gp100 targets DC-SIGN to enhance dendritic cell induced antigen presentation to T cells. *Int. J. cancer* 2008. 122: 839–846.

5

19. Yang, L., H. Yang, K. Rideout, T. Cho, K. Il Joo, L. Ziegler, A. Elliot, A. Walls, D. Yu, D. Baltimore, and P. Wang. Engineered lentivector targeting of dendritic cells for in vivo immunization. *Nat. Biotechnol.* 2008. 26: 326–334.

20. Singh, S. K., I. Streng-Ouwehand, M. Litjens, H. Kalay, S. Burgdorf, E. Saeland, C. Kurts, W. W. Unger, and Y. van Kooyk. Design of neo-glycoconjugates that target the mannose receptor and enhance TLR-independent cross-presentation and Th1 polarization. *Eur. J. Immunol.* 2011. 41: 916–925.

21. Burgdorf, S., C. Schölz, A. Kautz, R. Tampé, and C. Kurts. Spatial and mechanistic separation of cross-presentation and endogenous antigen presentation. *Nat. Immunol.* 2008. 9: 558–566.

22. Burgdorf, S., A. Kautz, V. Böhnert, P. A. Knolle, and C. Kurts. Distinct pathways of antigen uptake and intracellular routing in CD4 and CD8 T cell activation. *Science* 2007. 316: 612–616.

23. Taylor, M. E., K. Bezouska, and K. Drickamer. Contribution to ligand binding by multiple carbohydrate-recognition domains in the macrophage mannose receptor. *J. Biol. Chem.* 1992. 267: 1719–1726.

24. Singh, S. K., I. Streng-Ouwehand, M. Litjens, D. R. Weelij, J. J. García-Vallejo, S. J. van Vliet, E. Saeland, and Y. van Kooyk. Characterization of murine MGL1 and MGL2 C-type lectins: Distinct glycan specificities and tumor binding properties. *Mol. Immunol.* 2009. 46: 1249–1249.

25. Dupasquier, M., P. Stoitzner, H. Wan, D. Cerqueira, A. Van Oudenaren, J. S. A. Voerman, K. Denda-Nagai, T. Irimura, G. Raes, N. Romani, and P. J. M. Leenen. The dermal microenvironment induces the expression of the alternative activation marker CD301/mMGL in mononuclear phagocytes, independent of IL-4/IL-13 signaling. *J. Leukoc. Biol.* 2006. 80: 838–849.

26. Tsuiji, M., M. Fujimori, Y. Ohashi, N. Higashi, T. M. Onami, S. M. Hedrick, and T. Irimura. Molecular cloning and characterization of a novel mouse macrophage C-type lectin, mMGL2, which has a distinct carbohydrate specificity from mMGL1. *J. Biol. Chem.* 2002. 277: 28892–28901.

27. Denda-Nagai, K., S. Aida, K. Saba, K. Suzuki, S. Moriyama, S. Oo-puthinan, M. Tsuiji, A. Morikawa, Y. Kumamoto, D. Sugiura, A. Kudo, Y. Akimoto, H. Kawakami, N. V. Bovin, and T. Irimura. Distribution and function of macrophage galactose-type C-type lectin 2 (MGL2/CD301b): Efficient uptake and presentation of glycosylated antigens by dendritic cells. *J. Biol. Chem.* 2010. 285: 19193–19204.

28. Segura, E., E. Kapp, N. Gupta, J. Wong, J. Lim, H. Ji, W. R. Heath, R. Simpson, and J. A. Villadangos. Differential expression of pathogen-recognition molecules between dendritic cell subsets revealed by plasma membrane proteomic analysis. *Mol. Immunol.* 2010. 47: 1765–1773.

29. van Vliet, S. J., E. Saeland, and Y. van Kooyk. Sweet preferences of MGL: carbohydrate specificity and function. *Trends Immunol.* 2008. 29: 83–90.

30. van Vliet, S. J., C. A. Aarnoudse, V. C. M. Broks-van den Nerg, M. Boks, T. B. H. Geijtenbeek, and Y. van Kooyk. MGL-mediated internalization and antigen presentation by dendritic cells: A role for tyrosine-5. *Eur. J. Immunol.* 2007. 37: 2075–2081.

31. Yuita, H., M. Tsuiji, Y. Tajika, Y. Matsumoto, K. Hirano, N. Suzuki, and T. Irimura. Retardation of removal of radiation-induced apoptotic cells in developing neural tubes in macrophage galactose-type C-type lectin-1-deficient mouse embryos. *Glycobiology* 2005. 15: 1368–1375.

32. Gringhuis, S. I., T. M. Kaptein, B. A. Wevers, M. Van Der Vlist, E. J. Klaver, I. Van Die, L. E. M. Vriend, M. A. W. P. De Jong, and T. B. H. Geijtenbeek. Fucose-based PAMPs prime dendritic cells for follicular T helper cell polarization via DC-SIGN-dependent IL-27 production. *Nat. Commun.* 2014. 5: 5074.

33. Taylor, M. E., and K. Drickamer. Structural requirements for high affinity binding of complex ligands by the macrophage mannose receptor. *J. Biol. Chem.* 1993. 268: 399–404.

34. Burgdorf, S., V. Lukacs-Kornek, and C. Kurts. The mannose receptor mediates uptake of soluble but not of cell-associated antigen for cross-presentation. *J. Immunol.* 2006. 176: 6770–6776.

35. Gervais, F., M. Stevenson, and E. Skamene. Genetic control of resistance to Listeria monocytogenes: regulation of leukocyte inflammatory responses by the Hc locus. *J. Immunol.* 1984. 132: 2078–83.

36. Hsieh, C. S., S. E. Macatonia, A. O'Garra, and K. M. Murphy. T cell genetic background determines default t helper phenotype development in vitro. *J. Exp. Med.* 1995. 181: 713–721.

37. Blander, J. M., and R. Medzhitov. On regulation of phagosome maturation and antigen presentation. *Nat. Immunol.* 2006. 7: 1029–1035.

38. Amigorena, S., and A. Savina. Intracellular mechanisms of antigen cross presentation in dendritic cells. *Curr. Opin. Immunol.* 2010. 22: 109–117.

39. Adiko, A. C., J. Babdor, E. Gutiérrez-Martínez, P. Guermonprez, and L. Saveanu. Intracellular transport routes for MHC I and their relevance for antigen cross-presentation. *Front. Immunol.* 2015. 6: 335.

40. Shen, L., L. J. Sigal, M. Boes, and K. L. Rock. Important role of cathepsin S in generating peptides for TAP-independent MHC class I crosspresentation in vivo. *Immunity* 2004. 21: 155–165.

41. Nakagawa, T. Y., W. H. Brissette, P. D. Lira, R. J. Griffiths, N. Petrushova, J. Stock, J. D. McNeish, S. E. Eastman, E. D. Howard, S. R. Clarke, E. F. Rosloniec, E. A. Elliott, and A. Y. Rudensky. Impaired invariant chain degradation and antigen presentation and diminished collagen-induced arthritis in cathepsin S null mice. *Immunity* 1999. 10: 207–217.

42. Van Montfoort, N., M. G. Camps, S. Khan, D. V. Filippov, J. J. Weterings, J. M. Griffith, H. J. Geuze, T. van Hall, J. S. Verbeek, C. J. Melief, and F. Ossendorp. Antigen storage compartments in mature dendritic cells facilitate prolonged cytotoxic T lymphocyte cross-priming capacity. *Proc. Natl. Acad. Sci. U. S. A.* 2009. 106: 6730–6735.

43. Kovacsovics-Bankowski, M., and K. L. Rock. A phagosome-to-cytosol pathway for exogenous antigens presented on MHC class I molecules. *Science* 1995. 267: 243–246.

44. Sancho, D., D. Mourão-Sá, O. P. Joffre, O. Schulz, N. C. Rogers, D. J. Pennington, J. R. Carlyle, and C. R. Sousa. Tumor therapy in mice via antigen targeting to a novel, DC-restricted C-type lectin. *J. Clin. Invest.* 2008. 118: 2098–2110.

45. Segura, E., A. L. Albiston, I. P. Wicks, S. Y. Chai, and J. A. Villadangos. Different cross-presentation pathways in steady-state and inflammatory dendritic cells. *Proc. Natl. Acad. Sci. U. S. A.* 2009. 106: 20377–20381.

46. Sancho, D., O. P. Joffre, A. M. Keller, N. C. Rogers, D. Martínez, P. Hernanz-Falcón, I. Rosewell, and C. R. E. Sousa. Identification of a dendritic cell receptor that couples sensing of necrosis to immunity. *Nature* 2009. 458: 899–903.

47. Li, D., G. Romain, A.-L. Flamar, D. Duluc, M. Dullaers, X.-H. Li, S. Zurawski, N. Bosquet, A. K. Palucka, R. Le Grand, A. O'Garra, G. Zurawski, J. Banchereau, and S. Oh. Targeting self- and foreign antigens to dendritic cells via DC-ASGPR generates IL-10-producing suppressive CD4+ T cells. *J. Exp. Med.* 2012. 209: 109–121.

48. van Vliet, S. J., S. Bay, I. M. Vuist, H. Kalay, J. J. García-Vallejo, C. Leclerc, and Y. van Kooyk. MGL signaling augments TLR2-mediated responses for enhanced IL-10 and TNF-α secretion. *J. Leukoc. Biol.* 2013. 94: 315–323.

49. Saba, K., K. Denda-Nagai, and T. Irimura. A C-type lectin MGL1/CD301a plays an anti-inflammatory role in murine experimental colitis. *Am. J. Pathol.* 2009. 174: 144–152.

50. Westcott, D. J., J. B. Delproposto, L. M. Geletka, T. Wang, K. Singer, A. R. Saltiel, and C. N. Lumeng. MGL1 promotes adipose tissue inflammation and insulin resistance by regulating 7/4hi monocytes in obesity. *J. Exp. Med.* 2009. 206: 3143–3156.

51. Guermonprez, P., L. Saveanu, M. Kleijmeer, J. Davoust, P. Van Endert, and S. Amigorena. ER-phagosome fusion defines an MHC class I cross-presentation compartment in dendritic cells. *Nature* 2003. 425: 397–402.

52. Houde, M., S. Bertholet, E. Gagnon, S. Brunet, G. Goyette, A. Laplante, M. F. Princiotta, P. Thibault, D. Sacks, and M. Desjardins. Phagosomes are competent organelles for antigen cross-presentation. *Nature* 2003. 425: 402–406.

53. Burgdorf, S., and C. Kurts. Endocytosis mechanisms and the cell biology of antigen presentation. *Curr. Opin. Immunol.* 2008. 20: 89–95.

54. Mintern, J. D., C. Macri, and J. A. Villadangos. Modulation of antigen presentation by intracellular trafficking. *Curr. Opin. Immunol.* 2015. 34: 16–21.

55. Nair-Gupta, P., A. Baccarini, N. Tung, F. Seyffer, O. Florey, Y. Huang, M. Banerjee, M. Overholtzer, P. A. Roche, R. Tampé, B. D. Brown, D. Amsen, S. W. Whiteheart, and J. M. Blander. TLR signals induce phagosomal MHC-I delivery from the endosomal recycling compartment to allow cross-presentation. *Cell* 2014. 158: 506–521.

56. Cebrian, I., G. Visentin, N. Blanchard, M. Jouve, A. Bobard, C. Moita, J. Enninga, L. F. Moita, S. Amigorena, and A. Savina. Sec22b regulates phagosomal maturation and antigen crosspresentation by dendritic cells. *Cell* 2011. 147: 1355–1368.

57. Lieberoth, A., F. Splittstoesser, N. Katagihallimath, I. Jakovcevski, G. Loers, B. Ranscht, D. Karagogeos, M. Schachner, and R. Kleene. Lewis x and α2,3-sialyl glycans and their receptors TAG-1, contactin, and L1 mediate CD24-dependent neurite outgrowth. *J. Neurosci.* 2009. 29: 6677–6690.

58. Read, T.-A., M. P. Fogarty, S. L. Markant, R. E. McLendon, Z. Wei, D. W. Ellison, P. G. Febbo, and R. J. Wechsler-Reya. Identification of CD15 as a marker for tumor-propagating cells in a mouse model of medulloblastoma. *Cancer Cell* 2009. 15: 135–147.

5

59. Hittelet, A., I. Camby, N. Nagy, H. Legendre, Y. Bronckart, C. Decaestecker, H. Kaltner, N. E. Nifant'ev, N. V Bovin, J.-C. Pector, I. Salmon, H.-J. Gabius, R. Kiss, and P. Yeaton. Binding sites for Lewis antigens are expressed by human colon cancer cells and negatively affect their migration. *Lab. Invest.* 2003. 83: 777–87.

60. Ohana-Malka, O., D. Benharroch, N. Isakov, I. Prinsloo, G. Shubinsky, M. Sacks, and J. Gopas. Selectins and anti-CD15 (Lewis x/a) antibodies transmit activation signals in Hodgkin's lymphoma-derived cell lines. *Exp. Hematol.* 2003. 31: 1057–1065.

61. Bergman, M. P., A. Engering, H. H. Smits, S. J. Van Vliet, A. A. Van Bodegraven, H. P. Wirth, M. L. Kapsenberg, C. M. J. E. Vandenbroucke-Grauls, Y. Van Kooyk, and B. J. Appelmelk. Helicobacter pylori modulates the T helper cell 1/T helper cell 2 balance through phase-variable interaction between lipopolysaccharide and DC-SIGN. *J. Exp. Med.* 2004. 200: 979–990.

62. Saeland, E., and Y. Van Kooyk. Highly glycosylated tumour antigens: Interactions with the immune system. *Biochem. Soc. Trans.* 2011. 39: 388–392.

63. Kalay, H., M. Ambrosini, P. H. C. Van Berkel, P. W. H. I. Parren, Y. Van Kooyk, and J. J. García Vallejo. Online nanoliquid chromatography-mass spectrometry and nanofluorescence detection for high-resolution quantitative N-glycan analysis. *Anal. Biochem.* 2012. 423: 153–162.
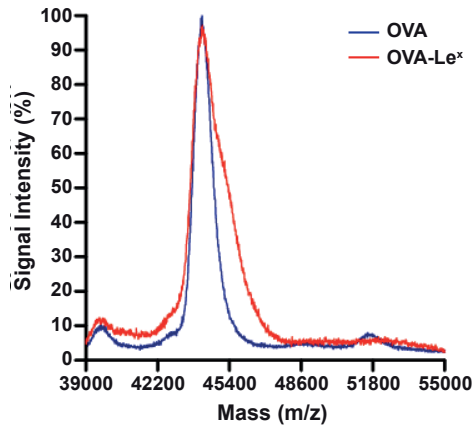
Figure 1-figure supplement 1. The MALDI-TOF/TOF mass spectrum of OVA-Le^x (Red) shows an increase of 1,2 KDa compared to unconjugated OVA (Blue), corresponding to addition of two Le^x molecules per OVA molecule.

A

B
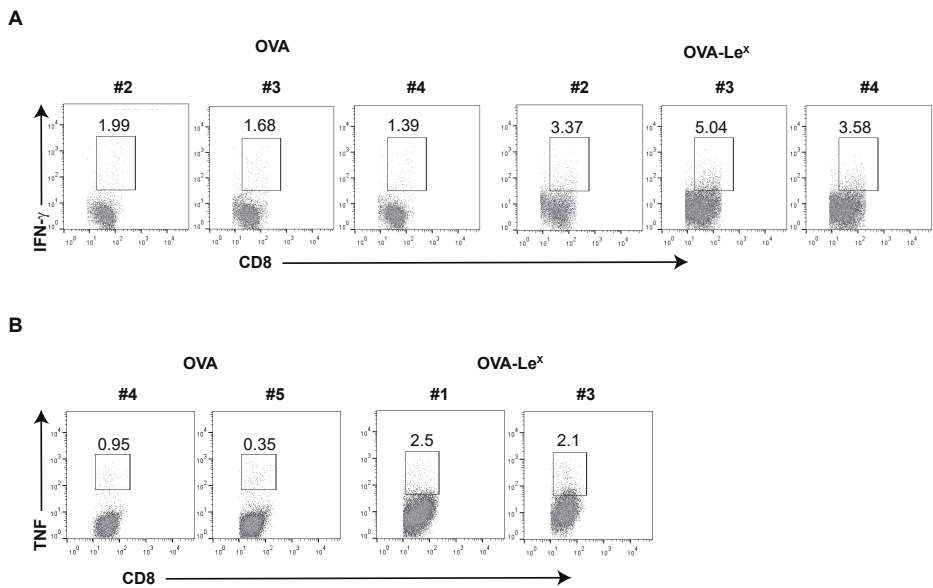
Figure 2-figure supplement 1. Representative flow cytometry plots of **(A)** IFN-γ and **(B)** TNF- producing CD8$^+$ T cells in spleens of C57BL/6 mice that were immunized with either OVA-Le^x or native OVA mixed with anti-CD40 using a prime-boost protocol; numbers above the gates designate the percentage of IFN-γ$^+$ or TNF$^+$ CD8$^+$ T cells.
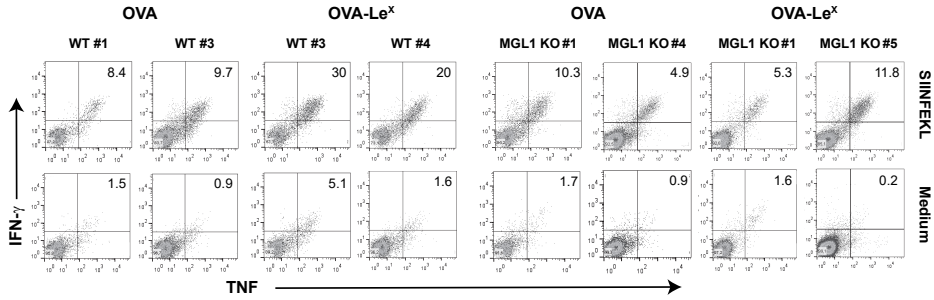
Figure 2-figure supplement 2. C57BL/6 and MGL1 KO mice were prime-boosted with either OVA-Le^x or native OVA mixed with anti-CD40. Frequencies of IFN-γ and TNF-double-producing CD8$^+$ T cells were determined by intracellular staining after re-stimulation of splenocytes *ex vivo*. Representative FACS plots of indicated mice are shown; numbers designate the percentage of IFN-γ and TNF-double positive CD8$^+$ T cells.
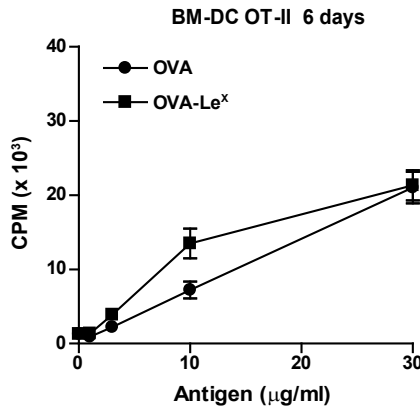
Figure 3-figure supplement 1. No enhanced expansion of OT-II T cells when co-cultured for six days with OVA-Le^x pulse-loaded DCs. WT BM-DCs were loaded with OVA-Le^x or native OVA for 4h and subsequently co-cultured with OT-II T cells for six days. Proliferation of OT-II T cells was determined by [^{3}H]-thymidine uptake and presented as mean±SD of triplicate cultures. Data shown are representative of two independent experiments.
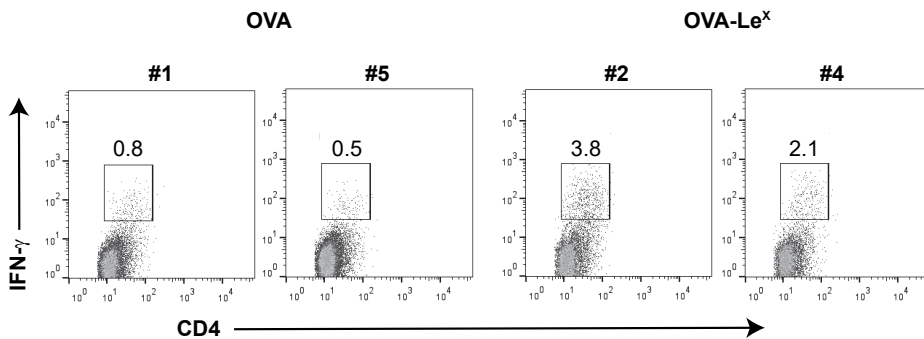
Figure 3-figure supplement 2. C57BL/6 mice were immunized s.c. with either OVA-Le^x or native OVA mixed with anti-CD40 using a prime-boost protocol and the frequency of IFN-γ-producing activated CD4$^+$ T cells in spleen was determined by intracellular staining after OVA-specific re-stimulation *ex vivo*. Representative FACS plots of indicated mice are shown; numbers above the gates designate the percentage of IFN-γ$^+$ CD4$^+$ T cells.
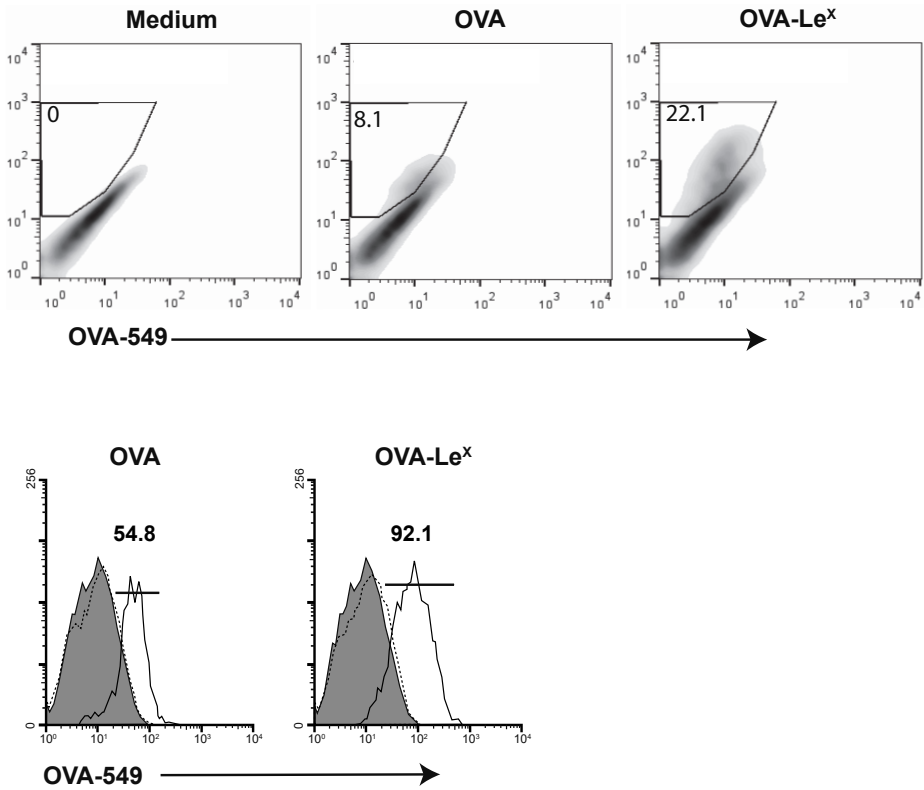
Figure 4-figure supplement 1. Uptake of fluorescent-labeled OVA-Le^x or native OVA (30 µg/ml) by WT BM-DCs was analyzed by flow cytometry after 90 min (upper panel). Control cells were incubated with medium. The percentage of gated antigen- positive DCs are indicated. Lower panel: histograms indicating the mean uptake of OVA (left, black line) or OVA-Le^x (right, black line) versus medium (grey filled histograms) and EGTA (dashed lines) controls. Numbers indicate the MFI of OVA- positive DCs.
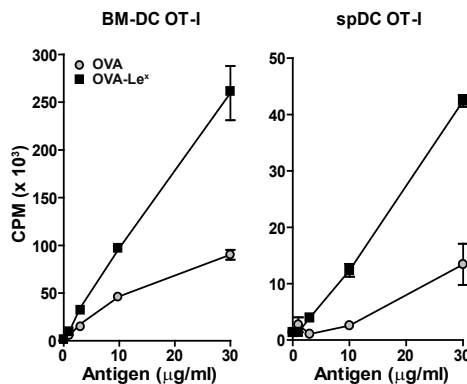
Figure 4-figure supplement 2. Enhanced cross-presentation of OVA-Le^x by DCs as measured by 3H-Thymidine incorporation. BM-DCs and CD11c$^+$ spDCs loaded with OVA-Le^x enhanced OT-I proliferation compared to native OVA loaded DCs. Proliferation was determined on day 3 by [3H]-Thymidine uptake and presented as mean±SD of triplicate cultures. Data are representative of four independent experiments.

OVA   **OVA-Le^x**
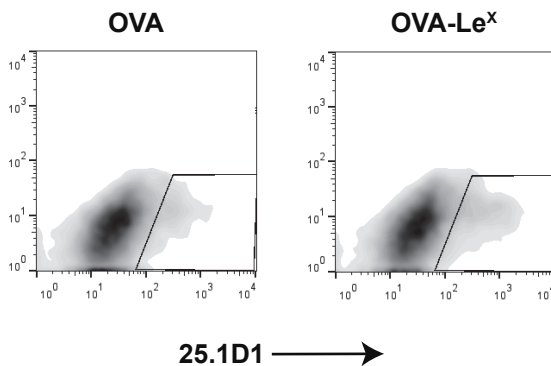
25.1D1 ⟶

Figure 4-figure supplement 3. Representative flow cytometry plots of 25.1D1 staining of BM-DCs 18h after pulse loading with OVA-Le^x or native OVA (750 ug/ml).
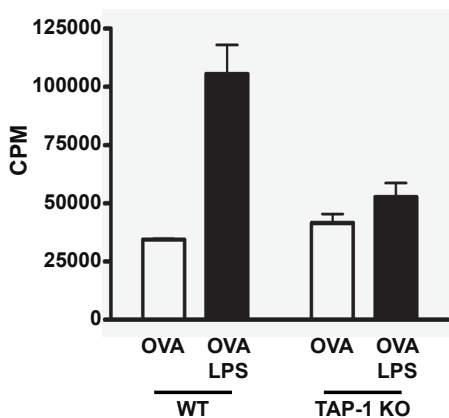
Figure 4-figure supplement 4. Cross-presentation of OVA requires TLR4 triggering and is TAP-dependent. WT or TAP-1-deficient BM-DCs were loaded with OVA (0.5 mg/ml) in the presence or absence of 100 ng/ml LPS and subsequently co-cultured with purified OT-I T cells for 3 days. [3H]-Thymidine is incorporated during the last 18h and is presented as mean±SD of triplicate cultures. Data are representative of two independent experiments.
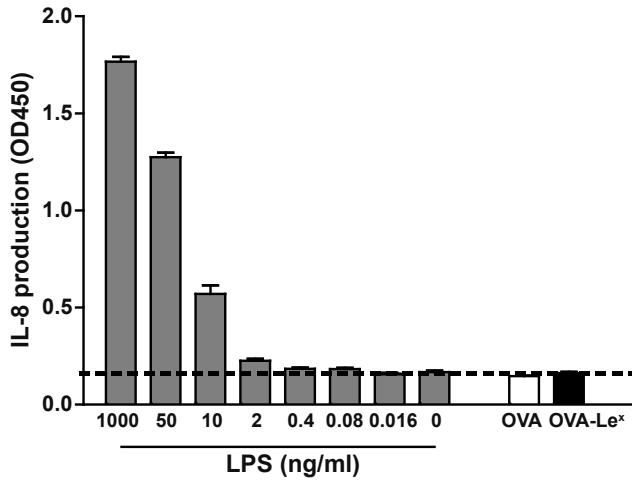
Figure 4-figure supplement 5. OVA-Le^x formulations are free of endotoxins. Both OVA and OVA-Le^x were tested for endotoxin levels. Human embryonic kidney (HEK)293-TLR4/MyD88 transfectants (kind gift of Dr. D. Golenbock) were cultured in the presence of either antigen preparation (30 µg/ml) or indicated amounts of E. coli- derived LPS (Sigma Aldrich). The HEK transfectants respond to LPS by secreting IL-8. In both preparations, LPS was below detection limits (dashed line). Results are representative of two independent experiments.

5
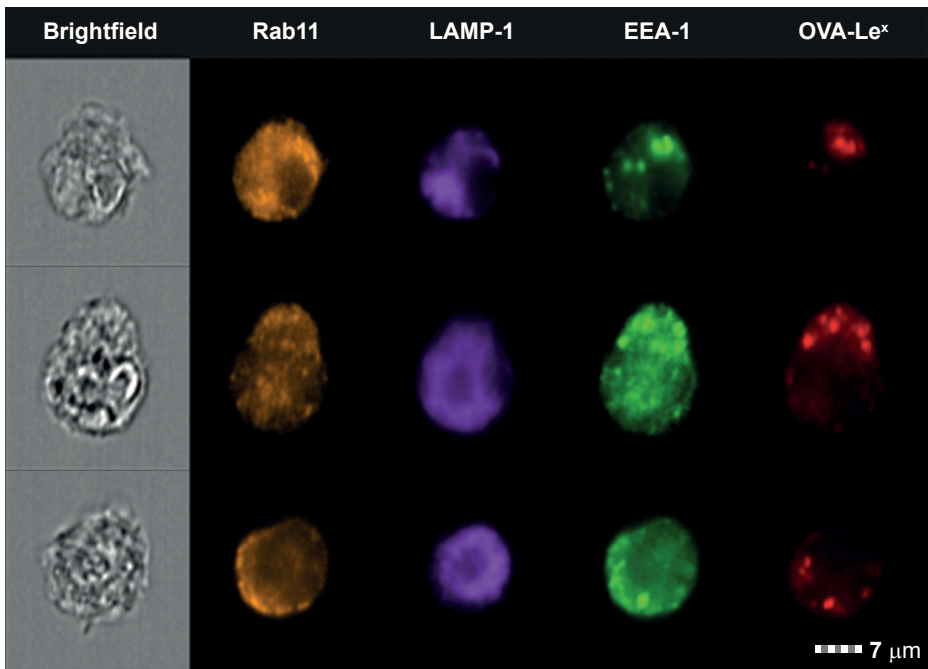
Figure 6-figure supplement 1. Examples of WT BM-DCs pulsed with Alexa Fluor 674-OVA-Le^x displaying high co-localization of OVA-Le^x with EEA-1 and Rab11 as measured by imaging flow cytometry.
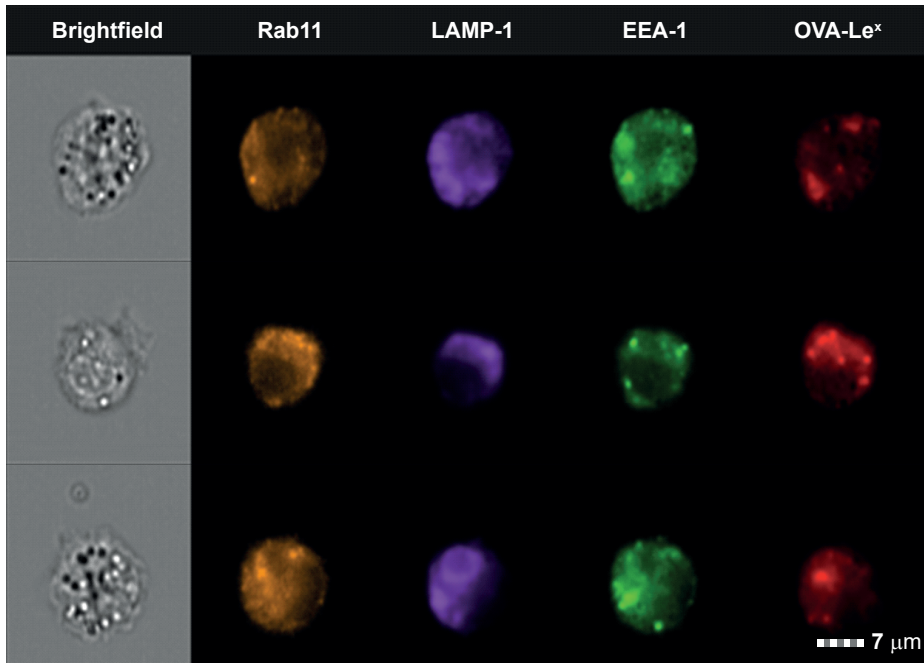
Figure 6-figure supplement 2. Examples of WT BM-DCs pulsed with Alexa Fluor 674-OVA-Le^x displaying high co-localization of OVA-Le^x with LAMP1 and Rab11 as measured by imaging flow cytometry.
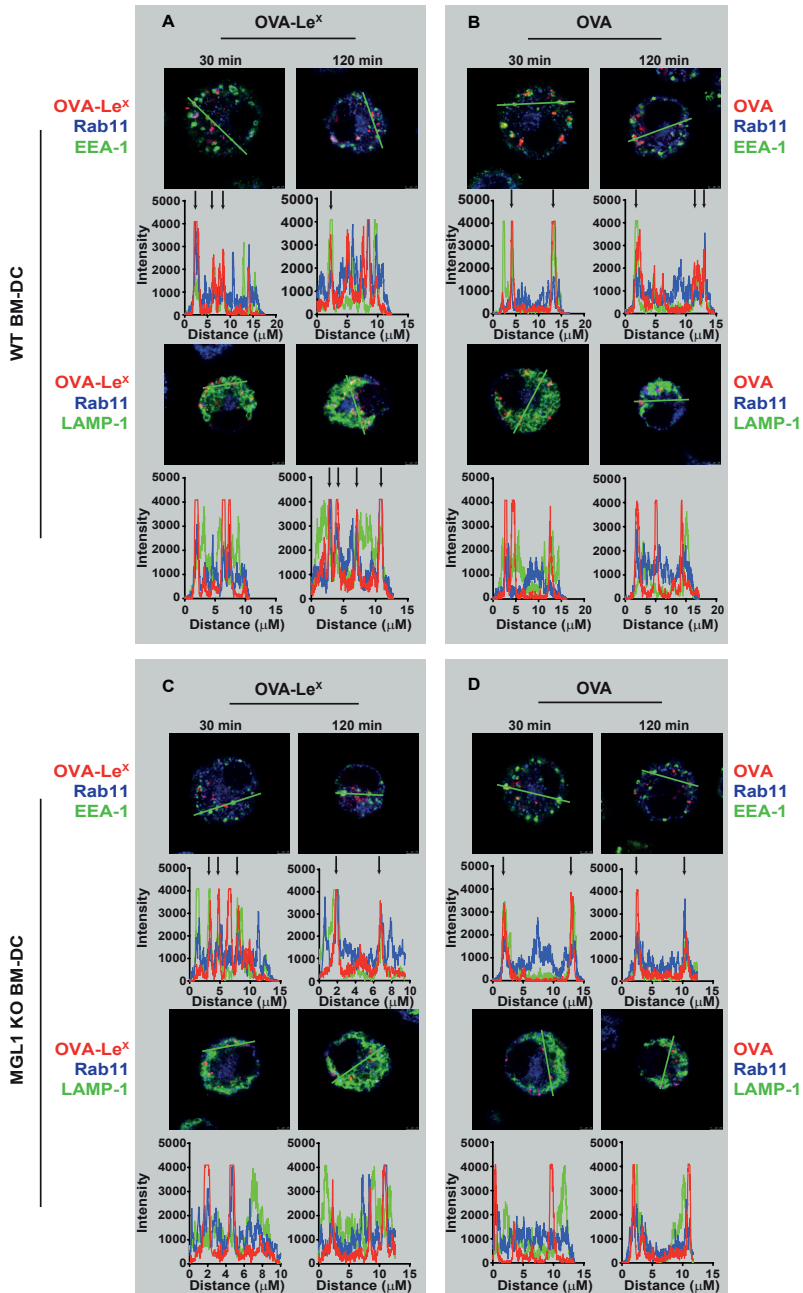
Figure 6-figure supplement 3. WT (upper panels) and MGL1 KO (lower panels) BM-DCs were incubated with Dylight-633-OVA-Le^x or native OVA (30 µg/ml) and 30min or 2h later co-localization of OVA antigen (Red) with early endosomal (EEA-1, Green) or endosomal/lysosomal (LAMP1, Green) and recycling endosomal (Rab11, Blue) compartments was analyzed using CSLM. From a z-stack, histograms were created for a selected area (indicated by a line) using the Leica confocal software. Histograms were created from each fluorochrome and overlays were made by the program. Arrows indicate co-localization of antigen (Red) with EEA1&Rab11 or LAMP1&Rab11.

6
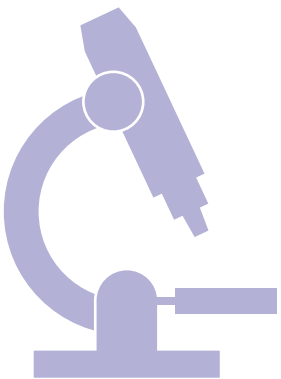
Autophagy regulates long-term cross-presentation by dendritic cells

Nataschja I. Ho, Marcel G. M. Camps, Martijn Verdoes, Christian Münz, Ferry Ossendorp

ABSTRACT

Autophagy has been reported to be involved in supporting antigen cross-presentation by dendritic cells (DCs). We have shown that DCs have the ability to store antigen for a prolonged time in lysosomal compartments and thereby sustain MHCI antigen cross-presentation to CD8$^+$ T cells. In the current study, we investigated the role of autophagy in long-term antigen presentation. We show that the autophagy machinery has a negative impact on storage of antigen in DCs. Atg5$^{-/-}$ DCs which are deficient in autophagy or DCs treated with common autophagy inhibitors showed enhanced antigen storage and antigen cross-presentation. This augmented antigen cross-presentation effect is independent of proteasome enzyme activity or MHCI surface expression on DCs. We visualized that the storage compartments are in close proximity to LC3 positive autophagosomes. Our results indicate that autophagosomes disrupt antigen storage in DCs and thereby regulate long-term MHCI cross-presentation.

INTRODUCTION

Dendritic cells (DCs) have been extensively investigated for their superiority in antigen cross-presentation. Their ability to present exogenous antigen on MHCI molecules to CD8^{+} T cells has given DCs a key role in immune surveillance of cancers and infectious diseases. The mechanisms and pathways how DCs internalize, process and present protein antigens on MHCI are studied broadly but generally under short term conditions, only several hours up to 18 h after antigen uptake (1–5). We have previously demonstrated that DCs can store protein antigen for several days in a lysosomal-like organelle which supplies antigen for sustained and functional antigen presentation *in vitro* and *in vivo* (6). This compartment is distinct from MHCII loading or early endosomal compartments and constitutes an internal source for the continuous supply of ligands for MHCI loading, and thereby enhancing prolonged cross-presentation to CD8^{+} T cells. We have shown that the antigen processing from the storage organelle in DCs is TAP and proteasome dependent since inhibiting the activity of either one almost completely inhibits MHCI cross-presentation. Therefore, it is likely that the stored antigen is translocated into the cell cytosol and degraded by the proteasome and peptidases before MHCI loading (7, 8).

Autophagy plays an important role in the degradation of endogenous proteins and organelles in cells (9). The autophagy machinery is known for its importance in regulating endogenous as well as exogenous antigen processing for MHCII presentation by fusion of autophagosomes with MHCII loading compartments (MIIC) or via LC3-associated phagocytosis (LAP), respectively (10–14). There have been reports suggesting the importance of autophagy in enhancing MHCI cross-presentation (15–17), whereas others showed the opposite (18, 13). Macroautophagy, which is one of the three distinct types of autophagy, is characterized by the formation of double-membrane autophagosomes which subsequently fuse with lysosomes and release their cargo for degradation (19). Several units, including the Atg1 complex, the PI3K complex, Atg9, the Atg2-Atg18 complex, the Atg12 conjugation system and the Atg8 (LC3) conjugation system, are involved in the formation of autophagosomes. Atg5 gets covalently coupled to Atg12 and then forms with Atg16L1 the E3-like ligase of the Atg8 (LC3) conjugation system. Therefore, Atg5 it is an essential protein for elongation of phagophoric membranes and substrate recruitment during autophagosome formation (20). Atg5-deficient DCs were impaired in their ability to present antigen on MHCII to CD4^{+} T cells due to impaired phagosomal-to-lysosome fusion and delivery of lysosomal proteases to the phagosomes (13).

In the current study we used DCs from mice in which Atg5 was conditionally deleted in CD11c-positive DCs and macrophages. We show that by blocking autophagy, antigen presence in storage compartments is prolonged, as well greatly enhancing antigen cross-presentation to CD8^{+} T cells. Using Atg8 (LC3), which gets covalently coupled to

6

membranes of autophagosomes, we show that the storage compartments are associated with autophagosomes in DCs. Our results suggest that autophagosomes disrupt antigen storage in DCs and thereby regulate late MHCI cross-presentation.

RESULTS

Antigen storage in DCs is not disrupted by autophagy inhibitors

We have reported earlier that DCs have the ability to store antigen for several days in endo/lysosomal compartments (6). We suggested that antigen storage is beneficial for prolonged antigen cross-presentation to CD8^{+} T cells *in vivo*. As MHCI-peptide complexes have a relatively high turnover rate on the DC cell surface, these antigen storage compartment allow sustained antigen presentation for several days. We investigated whether autophagy could affect the storage of antigen in DCs by using the autophagy inhibitors Wortmannin (WM) and 3-Methyladenine (3-MA). DCs were first pulse-loaded with antigen-antibody immune complexes (OVA IC) for 2 h and chased for 24 h, followed by incubation of autophagy inhibitors. DCs that were incubated with 3-MA or WM showed decreased LC3 coupling to autophagic membranes, as measured by LC3-II expression, indicating reduced formation of autophagosomes (Fig. 1A, upper panel). Proteasome activity, as detected with an activity-based fluorescent probe, was not affected by the inhibition of autophagy (Fig. 1A, lower panel). The amount of antigen conserved in DCs in the presence of WM (MFI 761) is similar without inhibitors (MFI 775), and slightly increased when incubated with 3-MA (MFI 987) (Fig. 1B). Inhibiting autophagy did not affect the expression levels of MHCI on DCs (Fig. 1C). After 2 h pulse and 24 h chase, antigen was stored in DCs in LAMP1 positive compartments, located perinuclear in the cell cytosol (Fig. 1D, upper panel). It showed similar outcome when DCs were incubated with either 3-MA or WM (Fig. 1D, middle and lower panel). The storage compartments are distinct from EEA-1 loading compartments, no co-localization was found with antigen and EEA-1 marker whether DCs were incubated with or without autophagy inhibitors (Supplemental Fig. 1). These results indicate that using inhibitors to block autophagosome formation does not detectably disrupt antigen storage in LAMP1 positive endosomal compartments in DCs.
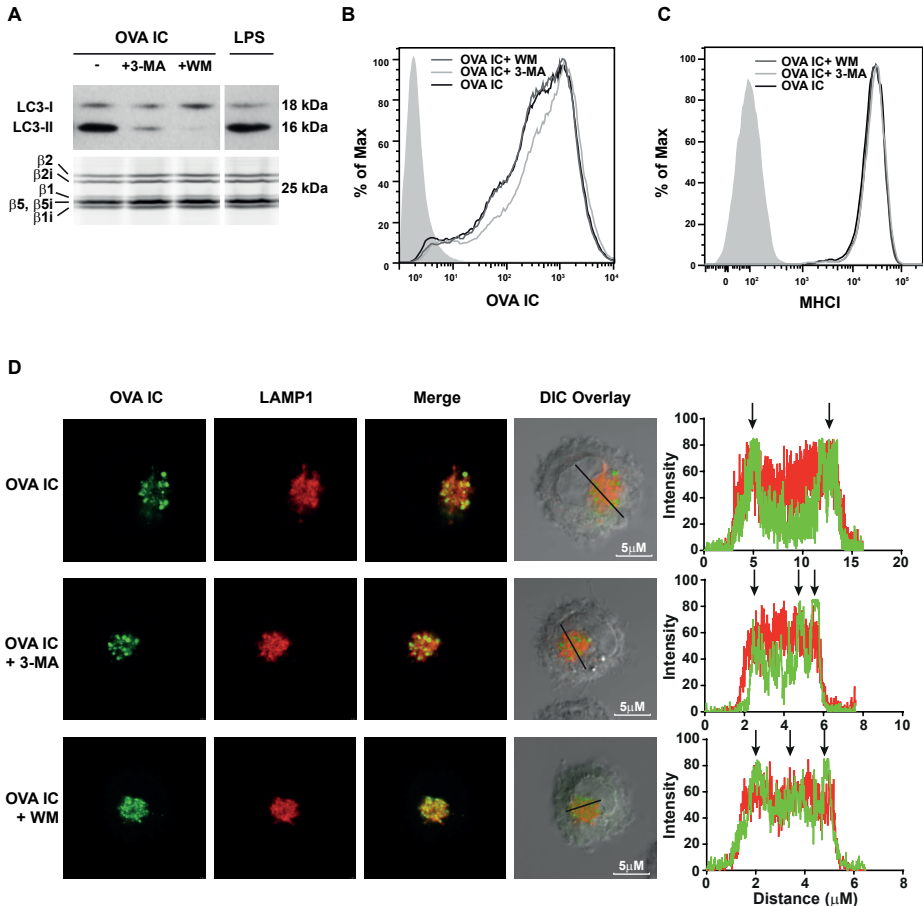
Figure 1. Antigen storage in DCs is not disrupted by autophagy inhibitors. DCs were pulse-loaded with OVA IC for 2 h and chased for 48 h. Autophagy inhibitors 3-MA or WM were added for 2 h. LPS was used as positive control for DC maturation. During the last 30 min of autophagy inhibitors incubation an activity-based proteasome probe (BODIPY-TMR labeled) was added to visualize the active β subunits of the proteasome. Proteins from total cell lysates were separated on SDS-PAGE gel and BODIPY-TMR labeled activity proteasome subunits were measured directly from the gel using a Typhoon 9410 variable mode imager. Proteins were transferred to a nitrocellulose membrane and LC3-I and LC3-II expression was visualized by western blot **(A)**. D1 cells were incubated with OVA IC (OVA Alexa Fluor 488 labeled) for 2 h and chased for 24 h. Cells were then incubated with 3-MA or WM for 24 h. Antigen presence in DCs was measured by flow cytometry **(B)**. D1 cells were incubated for 2 h with OVA IC (OVA Alexa Fluor 488 labeled) and chased for 24 h followed by incubation with 3-MA or WM for 48 h. MHCI expression levels were measured by flow cytometry **(C)**. D1 cells were pulse-loaded with OVA IC (Alexa Fluor 488 labeled OVA) for 2 h and chased for 24 h followed by incubation with 3-MA or WM for 24 h. Cells were then incubated with LAMP1 (Alexa Fluor 647 labeled) antibody and imaged by confocal microscopy. Differential interference contrast (DIC) was additionally used to image cell contrast. Histograms for each fluorophore were created for a selected area (indicated by a line on the image) and overlays were made with the ImageJ software. Arrows indicate co-localization between OVA IC (green) and LAMP1 (red) **(D)**. Representative results are shown here from two independent experiments.

Long term cross-presentation is enhanced by autophagy inhibitors

Several reports have shown the inhibitory effect of autophagy on MHCI cross-presentation by DCs, however they were mostly measured a few hours after antigen uptake (16, 17). We could show comparable results when DCs were pre-incubated with 3-MA or WM and incubated with OVA IC for 2 h (Fig. 2A, left graph). In the presence of autophagy inhibitors, early antigen cross-presentation by DCs was significantly impaired. DC cell surface loading with minimal peptide OVA-8 (SIINFEKL) indicated that the treated DCs were not hampered in their antigen presentation capacity (Fig. 2A, right graph). To investigate the impact of autophagy on long term DC cross-presentation, DCs were pulse-loaded with OVA IC for 2 h and chased for 24 h, followed by incubation with autophagy inhibitors. In contrast, antigen presentation was significantly enhanced in the presence of 3-MA or WM (Fig. 2B, left graph), whereas exogenous minimal peptide OVA-8 loading showed again no differences (Fig. 2B, right graph). To establish that presented antigenic peptides were derived from internal sources we stripped the cell surface of DC cells which were pulse-loaded with OVA IC and chased for 24 h in the presence or absence of autophagy inhibitors. Cell surface peptides were stripped with a mild acidic elution buffer and the recovery of newly synthesized peptides from the storage compartment loaded on MHCI was measured. All conditions showed undetectable antigen presentation when the DC cell surface was stripped with elution buffer (Fig. 2C). DCs without inhibitors were able to recover newly synthesized peptides on the surface, although to a lesser extent (~30%) compared to before the elution (Fig. 2C, dark bars) as we have published previously (21). Both 3-MA and WM significantly enhanced peptide recovery from the storage compartment compared to recovery without inhibitors (Fig. 2C, grey and white bars). These results indicate that by blocking autophagy, antigen presentation from internal storage compartments is increased, in contrast to short term cross-presentation which is inhibited.

Antigen storage is prolonged in autophagy-deficient DCs

We generated BMDCs from autophagy-deficient mice lacking Atg5 in CD11c positive cells (Atg5$^{-/-}$) to further investigate the effect of autophagy on antigen storage in DCs. Atg5 forms a complex together with Atg12 and Atg16L1 which is required for the association of LC3 with the autophagosomal membrane during the early stages of autophagosome formation. BMDCs are known to be a heterogeneous population (22),we used the following gating strategy to isolate DCs: CD11c$^+$ CD11b^{lo} MHCII^{int} (Fig. 3A). Atg5$^{-/-}$ DCs have higher LC3-I and totally lacked LC3-II expression compared to control mice (Atg5$^{fl/fl}$), whereas proteasome activity remained the same (Fig. 3B). Atg5$^{-/-}$ DCs were pulsed for 1 h with OVA IC and chased for different time points. After the initial 2 h pulse of antigen and 5 h chase, the amount of antigen uptake is similar in both Atg5$^{-/-}$ and Atg5$^{fl/fl}$ DCs (Fig. 3C).
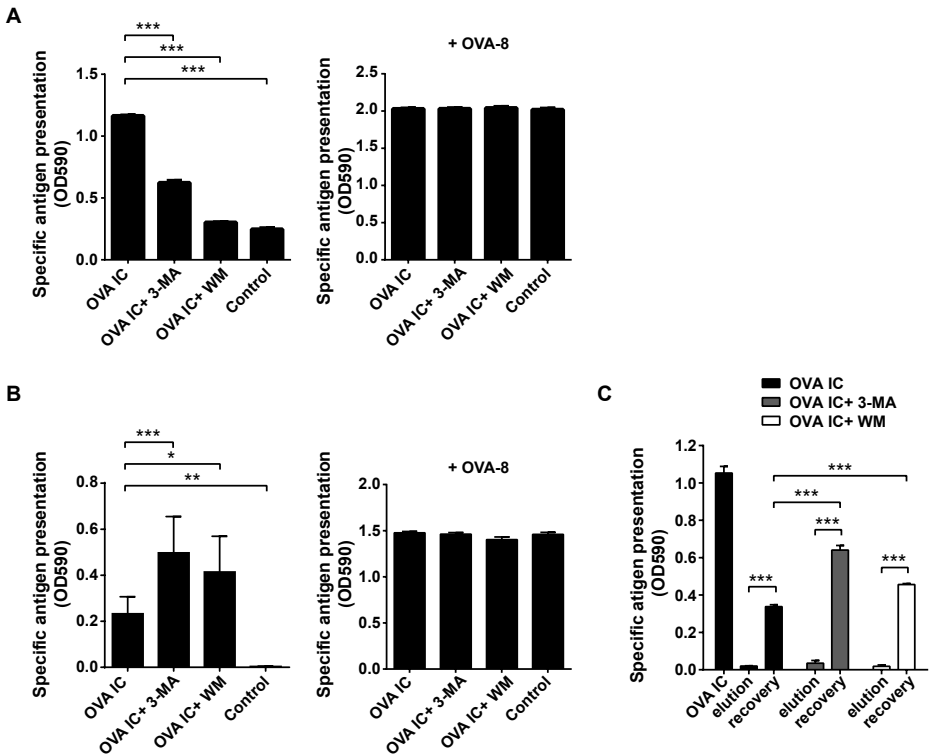
Figure 2. DC cross-presentation is enhanced by autophagy inhibitors. DCs were pre-incubated with 3-MA or WM for 2 h before incubation with OVA IC for 2 h. Antigen presentation was measured by adding B3Z CD8+ T cell hybridoma overnight (left graph). Minimal peptide OVA-8 SIINFEKL (right graph) was added as positive control **(A)**. DCs were incubated with OVA IC for 2 h and chased for 24 h. Cells were then incubated with 3-MA or WM for 24 h. Antigen presentation was measured with B3Z cells **(B)**. DCs were pulse loaded with OVA IC for 2 h followed by 24 h chase. Cells were then incubated with 3-MA or WM for 24 h. Cell surface peptides on MHCI molecules were stripped by mild acid citrate/phosphate elution buffer and incubated again with 3-MA or WM during 6 h of peptide recovery and antigen presentation was measured overnight with B3Z T cells (indicated by OD590) **(C)**. Representative results are shown here from three independent experiments. * p<0.05, ** p<0.01, *** p<0.001.

6

However, after 24 h or longer, significantly more antigen was detectable in DCs lacking Atg5. MHCI expression was comparable in Atg5$^{-/-}$ and Atg5$^{fl/fl}$ after 24 h antigen chase (Fig. 3D). The pH of the antigen containing compartments in both Atg5$^{-/-}$ and Atg5$^{fl/fl}$ were similar after 1 h antigen pulse, and decreased gradually but remained comparable in time towards pH 4 in the storage compartments (Fig. 3E). These results indicate that in absence of autophagy mediator Atg5 the presence of antigen in DCs is prolonged, which is not related to significant changes in phagosomal acidification.
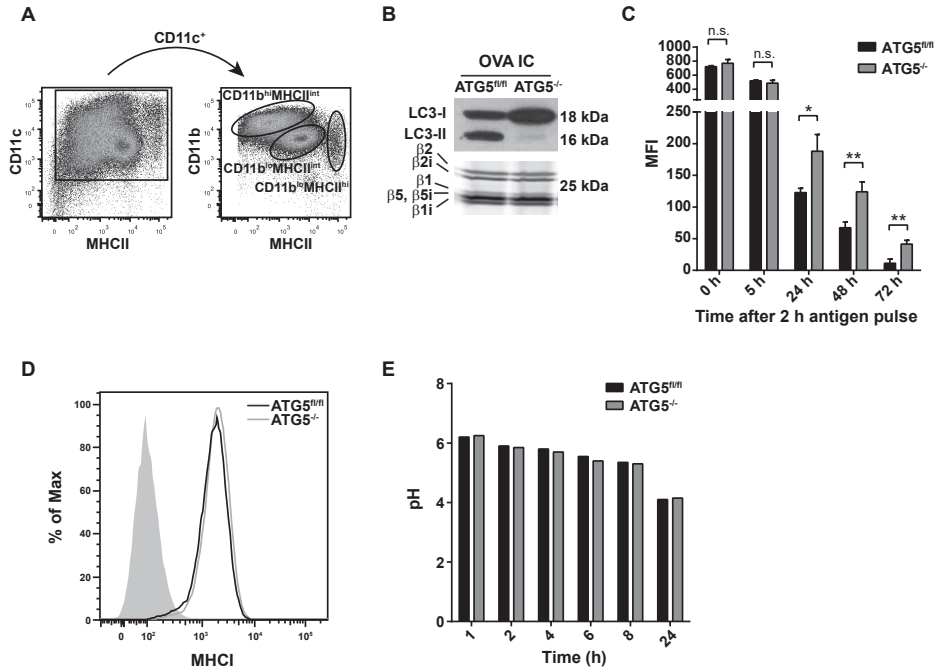
Figure 3. Antigen storage is enhanced in autophagy-deficient DCs. Bone marrow dendritic cells (BMDCs) were gated according to the following markers: CD11c+ CD11b^{lo} MHCII^{int} **(A)**. BMDCs were pulsed with OVA IC for 2 h and chased for 48 h followed by 30 min incubation with activity-based proteasome probe (BODIPY-TMR labeled). Proteins from total cell lysates were separated on SDS-PAGE gel and BODIPY-TMR labeled activity proteasome subunits were measured directly from the gel using a Typhoon 9410 variable mode imager. Proteins were transferred to a nitrocellulose membrane and LC3-I and LC3-II expression was visualized by western blot **(B)**. BMDCs from Atg5$^{-/-}$ or Atg5$^{fl/fl}$ mice were incubated with OVA IC (OVA Alexa Fluor 488 labeled) for 2 h and chased for 0, 5, 24, 48 or 72 h. Antigen presence in DCs was measured by flow cytometry (indicated by MFI) **(C)**. BMDCs from Atg5$^{-/-}$ or Atg5$^{fl/fl}$ mice were incubated for 2 h with OVA IC (OVA Alexa Fluor 488 labeled) and chased for 24 h. MHCI expression levels were measured by flow cytometry **(D)**. pH of antigen containing compartments in BMDCs from Atg5$^{-/-}$ or Atg5$^{fl/fl}$ mice was measured. Cells were incubated with IC (partial OVA FITC (pH sensitive) and Alexa Fluor 647 labeled as described in material and methods) for 1 h and 1, 2, 4, 6, 8, or 24 h chase. The uptake of OVA antigen labeled with FITC and Alexa Fluor 647 were measured by flow cytometry. The ratio between OVA FITC and OVA Alexa Fluor 647 was calculated to determine the pH value of antigen compartments **(E)**. Representative results are shown here from two independent experiments. n.s non-significant, * p<0.05, ** p<0.01.

MHCI antigen cross-presentation is enhanced in autophagy-deficient DCs

Since blocking autophagy reduced antigen degradation in the storage compartments, we investigated the effect on antigen cross-presentation to CD8+ T cells. Atg5$^{-/-}$ DCs were pulse loaded with OVA IC and chased for 24, 48 or 72 h. Antigen cross-presentation after 24 h was detectably higher by Atg5$^{-/-}$ DCs compared to Atg5$^{fl/fl}$ DCs (Fig. 4A). Antigen presentation capacity of the Atg5$^{-/-}$ DCs sustained in time, even 72 h after the initial antigen pulse CD8+ T cell proliferation remained superior to Atg5$^{fl/fl}$ DCs. Comparable results were found when

using soluble OVA protein, Atg5$^{-/-}$ DCs induced higher T cell proliferation compared to Atg5$^{fl/fl}$ DCs (Supplemental Fig. 2). Moreover, mild acid elution was carried out to show peptide recovery from internal antigen sources. Atg5$^{-/-}$ DCs were pulse loaded with OVA IC, chased for 48 h and stripped from their cell surface peptides with an elution buffer. Prior to peptide elution, Atg5$^{-/-}$ DCs again showed higher antigen cross-presentation to CD8$^+$ T cells compared to Atg5$^{fl/fl}$ DCs (Fig. 4B, left panel). After peptide elution, antigen presentation reduced to similarly low levels in both Atg5$^{-/-}$ and Atg5$^{fl/fl}$ DCs (Fig. 4B, middle panel). Six hours recovery was sufficient to restore the initial antigen presentation capacity of the DCs, however, Atg5$^{-/-}$ DCs induced much higher CD8$^+$ T cell proliferation compared to Atg5$^{fl/fl}$ DCs (Fig. 4B, right panel). These data show that antigen presentation from internal sources in autophagy-deficient DCs is enhanced.

Antigen storage compartments are in close proximity to autophagosomes

Our results indicate that autophagosomes have negative effects on antigen storage in DCs and thereby affecting antigen cross-presentation. It is therefore likely that the antigen containing compartments and autophagosomes are in close proximity in the cell. DCs were pulse- loaded with OVA IC (Alexa Fluor 488 labeled) and chased in time up to 24 h. Using an LC3 marker that stains both LC3-I and LC3-II (Alexa Fluor 647 labeled), autophagosomes could be detected in DCs. After 30 min antigen pulse, LC3 showed punctuated "hotspots" spread in the cell cytosol distinct from antigen (Fig. 5A, upper panel). After 1 h, LC3 started to cluster more around the antigen compartments, and after 3 h, the majority of LC3 was located on the same perinuclear location as the antigen containing compartments as we have previously reported (21) (Fig. 5A, 2nd and 3rd panel). After 24 h, most LC3 is co-localizing or in close proximity with the storage compartments (Fig. 5A, bottom panel). Similar experiment with 30 min antigen pulse in Atg5$^{-/-}$ DCs showed no punctuated LC3 "hotspots" (LC3-II), but instead a diffuse cytosolic staining (LC3-I) (Fig. 5B, 2nd panel) compared to Atg5$^{fl/fl}$ DCs (Fig. 5B, upper panel). After 24 h LC3 "hotspots" were co-localizing with OVA IC in Atg5$^{fl/fl}$ DCs but not in Atg5$^{-/-}$ DCs (Fig. 5B, third and lower panel). These results show that the antigen containing compartments are co-localizing with or in close proximity to autophagosomes.

6

A
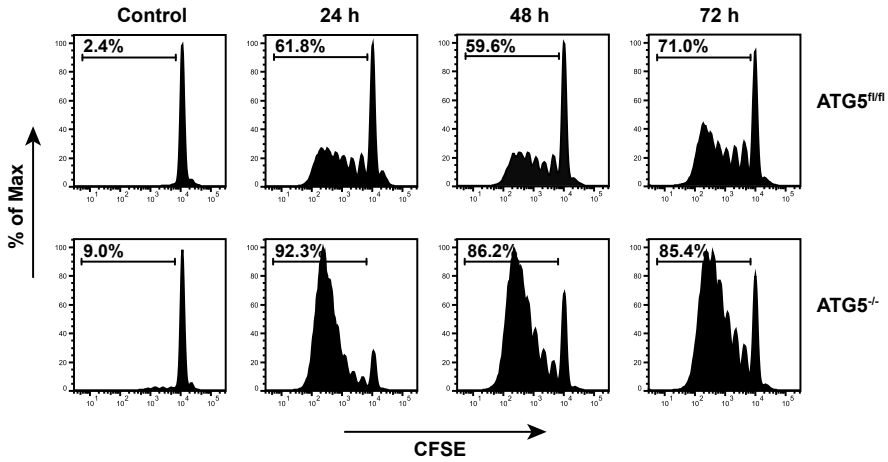
B
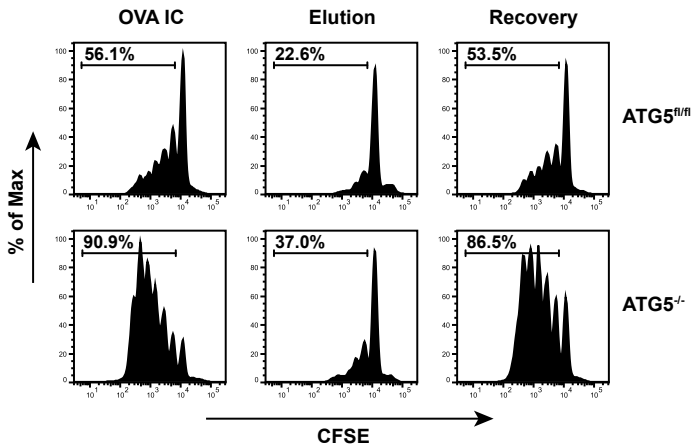
Figure 4. MHCI antigen cross-presentation is enhanced in autophagy-deficient DCs. BMDCs from Atg5^{-/-} or Atg5^{fl/fl} mice were sorted and pulsed for 2 h with OVA IC and chased for 24, 48 or 72 h. CFSE labeled CD8^{+} T cells from OTI mice were added and T cell proliferation was measured after 4 days by flow cytometry **(A)**. BMDCs from Atg5^{-/-} or Atg5^{fl/fl} mice were pulse-loaded with OVA IC for 2 h followed by 48 h chase. Cells were then stripped for surface MHCI molecules with mild acid citrate/phosphate elution buffer and recovered for 6 h. CFSE labeled CD8^{+} T cells from OTI mice were added and T cell proliferation was measured after 3 days by flow cytometry **(B)**. Representative results are shown here from two independent experiments.
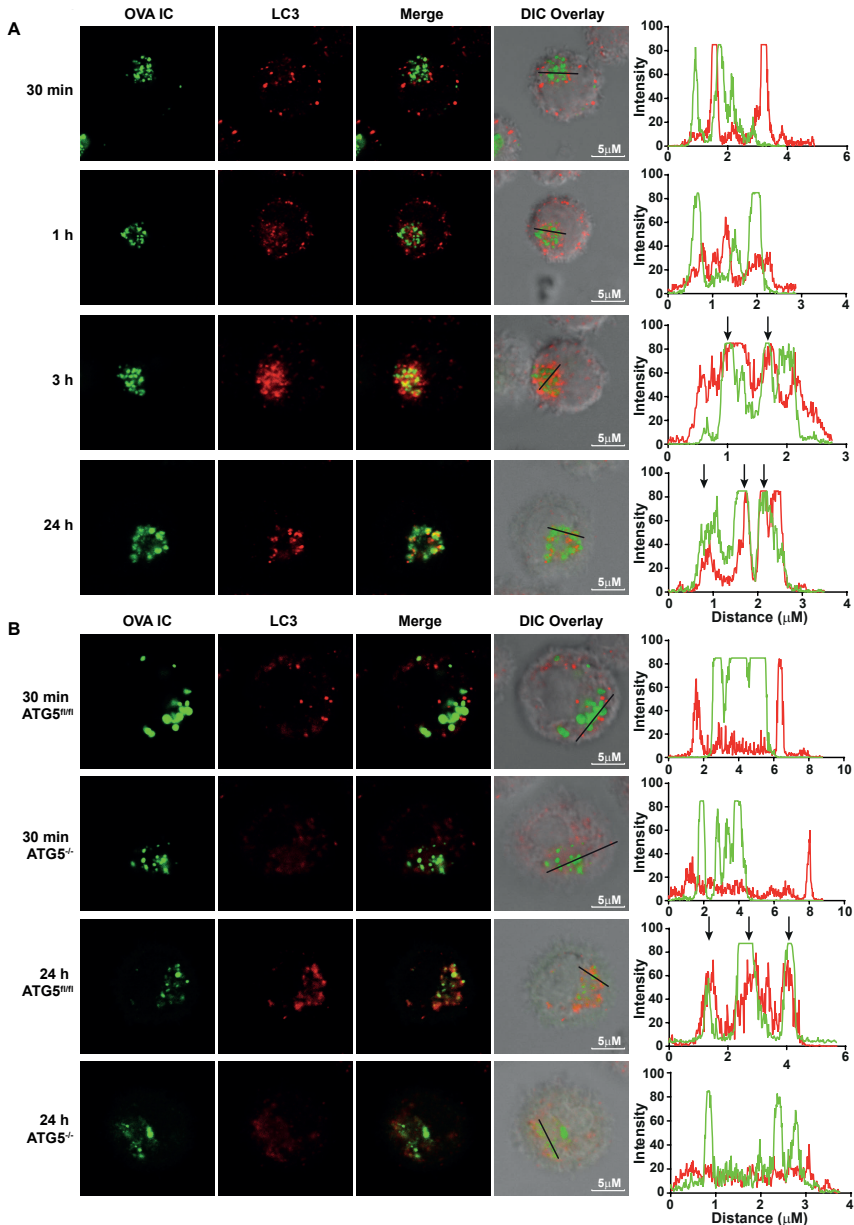
Figure 5. Antigen storage compartments are in close proximity with autophagosomes.
Dendritic cells were pulse-loaded with OVA IC (Alexa Fluor 488 labeled OVA) for 30 min and chased for 1, 3, or 24 h and stained with LC3 marker (Alexa Fluor 647 labeled) **(A)**. BMDCs from Atg5$^{-/-}$ or Atg5$^{fl/fl}$ mice were incubated with OVA IC (Alexa Fluor 488 labeled OVA) for 30 min or pulse-loaded for 2 h and chased for 24 h. In addition, 10 μM Chloroquine was added for 30 min to induce higher LC3 expression levels and cells were stained with LC3 marker (Alexa Fluor 647 labeled) **(B)**. Cells were imaged by confocal microscopy and differential interference contrast (DIC) was additionally used to image cell contrast. Histograms for each fluorophore were created for a selected area (indicated by a line on the image) and overlays were made with the ImageJ software. Arrows indicate co-localization between OVA IC (green) and LC3 (red). Representative results are shown here from two independent experiments.

DISCUSSION

Dendritic cells (DCs) have been recognized for their superiority in cross-presenting exogenous antigen to CD8^{+} T cells. We have previously reported that DCs can store antigen for several days in a lysosome-like storage compartment which contributes to sustained antigen presentation to T cells (21). In the current study we demonstrated, with the use of antibody-bound antigen which is effectively engulfed by Fc receptor-mediated uptake, that autophagy has a severe impact on the amount of antigen stored in the storage compartments and thereby affecting antigen cross-presentation outcome. DCs that were treated with common autophagy inhibitors or gained from Atg5^{-/-} mice showed prolonged antigen storage and significantly enhanced antigen cross-presentation to CD8^{+} T cells. This was rather unexpected since it was reported that autophagy inhibition can negatively influence MHCI cross-presentation (15–17). We could confirm this in short term antigen presentation assays. However, we observed the opposite enhancing effect on long term antigen cross-presentation which can be explained by inhibition of autophagosomal degradation of internal antigen containing compartments.

An alternative explanation for enhanced MHCI antigen cross-presentation upon autophagy inhibition was described by Loi et al. showing elevated MHCI surface levels on Atg5 or Atg7 deficient DCs (23). This might be a cellular mechanism to balance the MHCI and MHCII antigen presentation by DCs, and was mainly observed on DCs and alveolar macrophages *ex vivo*. However, in our study conditions we did not find significant differences in MHCI surface expression levels on Atg5 deficient DCs upon maturation, suggesting the enhanced cross-presentation is rather caused by increased peptide production. Moreover, we showed that proteasomal enzyme activity was not affected in autophagy deficient DCs or by treating DCs with autophagy inhibitors, thereby excluding a significant role of proteasome activity in enhancing cross-presentation upon autophagy inhibition.

LC3-associated phagocytosis (LAP), an autophagy pathway initiated by pattern recognition receptors and mainly described as machinery for extracellular MHCII presentation, leads to the recruitment of LC3 to form single-membrane phagosomes (24, 14). There is a possibility that LAP also plays a role in MHCI cross-presentation. Both the Atg5-12-16L and Atg8 (LC3) conjugation system are required for lysosomal fusion and maturation of the LAP-engaged phagosome, facilitating degradation of engulfed pathogens and modulation of immune responses. Moreover, it has been shown that a Class III PI3K-associated protein, Rubicon, which is required for LAP, can stabilize NOX2 complex for ROS production in LAP (25). There have been reports showing the effect of NOX2-generated ROS on phagosomal pH induction and thereby reducing antigen degradation in phagosomes resulting in enhanced antigen cross-presentation (26, 27). We showed in the current study that antigen containing storage compartments are co-localizing or at

least in very close proximity with LC3-positive autophagosomes, however we did not find any detectable differences in antigen containing compartment-pH between wildtype and Atg5 deficient DCs. It seems that antigen degradation in the storage compartments is not controlled by lysosomal enzyme activity within the compartments, but rather degraded by autophagosomes in a different manner. It has been reported that during autophagy it is important that the edges of the isolation membrane of autophagosomes are sealed. This is to prevent leakage of hydrolases that can cause cellular damage and apoptosis (28, 29). Therefore, it is conceivable that autophagosomes prevent translocation of antigen from the storage compartment to the cytosol. Another possibility is that, under normal conditions, the storage compartments are slowly leaking antigen to the cytosol for antigen processing and MHCI presentation. However this process might be disrupted by autophagy since it has been reported that autophagosomes can degrade leaky endosomes (30). This might regulate the long-term storage of antigen in the storage compartments and thereby the sustained cross-presentation ability of DCs. How protein antigen is stored in the storage compartments is still not clear. There might be specific hydrolases or cathepsins lacking in the storage compartments.

Several studies have investigated the role of autophagy in DC cross-presentation with contradictory results. Some groups showed elevated CD8+ T cell responses upon autophagy inhibition in DCs with different antigen targeting systems (23), while others showed autophagy-independent cross-presentation (13) or even lowered immune responses upon blocking autophagy (16, 18). It seems that the outcome depends on the type of antigen, cell subset and time point of measuring antigen presentation. Most studies show DC antigen presentation already after a few hours, whereas we have studied prolonged antigen presentation capacity of DCs several days after the initial antigen pulse. In the current report we showed that blocking autophagy inhibits breakdown of antigen containing compartments and thereby enhancing the presence of protein antigen in DCs available for antigen cross-presentation to CD8+ T cells. We therefore propose that autophagy can regulate long term antigen cross-presentation capacity of DCs.

6

MATERIALS & METHODS

Cells
The D1 cells, a long-term growth factor dependent immature splenic DC line derived from C57BL/6 (BL/6) mice, were kindly provided by P. Ricciardi-Castagnoli (University of Milano-Bicocca, Italy) and cultured as described (31). Bone marrow cells from Atg5-/- and Atg5fl/fl mice (provided by C. Münz) were cultured in the presence of 30% R1 supernatant from NIH3T3 fibroblasts transfected with GM-CSF for 10 days. Atg5-/- mice were conditionally deleted in

CD11c-positive DCs and macrophages by crossing CD11c-cre mice with Atg5$^{fl/fl}$ mice. From this source, bone marrow-derived dendritic cells (BMDCs) were generated and gated in flow cytometry according to the following markers: CD11c$^+$ CD11b^{lo} MHCII^{int}. CD8$^+$ T cells (CD8$^+$/CD45.1$^+$) were purified (Mouse CD8 T Lymphocyte Enrichment Set, BD Biosciences) from the spleen of OTI mice (CD8$^+$ T cell transgenic mice expressing a TCR recognizing the OVA derived K^b associated epitope SIINFEKL) that were bred and kept at the LUMC animal facility under SPF conditions. B3Z is a CD8$^+$ T cell hybridoma specific for SIINFEKL on H2-K^b MHCI molecules and expresses LacZ upon activation.

Ag-IgG immune complexes

OVA-IgG immune complexes (OVA IC) were formed by incubating 1 µg/ml OVA (unconjugated; Worthington Biochemical, or Alex Fluor 488 conjugated; Life Technologies) and 300 µg/ml anti-OVA IgG (rabbit polyclonal, LSBio) for 30 min at 37^{0}C *in vitro*. DCs were loaded with OVA IC as indicated in each experiment.

LC3 expression in DCs

Immature D1 DCs were pulsed with OVA IC (unconjugated OVA) for 2 h, washed and chased for 48 h followed by 2 h incubation with either 5 mM 3-Methyladenine (3-MA, Calbiochem), 0.5 µM Wortmannin (WM, Invivogen) or medium control. As a positive control for DC maturation, 5 µg/ml LPS (Sigma) was used. During the last 30 min of autophagy inhibitors incubation 2 µM activity-based proteasome probe MVB003 (BODIPY-TMR labeled), which was kindly provided by Hermen Overkleeft (Leiden Institute of Chemistry, The Netherlands), was added (32). BMDCs from Atg5$^{-/-}$ or Atg5$^{fl/fl}$ mice were generated, gated in flow cytometry as described above and sorted by BD FACSAria II SORP (BD Biosciences). BMDCs were pulsed with OVA IC (unconjugated OVA) for 2 h and chased for 48 h followed by 30 min incubation with the activity-based proteasome probe. Proteins from total cell lysates from D1 DCs or BMDCs were separated by 15% SDS-PAGE gel and BODIPY-TMR labeled activity proteasome subunits were measured directly from the gel by using a Typhoon 9410 variable mode imager (GE Healthcare Bio-Sciences). Proteins were then transferred to a nitrocellulose membrane and incubated with polyclonal rabbit IgG anti-LC3 (MBL) followed by Peroxidase-conjugated Goat anti-Rabbit IgG (H+L, Jackson ImmunoResearch) and visualized with an enhanced chemiluminescent substrate for the detection of HRP (Thermo Fisher Scientific) in western blot.

Antigen presence in dendritic cells

Immature D1 DCs were pulse-loaded with OVA IC (OVA Alexa Fluor 488 labeled) for 2 h and chased for 24 h. Cells were then incubated with 5 mM 3-MA, 0.5 µM WM or medium control for 24 h. BMDCs from Atg5$^{-/-}$ or Atg5$^{fl/fl}$ mice were incubated with OVA IC (OVA Alexa

Fluor 488 labeled) for 2 h and chased for 0, 5, 24, 48 or 72 h. Antigen presence in DCs was measured by flow cytometry.

DC antigen presentation

For early antigen presentation, immature D1 DCs were pre-incubated with 5 mM 3-MA or 0.5 µM WM for 2 h before incubation with OVA IC (unconjugated) for 2 h. Antigen presentation was measured by adding B3Z CD8+ T cell hybridoma overnight. Minimal peptide OVA-8 SIINFEKL (2 ng/ml), which binds directly to cell surface MHCI, was added as positive control. For late antigen presentation, immature D1 DCs were incubated with OVA IC (unconjugated OVA) for 2 h and chased for 24 h. Cells were then incubated with 5 mM 3-MA, 0.5 µM WM or medium control for 24 h. Antigen presentation was measured by adding B3Z CD8+ T cell hybridoma overnight. Minimal peptide OVA-8 SIINFEKL was added as positive control. BMDCs from Atg5-/- or Atg5fl/fl mice were sorted as described above and pulsed for 2 h with OVA IC (unconjugated OVA) and chased for 24, 48 or 72 h, or cells were pulsed for 2h with 500µg/ml OVA (unconjugated) and chased for 48 h. CFSE labeled CD8+ T cells (CD8+/CD45.1+) from OTI mice were added and T cell proliferation was measured 3 days later by flow cytometry.

DC peptide elution assay

Immature D1 DCs were pulse-loaded with OVA IC (unconjugated OVA) for 2 h followed by 24 h chase. Cells were then incubated with 5 mM 3-MA, 0.5 µM WM or medium control for 24 h. Cell surface peptides on MHCI molecules were stripped by mild acid citrate/phosphate buffer with pH3.3. Cells were again incubated with 3-MA, WM or medium control during 6 h of peptide recovery and fixated in 0.2% paraformaldehyde before T cell activation read-out with B3Z T cells. BMDCs from Atg5-/- or Atg5fl/fl mice were sorted as described above and pulse loaded with OVA IC (unconjugated OVA) for 2 h followed by 48 h chase, stripped for surface MHCI molecules and recovered for 6 h.

6

MHCI expression on DCs

Immature D1 DCs were incubated with OVA IC (Alexa Fluor 488 labeled OVA) for 24 h followed by 48 h with 5 mM 3-MA, 0.5 µM WM or medium control. BMDCs from Atg5-/- or Atg5fl/fl mice were gated and sorted as described above and treated similar as the D1 DCs. Cells were harvested and incubated with primary monoclonal MHCI H-2Kb (B8.24.3) antibody and secondary Goat anti-Mouse IgG Alexa Fluor 647 conjugated antibody. MHCI expression was measured by flow cytometry.

Antigen co-localization with markers in the presence of autophagy inhibitors

D1 cells were pulse-loaded with OVA IC (Alexa Fluor 488 labeled OVA) for 2 h and chased for 24 h followed by incubation with 5 mM 3-MA or 0.5 µM WM for 24 h. Cells were transferred to glass bottom dishes (MatTek corporation, Ashland, USA) and incubated with one of the following primary antibodies as indicated in each experiment: LAMP1 (CD107a, Alexa Fluor 647, Biolegend), EEA-1 (C-15, Santa Cruz), and secondary antibody: anti-goat IgG (Alexa Fluor 647, Invitrogen). Cells were imaged using Leica SP5 STED confocal microscope with a 63x objective lens. Differential interference contrast (DIC) was additionally used to image cell contrast. Images were acquired in 10x magnification and processed with Leica LAS AF Lite software.

Antigen co-localization with LC3 positive compartments

D1 cells were pulse-loaded with OVA IC (Alexa Fluor 488 labeled OVA) for 30 min and chased for 1, 3, or 24 h. BMDCs from Atg5^{-/-} or Atg5^{fl/fl} mice were incubated with OVA IC (Alexa Fluor 488 labeled OVA) for 30 min and chased for 24 h. In addition, 10 µM Chloroquine was added for 30 min to block autophagosome turnover and LC3 degradation. Cells were then stained with LC3 antibody (4E12, MBL) and secondary antibody anti-mouse IgG (Alexa Fluor 647, Invitrogen). Cells were imaged using Leica SP5 STED confocal microscope with a 63x objective lens. Differential interference contrast (DIC) was additionally used to image cell contrast. Images were acquired in 10x magnification and processed with Leica LAS AF Lite software.

pH measurements in storage compartments

BMDCs from Atg5^{-/-} or Atg5^{fl/fl} mice were gated and sorted as described above and incubated with IC (1 h pulse and 1, 2, 4, 6, 8, or 24 h chase) formed from: 3.8 µg/ml OVA FITC (ThermoFisher Scientific), 0.2 µg/ml OVA Alexa Fluor 647 (Biolegend) and 1.6 mg/ml anti-OVA IgG (rabbit polyclonal, LSBio). The uptake of OVA antigen labeled with FITC and Alexa Fluor 647 were measured by flow cytometry indicated by MFI. Since the FITC signal will be reduced upon encountering acidic environments, the MFI ratio between OVA FITC and OVA Alexa Fluor 647 was calculated to determine the pH value of storage compartments. A standard curve of MFI ratio-pH was made by incubating OVA IC positive-BMDCs with a range of different pH buffers.

Statistical analysis

Statistical analysis was performed using one-way analysis of variance (ANOVA) test. Tukey's *post hoc* test was performed to correct for multiple comparisons. The following indications are used in all figures: n.s: non-significant, * $p<0.05$, ** $p<0.01$, *** $p<0.001$.

ACKNOWLEDGEMENTS

6

REFERENCES

1.   Rodriguez, A., A. Regnault, M. Kleijmeer, P. Ricciardi-Castagnoli, and S. Amigorena. Selective transport of internalized antigens to the cytosol for MHC class I presentation in dendritic cells. *Nat. Cell Biol.* 1999. 1: 362–368.
2.   Pooley, J. L., W. R. Heath, and K. Shortman. Cutting edge: intravenous soluble antigen is presented to CD4 T cells by CD8- dendritic cells, but cross-presented to CD8 T cells by CD8+ dendritic cells. *J. Immunol.* 2001. 166: 5327–5330.
3.   den Haan, J. M. M., and M. J. Bevan. Constitutive versus activation-dependent cross-presentation of immune complexes by CD8(+) and CD8(-) dendritic cells in vivo. *J. Exp. Med.* 2002. 196: 817–827.
4.   Grotzke, J. E., P. Kozik, J.-D. Morel, F. Impens, N. Pietrosemoli, P. Cresswell, S. Amigorena, and C. Demangel. Sec61 blockade by mycolactone inhibits antigen cross-presentation independently of endosome-to-cytosol export. *Proc. Natl. Acad. Sci. U. S. A.* 2017. 114: E5910–E5919.
5.   Alloatti, A., D. C. Rookhuizen, L. Joannas, J.-M. Carpier, S. Iborra, J. G. Magalhaes, N. Yatim, P. Kozik, D. Sancho, M. L. Albert, and S. Amigorena. Critical role for Sec22b-dependent antigen cross-presentation in antitumor immunity. *J. Exp. Med.* 2017. 214: 2231–2241.
6.   Ho, N. I., M. G. M. Camps, E. F. E. de Haas, and F. Ossendorp. Sustained cross-presentation capacity of murine splenic dendritic cell subsets in vivo. *Eur. J. Immunol.* 2018. 48: 1164–1173.
7.   Kovacsovics-Bankowski, M., and K. L. Rock. A phagosome-to-cytosol pathway for exogenous antigens presented on MHC class I molecules. *Science* 1995. 267: 243–246.
8.   Palmowski, M. J., U. Gileadi, M. Salio, A. Gallimore, M. Millrain, E. James, C. Addey, D. Scott, J. Dyson, E. Simpson, and V. Cerundolo. Role of Immunoproteasomes in Cross-Presentation. *J. Immunol.* 2006. 177: 983–990.
9.   Murrow, L., and J. Debnath. Autophagy as a Stress-Response and Quality-Control Mechanism: Implications for Cell Injury and Human Disease. *Annu. Rev. Pathol. Mech. Dis.* 2013. 8: 105–137.
10.   Dengjel, J., O. Schoor, R. Fischer, M. Reich, M. Kraus, M. Muller, K. Kreymborg, F. Altenberend, J. Brandenburg, H. Kalbacher, R. Brock, C. Driessen, H.-G. Rammensee, and S. Stevanovic. Autophagy promotes MHC class II presentation of peptides from intracellular source proteins. *Proc. Natl. Acad. Sci. U. S. A.* 2005. 102: 7922–7927.
11.   Schmid, D., M. Pypaert, and C. Münz. Antigen-Loading Compartments for Major Histocompatibility Complex Class II Molecules Continuously Receive Input from Autophagosomes. *Immunity* 2007. 26: 79–92.
12.   Kasai, M., I. Tanida, T. Ueno, E. Kominami, S. Seki, T. Ikeda, and T. Mizuochi. Autophagic Compartments Gain Access to the MHC Class II Compartments in Thymic Epithelium. *J. Immunol.* 2009. 183: 7278–7285.
13.   Lee, H. K., L. M. Mattei, B. E. Steinberg, P. Alberts, Y. H. Lee, A. Chervonsky, N. Mizushima, S. Grinstein, and A. Iwasaki. In Vivo Requirement for Atg5 in Antigen Presentation by Dendritic Cells. *Immunity* 2010. 32: 227–239.
14.   Romao, S., N. Gasser, A. C. Becker, B. Guhl, M. Bajagic, D. Vanoaica, U. Ziegler, J. Roesler, J. Dengjel, J. Reichenbach, and C. Münz. Autophagy proteins stabilize pathogen-containing phagosomes for prolonged MHC II antigen processing. *J. Cell Biol.* 2013. 203: 757–766.
15.   Tey, S. K. S.-K., and R. Khanna. Autophagy mediates transporter associated with antigen processing- independent presentation of viral epitopes through MHC class I pathway. *Blood* 2012. 120: 994–1004.
16.   Ravindran, R., N. Khan, H. I. Nakaya, S. Li, J. Loebbermann, M. S. Maddur, Y. Park, D. P. Jones, P. Chappert, J. Davoust, D. S. Weiss, H. W. Virgin, D. Ron, and B. Pulendran. Vaccine activation of the nutrient sensor GCN2 in dendritic cells enhances antigen presentation. *Science* 2014. 343: 313–317.
17.   Li, H., Y. Li, J. Jiao, and H. M. Hu. Alpha-alumina nanoparticles induce efficient autophagy-dependent cross-presentation and potent antitumour response. *Nat. Nanotechnol.* 2011. 6: 645–650.
18.   Mintern, J. D., C. Macri, W. J. Chin, S. E. Panozza, E. Segura, N. L. Patterson, P. Zeller, D. Bourges, S. Bedoui, P. J. Mcmillan, A. Idris, C. J. Nowell, A. Brown, K. J. Radford, A. P. R. Johnston, and J. A. Villadangos. Differential use of autophagy by primary dendritic cells specialized in cross-presentation. *Autophagy* 2015. 11: 906–917.
19.   Mizushima, N., T. Yoshimori, and Y. Ohsumi. The Role of Atg Proteins in Autophagosome Formation. *Annu. Rev. Cell Dev. Biol.* 2011. 27: 107–132.

20. Mizushima, N., A. Yamamoto, M. Hatano, Y. Kobayashi, Y. Kabeya, K. Suzuki, T. Tokuhisa, Y. Ohsumi, and T. Yoshimori. Dissection of autophagosome formation using Apg5-deficient mouse embryonic stem cells. *J. Cell Biol.* 2001. 152: 657–668.

21. Van Montfoort, N., M. G. Camps, S. Khan, D. V. Filippov, J. J. Weterings, J. M. Griffith, H. J. Geuze, T. van Hall, J. S. Verbeek, C. J. Melief, and F. Ossendorp. Antigen storage compartments in mature dendritic cells facilitate prolonged cytotoxic T lymphocyte cross-priming capacity. *Proc. Natl. Acad. Sci. U. S. A.* 2009. 106: 6730–6735.

22. Helft, J., J. Böttcher, P. Chakravarty, S. Zelenay, J. Huotari, B. U. Schraml, D. Goubau, and C. Reis e Sousa. GM-CSF Mouse Bone Marrow Cultures Comprise a Heterogeneous Population of CD11c(+) MHCII(+) Macrophages and Dendritic Cells. *Immunity* 2015. 42: 1197–211.

23. Loi, M., A. Müller, K. Steinbach, J. Niven, R. Barreira da Silva, P. Paul, L. A. Ligeon, A. Caruso, R. A. Albrecht, A. C. Becker, N. Annaheim, H. Nowag, J. Dengjel, A. García-Sastre, D. Merkler, C. Münz, and M. Gannagé. Macroautophagy Proteins Control MHC Class I Levels on Dendritic Cells and Shape Anti-viral CD8+ T Cell Responses. *Cell Rep.* 2016. 15: 1076–1087.

24. Sanjuan, M. A., C. P. Dillon, S. W. G. Tait, S. Moshiach, F. Dorsey, S. Connell, M. Komatsu, K. Tanaka, J. L. Cleveland, S. Withoff, and D. R. Green. Toll-like receptor signalling in macrophages links the autophagy pathway to phagocytosis. *Nature* 2007. 450: 1253–1257.

25. Martinez, J., R. K. S. Malireddi, Q. Lu, L. D. Cunha, S. Pelletier, S. Gingras, R. Orchard, J. L. Guan, H. Tan, J. Peng, T. D. Kanneganti, H. W. Virgin, and D. R. Green. Molecular characterization of LC3-associated phagocytosis reveals distinct roles for Rubicon, NOX2 and autophagy proteins. *Nat. Cell Biol.* 2015. 17: 893–906.

26. Mantegazza, A. R., A. Savina, M. Vermeulen, L. Pérez, J. Geffner, O. Hermine, S. D. Rosenzweig, F. Faure, and S. Amigorena. NADPH oxidase controls phagosomal pH and antigen cross-presentation in human dendritic cells. *Blood* 2008. 112: 4712–4722.

27. Savina, A., A. Peres, I. Cebrian, N. Carmo, C. Moita, N. Hacohen, L. F. Moita, and S. Amigorena. The Small GTPase Rac2 Controls Phagosomal Alkalinization and Antigen Crosspresentation Selectively in CD8+Dendritic Cells. *Immunity* 2009. 30: 544–555.

28. Fujita, N., M. Hayashi-Nishino, H. Fukumoto, H. Omori, A. Yamamoto, T. Noda, and T. Yoshimori. An Atg4B mutant hampers the lipidation of LC3 paralogues and causes defects in autophagosome closure. *Mol. Biol. Cell* 2008. 19: 4651–4659.

29. Kawabata, T., and T. Yoshimori. Beyond starvation: An update on the autophagic machinery and its functions. *J. Mol. Cell. Cardiol.* 2016. 95: 2–10.

30. Boyle, K. B., and F. Randow. The role of "eat-me" signals and autophagy cargo receptors in innate immunity. *Curr. Opin. Microbiol.* 2013. 16: 339–348.

31. Winzler, C., P. Rovere, M. Rescigno, F. Granucci, G. Penna, L. Adorini, V. S. Zimmermann, J. Davoust, and P. Ricciardi-Castagnoli. Maturation stages of mouse dendritic cells in growth factor-dependent long-term cultures. *J. Exp. Med.* 1997. 185: 317–328.

32. Florea, B. I., M. Verdoes, N. Li, W. A. Van Der Linden, P. P. Geurink, H. Van Den Elst, T. Hofmann, A. De Ru, P. A. Van Veelen, K. Tanaka, K. Sasaki, S. Murata, H. Den Dulk, J. Brouwer, F. A. Ossendorp, A. F. Kisselev, and H. S. Overkleeft. Activity-based profiling reveals reactivity of the murine thymoproteasome-specific subunit β5t. *Chem. Biol.* 2010. 17: 795–801.

6
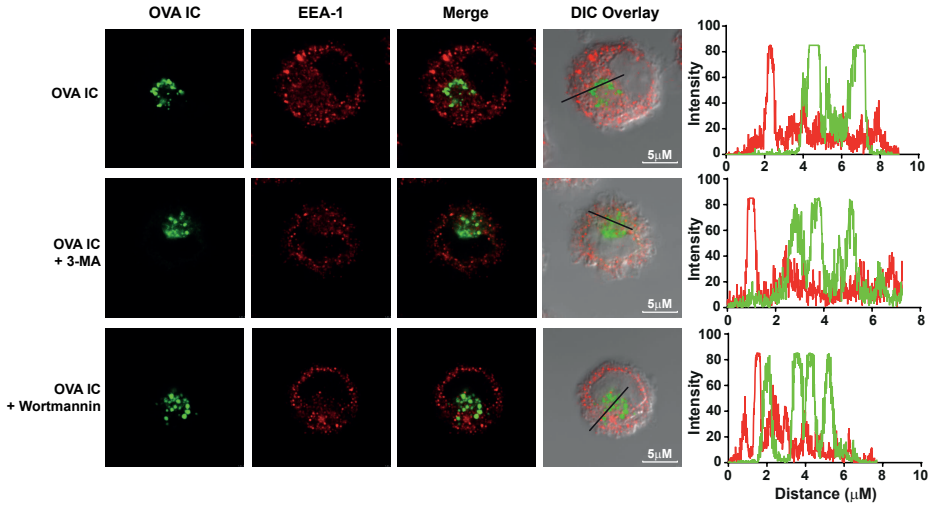
Supplemental Figure 1. Antigen storage compartment co-staining with EEA-1. DCs were pulse-loaded with OVA IC (Alexa Fluor 488 labeled OVA) for 2 h and chased for 24 h followed by incubation with 3-MA or WM for 24 h. Cells were then incubated with EEA-1 antibody and imaged by confocal microscopy. Differential interference contrast (DIC) was additionally used to image cell contrast. Histograms for each fluorophore were created for a selected area (indicated by a line on the image) and overlays were made with the ImageJ software between OVA IC (green) and EEA-1 (red). Representative results are shown here from two independent experiments.
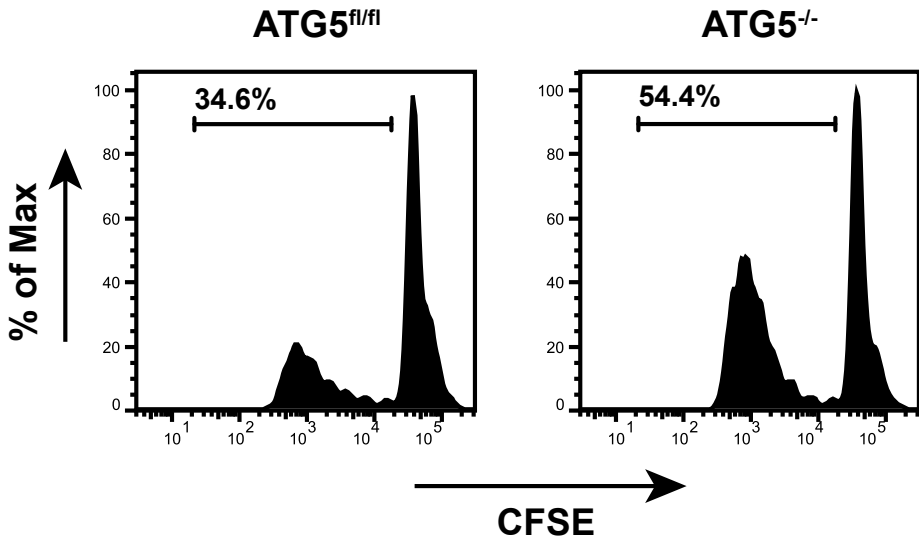
Supplemental Figure 2. Antigen presentation with soluble antigen is enhanced in autophagy-deficient DCs. BMDCs from Atg5$^{-/-}$ or Atg5$^{fl/fl}$ mice were pulse-loaded with 500ug/ml OVA for 2 h followed by 48 h chase. CFSE labeled CD8$^+$ T cells from OTI mice were added and T cell proliferation was measured after 4 days by flow cytometry. Representative results are shown here from two independent experiments.

6

7

Synthesis and evaluation of fluorescent TLR ligand-peptide conjugates in dendritic cells

Nataschja I. Ho, Geoffroy P. P. Gential, Fabrizio Chiodo, Nico Meeuwenoord, Ferry Ossendorp, Herman S. Overkleeft, Gijs A. van der Marel, Dmitri V. Filippov

ABSTRACT

Covalent conjugation of Toll-like receptors (TLRs) to synthetic antigen peptides have shown to be a promising tool for cancer vaccines. We have demonstrated before that TLR-2 ligand Pam_3CysSK_4 (Pam) linked to synthetic antigenic peptides was targeted into MHCI cross-presentation pathway and was able to strongly enhance the induction of specific CD8^{+} T cells. Moreover, the configuration at the C-2 position of the glycerol moiety of the Pam linked to OVA peptide could affect its ability to activate dendritic cells (DCs). The *R*-Pam-peptide conjugate was superior in activating DCs and inducing specific CD8^{+} T cells compared to *S*-Pam-peptide conjugate. In order to visualize and track these TLR ligand-peptide conjugates in DCs after uptake, we fluorescently labeled Pam conjugated to an OVA peptide with TAMRA or Cy5. Chirally pure *R*- and *S*-epimers of Pam were prepared and separately conjugated to an OVA model epitope, in which lysine was replaced by azidonorleucine. The azide function in the conjugate permitted labelling with different fluorophores by use of strain-promoted [3+2] cycloaddition. Combining the lipophilicity of Pam ligand with fluorophores influenced the solubility of the resulting conjugates in an unpredictable way and only the conjugates labeled with Cy5 were suitable for confocal fluorescence microscopy experiments. We show here that both epimers of the Cy5 labeled lipopeptides were internalized equally well. The presented results demonstrate the usefulness of strain-promoted azide-alkyne cycloaddition in the labelling of highly lipophilic lipopeptides without disturbing the *in vitro* activity of these conjugates with respect to activation of TLR-2. Further comparison between different types of fluorophores on CpG-peptide conjugates revealed that also these conjugates can activate DCs and efficiently be taken up in endosomal compartments.

INTRODUCTION

Conjugated cancer vaccines have attracted much attention as a promising lead for innovative therapeutic interventions (1–5). A particular flavor of conjugated vaccines, that has been extensively investigated through the years, comprises a structurally defined construct of a Toll-like receptor (TLR) agonist covalently attached to a synthetic peptide, that contains a T-cell epitope, either model or tumor associated (6). It has been discovered that a conjugate of this kind showed improved T-cell priming and tumor protection compared to a mixture of the individual antigenic peptide and TLR agonist (7, 8). The usefulness of such synthetic peptide-based conjugates in tumor vaccination has been demonstrated as well. A commonly used agonist in these studies is a lipopeptide known as Pam_3CysSK_4 (Pam) that binds to TLR-2/TLR-1 (9–11). This compound has been derived from the N-terminus of bacterial lipoprotein of, among others, Escherichia coli (12). Notably, when Pam was applied as a component of a vaccine candidate, either covalently attached to a longer peptide sequence or simply admixed with a peptide, it was often present as a mixture of R- and S-epimers at the glycerol moiety (10, 13–16, 8). However, it is known that the R-epimer is the biologically active one (9, 17). With the aid of non-labeled Pam conjugates it has been shown that R-epimer of Pam is indeed the one responsible for dendritic cell (DC) activation, which directly contributed to enhanced CD8+ T cell responses, whereas the S-epimer did not activate DCs and therefore unable to prime CD8+ T cells (17). Moreover, the uptake of both chirality of Pam was comparable, although in a TLR-2 independent manner, indicating that DC activation was mainly the cause of the observed differences in CD8+ T cell priming.

In the current study, we show that fluorescently labeled and chirally pure Pam-lipopeptides represent useful tools in the studies of antigen processing since these constructs allow a visual evaluation of the antigen uptake irrespective of the DC-maturation status. Towards this end, we synthesized Pam-peptide conjugates with the fluorescent label (TAMRA or Cy5) covalently attached to the modified side chain of a lysine residue in the commonly used model MHC-I epitope (SIINFEKL). This design of the labeled construct proved to be successful in our past studies that involved the monitoring of the intracellular trafficking of Pam-lipopeptides as mixtures of epimers at C-2 of the glycerol moiety (7). To be able to vary the type of fluorophore more readily, a convergent approach based on copper free click chemistry has been chosen in the present work (18–20). The fluorescent labels TAMRA and Cy5 were connected to the Pam-peptide conjugates. We showed that with the use of strain-promoted [3+2] cycloaddition, Pam-peptide conjugates could be successfully labeled with TAMRA and Cy5. The R-, but not S-epimer of fluorescently labeled Pam- peptide conjugates was able to activate DCs in a TLR-2-dependent manner, comparable to their unlabeled analogues. However, the uptake of the fluorescently labeled R- and S- Pam-peptide conjugates by DCs was comparable as shown by confocal microscopy. Combining TAMRA

7

with Pam-peptide conjugates influenced the solubility of the conjugates in such a manner that it was difficult to use for confocal experiments. To further investigate a different TLR-ligand and its properties when fluorescently labeled, we compared CpG- peptide conjugates labeled with Alexa Fluor 488 (A488) or Cy5. We have published before that CpG (a TLR-9 agonist) is taken up independently of TLR-9, but DC activation through TLR-9 is crucial for efficient CD8+ T cell priming (7). We show here that both A488 and Cy5 labeled CpG-peptide conjugates induced comparable activation of DCs and are taken up efficiently in endosomal compartments.

RESULTS

Synthesis of fluorescently labeled TLR- peptide conjugates

In order to study the uptake and trafficking of TLR-peptide conjugates in DCs, TLR-2 ligand Pam$_3$CysSK$_4$ and TLR-9 ligand CpG were used. The *R*- and *S*- epimers of Pam$_3$CysSK$_4$(Pam)-OVA peptide conjugates were labeled with TAMRA or Cy5 and described in more detail in de published version of this study (21). In short, chirally pure *R*- and *S*- epimers of Pam were prepared and separately conjugated to an OVA model peptide (DEVSGLEQLESIINFEKL, OVA$_{247-264}$), in which lysine was replaced by azidonorleucine (Fig. 1). The azide function in the conjugate permitted labelling with different fluorophores by use of strain-promoted 3+2 cycloaddition. The synthesis of labeled CpG-OVA peptide conjugates was done as described before (7).
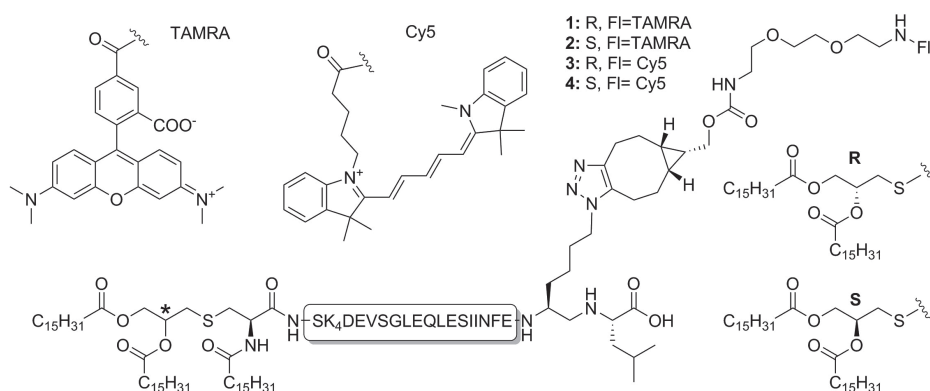
Figure 1. **Schematic overview of fluorescent labeling of TLR-ligand peptide conjugates.** Synthesis of TAMRA or Cy5 labeled *R*- and *S*- Pam$_3$CysSK$_4$ conjugated to OVA peptide (DEVSGLEQLESIINFEKL, OVA$_{247-264}$).

Fluorescently labeled Pam$_3$CysSK$_4$- peptide conjugates are efficiently taken up by DCs

To investigate the immunological function of the fluorescently labeled Pam$_3$CysSK$_4$ (Pam)-peptide conjugates, we compared the unlabeled *R*-and *S*- epimers of Pam-peptide conjugates with the TAMRA and Cy5 labeled variants on DC activation. We have shown before that the *R*-Pam is the active form which could efficiently activate DCs and promote CD8^{+} T cell priming, whereas the *S*- Pam is the inactive form and failed to induce DC activation and specific T cell priming (17). DCs were stimulated with unlabeled or labeled *R*- or *S*- Pam-peptide conjugates for 48 hours and DC maturation was measured by IL-12 production. Similar to our previous findings, unlabeled *R*- Pam-peptide conjugate induced more IL-12 production by DCs than unlabeled *S*- Pam-peptide conjugate (Fig. 2A). Comparable results were found for the TAMRA or Cy5 labeled *R*- and *S*- Pam-peptide conjugates, showing intact immunogenicity of the fluorophore-labeled conjugates. However, TAMRA appeared to influence the solubility of the Pam-peptide conjugates in an unpredictable way, therefore the TAMRA variant of the conjugates will be excluded for the following experiments.

To corroborate the TLR-2 dependent activation of DCs by the fluorescent conjugates, the compounds were next assessed using HEK-cells transfected with TLR2. The level of IL-8 produced in the assay reflects the capacity of the conjugates to activate the receptor. Both unlabeled and Cy5 labeled *R*- Pam-peptide conjugates were able to trigger human TLR-2 and induced IL-8 production by HEK cells (Fig 2B). The *S*- Pam-peptide conjugate did not induce IL-8 production, regardless of labeled or unlabeled form, indicating the lack of triggering human TLR-2. To determine the receptor specificity of immunogenic lipopeptides for TLR-2, HEK cells expressing TLR-4 were stimulated with unlabeled or Cy5 labeled *R*- or *S*- Pam-peptide conjugates. None of the compounds were able to trigger human TLR-4 indicating not only the high specificity of the immunogenic lipopeptides for TLR-2, but also the absence of any inadvertent LPS contamination in the samples of the TLR-2 activating conjugates (Fig. 2C).

The uptake of Cy5 labeled *R*- and *S*- Pam-peptide conjugates by DCs was measured with confocal microscopy. After 15 min, both compounds were efficiently internalized by DCs (shown in red and overlay with DIC) and accumulated in hot spots surrounding the nucleus (Fig. 3). Similar as we have previously reported, no differences in localization or uptake were observed (7, 17).

7
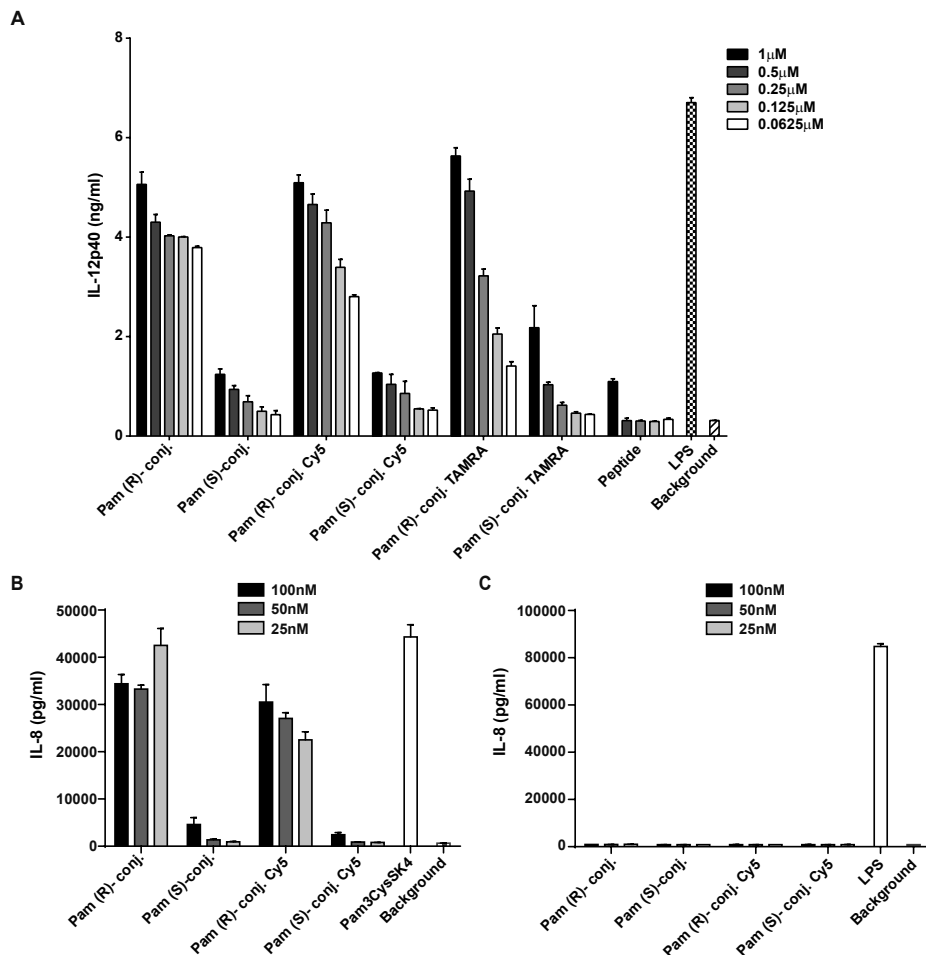
Figure 2. Activation of dendritic cells by Pam-peptide conjugates. (A) DCs were stimulated with titrated amounts of either unlabeled, TAMRA or Cy5 labeled, *R-* or *S*-Pam for 48 hours. LPS (1.25 µg/ml) and peptide (DEVSGLEQLESIINFEKL) were used as positive and negative control, respectively. Untreated cells were depicted as background signal. Supernatants were harvested and analyzed for IL-12 cytokine secretion by ELISA. One representative from three independent experiments is shown. Error bars represent SD**. (B)** Ability of immunogenic lipopeptides in triggering human IL-8 production via TLR-2. HEK TLR-2 cells were incubated with titrated amounts of unlabeled or Cy5 labeled, *R-* or *S*-Pam for 24 hours. Untreated cells and cells treated with Pam3CysSK4 (100 ng/ml) were used as negative and positive control, respectively. Error bars represent SD. **(C)** HEK TLR-4 cells were incubated with titrated amounts of unlabeled or Cy5 labeled, *R-* or *S*-Pam for 24 hours. Untreated cells and LPS (10 ng/ml) treated cells were used as negative and positive control, respectively. Supernatants were subsequently analyzed for IL-8 production by ELISA. The graphs are representative of two different independent experiments performed in duplicate. Error bars represent SD.
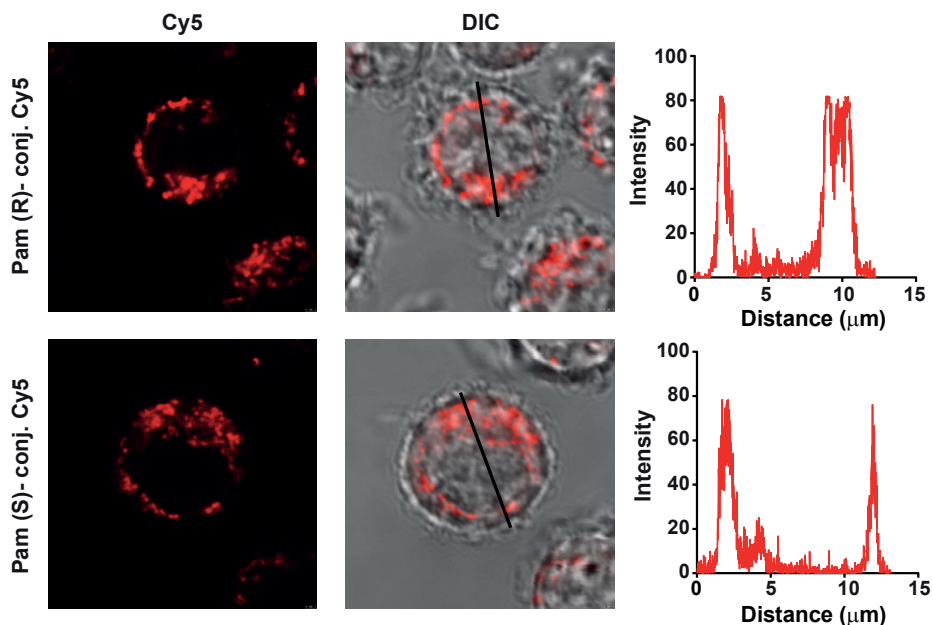
Figure 3. Uptake of *R-* and *S-* Pam-peptide conjugates by dendritic cells. DCs were incubated for 15 min with Cy5 labeled *R-* or *S-* Pam-peptide conjugates (1 μM). The uptake and localization of the compounds were analyzed with confocal laser scanning microscopy. Differential interference contrast (DIC) was used to image cell contrast. Intensity histograms were created for a selected area (indicated by a line on the image) with the ImageJ software. The images are representative for multiple cells from at least 3 experiments.

DC handling of fluorophore labeled CPG-conjugates

To further investigate a different TLR-ligand and its properties when fluorescently labeled, we used Alexa Fluor 488 (A488) or Cy5 labeled CpG-peptide conjugates. DC activation was measured by stimulating DCs with unlabeled or labeled CpG-peptide conjugates for 48 hours. All CpG-peptide conjugates significantly induced IL-12 production by DCs, regardless whether the conjugates were labeled or unlabeled (Fig. 4A). Moreover, both A488 and Cy5 labeled CpG-peptide conjugates were able to induce CD40 and CD86 expression on DCs (Fig. 4B). The uptake of the labeled CpG-peptide conjugates by DCs was visualized by confocal microscopy. DCs were stimulated with either A488 or Cy5 labeled CpG-peptide conjugates, or incubated simultaneously with A488 and Cy5 CpG-peptide conjugates for 24 hours. Both A488 and Cy5 labeled compounds were efficiently taken up by DCs and accumulated in hot spots in the cell cytosol (Fig. 5, first and second panel), which is in line with our previous work (7).

7
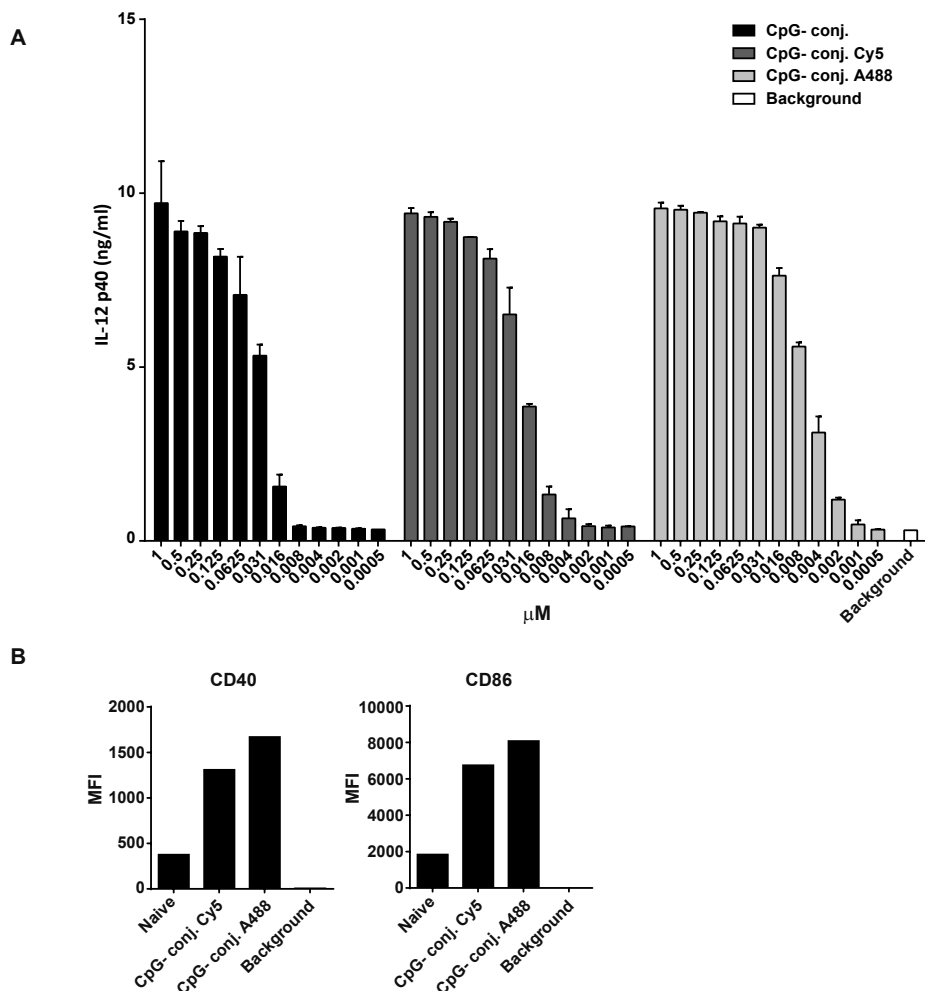
Figure 4. Activation of dendritic cells by CpG-peptide conjugates. (A) DCs were stimulated with titrated amounts of unlabeled, A488 or Cy5 labeled CpG-peptide conjugates for 48 hours. Untreated cells were depicted as background signal. Supernatants were harvested and analyzed for IL-12 cytokine secretion by ELISA. Error bars represent SD**. (B)** DCs were stimulated with A488 or Cy5 labeled CpG-peptide conjugates (1µM) for 48 hours. Naïve DCs were not treated with any compounds, and cells not stained with antibodies were used as background. CD40 and CD86 expression on DCs was measured by flow cytometry and depicted in mean fluorescence intensity (MFI).
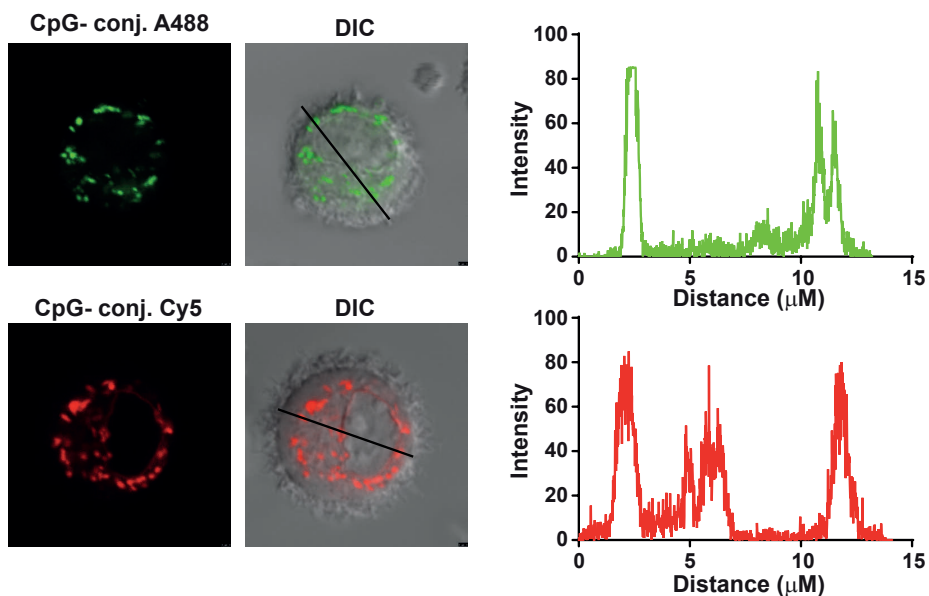
Figure 5. Uptake of CpG-peptide conjugates. DCs were incubated with A488 (green) or Cy5 (red) labeled CpG-peptide conjugates (1µM) for 2 hours and chased for 24 hours. The uptake and localization of the compounds were analyzed with confocal laser scanning microscopy. Differential interference contrast (DIC) was used to image cell contrast. Intensity histograms and overlays were created for a selected area (indicated by a line on the image) with the ImageJ software.

DISCUSSION

TLR-ligands covalently conjugated to synthetic peptides have been an attractive target for cancer vaccination strategies, especially when the peptide antigen and a defined adjuvant are combined in one compound. We have demonstrated before that TLR-2 ligand Pam_3CysSK_4 (Pam) linked to synthetic antigenic peptides was targeted into MHCI cross-presentation pathway, strongly enhancing the induction of specific CD8^{+} T cells, and efficiently inducing antitumor immunity (17, 8). In the current study we investigated the possibilities in coupling different fluorescent dyes to the *R* (active)- and *S* (inactive)- Pam conjugated to an OVA peptide. Using strain-promoted [3+2] cycloaddition, a small set of TAMRA and Cy5 labeled Pam-lipopeptides was successfully synthesized. The *R*- but not *S*-epimer of Pam in the prepared fluorescent lipopeptides triggered DC maturation in a TLR-2-dependent manner and at comparable levels as their unlabeled analogues. However, the poor aqueous solubility of the conjugates containing TAMRA precluded the use of those for microscopy studies. This reminds that attaining sufficient solubility remains a major challenge in the synthesis of Pam-based constructs labeled with fluorophores. Nevertheless, Cy5 labeled *R*- and *S*-Pam-peptide conjugates could successfully be used for confocal microscopy and were both

7

taken up by dendritic cells to the same extent. These results corroborate previous findings that suggested a TLR-independent uptake of the peptides conjugated to a TLR-ligand (7). Furthermore, we used A488 and Cy5 to label CpG-peptide conjugates and showed similar DC activation and uptake in endosomal compartments. However, interpreting data by using fluorescently labeled compounds could sometimes be challenging and new approaches to track chemically defined synthetic peptide vaccines should be investigated. Not only can fluorophores affect the uptake and routing of the compounds of interest, but it can also interrupt with antigen processing due to their bulky and hydrophobic structures compared to the relatively small peptides. One of the new possibilities to overcome these problems is the use of click chemistry (reviewed in (22)). By using biorthogonal peptides and ligation of a complementary fluorophore to the biorthogonal amino acid side chain at the end of the experiment, surface labeling of MHCI loaded minimal epitopes was quantified on APCs (23). One can imagine the possibilities with this new technique for accurate tracking of the compound of interest, even *in vivo*, bypassing solubility problems or characteristic changes caused by the type of fluorophore. However, the click chemistry technique is still limited by poor signal-to-noise ratios and further optimization is needed for future use.

MATERIALS AND METHODS

IL-12p40 ELISA

D1 dendritic cells (immature splenic dendritic cell line derived from B6 (H-2b) mice) were plated in a 96-wells plate and incubated with a titration of the compounds for 48 hours. Supernatants were collected and tested with ELISA for IL-12p40 using a standard sandwich ELISA. Coating Ab: rat anti-mouse IL-12p40 mAb (clone C15.6, Biolegend). Detection Ab: biotinylated rat anti-mouse IL-12p40 mAb (clone C17.8, Biolegend). Streptavidin-Poly-HRP (Sanquin) and 3,3',5,5' Tetramethylbenzidine (Sigma-Aldrich) were used as enzyme and substrate, respectively.

Confocal microscopy

D1 dendritic cells were incubated with Cy5 labeled *R*- or S- Pam-peptide conjugates (1 μM) for 15 min at 37 ˚C and washed with culture medium. Alexa 488 or Cy5 labeled CpG-peptide conjugates (1μM) were added to dendritic cells for 24 hours. The cells were plated out into glass-bottom Petri dishes (MatTek) and imaged using the Leica SP5-STED with a 63x objective lens. Differential interference contrast (DIC) was used to image cell contrast. Images were acquired in 10x magnification and processed with Leica LAS AF Lite software.

Activity assay on transfected TLR-2/4 HEK cells assay

Human TLR-expressing HEK cells were cultured in DMEM medium enriched with Penicillin/ Streptomycin/ Glutamine and 1% FCS. HEK TLR-2 and HEK TLR-4 cells were cultured in the presence of G418 (Geneticin, 0.5 mg/mL). Suspensions of 100 μL cells (1.106 cells/mL) were stimulated for 24 h with compounds unlabeled or Cy5 labeled *R*- or S- Pam-peptide conjugates. Pam3CysSK4 (100ng/mL) and LPS (10 ng/mL) were used as a positive control for TLR-2, and TLR-4, respectively. Supernatants were subsequently analyzed for IL-8 production by ELISA.

Flow cytometry

D1 DCs were incubated with A488 or Cy5 labeled CpG-peptide conjugates (1 μM) for 48 hours. Cells were the harvested and incubated for 20 min with CD40 (clone 3/23) and CD86 (clone GL-1) antibodies. Cells were washed twice and measured immediately with flow cytometry.

ACKNOWLEDGEMENTS

7

REFERENCES

1. Tighe, H., K. Takabayashi, D. Schwartz, G. Van Nest, S. Tuck, J. J. Eiden, A. Kagey-Sobotka, P. S. Creticos, L. M. Lichtenstein, H. L. Spiegelberg, and E. Raz. Conjugation of immunostimulatory DNA to the short ragweed allergen Amb a 1 enhances its immunogenicity and reduces its allergenicity. *J. Allergy Clin. Immunol.* 2000. 106: 124–134.

2. Maurer, T., A. Heit, H. Hochrein, F. Ampenberger, M. O'Keeffe, S. Bauer, G. B. Lipford, R. M. Vabulas, and H. Wagner. CpG-DNA aided cross-presentation of soluble antigens by dendritic cells. *Eur. J. Immunol.* 2002. 32: 2356–2364.

3. Heit, A., F. Schmitz, M. O'Keeffe, C. Staib, D. H. Busch, H. Wagner, and K. M. Huster. Protective CD8 T cell immunity triggered by CpG-protein conjugates competes with the efficacy of live vaccines. *J. Immunol.* 2005. 174: 4373–4380.

4. Zom, G. G. P., S. Khan, D. V. Filippov, and F. Ossendorp. TLR Ligand–Peptide Conjugate Vaccines: Toward Clinical Application. *Adv. Immunol.* 2012. 114: 177–201.

5. Chang, C., P. Varamini, A. K. Giddam, F. M. Mansfeld, M. J. D'Occhio, and I. Toth. Investigation of Structure-Activity Relationships of Synthetic Anti-Gonadotropin Releasing Hormone Vaccine Candidates. *ChemMedChem* 2015. 10: 901–910.

6. Jackson, D. C., Y. F. Lau, T. Le, A. Suhrbier, G. Deliyannis, C. Cheers, C. Smith, W. Zeng, and L. E. Brown. A totally synthetic vaccine of generic structure that targets Toll-like receptor 2 on dendritic cells and promotes antibody or cytotoxic T cell responses. *Proc. Natl. Acad. Sci. U. S. A.* 2004. 101: 15440–15445.

7. Khan, S., M. S. Bijker, J. J. Weterings, H. J. Tanke, G. J. Adema, T. van Hall, J. W. Drijfhout, C. J. M. Melief, H. S. Overkleeft, G. A. van der Marel, D. V. Filippov, S. H. van der Burg, and F. Ossendorp. Distinct Uptake Mechanisms but Similar Intracellular Processing of Two Different Toll-like Receptor Ligand-Peptide Conjugates in Dendritic Cells. *J. Biol. Chem.* 2007. 282: 21145–21159.

8. Zom, G. G., S. Khan, C. M. Britten, V. Sommandas, M. G. M. Camps, N. M. Loof, C. F. Budden, N. J. Meeuwenoord, D. V. Filippov, G. A. van der Marel, H. S. Overkleeft, C. J. M. Melief, and F. Ossendorp. Efficient induction of antitumor immunity by synthetic toll-like receptor ligand-peptide conjugates. *Cancer Immunol. Res.* 2014. 2: 756–764.

9. Metzger, J., G. Jung, W. G. Bessler, P. Hoffmann, M. Strecker, A. Lieberknecht, and U. Schmidt. Lipopeptides containing 2-(palmitoylamino)-6,7-bis(palmitoyloxy)heptanoic acid: synthesis, stereospecific stimulation of B-lymphocytes and macrophages and adjuvanticity in vivo and in vitro. *J. Med. Chem.* 1991. 34: 1969–1974.

10. Spohn, R., U. Buwitt-Beckmann, R. Brock, G. Jung, A. J. Ulmer, and K.-H. Wiesmüller. Synthetic lipopeptide adjuvants and Toll-like receptor 2—structure—activity relationships. *Vaccine* 2004. 22: 2494–2499.

11. Jin, M. S., S. E. Kim, J. Y. Heo, M. E. Lee, H. M. Kim, S.-G. Paik, H. Lee, and J.-O. Lee. Crystal Structure of the TLR1-TLR2 Heterodimer Induced by Binding of a Tri-Acylated Lipopeptide. *Cell* 2007. 130: 1071–1082.

12. Braun, V. Covalent lipoprotein from the outer membrane of escherichia coli. *Biochim. Biophys. Acta - Rev. Biomembr.* 1975. 415: 335–377.

13. Welters, M. J. P., M. S. Bijker, S. J. F. van den Eeden, K. L. M. C. Franken, C. J. M. Melief, R. Offringa, and S. H. van der Burg. Multiple CD4 and CD8 T-cell activation parameters predict vaccine efficacy in vivo mediated by individual DC-activating agonists. *Vaccine* 2007. 25: 1379–1389.

14. Caproni, E., E. Tritto, M. Cortese, A. Muzzi, F. Mosca, E. Monaci, B. Baudner, A. Seubert, and E. De Gregorio. MF59 and Pam3CSK4 boost adaptive responses to influenza subunit vaccine through an IFN type I-independent mechanism of action. *J. Immunol.* 2012. 188: 3088–3098.

15. Shakya, N., S. A. Sane, P. Vishwakarma, and S. Gupta. Enhancement in therapeutic efficacy of miltefosine in combination with synthetic bacterial lipopeptide, Pam3Cys against experimental Visceral Leishmaniasis. *Exp. Parasitol.* 2012. 131: 377–382.

16. Moyle, P. M., W. Dai, Y. Zhang, M. R. Batzloff, M. F. Good, and I. Toth. Site-Specific Incorporation of Three Toll-Like Receptor 2 Targeting Adjuvants into Semisynthetic, Molecularly Defined Nanoparticles: Application to Group A Streptococcal Vaccines. *Bioconjug. Chem.* 2014. 25: 965–978.

17. Khan, S., J. J. Weterings, C. M. Britten, A. R. de Jong, D. Graafland, C. J. M. Melief, S. H. van der Burg, G. van der Marel, H. S. Overkleeft, D. V. Filippov, and F. Ossendorp. Chirality of TLR-2 ligand Pam3CysSK4 in fully synthetic peptide conjugates critically influences the induction of specific CD8+ T-cells. *Mol. Immunol.* 2009. 46: 1084–1091.
18. Sletten, E. M., and C. R. Bertozzi. From Mechanism to Mouse: A Tale of Two Bioorthogonal Reactions. *Acc. Chem. Res.* 2011. 44: 666–676.
19. Debets, M. F., J. C. M. van Hest, and F. P. J. T. Rutjes. Bioorthogonal labelling of biomolecules: new functional handles and ligation methods. *Org. Biomol. Chem.* 2013. 11: 6439.
20. Zheng, M., L. Zheng, P. Zhang, J. Li, and Y. Zhang. Development of bioorthogonal reactions and their applications in bioconjugation. *Molecules* 2015. 20: 3190–3205.
21. Gential, G. P. P., N. I. Ho, F. Chiodo, N. Meeuwenoord, F. Ossendorp, H. S. Overkleeft, G. A. van der Marel, and D. V. Filippov. Synthesis and evaluation of fluorescent Pam3Cys peptide conjugates. *Bioorganic Med. Chem. Lett.* 2016. 26: 3641–3645.
22. Hos, B. J., E. Tondini, S. I. van Kasteren, and F. Ossendorp. Approaches to Improve Chemically Defined Synthetic Peptide Vaccines. *Front. Immunol.* 2018. 9: 884.
23. Pawlak, J. B., B. J. Hos, M. J. van de Graaff, O. A. Megantari, N. Meeuwenoord, H. S. Overkleeft, D. V. Filippov, F. Ossendorp, and S. I. van Kasteren. The Optimization of Bioorthogonal Epitope Ligation within MHC-I Complexes. *ACS Chem. Biol.* 2016. 11: 3172–3178.

7
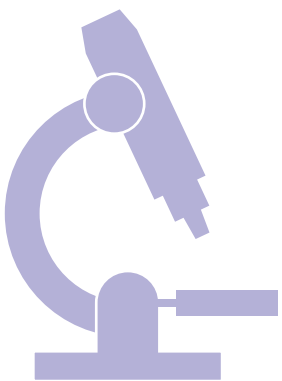
Summary and general discussion

In the current thesis, we provide novel insights in antigen uptake, storage, processing, and sustained cross-presentation mechanisms in dendritic cells (DCs) *in vitro* and *in vivo* (Fig. 1). We have studied antigen handling functions by dendritic cells in three different antigen delivery routes: antibody targeting involving Fcγ receptors (FcγRs) and complement factor C1q, C-type lectin receptor (CLR) targeting, and toll-like receptor (TLR) ligand targeting systems. Our data highlights that antigen storage in specialized compartments in DCs, despite the chosen uptake route, is beneficial for prolonged antigen cross-presentation by DCs and sustained T cell activation. Further *in vivo* studies in different antigen presenting cell (APC) subsets confirmed the presence of antigen storage compartments by isolating APC subsets after *in vivo* antigen uptake. Besides, we revealed a dominant role of C1q in antigen-antibody immune complex (IC) uptake and cross-presentation *in vivo* in contrast to the crucial role of FcγRs *in vitro*. Furthermore, we demonstrated that autophagosomes have a negative impact on the storage of antigen in those specialized compartments and thereby affecting DC cross-presentation efficiency. With the current studies, we unraveled some mechanics of antigen processing in DCs which contribute to future vaccine designs against diseases such as cancer. A general summary and more detailed discussion of remaining questions will be provided below. Finally, future applications and directions for DC-based immunotherapy will be discussed.

ANTIGEN STORAGE IN DENDRITIC CELLS

Prolonged cross-presentation by dendritic cells

What happens with antigen after its uptake by DCs? This is one of the questions that has gained lots of interest by researchers since the discovery of DCs and their key mediator function in bridging innate and adaptive immune responses. The distinction between MHCI and MHCII antigen presentation pathways in expressing intracellular and extracellular antigens, respectively, is well known now. But the mechanisms of presenting exogenous antigen, derived from e.g. cancer cells, on MHCI to cytotoxic T cells require in depth unraveling of DC uptake, processing and cross-presentation machinery. This basic knowledge is of central importance to develop efficient cancer vaccines for the activation of immune responses to specific tumor antigens. One observation from our group was that antigen can be conserved in DCs for several days in specialized intracellular storage compartments which facilitate prolonged antigen cross-presentation to CD8+ T cells (**chapter 4** and (1)) (Fig. 1). This storage compartment functions as a depot for the continuous supply of MHCI ligands. One can appreciate its importance since the trafficking of DCs from peripheral organs to lymphatic sites can take up to several days (2). In addition, due to the rapid turnover rate of MHCI-peptide complexes on the cell surface, newly synthesized peptide

loading could be beneficial to achieve long-lasting and potent antigen presentation capacities of DCs (3). Further characterization of this storage compartment with the use of different antigen targeting system (including FcγRs and C-type lectin receptor MGL1) revealed that, despite different antigen targeting routes, the antigens ended up in the same endosomal compartments (LAMP1⁺) in DCs (**chapter 4**) and induced sustained antigen cross-presentation by DCs (**chapter 4 and 5**). Importantly, the storage compartments are distinct from early endosomal (EEA1⁺/ Rab5⁺), MHCI or MHCII loading compartments. Our results indicate that these specialized storage compartments play a central role in DC cross-presentation where antigens, taken up via different surface receptors, are congregated in the same endosomal organelle for further processing.

One of the initial suggested concepts of endosomal routing of captured antigens is that antigens first enter early endosomes (Rab5⁺), then late endosomes (Rab7⁺), and end up in lysosomes (LAMP1⁺). The pH in these endosomes drops accordingly to the maturation state of the endosomes, which is in favor of antigen degradation. Despite the fact that an overall pH of 4 was reached by DCs after 24 hours of IC uptake, antigen degradation was limited (**chapter 6** and (1)). How antigen is protected from degradation in the storage compartments is still not fully understood. We have shown in **chapter 4** that the activity of cathepsin S was lacking in the compartments where antigen was stored, which could explain why antigen was degraded at a slower rate. Besides, there is a possibility that antigens in ICs are protected by the bound antibodies. It has also been suggested that the intracellular neonatal FcR (FcRn) facilitates the transport of IgG-bound antigens, but not monomeric IgG, to endosomes where it protects the degradation of antigen and mediates efficient antigen delivery to the cytosol (4, 5). However, preliminary studies with FcRn deficient mice in our group suggested no clear involvement of this receptor in antigen cross-presentation of immune-complexed OVA (unpublished data).

An interesting finding we observed in **chapter 4** was the presence of cathepsin X in the storage compartments. It has been described that cathepsin X expression is restricted to immune cells, such as monocytes, macrophages, and dendritic cells (6). It can regulate the proliferation, maturation, migration, and adhesion of immune cells. Inhibition of cathepsin X resulted in lower expression of co-stimulatory molecules, hampered cytokine production, diminished DC migration, and decreased stimulation of CD4⁺ T cells (7). During DC maturation, cathepsin X translocates to the membrane, where it activates Mac-1 integrin receptor, resulting in cell adhesion and development of podosomes (8). After DC maturation, cathepsin X redistributes from the membrane to the perinuclear region, resulting in de-adhesion of DCs. In **chapter 4,** we observed similar redistribution of cathepsin X towards the perinuclear region and co-localization with antigen in storage after FcγR targeting. Cathepsin X is a fairly new discovered cathepsin, and its role in DC cross-presentation is not known yet. However, the presence of this particular cathepsin in the storage compartments could

8

imply a role in antigen processing for cross-presentation. Interestingly, preliminary data from our group observed a higher presence of cathepsin X in CD8α+ DCs compared to CD8α- DCs, pDCs, and macrophages (unpublished data). Further studies with cathepsin X deficient DCs are needed to elucidate whether there is a direct role of cathepsin X in antigen cross-presentation.
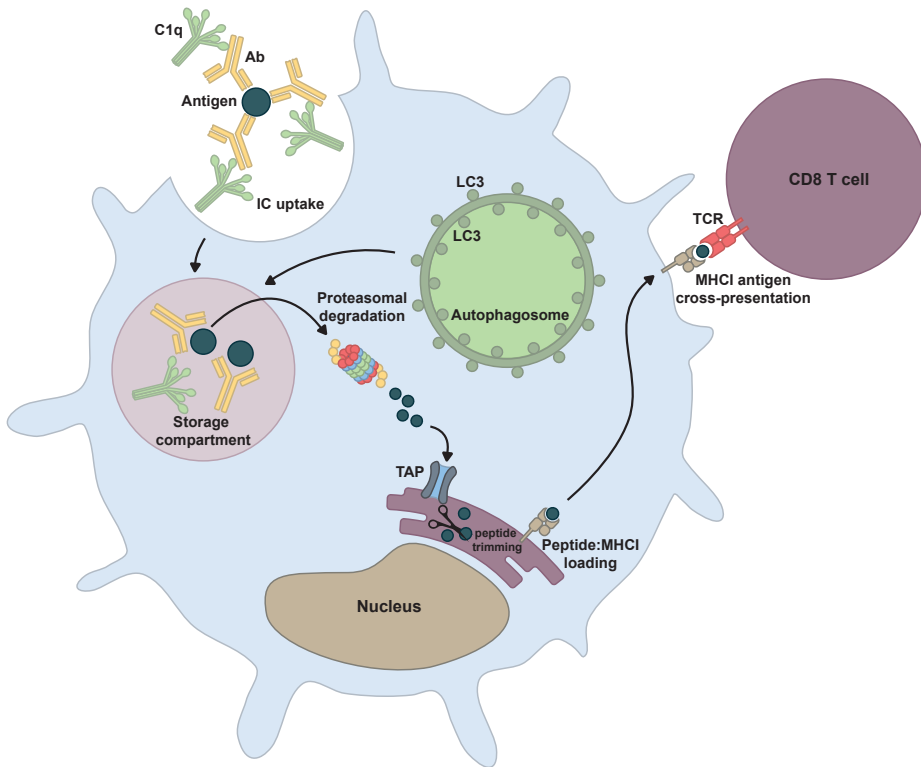
Figure 1. Overview of antigen cross-presentation mechanisms by DCs studied in the current thesis. Soluble protein antigen binds to antibodies in circulation to form antigen–antibody immune complexes (IC). C1q facilitates the uptake of these complexes by DCs via an as yet undefined uptake route *in vivo*. After uptake, antigens are conserved in storage compartments for prolonged antigen presentation. Antigen from the storage compartment is translocated to the cell cytosol where it is degraded by the proteasome and transported by TAP to the ER for MHCI loading and subsequently antigen cross-presentation on the cell surface to CD8+ T cell through the T cell receptor (TCR). Moreover, autopaghosomes (positive for LC3) can degrade antigen storage compartments and thereby affecting the sustained cross-presentation capacity of DCs.

Differential cross-presentation ability by dendritic cell subsets *in vivo*

Since we have observed the existence of antigen storage compartments in DCs cultured *in vitro* and their contribution to prolonged antigen cross-presentation, the next step was

to confirm their existence and role in the *in vivo* setting. In order to mimic the natural formation of antigen-antibody ICs, we injected mice sequentially with anti-OVA IgG and OVA to form OVA ICs *in vivo*, which previously have been shown by our group to induce efficient antigen cross-presentation to CD8$^+$ T cells (9). We now show in **chapter 2** for the first time that different APC subsets, including CD8α$^+$ DCs (also called cDC1), CD8α$^-$ DCs (also called cDC2), pDCs, and macrophages, have the ability to store antigens for several days *in vivo*. This corresponds with long-lasting *in vivo* antigen presentation to CD8$^+$ and CD4$^+$ T cells up to a week after antigen injection. These data confirm our earlier *in vitro* work and emphasize the importance of antigen storage also in DCs *in vivo*. Interestingly, a clear distinction between antigen presentation ability was found between CD8α$^-$ DCs and CD8α$^+$ DCs, where the later subset was superior in antigen cross-presentation. Other studies have shown similar distinction in antigen presentation capacities by CD8α$^+$ and CD8α$^-$ DCs (10–13). It is still unclear why specific APC subsets are more potent in cross-presenting antigen. It has been suggested that cross-presentation by CD8α$^-$ DCs depends on activating Fcγ receptors (FcγRs) (14) or an additional stimuli such as TLR ligands (15). MHCI antigen presentation by CD8α$^-$ DCs is hampered in γ-chain-deficient mice, but not in CD8α$^+$ DCs, indicating that the activation of CD8α$^+$ DCs is not required for efficient cross-presentation. However, we observed in **chapter 3** that complement factor C1q, rather than FcγRs, plays a major role in antibody-mediated antigen uptake from blood circulation and presentation *in vivo*, which will be discussed later in this chapter.

Other explanations for the superior cross-presentation ability of CD8α$^+$ DCs include lower degradation of antigen in endosomes by ROS production (16) or lower levels of lysosomal proteases (17). DCs have the ability to recruit NOX2 to the endosomes which mediates the generation of ROS that capture protons to build hydrogen peroxide. This results in active alkalization and impaired pH-dependent activation of lysosomal proteases. However, preliminary data from our group with NOX2 deficient mice did not show differences in antigen cross-presentation of IC (unpublished data). It has been demonstrated that DCs express lower levels of lysosomal proteases compared to other immune cells (17). Expression of cathepsins L, S, D, and B in phagosomes in DCs is also more reduced compared to the levels in macrophages. This results in slower phagolysosomal antigen degradation and prolonged antigen presence in DCs. Others showed more efficient transfer of exogenous antigens into the cytosol (18), and higher expression of components that are associated with MHCI processing pathway (12) in CD8α$^+$ DCs, which can also contribute to their potent cross-presentation capacity.

Despite the fact that we observed efficient antigen uptake by splenic pDCs and macrophages *in vivo*, strikingly both subsets showed no detectable antigen presentation to T cells *ex vivo* (**chapter 2**). pDCs are well known for their ability in producing large amounts of type I interferons. Some studies had shown their potential role in cross-presentation *in*

8

vitro or *ex vivo* (19–21), however their cross-presentation capacity *in vivo* seemed lacking which is in line with our observations (22, 23). It is also important to take into account that pDCs only express the inhibitory FcγRII, suggesting a role in controlling tolerance in steady state. Although, it has been demonstrated that pDCs are capable in inducing effective cross-presentation upon TLR stimulation (20). A more recent study showed that the activation of pDCs by TLR ligands induced the production of mitochondrial ROS and thereby increased the cross-presentation capacity by pDCs (24). Macrophages mostly function as a first line defense against pathogens by their rapid degradation ability and are less well known for their role in antigen cross-presentation. Although it has been suggested that macrophages have a more acidic endosomal environment compared to DCs (17, 25), in our current system we could still detect similar amounts of antigen stored in splenic macrophages compared to DCs several days after antigen and antibody injection without detectable MHCI or MHCII presentation.

Antigen transfer between APC subsets: A role for antigen storage compartments?
Although only specific APC subsets can cross-present antigen, that does not mean that other APC subsets are not relevant for efficient T cell induction. There are studies suggesting that macrophages and pDCs act in concert with DCs to promote cross-priming to T cells (reviewed in (26)). Upon infection, pDCs migrate to lymphoid organ areas which are rich in CD169^{+} macrophages, and produce large amounts of IFN-I (27). It has been shown that IFN-I is critical for the antigen cross-presentation by DCs and that pDCs can promote the generation and survival of antigen-specific CD8^{+} T cells upon infection (28–31). Moreover, several studies suggested antigen transfer from CD169^{+} macrophages to DCs for CTL induction (32, 33). A more recent study discovered that CD169, a sialic acid binding lectin involved in cell-cell contact, preferentially binds to sialic acid containing ligands on CD8α[+] DCs and thereby facilitated antigen transfer to DCs (34). In addition, also carry-over of antigen from one DC type to another is currently accepted as a feasible model of cross presentation (35–37) especially when different DC subsets seem to have different roles in a two-step T cell priming model (38–41). In this two-step priming model, naïve CD4^{+} and CD8^{+} T cells are activated by different DC populations. The activated CD8^{+} T cells recruit lymph node-resident XCR1^{+} DCs which receive cross-presented antigen from the DCs that carried out the first priming step (42, 43). The XCR1^{+} DCs interact with both activated CD4^{+} and CD8^{+} T cells and thereby inducing optimal signals for CD8^{+} T cell differentiation into cytotoxic T lymphocytes (CTLs) and memory CTLs. We showed with multiple antigen-targeting systems that antigen could be conserved in DCs for sustained cross-presentation. This does not only increase the significance of antigen storage by different cell types, but we speculate that prolonged antigen storage and presentation would be beneficial for antigen transfer between subsets and multi-step T cell priming mechanisms.

FATE OF ANTIGEN IN DENDRITIC CELLS

Antigen routing in dendritic cells

One remarkable observation we had was that timing seemed to correlate with different antigen processing phases in DCs. Despite the fact that antigen targeted to either FcγR or MGL1 ended up in the same storage compartment, antigen targeted to MGL1 induced DC cross-presentation which was TAP independent (**chapter 5**). This seemed to be in contradiction with our previous work showing TAP and proteasome dependent antigen cross-presentation after FcγRs targeting on DCs (1). However, an important note is that relatively early cross-presentation was measured in the MGL1 setting, only 4 hours after antigen pulse, whereas antigen cross-presentation from the storage compartments mediated by FcγRs targeting was measured after 2 hours antigen pulse and 48 hours chase. It could be possible that there is a distinction between early and late antigen processing and cross-presentation in DCs. One can speculate that during the early stage after antigen uptake, antigen is processed and loaded on MHCI directly in early endosomes, which is TAP and proteasome independent. In this case, MHCI molecules could be derived from Rab11 positive endosomal recycling compartments (44). Similar antigen routing had been shown before for antigens targeted to the mannose receptor and DC-SIGN, where antigens were mainly residing and presented from early endosomal compartments (45, 46). However, when antigen stays longer in DCs and resides in LAMP1 positive compartments, which lack direct processing and loading machineries, it requires antigen translocation from the storage compartments to the cytosol for proteasomal degradation and subsequently transportation via TAP to MHCI loading sites. Indeed, the lack of TAP-1 and PA28 in the storage compartments suggests that antigen is rather translocated from the endosomes back into the cell cytosol for further processing and loading of MHCI in the ER for antigen cross-presentation (**chapter 4**). We had previously demonstrated almost complete inhibition of MHCI cross-presentation by DCs from the storage organelles upon inhibition of proteasomal activity or using TAP deficient DCs (1). Although it is not excluded that peptides, after proteasome degradation, are transported back into endocytic compartments and trimmed by IRAP and loaded on MHCI (47).

The ability of antigens to induce DC maturation signaling pathways might also contribute to the maturation and reorganization of endosomes and further trafficking of antigens from early endosomes to late endosomes. We showed in **chapter 5** that the modification of OVA with the glycan-structure Lewis[x] (Le[x]) re-directs OVA to the C-type lectin receptor MGL1, skewing naïve CD4^{+} T cell differentiation towards IFNγ-producing Th1 cells. MR targeting often requires high amounts of soluble OVA and additional activation signals from e.g. TLR ligands. Le[x] modification did not only reduce the required OVA amount by 100-fold, but also obviated the additional TLR activation signal. More importantly, OVA-Le[x] was routed to

8

Rab11[+] LAMP1^{+} compartments where it was stored for sustained antigen cross-presentation, whereas soluble OVA was routed towards EEA1^{+} Rab11^{+} compartments. Targeting different regions of the same receptor might also influence the routing and processing of antigen by DCs, as shown by a study targeting the carbohydrate-recognition domain (CRD) and the neck region of DC-SIGN (46). Antigens coupled to antibodies specific for CRD were delivered to lysosomal compartments, resulting in rapid antigen degradation and poor cross-presentation, whereas antigens coupled to antibodies specific for the neck region were directed to early endosomal compartments and induced effective cross-presentation.

Different categories of endosomes with distinct functions had been proposed before where endosomes were described as "dynamic" or "static" (48) (reviewed in (49)). The "dynamic" endosomes were suggested to mature rapidly towards late endosomes and provide antigens for MHCII loading, whereas "static" endosomes (Rab14 positive) were matured more slowly towards late endosomes and favor cross-presentation due to lower proteolytic activity and antigen degradation. However, since these "static" endosomes possess MHCI loading components, such as MHCI and IRAP (47), it is unlikely that the endosomal storage compartments that we described here are the same. A distinct marker expressed on storage compartments is LAMP1. Although LAMP1 is a classical lysosomal marker, it is unlikely that the storage compartment is a classical lysosome due to the lack of active proteases such as cathepsin S (**chapter 4**) and slow antigen degradation rate. However, endosomal trafficking and maturation pathways are dynamic and complex, it would be interesting to further investigate the expression of other endo-lysosomal or subcellular markers on the storage compartments, for instance by proteomic analysis of isolated organelles.

In addition, new approaches for tracking antigen in DCs will be available. Currently, most of the fluorophores are chemically conjugated to the molecule of interest which may influence the experimental outcome. In **chapter 7** we investigated new possibilities in coupling different fluorophores to TLR-ligand conjugated peptides. However, interpreting data by using fluorescently labeled compounds could sometimes be challenging due to their bulky and hydrophobic structures compared to the relatively small peptides. One of the new possibilities to overcome these problems is the use of click chemistry (reviewed in (50)). By using biorthogonal peptides and ligation of a complementary fluorophore to the biorthogonal amino acid side chain at the end of the experiment, surface labeling of MHCI loaded minimal epitopes was quantified on APCs (51). Potentially this technique can be used for accurate tracking of the compound of interest, even in vivo, bypassing solubility problems or characteristic changes caused by the type of fluorophore. However, the click chemistry approach is still technically difficult in cells and further optimization is needed for future use. When optimized, this could further unravel the routing and processing of antigens in DCs in subcellular detail.

Autophagy and antigen degradation

Since the fate of antigen from the DC storage compartment is still unclear, we investigated the possible role of autophagy in antigen storage and cross-presentation. In **chapter 6** we revealed that DCs treated with common autophagy inhibitors or gained from Atg5$^{-/-}$ mice showed prolonged antigen storage and significantly enhanced antigen cross-presentation to CD8$^+$ T cells. Thus, autophagosomes degrade antigen storage compartments and consequently less antigens will be available for cross-presentation (Fig. 1). This was rather unexpected since it was reported that autophagy inhibition can negatively influence MHCI cross-presentation (52–54). We could confirm that blocking autophagy at an early stage inhibited MHCI cross-presentation, but the opposite enhancing effect was found on long term antigen cross-presentation. The discrepancies between the beneficial or detrimental role of autophagy in DC cross-presentation were reflected in studies providing evidence for both. Some groups showed elevated CD8$^+$ T cell responses upon autophagy inhibition in DCs (55), while others showed that MHCI cross-presentation by DCs was still intact in the absence of Atg5 (56). Tumor antigens conjugated to nanoparticles delivered to autophagosomes were efficiently cross-presented to CD8$^+$ T cells resulting in potent antitumor responses (54). Interestingly, it had been shown that XCR1 positive DCs had the highest steady-state levels of macroautophagy, indicating that autophagy is highly active in specialized cross-presenting DCs (57). The reasons for these discrepancies are unclear, although it seems that the outcome depends on the type of antigen, cell subset and time point of measuring antigen presentation, as we already pointed out in the section above. Nevertheless, our data provide new insight in the role of autophagy in antigen degradation and thereby affecting cross-presentation to T cells. It had been suggested that Atg5 or Atg7 deficient DCs had decreased endocytosis and degradation of MHCI molecules resulting in elevated surface expression of MHCI (55). This could subsequently induce antigen cross-presentation to CD8$^+$ T cells. However, in our study conditions in **chapter 6**, we did not find significant differences in MHCI surface expression levels on Atg5 deficient DCs upon maturation. We propose that enhanced cross-presentation is rather caused by increased peptide production.

In addition, we showed in **chapter 6** that LC3 positive autophagosomes were in close proximity with the antigen storage compartments. However, it cannot be ruled out that the LC3 positive compartments are vesicles mediated by LC3-associated phagocytosis (LAP). Some receptors that can stimulate LAP include FcγRs, TLRs, CLR Dectin-1, and the phosphatidylserine binding receptor TIM4 (58–61). Therefore, additional staining for p62, which is present on autophagosomes, could distinguish LAP from autophagosomes. However, it has been shown that LAP formation is dependent on the recruitment of NOX2 to the membranes and the generation of ROS (59, 62, 63). Preliminary functional studies with NOX2-deficient mice showed no effect on sustained antigen cross-presentation by DCs (unpublished data), therefore it is unlikely that LAP is playing a crucial role in our setting.

8

How autophagosomes are affecting antigen degradation in the storage compartment still needs to be elucidated. It seems that it is not controlled by lysosomal activity within the compartments since we could not detect significant differences in the pH of antigen containing compartments between wildtype and Atg5 deficient DCs. Moreover, we already showed in **chapter 4** that the activity of endosomal proteases, such as cathepsin S, was lacking in the antigen storage compartments. One possible explanation is that autophagosomes prevent translocation of antigen from the storage compartment to the cytosol for further processing and loading on MHCI molecules. It had been reported that during autophagy, the edges of the isolation membrane of autophagosomes were sealed to prevent leakage of hydrolases which could cause cellular damage and apoptosis (64, 65). Another possibility is that, under normal conditions, antigens are slowly leaked from the storage compartments into the cytosol for further processing. It had been shown that autophagosomes can degrade leaky endosomes (66), which makes it plausible that autophagosomes degrade antigen storage compartments and thereby hampering antigen cross-presentation.

THE ROLE OF FCΓRS AND C1Q IN ANTIBODY-MEDIATED ANTIGEN TARGETING TO DCS

The importance of antigen targeted to FcγRs in T cell-mediated anti-tumor responses had been documented well by our group and others (1, 67–69). However, to our surprise, FcγRs seem to play a limited role in the uptake of ICs by DCs *in vivo* (**chapter 3**). We discovered that the uptake of *in vivo*- formed OVA ICs, by injecting mice sequentially with anti-OVA IgG and OVA, was not hampered in DCs from mice lacking FcγRI/II/III/IV (FcγR quadruple^{-/-}). More interestingly, our results indicate a dominant role of complement factor C1q in controlling antigen targeting and handling by DCs *in vivo* (Fig. 1). Mice lacking C1q (C1qa^{-/-}) showed no antigen uptake in APCs and severely reduced antigen presentation to T cells.

Complement plays a main role as effector mechanism of antibody-mediated immunity and one of its function is to dispose immune complexes from circulation. C1q was initially discovered as part of the C1 initiation component of the classical complement pathway upon binding to antigen-bound IgM or IgG (70). However it has been shown that C1q regulates a variety of cellular processes independent of complement activation, such as enhancement of phagocytosis of apoptotic cells, decrease in pro-inflammatory cytokine release and induction of anti-inflammatory mediators in macrophages and DCs, skewing the adaptive immune system towards a more regulatory state (71).

Although many potential C1q receptors has been described, it is still unclear which C1q receptor is expressed on DCs to mediate IC uptake. C1q receptors that are known

to be expressed on DCs, such as RAGE and DC-SIGN, mainly function for apoptotic cell phagocytosis and DC differentiation, respectively (71). Both the collagen-like region and the globular head are suggested as binding sites for C1q receptors. Importantly, it has been suggested that monomeric IgG binding to one C1q head is of low affinity and results in poor complement activation. IgG molecules form hexamers after binding to antigens and bind to C1q with high affinity promoting efficient complement activation (72). Further work by the same group, using different Ab mutants which promote or inhibit hexamerization in solution, showed that IgG hexamerization was a prerequisite to C1q binding and C1 activation (73). More recently, it has been shown that the C1q arms were condensed upon hexameric antibody binding, resulting in the rearrangement of the $C1r_2$-$C1S_2$ proteases and tilting the C1q's cone-shaped stalk. C1r could therefore activate C1s within single, strained C1 complexes, or between neighboring C1 complexes (74). These data suggest flexible movements of C1q which can modulate the positions of the six globular domains and cross-activities with neighboring C1 complexes. Additional studies on the interaction between C1q and ICs, and the identification of the C1q-IC uptake receptor on DCs are needed to further fine-tune C1q-mediated IC uptake and immune responses by DCs.

It is still puzzling why FcγRs have a less essential role in IC uptake *in vivo*, while *in vitro* we had demonstrated that the uptake of OVA IC by FcR γ-chain^{-/-} BMDCs was hampered (1). In **chapter 3** we also showed hampered IC uptake and cross-presentation by FcγR quadruple^{-/-} BMDCs *in vitro*. Although FcγRs are known to enable DC activation to augment antigen cross-presentation *in vitro*, mainly through signaling of ITAM, we did not detect an increase in DC maturation after co-injection of antigen and antibody *in vivo* (data not shown). These results indicate that FcγRs are the more dominant uptake and activation receptors under *in vitro* conditions and that there is a distinct contribution of FcγRs in antibody-mediated antigen uptake by DCs *in vitro* and *in vivo*. The elimination of circulating antigen-antibody ICs is generally assumed to be mediated by Kupffer cells and endothelial cells expressing FcγRs in the liver. It is presumable that FcγRs *in vivo* are more important in IC clearance from the circulation by FcγR expressing liver cells than in IC uptake by DCs in the spleen. Indeed, serum from FcγR quadruple^{-/-} mice showed slower clearance of antigen from circulation, prolonged presence of antigen in circulation, and slightly higher antigen uptake by APCs *in vivo* (**chapter 3**). It has been suggested that FcRn mediates cross-presentation of ICs by CD8α[-] DCs and that FcRn and FcγRs work in cooperation (5). Since we showed hampered antigen cross-presentation by CD8α[-] DCs in FcγR quadruple^{-/-} mice, it is not excluded that FcγRs or FcRn play a role in the activation and signaling pathway for cross-presentation in this particular subset.

Another possible explanation for the distinct role of FcγRs *in vivo* could be the fact that DCs *in vivo* are strategically positioned for efficient uptake of antigen to initiate adaptive immunity. Studies on the anatomy of mouse spleen showed high organization

8

of immune cells in different zones within the spleen. CD8α+ DCs that express higher levels of DEC205 are more restricted to periarterial lymphoid sheaths in the spleen, whereas DCIR2 expressing CD8α- DCs are restricted to the bridging region of the marginal zone (75). Langerin/CD207+CD103+ CD8α+ DCs are mainly localized in the marginal zone, but upon phagocytosis of apoptotic cells they migrate into T cells zones for cross-presentation (76). Since DC populations are distributed differently in the spleen, and considering the fact that we only found a small percentage of antigen-positive cells within each APC subset, it is possible that DCs expressing a receptor for C1q-mediated IC uptake are positioned more favorable for better access to circulating ICs compared to DCs that lack the C1q receptor. Although higher C1q receptor expression levels in DC populations cannot be ruled out. Further anatomic studies on the spleen are required to determine the position of FcγR- and C1q receptor-expressing DC subsets.

CONCLUSION AND FUTURE PROSPECTIVE

Dendritic cells have an increasing role as foundation for effective cancer immunotherapy. As central regulators of the adaptive immune responses, DCs are crucial for antigen recognition, transport to draining lymph nodes and cross-presentation to T cells. However, the precise mechanisms of antigen cross-presentation by DCs are still not fully unraveled. Nevertheless, DCs became an attractive target for vaccination against diseases, such as cancer, for which cellular immunity is important. Different strategies were explored for the development of DC vaccines, including *ex vivo* generated DCs and *in vivo* DC targeting. The majority of *ex vivo* generated DCs are monocyte-derived DCs (moDCs) differentiated from purified blood monocytes in the presence of cytokines and subsequently loaded with tumor-derived antigens. Although moDCs have the advantage in terms of practicality, since monocytes are easy to isolate in high amounts and efficiently differentiated into moDCs, it is important to keep in mind that *ex vivo* generated moDCs could be functionally different from natural DCs. Some studies showed that moDCs differ in their lysosomal pH and are limited in their ability to migrate *in vivo* with most moDCs residing at the injection site (77–79). Another approach for DC based anti-cancer therapy is using *In vivo* DC targeting. By coupling tumor antigens to specific monoclonal antibodies (mAbs), DC receptors can be targeted *in vivo*. Many studies have been investigating C-type lectin receptors, such as DEC-205, fused with tumor antigen, however most of the time an additional adjuvant is needed to activate DCs in order to overcome tolerance (80–83).

We have published before that targeting FcγRs on DCs with IC can efficiently activate DCs and prime T cells leading to prophylactic and therapeutic tumor control *in vivo* (84). In **chapter 2**, we discovered that DC subsets *in vivo* have the capacity to store antigen

for several days in specialized antigen storage compartments, which corresponds with sustained antigen cross-presentation to CD8^{+} T cells. Prolonged antigen cross-presentation is crucial since it takes time for DCs to mature and travel to lymph nodes to encounter T cells. It is important for the development of next generation DC vaccines to consider DC targeting which can enhance antigen storage in DCs and induce efficient DC maturation. Since a natural infection usually includes multiple antigenic ligands, it is plausible to further enhance DC targeting and activation by combining different patter-recognition receptor (PRR) ligands. Our group has shown before that TLR-ligand- peptide conjugates also lead to the formation of intracellular antigen depot and induce CD8^{+} and CD4^{+} T-cell priming capacity leading to efficient induction of antitumor immunity in mice (1, 85). In **chapter 5**, we showed that targeting C-type lectin receptor MGL can also lead to prolonged antigen storage and antigen cross-presentation by DCs. Several studies have suggested cross talk between multiple PRRs, such as TLR and NLR (86–88). Moreover, triggering TLRs, NLRs, and CLRs can all activate downstream NFκB activation, indicating the signaling pathways of different PRRs contain overlapping functions. Therefore, combining different PRR ligands might induce a synergistic effect on DC activation and antigen cross-presentation.

In **chapter 3**, we showed that *in vivo* DC targeting is much more complex and not all *in vitro* DC studies can be directly translated to the *in vivo* situation. Therefore, *In vivo* targeting of DCs by using antibodies can be a difficult approach since antibodies can be taken up by other cell types expressing similar receptors and filtered out of the system before reaching the targeted DCs. Understanding the *in vivo* uptake mechanisms of DCs might improve the design of modified antibodies which can be specifically targeted to DCs. Other promising targeting approaches are using nanoparticles or liposomes to deliver antigens specifically to DCs. One of the FDA approved nanoparticles is PLGA-based, a biodegradable slow-release polymer that effectively encapsulates drugs and antigens (89, 90). An advantage of these antigen carriers is the flexibility in property modulation, e.g., size, charge, and composition, which can influence the outcome of the vaccine (91).

Targeting the right APC subsets is also a crucial aspect for an effective vaccine. As discussed in **chapter 2**, all APC subsets have the capacity to take up and store antigen for several days, but only the CD8α^{+} DCs showed superior antigen cross-presentation ability to CD8^{+} T cells, while the CD8α^{-} DCs were better antigen presenters to CD4^{+} T cells. Although CD8α^{+} DCs are effective inducers of CD8^{+} T cell priming and cytotoxic killing of tumor cells, the role of CD4^{+} T cells cannot be neglected. It was already demonstrated by our group and others that the Th response is essential for the induction of antitumor immunity, which is mainly mediated by the upregulation of CD40L on CD4^{+} T cells triggered by MHCII presentation by DCs (92–94). CD40L will engage CD40 on DCs to cause maturation of the DCs and efficient induction of CD8^{+} killer T cells. Therefore, it is important for a vaccine to deliver

8

antigens both to the CD8α$^+$ and the CD8α$^-$ DCs. Designing vaccines that contain both CD8$^+$ as CD4$^+$ epitopes of the target antigens have already shown effective antitumor immunity (85).

Beside specific targeting and activating DCs, choosing a highly tumor specific antigen that is delivered to the DCs is also an important aspect for designing an effective antitumor therapy which evades tolerance induction. Many sources of antigen have been used in DC vaccines, including e.g. short peptides, synthetic long peptides, tumor cell lysates, and DNA/RNA transduction with viral vectors (95–99). Although these approaches show promising results in combination with maturation signals, it remains unclear what the optimal method for antigen loading is. A different approach to improve DC vaccines might be the use of neoantigens, which are generated by somatic mutations in the tumor. Vaccination with neoantigen-loaded DCs have shown to promote neoantigen-specific T cell responses (100). However, neoantigens requires labor-intensive sequencing of the tumor of patients, and the frequency of neoantigens is strongly dependent of the tumor type (101). One of the most recent and innovative developments in DC vaccine is the use of RNA encoding tumor antigen derived epitopes combined with immunostimulatory motifs which were delivered by nano-sized lipoplexes to DCs (102, 103).

Future directions for specific immunotherapy include combining DC targeted vaccination with the now widely clinically applied immune checkpoint blockade antibodies like PD-1 and CTLA-4 to block the interactions between APCs and T cells and thereby releasing the inhibitory signals for tumor-specific T cells. Moreover, the combination of immunotherapy with other therapies such as chemotherapy or tumor ablation techniques has been shown to be beneficial for improved tumor eradication. Since the discovery of DCs more than a century ago, these specialized cells have established a crucial role, either directly or indirectly in immunotherapeutic strategies of cancer. More studies on the mechanisms of DC cross-presentation are required to use these cells, gifted by nature, to their full potential.

REFERENCES

1. Van Montfoort, N., M. G. Camps, S. Khan, D. V. Filippov, J. J. Weterings, J. M. Griffith, H. J. Geuze, T. van Hall, J. S. Verbeek, C. J. Melief, and F. Ossendorp. Antigen storage compartments in mature dendritic cells facilitate prolonged cytotoxic T lymphocyte cross-priming capacity. *Proc. Natl. Acad. Sci. U. S. A.* 2009. 106: 6730–6735.

2. MartIn-Fontecha, A., S. Sebastiani, U. E. Höpken, M. Uguccioni, M. Lipp, A. Lanzavecchia, and F. Sallusto. Regulation of dendritic cell migration to the draining lymph node: impact on T lymphocyte traffic and priming. *J. Exp. Med.* 2003. 198: 615–621.

3. Eberl, G., C. Widmann, and G. Corradin. The functional half-life of H-2Kd-restricted T cell epitopes on living cells. *Eur. J. Immunol.* 1996. 26: 1993–1999.

4. Qiao, S.-W., K. Kobayashi, F.-E. Johansen, L. M. Sollid, J. T. Andersen, E. Milford, D. C. Roopenian, W. I. Lencer, and R. S. Blumberg. Dependence of antibody-mediated presentation of antigen on FcRn. *Proc. Natl. Acad. Sci. U. S. A.* 2008. 105: 9337–9342.

5. Baker, K., S.-W. Qiao, T. T. Kuo, V. G. Aveson, B. Platzer, J.-T. Andersen, I. Sandlie, Z. Chen, C. de Haar, W. I. Lencer, E. Fiebiger, and R. S. Blumberg. Neonatal Fc receptor for IgG (FcRn) regulates cross-presentation of IgG immune complexes by CD8-CD11b+ dendritic cells. *Proc. Natl. Acad. Sci. U. S. A.* 2011. 108: 9927–9932.

6. Perišić Nanut, M., J. Sabotič, A. Jewett, and J. Kos. Cysteine cathepsins as regulators of the cytotoxicity of NK and T cells. *Front. Immunol.* 2014. 5: 616.

7. Kos, J., Z. Jevnikar, and N. Obermajer. The role of cathepsin X in cell signaling. *Cell Adh. Migr.* 2009. 3: 164–166.

8. Obermajer, N., U. Svajger, M. Bogyo, M. Jeras, and J. Kos. Maturation of dendritic cells depends on proteolytic cleavage by cathepsin X. *J. Leukoc. Biol.* 2008. 84: 1306–1315.

9. van Montfoort, N., S. M. Mangsbo, M. G. M. M. Camps, W. W. C. C. van Maren, I. E. C. C. Verhaart, A. Waisman, J. W. Drijfhout, C. J. M. M. Melief, J. S. Verbeek, and F. Ossendorp. Circulating specific antibodies enhance systemic cross-priming by delivery of complexed antigen to dendritic cells in vivo. *Eur. J. Immunol.* 2012. 42: 598–606.

10. den Haan, J. M., S. M. Lehar, and M. J. Bevan. CD8(+) but not CD8(-) dendritic cells cross-prime cytotoxic T cells in vivo. *J. Exp. Med.* 2000. 192: 1685–1696.

11. Pooley, J. L., W. R. Heath, and K. Shortman. Cutting edge: intravenous soluble antigen is presented to CD4 T cells by CD8- dendritic cells, but cross-presented to CD8 T cells by CD8+ dendritic cells. *J. Immunol.* 2001. 166: 5327–5330.

12. Dudziak, D., A. O. Kamphorst, G. F. Heidkamp, V. R. Buchholz, C. Trumpfheller, S. Yamazaki, C. Cheong, K. Liu, H.-W. H.-W. H. W. Lee, G. P. Chae, R. M. Steinman, M. C. Nussenzweig, C. G. Park, R. M. Steinman, and M. C. Nussenzweig. Differential antigen processing by dendritic cell subsets in vivo. *Science* 2007. 315: 107–111.

13. Hildner, K., B. T. Edelson, W. E. Purtha, M. S. Diamond, H. Matsushita, M. Kohyama, B. Calderon, B. U. Schraml, E. R. Unanue, M. S. Diamond, R. D. Schreiber, T. L. Murphy, and K. M. Murphy. Batf3 deficiency reveals a critical role for CD8α+ dendritic cells in cytotoxic T cell immunity. *Science* 2008. 322: 1097–1100.

14. den Haan, J. M. M., and M. J. Bevan. Constitutive versus activation-dependent cross-presentation of immune complexes by CD8(+) and CD8(-) dendritic cells in vivo. *J. Exp. Med.* 2002. 196: 817–827.

15. Neubert, K., C. H. K. Lehmann, L. Heger, A. Baranska, A. M. Staedtler, V. R. Buchholz, S. Yamazaki, G. F. Heidkamp, N. Eissing, H. Zebroski, M. C. Nussenzweig, F. Nimmerjahn, and D. Dudziak. Antigen Delivery to CD11c + CD8 − Dendritic Cells Induces Protective Immune Responses against Experimental Melanoma in Mice In Vivo. *J. Immunol.* 2014. 192: 5830–5838.

16. Savina, A., A. Peres, I. Cebrian, N. Carmo, C. Moita, N. Hacohen, L. F. Moita, and S. Amigorena. The Small GTPase Rac2 Controls Phagosomal Alkalinization and Antigen Crosspresentation Selectively in CD8+Dendritic Cells. *Immunity* 2009. 30: 544–555.

17. Delamarre, L., M. Pack, H. Chang, I. Mellman, and E. S. Trombetta. Differential Lysosomal Proteolysis in Antigen-Presenting Cells Determines Antigen Fate. *Science* 2005. 307: 1630–1634.

18. Lin, M. L., Y. Zhan, A. I. Proietto, S. Prato, L. L. Wu, W. R. Heath, J. A. Villadangos, and A. M. Lew. Selective suicide of cross-presenting CD8+ dendritic cells by cytochrome c injection shows functional heterogeneity within this subset. *Proc. Natl. Acad. Sci. U. S. A.* 2008. 105: 3029–3034.

8

19. Di Pucchio, T., B. Chatterjee, A. Smed-Sörensen, S. Clayton, A. Palazzo, M. Montes, Y. Xue, I. Mellman, J. Banchereau, and J. E. Connolly. Direct proteasome-independent cross-presentation of viral antigen by plasmacytoid dendritic cells on major histocompatibility complex class I. *Nat. Immunol.* 2008. 9: 551–557.

20. Mouries, J., G. Moron, G. Schlecht, N. Escriou, G. Dadaglio, and C. Leclerc. Plasmacytoid dendritic cells efficiently cross-prime naive T cells in vivo after TLR activation. *Blood* 2008. 112: 3713–3722.

21. Moffat, J. M., E. Segura, G. Khoury, I. Caminschi, P. U. Cameron, S. R. Lewin, J. A. Villadangos, and J. D. Mintern. Targeting antigen to bone marrow stromal cell-2 expressed by conventional and plasmacytoid dendritic cells elicits efficient antigen presentation. *Eur. J. Immunol.* 2013. 43: 595–605.

22. GeurtsvanKessel, C. H., M. A. M. Willart, L. S. van Rijt, F. Muskens, M. Kool, C. Baas, K. Thielemans, C. Bennett, B. E. Clausen, H. C. Hoogsteden, A. D. M. E. Osterhaus, G. F. Rimmelzwaan, and B. N. Lambrecht. Clearance of influenza virus from the lung depends on migratory langerin+CD11b- but not plasmacytoid dendritic cells. *J. Exp. Med.* 2008. 205: 1621–1634.

23. Lee, H. K., M. Zamora, M. M. Linehan, N. Iijima, D. Gonzalez, A. Haberman, and A. Iwasaki. Differential roles of migratory and resident DCs in T cell priming after mucosal or skin HSV-1 infection. *J. Exp. Med.* 2009. 206: 359–370.

24. Oberkampf, M., C. Guillerey, J. Mouriès, P. Rosenbaum, C. Fayolle, A. Bobard, A. Savina, E. Ogier-Denis, J. Enninga, S. Amigorena, C. Leclerc, and G. Dadaglio. Mitochondrial reactive oxygen species regulate the induction of CD8+ T cells by plasmacytoid dendritic cells. *Nat. Commun.* 2018. 9: 2241.

25. Savina, A., C. Jancic, S. Hugues, P. Guermonprez, P. Vargas, I. C. Moura, A.-M. M. Lennon-Duménil, M. C. Seabra, G. Raposo, and S. Amigorena. NOX2 Controls Phagosomal pH to Regulate Antigen Processing during Crosspresentation by Dendritic Cells. *Cell* 2006. 126: 205–218.

26. Grabowska, J., M. A. Lopez-Venegas, A. J. Affandi, and J. M. M. Den Haan. CD169+ macrophages capture and dendritic cells instruct: The interplay of the gatekeeper and the general of the immune system. *Front. Immunol.* 2018. 9: 2472.

27. Iannacone, M., E. A. Moseman, E. Tonti, L. Bosurgi, T. Junt, S. E. Henrickson, S. P. Whelan, L. G. Guidotti, and U. H. Von Andrian. Subcapsular sinus macrophages prevent CNS invasion on peripheral infection with a neurotropic virus. *Nature* 2010. 465: 1079–1083.

28. Diamond, M. S., M. Kinder, H. Matsushita, M. Mashayekhi, G. P. Dunn, J. M. Archambault, H. Lee, C. D. Arthur, J. M. White, U. Kalinke, K. M. Murphy, and R. D. Schreiber. Type I interferon is selectively required by dendritic cells for immune rejection of tumors. *J. Exp. Med.* 2011. 208: 1989–2003.

29. Fuertes, M. B., A. K. Kacha, J. Kline, S. R. Woo, D. M. Kranz, K. M. Murphy, and T. F. Gajewski. Host type I IFN signals are required for antitumor CD8+ T cell responses through CD8α+ dendritic cells. *J. Exp. Med.* 2011. 208: 2005–2016.

30. Le Bon, A., N. Etchart, C. Rossmann, M. Ashton, S. Hou, D. Gewert, P. Borrow, and D. F. Tough. Cross-priming of CD8+ T cells stimulated by virus-induced type I interferon. *Nat. Immunol.* 2003. 4: 1009–1015.

31. Swiecki, M., Y. Wang, S. Gilfillan, and M. Colonna. Plasmacytoid dendritic cells contribute to systemic but not local antiviral responses to HSV infections. *PLoS Pathog.* 2013. 9: e1003728.

32. Backer, R., T. Schwandt, M. Greuter, M. Oosting, F. Jüngerkes, T. Tüting, L. Boon, T. O'Toole, G. Kraal, A. Limmer, and J. M. M. Den Haan. Effective collaboration between marginal metallophilic macrophages and CD8+ dendritic cells in the generation of cytotoxic T cells. *Proc. Natl. Acad. Sci. U. S. A.* 2010. 107: 216–221.

33. Bernhard, C. A., C. Ried, S. Kochanek, and T. Brocker. CD169+ macrophages are sufficient for priming of CTLs with specificities left out by cross-priming dendritic cells. *Proc. Natl. Acad. Sci. U. S. A.* 2015. 112: 5461–5466.

34. van Dinther, D., H. Veninga, S. Iborra, E. G. F. Borg, L. Hoogterp, K. Olesek, M. R. Beijer, S. T. T. Schetters, H. Kalay, J. J. Garcia-Vallejo, K. L. Franken, L. B. Cham, K. S. Lang, Y. van Kooyk, D. Sancho, P. R. Crocker, and J. M. M. den Haan. Functional CD169 on Macrophages Mediates Interaction with Dendritic Cells for CD8 + T Cell Cross-Priming. *Cell Rep.* 2018. 22: 1484–1495.

35. Allan, R. S., J. Waithman, S. Bedoui, C. M. Jones, J. A. Villadangos, Y. Zhan, A. M. Lew, K. Shortman, W. R. Heath, and F. R. Carbone. Migratory Dendritic Cells Transfer Antigen to a Lymph Node-Resident Dendritic Cell Population for Efficient CTL Priming. *Immunity* 2006. 25: 153–162.

36. Srivastava, S., and J. D. Ernst. Cell-to-cell transfer of M. tuberculosis antigens optimizes CD4 T cell priming. *Cell Host Microbe* 2014. 15: 741–752.

37. Gurevich, I., T. Feferman, I. Milo, O. Tal, O. Golani, I. Drexler, and G. Shakhar. Active dissemination of cellular antigens by DCs facilitates CD8+ T-cell priming in lymph nodes. *Eur. J. Immunol.* 2017. 47: 1802–1818.

38. Eickhoff, S., A. Brewitz, M. Y. Gerner, F. Klauschen, K. Komander, H. Hemmi, N. Garbi, T. Kaisho, R. N. Germain, and W. Kastenmüller. Robust Anti-viral Immunity Requires Multiple Distinct T Cell-Dendritic Cell Interactions. *Cell* 2015. 162: 1322–1337.

39. Hor, J. L., P. G. Whitney, A. Zaid, A. G. Brooks, W. R. Heath, and S. N. Mueller. Spatiotemporally Distinct Interactions with Dendritic Cell Subsets Facilitates CD4+ and CD8+ T Cell Activation to Localized Viral Infection. *Immunity* 2015. 43: 554–565.

40. Kitano, M., C. Yamazaki, A. Takumi, T. Ikeno, H. Hemmi, N. Takahashi, K. Shimizu, S. E. Fraser, K. Hoshino, T. Kaisho, and T. Okada. Imaging of the cross-presenting dendritic cell subsets in the skin-draining lymph node. *Proc. Natl. Acad. Sci. U. S. A.* 2016. 113: 1044–1049.

41. Borst, J., T. Ahrends, N. Bąbała, C. J. M. Melief, and W. Kastenmüller. CD4+ T cell help in cancer immunology and immunotherapy. *Nat. Rev. Immunol.* 2018. 18: 635–647.

42. Bachem, A., S. Güttler, E. Hartung, F. Ebstein, M. Schaefer, A. Tannert, A. Salama, K. Movassaghi, C. Opitz, H. W. Mages, V. Henn, P.-M. Kloetzel, S. Gurka, and R. A. Kroczek. Superior antigen cross-presentation and XCR1 expression define human CD11c+CD141+ cells as homologues of mouse CD8+ dendritic cells. *J. Exp. Med.* 2010. 207: 1273–1281.

43. Brewitz, A., S. Eickhoff, S. Dähling, T. Quast, S. Bedoui, R. A. Kroczek, C. Kurts, N. Garbi, W. Barchet, M. Iannacone, F. Klauschen, W. Kolanus, T. Kaisho, M. Colonna, R. N. Germain, and W. Kastenmüller. CD8 + T Cells Orchestrate pDC-XCR1 + Dendritic Cell Spatial and Functional Cooperativity to Optimize Priming. *Immunity* 2017. 46: 205–219.

44. Nair-Gupta, P., A. Baccarini, N. Tung, F. Seyffer, O. Florey, Y. Huang, M. Banerjee, M. Overholtzer, P. A. Roche, R. Tampé, B. D. Brown, D. Amsen, S. W. Whiteheart, and J. M. Blander. TLR signals induce phagosomal MHC-I delivery from the endosomal recycling compartment to allow cross-presentation. *Cell* 2014. 158: 506–521.

45. Burgdorf, S., A. Kautz, V. Böhnert, P. A. Knolle, and C. Kurts. Distinct pathways of antigen uptake and intracellular routing in CD4 and CD8 T cell activation. *Science* 2007. 316: 612–616.

46. Tacken, P. J., W. Ginter, L. Berod, L. J. Cruz, B. Joosten, T. Sparwasser, C. G. Figdor, and A. Cambi. Targeting DC-SIGN via its neck region leads to prolonged antigen residence in early endosomes, delayed lysosomal degradation, and cross-presentation. *Blood* 2011. 118: 4111–4119.

47. Saveanu, L., O. Carroll, M. Weimershaus, P. Guermonprez, E. Firat, V. Lindo, F. Greer, J. Davoust, R. Kratzer, S. R. Keller, G. Niedermann, and P. van Endert. IRAP Identifies an Endosomal Compartment Required for MHC Class I Cross-Presentation. *Science* 2009. 325: 213–217.

48. Lakadamyali, M., M. J. Rust, and X. Zhuang. Ligands for clathrin-mediated endocytosis are differentially sorted into distinct populations of early endosomes. *Cell* 2006. 124: 997–1009.

49. Neefjes, J., and C. Sadaka. Into the Intracellular Logistics of Cross-Presentation. *Front. Immunol.* 2012. 3: 31.

50. Hos, B. J., E. Tondini, S. I. van Kasteren, and F. Ossendorp. Approaches to Improve Chemically Defined Synthetic Peptide Vaccines. *Front. Immunol.* 2018. 9: 884.

51. Pawlak, J. B., B. J. Hos, M. J. van de Graaff, O. A. Megantari, N. Meeuwenoord, H. S. Overkleeft, D. V. Filippov, F. Ossendorp, and S. I. van Kasteren. The Optimization of Bioorthogonal Epitope Ligation within MHC-I Complexes. *ACS Chem. Biol.* 2016. 11: 3172–3178.

52. Tey, S. K. S.-K., and R. Khanna. Autophagy mediates transporter associated with antigen processing- independent presentation of viral epitopes through MHC class I pathway. *Blood* 2012. 120: 994–1004.

53. Ravindran, R., N. Khan, H. I. Nakaya, S. Li, J. Loebbermann, M. S. Maddur, Y. Park, D. P. Jones, P. Chappert, J. Davoust, D. S. Weiss, H. W. Virgin, D. Ron, and B. Pulendran. Vaccine activation of the nutrient sensor GCN2 in dendritic cells enhances antigen presentation. *Science* 2014. 343: 313–317.

54. Li, H., Y. Li, J. Jiao, and H. M. Hu. Alpha-alumina nanoparticles induce efficient autophagy-dependent cross-presentation and potent antitumour response. *Nat. Nanotechnol.* 2011. 6: 645–650.

55. Loi, M., A. Müller, K. Steinbach, J. Niven, R. Barreira da Silva, P. Paul, L. A. Ligeon, A. Caruso, R. A. Albrecht, A. C. Becker, N. Annaheim, H. Nowag, J. Dengjel, A. García-Sastre, D. Merkler, C. Münz, and M. Gannagé. Macroautophagy Proteins Control MHC Class I Levels on Dendritic Cells and Shape Anti-viral CD8+ T Cell Responses. *Cell Rep.* 2016. 15: 1076–1087.

8

56. Lee, H. K., L. M. Mattei, B. E. Steinberg, P. Alberts, Y. H. Lee, A. Chervonsky, N. Mizushima, S. Grinstein, and A. Iwasaki. In Vivo Requirement for Atg5 in Antigen Presentation by Dendritic Cells. *Immunity* 2010. 32: 227–239.

57. Mintern, J. D., C. Macri, W. J. Chin, S. E. Panozza, E. Segura, N. L. Patterson, P. Zeller, D. Bourges, S. Bedoui, P. J. Mcmillan, A. Idris, C. J. Nowell, A. Brown, K. J. Radford, A. P. R. Johnston, and J. A. Villadangos. Differential use of autophagy by primary dendritic cells specialized in cross-presentation. *Autophagy* 2015. 11: 906–917.

58. Sanjuan, M. A., C. P. Dillon, S. W. G. Tait, S. Moshiach, F. Dorsey, S. Connell, M. Komatsu, K. Tanaka, J. L. Cleveland, S. Withoff, and D. R. Green. Toll-like receptor signalling in macrophages links the autophagy pathway to phagocytosis. *Nature* 2007. 450: 1253–1257.

59. Huang, J., V. Canadien, G. Y. Lam, B. E. Steinberg, M. C. Dinauer, M. A. O. Magalhaes, M. Glogauer, S. Grinstein, and J. H. Brumell. Activation of antibacterial autophagy by NADPH oxidases. *Proc. Natl. Acad. Sci. U. S. A.* 2009. 106: 6226–6231.

60. Martinez, J., J. Almendinger, A. Oberst, R. Ness, C. P. Dillon, P. Fitzgerald, M. O. Hengartner, and D. R. Green. Microtubule-associated protein 1 light chain 3 alpha (LC3)-associated phagocytosis is required for the efficient clearance of dead cells. *Proc. Natl. Acad. Sci. U. S. A.* 2011. 108: 17396–17401.

61. Ma, J., C. Becker, C. A. Lowell, and D. M. Underhill. Dectin-1-triggered Recruitment of Light Chain 3 Protein to Phagosomes Facilitates Major Histocompatibility Complex Class II Presentation of Fungal-derived Antigens. *J. Biol. Chem.* 2012. 287: 34149–34156.

62. Romao, S., N. Gasser, A. C. Becker, B. Guhl, M. Bajagic, D. Vanoaica, U. Ziegler, J. Roesler, J. Dengjel, J. Reichenbach, and C. Münz. Autophagy proteins stabilize pathogen-containing phagosomes for prolonged MHC II antigen processing. *J. Cell Biol.* 2013. 203: 757–766.

63. Martinez, J., R. K. S. Malireddi, Q. Lu, L. D. Cunha, S. Pelletier, S. Gingras, R. Orchard, J. L. Guan, H. Tan, J. Peng, T. D. Kanneganti, H. W. Virgin, and D. R. Green. Molecular characterization of LC3-associated phagocytosis reveals distinct roles for Rubicon, NOX2 and autophagy proteins. *Nat. Cell Biol.* 2015. 17: 893–906.

64. Fujita, N., M. Hayashi-Nishino, H. Fukumoto, H. Omori, A. Yamamoto, T. Noda, and T. Yoshimori. An Atg4B mutant hampers the lipidation of LC3 paralogues and causes defects in autophagosome closure. *Mol. Biol. Cell* 2008. 19: 4651–4659.

65. Kawabata, T., and T. Yoshimori. Beyond starvation: An update on the autophagic machinery and its functions. *J. Mol. Cell. Cardiol.* 2016. 95: 2–10.

66. Boyle, K. B., and F. Randow. The role of "eat-me" signals and autophagy cargo receptors in innate immunity. *Curr. Opin. Microbiol.* 2013. 16: 339–348.

67. Kalergis, A. M., and J. V. Ravetch. Inducing tumor immunity through the selective engagement of activating Fcγ receptors on dendritic cells. *J. Exp. Med.* 2002. 195: 1653–1659.

68. Rafiq, K., A. Bergtold, and R. Clynes. Immune complex-mediated antigen presentation induces tumor immunity. *J. Clin. Invest.* 2002. 110: 71–79.

69. Schuurhuis, D. H., A. Ioan-Facsinay, B. Nagelkerken, J. J. van Schip, C. Sedlik, C. J. M. Melief, J. S. Verbeek, and F. Ossendorp. Antigen-Antibody Immune Complexes Empower Dendritic Cells to Efficiently Prime Specific CD8 + CTL Responses In Vivo. *J. Immunol.* 2002. 168: 2240–2246.

70. Daha, N. A., N. K. Banda, A. Roos, F. J. Beurskens, J. M. Bakker, M. R. Daha, and L. A. Trouw. Complement activation by (auto-) antibodies. *Mol. Immunol.* 2011. 48: 1656–1665.

71. Thielens, N. M., F. Tedesco, S. S. Bohlson, C. Gaboriaud, and A. J. Tenner. C1q: A fresh look upon an old molecule. *Mol. Immunol.* 2017. 89: 73–83.

72. Diebolder, C. A., F. J. Beurskens, R. N. de Jong, R. I. Koning, K. Strumane, M. A. Lindorfer, M. Voorhorst, D. Ugurlar, S. Rosati, A. J. R. R. Heck, J. G. J. J. Van De Winkel, I. A. Wilson, A. J. Koster, R. P. Taylor, E. O. Saphire, D. R. Burton, J. Schuurman, P. Gros, and P. W. H. I. H. I. Parren. Complement is activated by IgG hexamers assembled at the cell surface. *Science* 2014. 343: 1260–1263.

73. Wang, G., R. N. de Jong, E. T. J. van den Bremer, F. J. J. Beurskens, A. F. F. Labrijn, D. Ugurlar, P. Gros, J. Schuurman, P. W. H. I. W. H. I. Parren, A. J. R. J. R. Heck, R. N. de Jong, E. T. J. van den Bremer, F. J. J. Beurskens, A. F. F. Labrijn, D. Ugurlar, P. Gros, J. Schuurman, P. W. H. I. W. H. I. Parren, and A. J. R. J. R. Heck. Molecular Basis of Assembly and Activation of Complement Component C1 in Complex with Immunoglobulin G1 and Antigen. *Mol. Cell* 2016. 63: 135–145.

74. Ugurlar, D., S. C. Howes, B.-J. de Kreuk, R. I. Koning, R. N. de Jong, F. J. Beurskens, J. Schuurman, A. J. Koster, T. H. Sharp, P. W. H. I. Parren, and P. Gros. Structures of C1-IgG1 provide insights into how danger pattern recognition activates complement. *Science* 2018. 359: 794–797.

75. Qiu, C.-H., Y. Miyake, H. Kaise, H. Kitamura, O. Ohara, and M. Tanaka. Novel Subset of CD8 + Dendritic Cells Localized in the Marginal Zone Is Responsible for Tolerance to Cell-Associated Antigens. *J. Immunol.* 2009. 182: 4127–4136.

76. Idoyaga, J., N. Suda, K. Suda, C. G. Park, and R. M. Steinman. Antibody to Langerin/CD207 localizes large numbers of CD8 + dendritic cells to the marginal zone of mouse spleen. *Proc. Natl. Acad. Sci. U. S. A.* 2009. 106: 1524–1529.

77. Morse, M. A., R. E. Coleman, G. Akabani, N. Niehaus, D. Coleman, and H. K. Lyerly. Migration of human dendritic cells after injection in patients with metastatic malignancies. *Cancer Res.* 1999. 59: 56–58.

78. McCurley, N., and I. Mellman. Monocyte-derived dendritic cells exhibit increased levels of lysosomal proteolysis as compared to other human dendritic cell populations. *PLoS One* 2010. 5: e11949.

79. De Vries, I. J. M., D. J. E. B. Krooshoop, N. M. Scharenborg, W. J. Lesterhuis, J. H. S. Diepstra, G. N. P. Van Muijen, S. P. Strijk, T. J. Ruers, O. C. Boerman, W. J. G. Oyen, G. J. Adema, C. J. A. Punt, and C. G. Figdor. Effective migration of antigen-pulsed dendritic cells to lymph nodes in melanoma patients is determined by their maturation state. *Cancer Res.* 2003. 63: 12–17.

80. Bonifaz, L., D. Bonnyay, K. Mahnke, M. Rivera, M. C. Nussenzweig, and R. M. Steinman. Efficient targeting of protein antigen to the dendritic cell receptor DEC-205 in the steady state leads to antigen presentation on major histocompatibility complex class I products and peripheral CD8+ T cell tolerance. *J. Exp. Med.* 2002. 196: 1627–1638.

81. Tacken, P. J., I. J. M. de Vries, K. Gijzen, B. Joosten, D. Wu, R. P. Rother, S. J. Faas, C. J. A. Punt, R. Torensma, G. J. Adema, and C. G. Figdor. Effective induction of naive and recall T-cell responses by targeting antigen to human dendritic cells via a humanized anti-DC-SIGN antibody. *Blood* 2005. 106: 1278–1285.

82. Ni, L., I. Gayet, S. Zurawski, D. Duluc, A.-L. Flamar, X.-H. Li, A. O'Bar, S. Clayton, A. K. Palucka, G. Zurawski, J. Banchereau, and S. Oh. Concomitant activation and antigen uptake via human dectin-1 results in potent antigen-specific CD8+ T cell responses. *J. Immunol.* 2010. 185: 3504–3513.

83. Dhodapkar, M. V., M. Sznol, B. Zhao, D. Wang, R. D. Carvajal, M. L. Keohan, E. Chuang, R. E. Sanborn, J. Lutzky, J. Powderly, H. Kluger, S. Tejwani, J. Green, V. Ramakrishna, A. Crocker, L. Vitale, M. Yellin, T. Davis, and T. Keler. Induction of antigen-specific immunity with a vaccine targeting NY-ESO-1 to the dendritic cell receptor DEC-205. *Sci. Transl. Med.* 2014. 6: 232ra51.

84. Schuurhuis, D. H., N. van Montfoort, A. Ioan-Facsinay, R. Jiawan, M. Camps, J. Nouta, C. J. M. Melief, J. S. Verbeek, and F. Ossendorp. Immune Complex-Loaded Dendritic Cells Are Superior to Soluble Immune Complexes as Antitumor Vaccine. *J. Immunol.* 2006. 176: 4573–4580.

85. Zom, G. G., S. Khan, C. M. Britten, V. Sommandas, M. G. M. Camps, N. M. Loof, C. F. Budden, N. J. Meeuwenoord, D. V. Filippov, G. A. van der Marel, H. S. Overkleeft, C. J. M. Melief, and F. Ossendorp. Efficient induction of antitumor immunity by synthetic toll-like receptor ligand-peptide conjugates. *Cancer Immunol. Res.* 2014. 2: 756–764.

86. Takada, H., and C. Galanos. Enhancement of endotoxin lethality and generation of anaphylactoid reactions by lipopolysaccharides in muramyl-dipeptide-treated mice. *Infect. Immun.* 1987. 55: 409–413.

87. Fritz, J. H., S. E. Girardin, C. Fitting, C. Werts, D. Mengin-Lecreulx, M. Caroff, J.-M. Cavaillon, D. J. Philpott, and M. Adib-Conquy. Synergistic stimulation of human monocytes and dendritic cells by Toll-like receptor 4 and NOD1- and NOD2-activating agonists. *Eur. J. Immunol.* 2005. 35: 2459–2470.

88. Tada, H., S. Aiba, K.-I. Shibata, T. Ohteki, and H. Takada. Synergistic effect of Nod1 and Nod2 agonists with toll-like receptor agonists on human dendritic cells to generate interleukin-12 and T helper type 1 cells. *Infect. Immun.* 2005. 73: 7967–7976.

89. Cruz, L. J., P. J. Tacken, R. Fokkink, B. Joosten, M. C. Stuart, F. Albericio, R. Torensma, and C. G. Figdor. Targeted PLGA nano- but not microparticles specifically deliver antigen to human dendritic cells via DC-SIGN in vitro. *J. Control. Release* 2010. 144: 118–126.

90. Rosalia, R. A., L. J. Cruz, S. van Duikeren, A. T. Tromp, A. L. Silva, W. Jiskoot, T. de Gruijl, C. Löwik, J. Oostendorp, S. H. van der Burg, and F. Ossendorp. CD40-targeted dendritic cell delivery of PLGA-nanoparticle vaccines induce potent anti-tumor responses. *Biomaterials* 2015. 40: 88–97.

91. Silva, A. L., R. A. Rosalia, A. Sazak, M. G. Carstens, F. Ossendorp, J. Oostendorp, and W. Jiskoot. Optimization of encapsulation of a synthetic long peptide in PLGA nanoparticles: Low-burst release is crucial for efficient CD8+ T cell activation. *Eur. J. Pharm. Biopharm.* 2013. 83: 338–345.
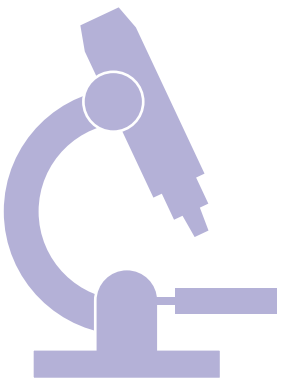
8

92. Bennett, S. R. M., F. R. Carbone, F. Karamalis, J. F. A. P. Miller, and W. R. Heath. Induction of a CD8+ cytotoxic T lymphocyte response by cross-priming requires cognate CD4+ T cell help. *J. Exp. Med.* 1997. 186: 65–70.

93. Schoenberger, S. P., R. E. M. Toes, E. I. H. van der Voort, R. Offringa, and C. J. M. Melief. T-cell help for cytotoxic T lymphocytes is mediated by CD40–CD40L interactions. *Nature* 1998. 393: 480–483.

94. Ossendorp, F., E. Mengedé, M. Camps, R. Filius, and C. J. Melief. Specific T helper cell requirement for optimal induction of cytotoxic T lymphocytes against major histocompatibility complex class II negative tumors. *J. Exp. Med.* 1998. 187: 693–702.

95. Takahashi, H., Y. Nakagawa, K. Yokomuro, and J. A. Berzofsky. Induction of CD8 [+] cytotoxic T lymphocytes by immunization with syngeneic irradiated HIV-1 envelope derived peptide-pulsed dendritic cells. *Int. Immunol.* 1993. 5: 849–857.

96. Arthur, J. F., L. H. Butterfield, M. D. Roth, L. A. Bui, S. M. Kiertscher, R. Lau, S. Dubinett, J. Glaspy, W. H. McBride, and J. S. Economou. A comparison of gene transfer methods in human dendritic cells. *Cancer Gene Ther.* 1997. 4: 17–25.

97. Meng, W. S., and L. H. Butterfield. Activation of antigen-presenting cells by DNA delivery vectors. *Expert Opin. Biol. Ther.* 2005. 5: 1019–1028.

98. Palucka, A. K., H. Ueno, J. Connolly, F. Kerneis-Norvell, J.-P. Blanck, D. A. Johnston, J. Fay, and J. Banchereau. Dendritic Cells Loaded With Killed Allogeneic Melanoma Cells can Induce Objective Clinical Responses and MART-1 Specific CD8+ T-cell Immunity. *J. Immunother.* 2006. 29: 545–557.

99. Rosalia, R. A., E. D. Quakkelaar, A. Redeker, S. Khan, M. Camps, J. W. Drijfhout, A. L. Silva, W. Jiskoot, T. van Hall, P. A. van Veelen, G. Janssen, K. Franken, L. J. Cruz, A. Tromp, J. Oostendorp, S. H. van der Burg, F. Ossendorp, and C. J. M. Melief. Dendritic cells process synthetic long peptides better than whole protein, improving antigen presentation and T-cell activation. *Eur. J. Immunol.* 2013. 43: 2554–2565.

100. Carreno, B. M., V. Magrini, M. Becker-Hapak, S. Kaabinejadian, J. Hundal, A. A. Petti, A. Ly, W.-R. Lie, W. H. Hildebrand, E. R. Mardis, and G. P. Linette. A dendritic cell vaccine increases the breadth and diversity of melanoma neoantigen-specific T cells. *Science* 2015. 348: 803–808.

101. Schumacher, T. N., and R. D. Schreiber. Neoantigens in cancer immunotherapy. *Science* 2015. 348: 69–74.

102. Kranz, L. M., M. Diken, H. Haas, S. Kreiter, C. Loquai, K. C. Reuter, M. Meng, D. Fritz, F. Vascotto, H. Hefesha, C. Grunwitz, M. Vormehr, Y. Hüsemann, A. Selmi, A. N. Kuhn, J. Buck, E. Derhovanessian, R. Rae, S. Attig, J. Diekmann, R. A. Jabulowsky, S. Heesch, J. Hassel, P. Langguth, S. Grabbe, C. Huber, Ö. Türeci, and U. Sahin. Systemic RNA delivery to dendritic cells exploits antiviral defence for cancer immunotherapy. *Nature* 2016. 534: 396–401.

103. Sahin, U., E. Derhovanessian, M. Miller, B.-P. Kloke, P. Simon, M. Löwer, V. Bukur, A. D. Tadmor, U. Luxemburger, B. Schrörs, T. Omokoko, M. Vormehr, C. Albrecht, A. Paruzynski, A. N. Kuhn, J. Buck, S. Heesch, K. H. Schreeb, F. Müller, I. Ortseifer, I. Vogler, E. Godehardt, S. Attig, R. Rae, A. Breitkreuz, C. Tolliver, M. Suchan, G. Martic, A. Hohberger, P. Sorn, J. Diekmann, J. Ciesla, O. Waksmann, A.-K. Brück, M. Witt, M. Zillgen, A. Rothermel, B. Kasemann, D. Langer, S. Bolte, M. Diken, S. Kreiter, R. Nemecek, C. Gebhardt, S. Grabbe, C. Höller, J. Utikal, C. Huber, C. Loquai, and Ö. Türeci. Personalized RNA mutanome vaccines mobilize poly-specific therapeutic immunity against cancer. *Nature* 2017. 547: 222–226.

8

Appendices

NEDERLANDSE SAMENVATTING

Ons immuunsysteem is het belangrijkste wapen dat wij van nature hebben meegekregen om ons te verdedigen tegen verschillende ziekteverwekkende indringers o.a. bacteriën en virussen. Het immuunsysteem bestaat uit verschillende cellen met ieder een eigen taak die vaak in verband staan met elkaar om samen als een legerfront te vechten tegen indringers. Eén van de cellen die een centrale rol speelt in het immuunsysteem is de dendritische cel (DC). Ze waren voor het eerst ontdekt door Paul Langerhans tegen het einde van de negentiende eeuw, en hebben hun naam te danken aan de voelsprieten (dendrieten) die de cellen hebben om de pathogene indringers op te sporen. Rond 1973 ontdekten Ralph Steinman en Zanvil Cohn dat DCs als een soort "scouts" in het lichaam patrouilleren om indringers op te sporen met hun voelsprieten. Vaak patrouilleren de DCs op plekken in het lichaam waar pathogenen binnendringen, zoals de huid en slijmvliezen. Op de voelsprieten zitten verschillende receptoren, zoals Toll-like receptoren (TLRs) and C-type lectine receptoren (CLRs), die delen van allerlei indringers kunnen herkennen. TLRs herkennen onderdelen van bijvoorbeeld bacteriën en virussen, CLRs herkennen suikerstructuren op onder andere bacteriën en schimmels. Daarnaast kunnen DCs ook antilichamen herkennen die gebonden zijn aan geïnfecteerde cellen of pathogenen door middel van Fcγ receptoren (FcγRs). Wanneer de receptoren op de DCs pathogenen herkennen worden de pathogenen opgenomen en de eiwitten daarvan (de antigenen) door de DCs verteerd tot kleinere stukjes. Deze stukjes worden daarna op het oppervlak van de DC gepresenteerd aan T-cellen, de "soldaten" van het immuunsysteem. Een unieke eigenschap van DCs is dat ze externe antigenen kunnen opnemen en aan specifieke "killer" T-cellen kunnen presenteren, ook wel "cross-presentatie" genoemd. Deze T-cellen worden geactiveerd zodra ze een DC "scout" zien die stukjes van een pathogeen presenteren waarmee de DC alarm slaat dat er ergens een vijand gesignaleerd is. De T-cellen gaan dan expanderen totdat ze een heel leger aan T-cel "soldaten" hebben die specifiek de vijand herkennen die eerder gerapporteerd werd door de DC. Het leger van T-cellen gaat dan naar de plek waar de pathogenen bevinden en ruimt ze dan op. Doordat DCs een onmisbare rol spelen in het activeren van het immuunsysteem en het aanzetten van T-cellen, worden er steeds meer onderzoeken gedaan naar hoe men deze DCs nog beter hun werk kunnen laten doen.

In dit proefschrift bestuderen we wat er met een antigeen gebeurt nadat het wordt opgenomen door DCs via receptoren op de voelsprieten. We maken gebruik van een model antigeen (OVA) en koppelen het aan antilichamen, die specifiek binden aan OVA, zodat er een immuuncomplex formatie van OVA met antilichamen (OVA IC) gevormd wordt. Deze OVA IC binden aan de FcγRs op de voelsprieten van de DCs en worden daarna opgenomen in de DCs. Onze onderzoeksgroep heeft al eerder laten zien dat deze OVA IC heel efficiënt worden opgenomen door DCs en ook DCs sterk kunnen activeren *in vitro*. Wanneer DCs

eerst beladen worden met tumor specifieke immuuncomplexen en ingespoten worden in muizen, wordt er een sterk CD8$^+$ T-cel respons opgewekt waardoor tumoren aangevallen worden. In **hoofdstuk 2** laten we zien dat DCs voor een lange tijd OVA IC kunnen opslaan in de cel nadat de OVA IC zijn opgenomen *in vivo*. Een belangrijk gegeven is dat we in deze studie gebruik hebben gemaakt van een natuurlijke formatie van OVA IC door eerst antilichamen in te spuiten in de muis en vervolgens het antigeen om op deze manier de immuuncomplexen zelf te laten vormen in circulatie. Hiermee bootsten we de natuurlijke vorming van immuuncomplexen na in het lichaam. In het lichaam zijn meerdere DC types te vinden, waaronder CD8α$^+$ (ook wel cDC1 genoemd), CD8α$^-$ (ook wel cDC2 genoemd), en pDCs. We zagen dat alle DC types OVA IC kunnen opnemen en opslaan, maar dat er een verschil was in welke type T cellen werden geactiveerd. De CD8α$^+$ DCs activeerden de CD8$^+$ T-cellen (ook wel de killer T-cellen genoemd), terwijl de CD8α$^-$ DCs veel beter de CD4$^+$ T-cellen (ook wel de helper T cellen genoemd) activeerden. De CD8$^+$ T-cellen kunnen tumorcellen aanvallen, waarbij CD4$^+$ T-cellen een extra boost kunnen geven aan de DCs om de CD8$^+$ T-cellen nog sterker te activeren. Opvallend was dat pDCs, die vaak een belangrijke rol spelen bij virale infecties, wel OVA IC konden opnemen en opslaan maar niet in staat waren om CD8$^+$ of CD4$^+$ T-cellen te activeren. In deze studie laten we zien dat DCs in staat zijn om antigenen voor lange duur op te slaan en daardoor ook voor lange duur antigenen kunnen presenteren aan T-cellen. Dit is van belang doordat DCs vaak tijd nodig hebben om te reizen vanaf de plek waar ze een pathogeen zijn tegengekomen tot de plekken (lymfeknopen) waar ze het antigeen presenteren aan T-cellen. Doordat DCs langdurig antigenen in hun opslag hebben en voor lange tijd aan T-cellen kunnen presenteren wordt een effectiever immuunrespons opgewekt.

Er werd altijd vanuit gegaan dat OVA IC worden opgenomen door DCs via de FcγRs op de voelsprieten van de DCs. We laten in **hoofdstuk 3** zien dat het echter veel complexer is. We hebben ontdekt dat C1q, die onderdeel is van het complementsysteem, een cruciale rol speelt in de opname van OVA IC door DCs *in vivo*. Hier hadden we ook weer gebruik gemaakt van natuurlijk gevormde immuuncomplexen in circulatie. Wanneer we muizen gebruikten die geen C1q hadden zagen we dat er geen OVA IC meer werden opgenomen door de DCs, waardoor er ook geen T-cellen meer werden geactiveerd. Het verbazingwekkende was dat we zelfs een verhoogde OVA IC opname zagen in DCs wanneer we gebruik maakten van muizen die geen FcγRs hadden *in vivo*. Het lijkt er op dat C1q een veel dominantere rol speelt dan FcγRs in OVA IC opname door DCs *in vivo*. Verder onderzoek naar de receptor voor C1q op de voelsprieten van DCs zou beter inzicht geven hoe IC worden opgenomen *in vivo*.

We hebben eerder door onze onderzoeksgroep en in **hoofdstuk 2** van dit proefschrift laten zien dat DCs voor lange tijd antigeen kunnen opslaan waardoor er langdurig T-cellen geactiveerd kunnen worden. In **hoofdstuk 4** onderzochten we meer in detail waar de antigenen worden opgeslagen in DCs. We maakten gebruik van fluorescerend gelabelde

A

OVA IC die we konden volgen in de DCs met behulp van confocale microscopie. We laten zien dat OVA IC worden opgeslagen in een compartiment die positief is voor LAMP1, maar niet hetzelfde is als de compartimenten waar antigeen wordt beladen op MHCI of MHCII-moleculen. Wanneer de antigenen via een andere receptor, de C-type lectin receptor MGL1, worden opgenomen zien we dat de antigenen uiteindelijk in dezelfde compartimenten terechtkomen. Onze data suggereren dat de compartimenten antigenen kunnen opslaan die vanuit verschillende opname routes worden opgenomen door de DCs.

Om antigenen te kunnen volgen in DCs worden vaak fluoroforen gekoppeld aan de antigenen die je wilt visualiseren. Je kan dan confocale microscopie gebruiken om de fluoroforen te zien in de cellen. Helaas zijn de antigenen waar interesse voor is niet altijd beschikbaar met een fluorofoor, daarom hebben we in **hoofdstuk 7** gekeken naar de mogelijkheden om met een nieuwe techniek fluoroforen te koppelen aan een TLR2 ligand (Pam) geconjugeerd met een OVA lang-peptide. We hebben eerder aangetoond dat de Pam in deze conjugaten DCs kunnen activeren en dat het OVA lang-peptide verwerkt wordt door de DC voor cross-presentatie aan CD8^{+} T-cellen. Deze combinatie is heel aantrekkelijk voor het ontwikkelen van vaccins tegen kanker doordat je met één conjugaat een specifiek antigeen en een adjuvans hebt voor het activeren van DCs. We zagen eerder dat DCs na opname van deze conjugaten ook voor meerdere dagen het antigeen konden cross-presenteren. Dit suggereert dat ook deze conjugaten worden opgeslagen in de DCs. Om de conjugaten te kunnen volgen in DCs hadden we de conjugaten gekoppeld aan fluorofoor TAMRA of Cy5. Vanwege de slechte oplosbaarheid van de conjugaten die gekoppeld waren aan TAMRA was het niet mogelijk deze conjugaten verder te gebruiken voor experimenten. De conjugaten die gekoppeld waren aan Cy5 werden efficiënt opgenomen door DCs en behielden de eigenschappen om DCs te activeren. Daarnaast hadden we ook een ander TLR-ligand (CpG) gekoppeld aan een OVA lang-peptide en gelabeld met Alexa 488 of Cy5. Beiden werden efficiënt opgenomen door DCs in endosomale compartimenten. Het is echter niet uitgesloten dat een fluorofoor de eigenschappen kunnen veranderen van een conjugaat, daarom is het belangrijk om nieuwe mogelijkheden in het labelen van conjugaten te ontdekken. Eén van de mogelijkheden is om eerst je antigeen te geven aan DCs en achteraf pas de fluorofoor vast te koppelen. Daar wordt nu intensief onderzoek aan gedaan.

In **hoofdstuk 5** modificeerden we het OVA-eiwit, dat normaal via de mannose receptor (MR) op DCs werd opgenomen, door er een suikerstructuur aan te koppelen. Door de koppeling van de suikerstructuur werd het OVA-eiwit opgenomen door de MGL1 receptor in plaats van MR. Dit zorgde ervoor dat naïeve CD4^{+} T-cellen veranderden naar IFNy-producerende Th1 cellen en een betere activatie van CD8^{+} T-cellen. De opnamen van OVA via de MR vereist meestal een hoge hoeveelheid van beschikbare OVA om een efficiënte opname te realiseren in DCs. Daarnaast is ook een additioneel signaal nodig via bijvoorbeeld TLRs om de DCs te activeren. Door de modifactie van OVA en de opname via MGL1 te laten verlopen,

is er veel minder OVA nodig en geen additioneel activatie signaal om DCs te matureren voor efficiënte T-cel activatie. Daarnaast laten we zien dat OVA zonder suikerstructuur wordt opgenomen in EEA1+ Rab11+ compartimenten in DCs. Echter, wanneer een suikerstructuur aan OVA is gekoppeld wordt OVA gestuurd naar Rab11+ LAMP1+ compartimenten waar het opgeslagen wordt voor langdurige antigeen cross-presentatie aan CD8+ T-cellen.

Wat er precies met het antigeen gebeurt nadat het opgeslagen wordt in DCs en de route die het antigeen aflegt voordat het op het celoppervlak in MHC-moleculen wordt gepresenteerd aan T-cellen is nog niet helemaal ontrafeld. We hebben eerder laten zien dat de route die het antigeen aflegt vanuit de opslag TAP en proteasoom afhankelijk is, maar hoe het antigeen uit het opslag-compartiment wordt getransporteerd of verder gedegradeerd wordt is nog onduidelijk. In **hoofdstuk 6** laten we zien dat het autofagie proces mogelijk de opslag-compartimenten afbreekt waardoor dit invloed kan hebben op de mate van antigeen cross-presentatie aan CD8+ T-cellen. Autofagie is een evolutionair geconserveerd systeem dat de degradatie van verschillende eiwitten en beschadigde organellen door lysosomen induceert. In dit hoofdstuk blokkeerden we autofagie met remmers of we gebruikten muizen die geen autofagie hadden en zagen dat DCs meer antigenen konden opslaan en een verhoogde antigeen cross-presentatie induceerden aan CD8+ T-cellen. Het lijkt er op dat autofagosomen de opslag compartimenten degraderen en daarbij de mate van antigeen cross-presentatie kunnen beïnvloeden.

In conclusie, in deze thesis is beschreven dat verschillende DC types capabel zijn om voor lange tijd verschillende typen antigenen op te slaan in speciale opslag-compartimenten. Dit draagt bij aan langdurige antigeen cross-presentatie aan T-cellen, waardoor een betere immuunrespons is op te wekken. Voor de ontwikkeling van toekomstige kankervaccins kan het van belang zijn dat de vaccin-antigenen langdurig opgeslagen worden in DCs en tegelijkertijd DCs kunnen activeren. Ook is het belangrijk om te weten door welke type DCs de antigenen opgenomen worden, aangezien verschillende DC types andere functies hebben. Het is gunstig als zowel de killer CD8+ T-cellen als de helper CD4+ T-cellen optimaal geactiveerd kunnen worden om de immuunrespons nog verder te kunnen versterken. Het immuunsysteem is echter zeer complex, er zijn veel factoren die een rol spelen bij immuuntherapie van patiënten met kanker. Vaak beïnvloeden tumorcellen de omgeving waardoor immuun cellen minder goed te tumorcellen kunnen bereiken of minder goed geactiveerd worden. In de toekomst zal steeds meer onderzoek gedaan worden om verschillende klassieke- en immuuntherapieën te combineren, waaronder specifieke kankervaccins met chemotherapie of tumor ablatie technieken om zo een sterke tumor specifieke immuunrespons op te wekken. Het is in ieder geval duidelijk dat DCs, sinds hun ontdekking, een dominante positie hebben verkregen in de ontwikkeling van vaccins tegen kanker. Verder onderzoek naar het mechanisme van DC cross-presentatie is noodzakelijk om deze cellen, die we van nature hebben meegekregen om te vechten tegen indringers, zo optimaal mogelijk te benutten.

A

ACKNOWLEDGEMENTS

Het heeft even geduurd, maar het ei is eindelijk gelegd. Ik kijk met plezier terug naar mijn jaren als PhD student en het prachtige bewijs ervan samengevat in dit boekje. Natuurlijk was dit alles niet mogelijk geweest in mijn eentje. Met deze laatste woorden wil ik iedereen in het zonnetje zetten die een bijdrage geleverd hebben.

Ferry, mijn promotor, ik wil je bedanken dat je mij onder de vleugels hebt genomen en dat ik aan dit project mocht deelnemen. Je was vanaf begin tot eind enthousiast en betrokken geweest bij het onderzoek. Je nam altijd de tijd om data te bespreken en dingen uit te leggen met uitgebreide schetsen tijdens onze wekelijkse werkbespreking. Ik heb veel van je geleerd. Bedankt voor het blijven geloven in mij en dat je samen met mij het traject tot het einde bewandeld hebt.

Marcel, mijn paranimf, vanaf dag één was je mijn rechterhand bij dit project. Niet alleen heb je mij alle kneepjes van het labwerk geleerd, maar jij bracht dagelijks plezier op de werkvloer met je humor. Ik wil je voornamelijk bedanken voor je onuitputtelijke inzet en hulp bij experimenten.

Alle collega's van tumorimmunologie en IHB, ik wil jullie allemaal bedanken voor de prettige werkomgeving en saamhorigheid als groep. Met name mijn kamergenoten, Tetje, Suzanne, Gijs, wil ik bedanken voor de gezellige tijd. Elena, my student and later on my colleague, I only had to explain things once and you catch up really quickly, I was lucky to have you. Edwin van de IHB, bedankt voor het sorteren van de cellen. De borrel commissieleden, Candido, Brett, Ruben, en Chih Kit, bedankt voor de leuke momenten en diepgaande gesprekken buiten werktijden.

Samenwerking is vaak de sleutel tot succes. Dima, mijn co-promotor, bedankt voor alle input en ideeën vanuit de chemie en dat je mij in dit project hebt begeleid. Geoffroy, en Gijs, ondanks de tegenslagen in het begin hebben we uiteindelijk mooie resultaten en een gezamenlijke publicatie kunnen waarmaken. Onze samenwerking met het VUMC, Yvette, Wendy, bedankt voor de mogelijkheid om samen een mooi paper te publiceren, and especially Juan, thank you for your time and effort in helping with all the flow cytometry imaging experiments. De elektronenmicroscopie experts van het LUMC, Bram en Erik, bedankt voor het maken van prachtige EM-plaatjes. Leendert, de specialist in het complement systeem in het LUMC, bedankt voor alle hulp en bijdrage voor ons C1q paper. Sander van het LIC en Martijn van het Radboudumc, jullie inzicht vanuit de chemie kant bracht altijd verassende en nieuwe ideeën om toe te passen in de immunologie. The autophagy expert Christian from the university of Zurich, thank you for your input and tools for our autophagy experiments. I am also grateful for our collaboration with Sven and Matthias from the Limes institute and the chance to visit your lab with Marcel.

Maria, mijn tweede paranimf, vanaf de dag dat we elkaar leerden kennen tijdens onze stages bij het "Neefjes" lab op het NKI waren we onafscheidelijk. Je hebt me tijdens mijn hoogte en dieptepunten meegemaakt en me altijd bijgestaan en bemoedigd.

Mom and dad, 非常感謝你們多年來的支持和鼓勵. 沒有你們, 我不會有今天的成就.

Andreas, älskling, you did not only add color to my dissertation but also to my life. Thank you for always supporting and encouraging me in everything I do.

A

CURRICULUM VITAE

Nataschja was born on the 28th of August 1986 in Amsterdam, The Netherlands. She obtained her VWO diploma in 2004 at the Fons Vitae lyceum in Amsterdam. She studied Biomedical Sciences and later on the master Oncology at the Vrije Universiteit in Amsterdam. During her first master internship she investigated the role of platelet-derived growth factor in tumor-stroma interaction between colon carcinoma cells and fibroblasts under the supervision of Prof. dr. Epie Boven (Medical Oncology, VUMC). She did her second internship under the supervision of Dr. Rik van der Kant and Prof. dr. Jacques Neefjes (Cell Biology II, Netherlands Cancer Institute) where she investigated the role of a multiprotein complex in the transport and fusion of late endosomes. Her interest in dendritic cells grew quickly after she did her literature study assignment under the supervision of Prof. dr. Tanja de Gruijl (Immunology, VUMC) where she focused on targeting different dendritic cell subsets for anti-cancer vaccination. She decided to pursue her career in de dendritic cell field and started her PhD in 2012 under the supervision of Prof. dr. Ferry Ossendorp (Tumor Immunology, LUMC) on a ZonMw TOP research project of which the results are described in this dissertation. She is currently working as post-doctoral researcher in the group of Prof. dr. Gosse Adema (Radiotherapy & Oncoimmunology, Radboudumc) where she further pursues her interest in human dendritic cells and cancer vaccines.

LIST OF PUBLICATIONS

Adjuvants Enhancing Cross-Presentation by Dendritic Cells: The Key to More Effective Vaccines?

Ho NI, Huis In 't Veld LGM, Raaijmakers TK, Adema GJ.
Front Immunol. 2018 Dec 13;9:2874.

Sustained cross-presentation capacity of murine splenic dendritic cell subsets in vivo.

Ho NI, Camps MGM, de Haas EFE, Ossendorp F.
Eur J Immunol. 2018 Jul;48(7):1164-1173.

C1q-Dependent Dendritic Cell Cross-Presentation of In Vivo-Formed Antigen-Antibody Complexes.

Ho NI, Camps MGM, de Haas EFE, Trouw LA, Verbeek JS, Ossendorp F.
J Immunol. 2017 Jun 1;198(11):4235-4243.

Synthesis and evaluation of fluorescent Pam3Cys peptide conjugates.

Gential GP, **Ho NI**, Chiodo F, Meeuwenoord N, Ossendorp F, Overkleeft HS, van der Marel GA, Filippov DV.
Bioorg Med Chem Lett. 2016 Aug 1;26(15):3641-5.

Glycan modification of antigen alters its intracellular routing in dendritic cells, promoting priming of T cells.

Streng-Ouwehand I, **Ho NI**, Litjens M, Kalay H, Boks MA, Cornelissen LA, Kaur Singh S, Saeland E, Garcia-Vallejo JJ, Ossendorp FA, Unger WW, van Kooyk Y.
Elife. 2016 Mar 21;5. pii: e11765.

Late endosomal transport and tethering are coupled processes controlled by RILP and the cholesterol sensor ORP1L.

van der Kant R, Fish A, Janssen L, Janssen H, Krom S, **Ho NI**, Brummelkamp T, Carette J, Rocha N, Neefjes J.
J Cell Sci. 2013 Aug 1;126(Pt 15):3462-74.

A